Integrins in muscle disease and repair

Thesis submitted to University of East Anglia for the degree of Doctor of Philosophy in the School of Biological Sciences

Devina Divekar

School of Biological Sciences

November 2014

Abstract

Integrin α7β1 plays an important role in maintaining adult skeletal muscle integrity and like dystrophin, provides anchorage and bidirectional signaling as a laminin receptor. The expression of α7β1 integrin was upregulated upon dystrophin deficiency arguing for the molecular compensation and thus considered as potential candidate for treatment of Duchenne Muscular Dystrophy (DMD).

The existence of developmentally regulated alternative splice variants makes the α7β1 integrin a complex integrin to study its function in skeletal muscle. In this study we show that increased levels of the adult extracellular variant X2 interfere with muscle integrity, while the presence of embryonic integrin α7 extracellular variant X1 results in normal skeletal muscle architecture. Furthermore, detailed analysis of *mdx*$^{\alpha 7tg}$ mice suggests that overexpression of integrin α7 made no difference on the dystrophic phenotype, in fact *mdx* $^{\alpha 7X2}$ mice show a more severe phenotype compared to *mdx* mice.

Our study also shed light on the importance of integrin α5 during the development of the skeletal muscle by means of generating conditional knockout (cKO) mice using HSA-Cre and Pax3-Cre promoter systems. Our findings show no obvious difference in the Itga5 cKO when the HSA promoter drives Cre recombinase, however conditional loss under the control of the Pax3 promoter leads perinatal lethality.

In addition we investigate the dosage effect of integrin α5 in integrin α7 knockout (KO) mice to understand the cross talk between these two integrins and to co-relate with previous data suggesting a gain of function phenotype by that existence of integrin α5 at the myotendinious junction (MTJ) in α7KO muscle (Nawrotzki et al., 2003)

From our data we know that gene therapy with integrin α7 is a challenge and is not a suitable alternative to cure dystrophy, at least not in *mdx* mice, we therefore switch our focus on looking into cell based therapies for DMD by investigating the potential role of perivascular cells (PVCs) using transplantation experiments in mice by artificially inducing muscle damage.

Table of Contents

Chapter 1: Introduction

Chapter 3 Integrin α5 in development and adult skeletal muscle

Chapter 4 Could integrin α7β1 be a potential therapeutic target for DMD?

Chapter 5 Do pericytes contribute to skeletal muscle regeneration?

Chapter 6 Summary

Chapter 1 Introduction

Chapter 2 Materials and Methods

Chapter 3 Integrin α5 in development and adult skeletal muscle

Chapter 4 Could integrin α7β1 be a potential therapeutic target for DMD?

Acknowledgements

There are many people I wish to thank in the preparation of this dissertation and their support throughout my PhD journey. A very special thank you goes to my mentor Prof. Uli Mayer. I would not have completed my PhD without her guidance and support the last few years. I am grateful for her extremely high standards in research and patience as I found my way. She took a chance by accepting a graduate student and gave me a lab "home" for which I am very grateful. I would also like to thank her for the time and lengths she went to make sure this thesis reflected my efforts.

I would like to thank Dr Ernst Pöschl for his unwavering enthusiasm and for always being there to offer advice. Dr Jelena Gavrivolica for being there as secondary supervisor and for being so supportive throughout my period of study.

I would also like to thank Melanie for generating the integrin α7over expresser constructs and all of her technical help. I have to thank the research associates and students I had the privilege of working with in the lab over the past few years; they have taught me just as much as I hope they have learned from me: Isabelle, Lisa Emily, Laura, Jamie, Chitra from the Mayer Lab; and Zhigang Zhou from the Pöschl Lab.

I would like to express my heartfelt gratitude to my husband, Prashant, who has been my backbone throughout this entire process even though he had to put up with my mood swings. A big thanks to my daughter, Parina, who makes me smile after an exhausting day.

Last, but certainly not least. To my family, thank you so much for your constant support even when it meant living 5,000 miles away from you! I am very lucky to have such a close family that supports and encouraged me to pursue my dreams. My parents and grandparents, who have always been world's best role models and cheerleaders, words cannot express just how grateful I am to you. Your love and support has been unwavering despite everything you were going through yourselves. You have given me the best possible start in life, and all of my achievements are directly attributable to you. Thank you.

1. Introduction

1.1 Skeletal Muscle:

Muscle is a specialised tissue that has both the ability to contract and to conduct electric impulses. There are three types of muscle tissue - skeletal, cardiac and smooth muscle. Skeletal muscle moves the body with the help of muscle fibre contraction, which is a result of the force generated by ATP consumption. The contractile force generated in the muscle must be passed through the muscle cell membrane, the sarcolemma, to the muscle surrounding basement membrane before being transferred through the tendon to the bone allowing for a joint movement. The complexity of muscle function requires a high degree of specialisation and organisation of muscle cell components, but this also leaves muscle susceptible to the effect of mutations. This is exemplified by the muscular dystrophies, of which many are caused by the disruption of the muscle cell anchorage between inside and outside of the cell.

Skeletal muscle integrity and its function are maintained by the interaction of the muscle cell with the surrounding extracellular matrix. Cell adhesion molecules, like integrin α7β1 and the Dystrophin Glyoprotein Complex (DGC) link the muscle cell to the surrounding basement membrane and thus play an important role in transferring signals between inside and outside of the muscle cell. It has been shown that in the absence of either of these cell-adhesion molecules muscle integrity is compromised leading to muscle wasting disease and myopathies. In order to develop potential therapies for the diseases it is important to understand the role cell-matrix interaction plays in normal development and maintenance of the adult muscle cell.

1.2 Muscle fibre development, structure and function

The first sign of commitment to the myogenic lineage in the mouse is seen around 8 days post coitum (Ott et al., 1991) when the precursor cells in the paraxial mesoderm (those adjacent to the notochord and neural tube) start to express the myogenic regulatory factors (MRFs). The promoter elements that control the specific temporo-spatial expression of the MRFs coordinating myogenesis have yet to be fully

elucidated, though it is known that the transcription of muscle specific proteins is a complex network of feedback loops and cascades allowing the precise control of the differentiation state.

Once committed to muscle cell lineage, myoblasts (muscle cell precursors) migrate to regions of muscle formation and start to proliferate. Some align with each other, withdraw from the cell cycle and fuse to form multi-nucleated primary myotubes. Subsequent migrating myoblasts then fuse to this primary structure and this process is termed secondary myogenesis. The fusion of myoblasts to form myotubes is termed terminal differentiation. The secondary myotubes continue to grow and elongate by cell fusion before eventually separating and maturing into adult muscle fibres (Fig. 1.1).

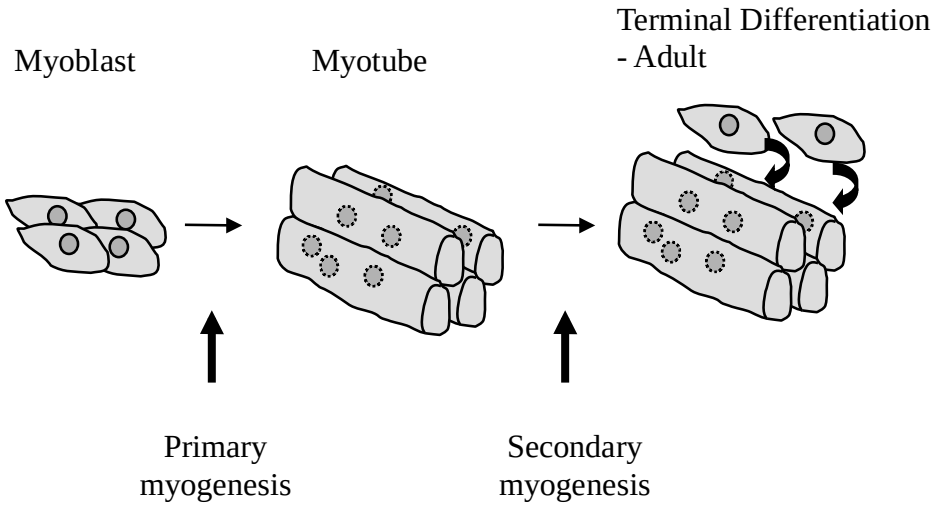

Figure 1.1: Schematic representation of myogenesis. *Myoblasts withdraw from the cell cycle and fuse to form primary myotubes. Further myoblast fusion is termed secondary myogenesis*

Over the course of this process, structural proteins and enzymes are synthesised and assembled into structural components or secreted to contribute to the specialised extracellular matrix surrounding muscle.

Secondary myotubes grow as a result of cell fusion and eventually separate and mature into adult skeletal muscle fibre. They are multinucleated and cylindrical in shape. A single myofibre contains bundles of myofibrils, which are divided into a serially arranged contractile apparatus called sarcomers. Each myofibre is surrounded by a plasma membrane called sarcolemma (Figure 1.2).

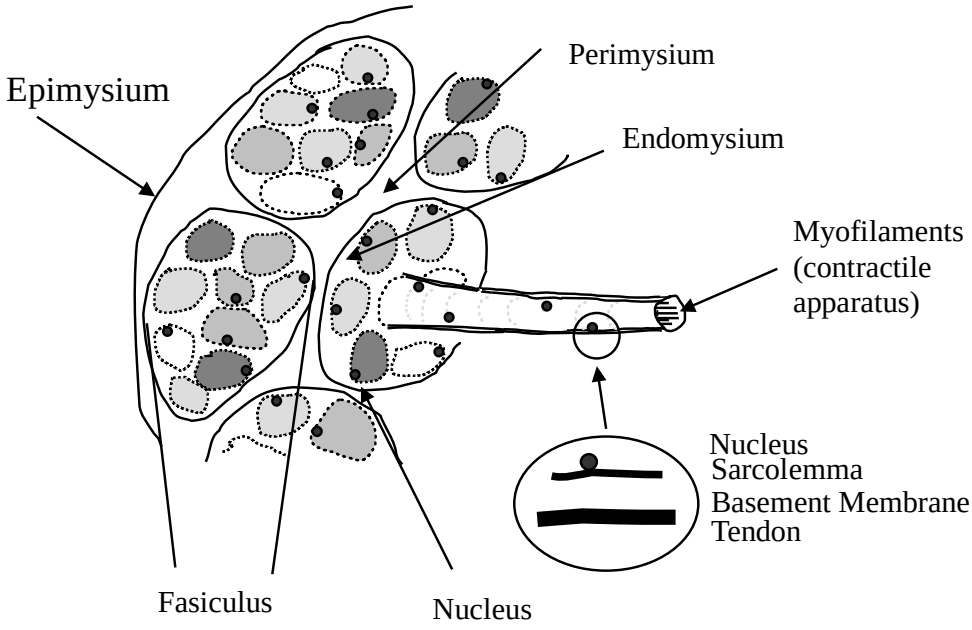

Figure 1.2: Adult skeletal muscle structure. *The myofilament proteins constituting the contractile apparatus are found within each individual myofibril. Myofibrils are bundled within the muscle fibre and encased by the sarcolemma (the muscle fibre plasma membrane) and a specialised extracellular matrix (ECM), the basement membrane, to form muscle fibres. The nuclei of each fibre lie just under the surface of the sarcolemma. Between muscle fibres is an interstital connective tissue termed the endomysium. A bundle of muscle fibres termed the fasiculus, is encased by the perimysium and forms the muscle unit. (Taken from Rogers and Mayer, 2006)*

Myofibres are attached to the sarcolemma at Z-disks by focal adhesion points called costameres. The muscle fibre is linked to the skeleton via the fibrous connective tissue called tendon. The site where the tendon meets the muscle fibre is called myotendinious junction (MTJ). At the MTJ the sarcolemma forms digit-like extensions into the tendon to increase the surface area of the MTJ and thus transferring tension into shear stress.

Myofibres are further classified into fibre types, oxidative/slow (type I) and glycolytic/fast (type II) fibres, depending upon their morphology, metabolic and physiological properties. Glycolytic fibres are further divided in the mouse, into subtypes IIa, IIb and IId. Each fibre type differs in the expression of the myosin heavy chain, structure and biochemistry (Payne et al., 1975; Moss et al., 1991). Adult skeletal

muscle has its own population of stem cells called satellite cells found between the muscle fibre sarcolemma and the basement membrane (Bishoff, 1994). They mediate repair of the adult muscle, being mitotically quiescent they are activated to re-enter the cell cycle in response to stress, induced for example by injury (Grounds, 1991) or diseases such as muscular dystrophies (Webster and Blau, 1990).

The main function of muscle fibres is to contract and as a result produce body movement. The contractile unit of the muscle is termed the sarcomere and is defined as the unit between two Z-lines (Figure 1.3).

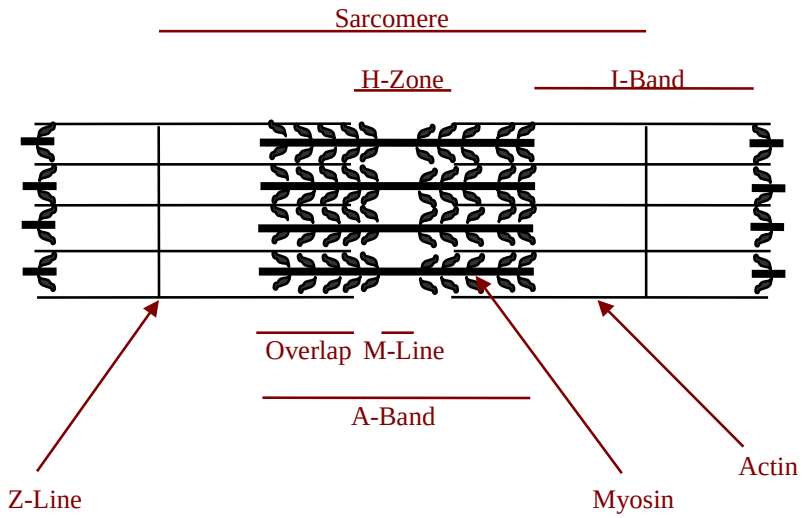

Figure 1.3: The contractile unit of muscle. Muscle fibres are striated due to the structure of the contractile unit. *The alignment of actin and myosin gives skeletal muscle its characteristic striations. Myosin fibres are thick and constitute the dark A-band, in the centre of which is the lighter H-Zone. Adjacent to the A-band is the lighter I-Band, this also contains the darker Z-line. The portion between two Z-lines is a single contractile unit, termed the sarcomere. Stimulation by a nerve impulse causes the globular head of myosin to bind actin. Once bound, ATP consumption results in movement of this head region, which pulls the actin into the centre of the sarcomere. The myosin head then releases the actin filament and the cycle is repeated. The sliding of myofilament components over each other via the consumption of ATP reduces muscle length by 70%. (Taken from Rogers and Mayer, 2005)*

Skeletal muscle function integrity and the transmission of chemical and mechanical signals are maintained by the interaction of the muscle cell with the surrounding extracellular matrix. As muscle cell contraction generates the force required for movement, muscle cell attachment to its surrounding matrix at the sites of force transmission is vital. In addition to the importance of force transmission,

interaction of muscle fibres with their surrounding matrix is also significant in the regulation of cell survival, proliferation and differentiation (Hynes, 2002). The correct attachment to a normal basement membrane is therefore as important to muscle fibre function as the integrity of the muscle fibre itself (Figure 1.4).

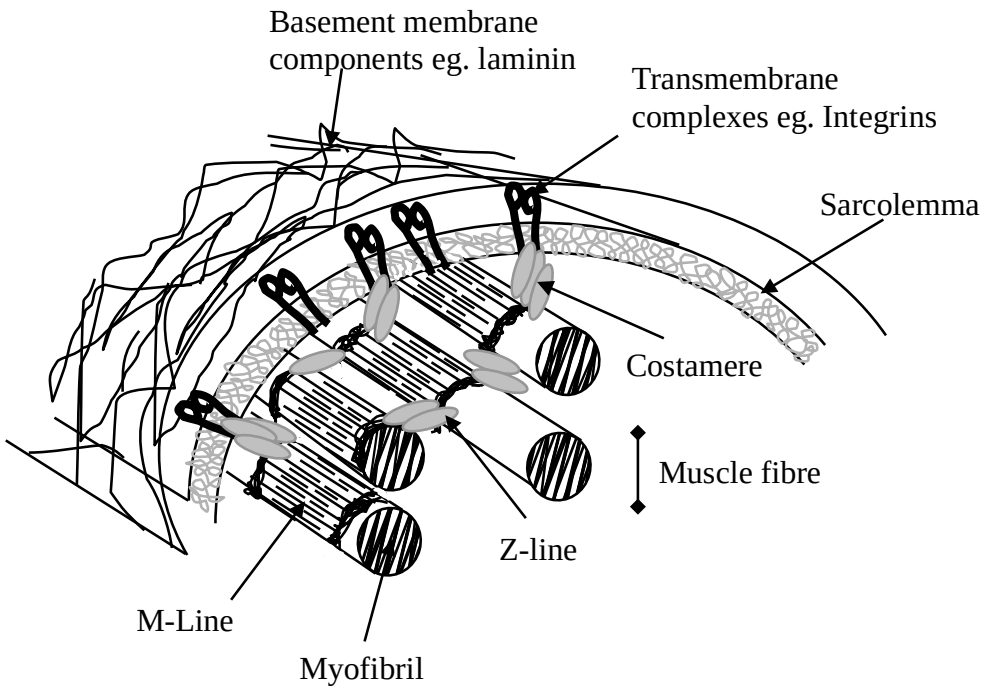

Figure 1.4: Anchorage of the contractile apparatus in adult skeletal muscle. *Contraction of muscle results when the myosin and actin filaments of the myofilaments slide over each other. The Z-line is the point at which the actin filaments are anchored. Myosin also has a base plate to which it is anchored, termed the M-line. The Z-line and to a lesser extent the M-line are the points at which the contractile unit attaches to the sarcolemma and therefore the basement membrane. These linkage points are termed the costameres (Pardo, Siliciano and Craig, 1983) and are rich in proteins such as vinculin, α-actinin, talin and the transmembrane adhesion receptors, the integrins. (Taken from Rogers and Mayer, 2006).*

Cell-matrix contact is predominantly maintained through the interaction of muscle cell transmembrane receptors and cell adhesive proteins found in the basement membranes.

1.3 Basement membrane

Basement membranes (BM) are a highly specialised element of extracellular matrix structure, which surrounds the skeletal muscle fibre and play an important role in muscle fibre regeneration. It was first described in 1840 by the histologist and surgeon Sir William Bowman (Bowman, 1940). In his publication Bowman described what is known as a BM to be highly delicate, transparent and elastic sheath encircling individual muscle fibres. Analysis at the level of electron microscopy revealed that the basement membrane is made up of two layers. The first being a sheet-like structure directly linked to the sarcolemma, called basal lamina (Figure 1.5) and the second an underlying fibrillar reticular lamina. The basal lamina consists of members of the laminin family, members of the type IV collagen family, the heparan sulphate proteoglycan perlecan, nidogen and additional molecules such as growth factors and agrin (Timple and Brown, 1996).

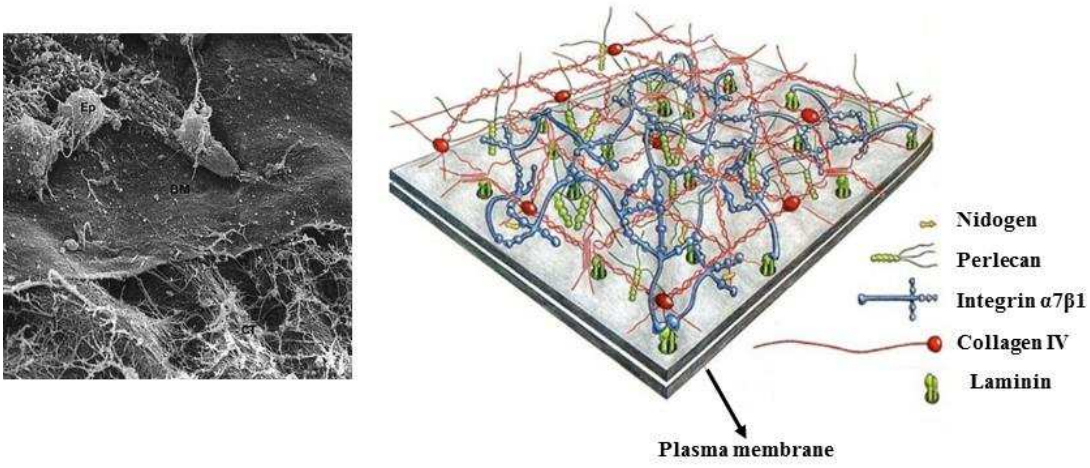

Figure 1.5: The basal lamina*- A) Scanning electron micrograph of the basal lamina taken from the cornea of the chick embryo, where the epithelial cells have been removed to reveal the sheet-like structure. B) The networks of collagen type IV and laminin connected through nidogen and perlecan. Integrin α7β1 and DGC (not shown in here) connect the basal lamina to the plasma membrane in skeletal muscle. (Adapted from Alberts, 2002).*

Within the ECM protein family, laminin has been shown to have a significant effect on cell behaviour. Laminin induces changes in myoblast cell shape, enhances migration and stimulate proliferation (Ocalan et al., 1988; Timpl and Brown 1996). Laminin is a trimer, composed of α, β and γ chains. Laminins-2, -4, -8, -9, -10 and -11,

containing the α2, α4 and α5 chains, respectively, are those predominant in skeletal muscle basement membranes during development. In the adult, laminin α4 and α5 chains become confined to the neuromuscular junction (NMJ) and blood vessels, while the α2 chain containing laminins (laminins-211 and -221) become the predominant forms (reviewed in Gullberg et al., 1999; Sanes, 2003).

Basement membranes are important for cell polarisation in the embryo and adult, for cell migration during development and for cell migration and adhesion in wound healing (Yurchenco et al., 1993). The change in expression pattern of basement membrane components reflects the degree of specialisation of the muscle ECM to muscle cell development and function. For example, terminal differentiation is characterised in part by a switch from a fibronectin-rich ECM to a laminin-rich basement membrane (Kuhl et al., 1986).

Fibronectin has pronounced effects on cell behaviour. It is implicated in many processes in the developing embryo such as gastrulation, migration of neural crest cells and germ cells, somitogenesis and the development of the heart and vasculature. Its importance is reflected by the embryonic lethality of functional null mutant mice. These mice have mesodermal defects and fail to develop notochords or somites (Georges-Labouesse et al., 1996). Fibronectin is first present at the blastocyst stage of development in mouse embryos and is abundant at sites of active cell migration (Hynes and Yamada, 1982). Within the adult, fibronectin is involved in processes such as wound healing and pathological processes such as thrombosis, fibrosis and neoplastic transformation (George et al., 1993). In muscle, fibronectin is down regulated in the basement membrane surrounding newly formed muscle fibres at terminal differentiation, though its expression remains in the endomysium between them.

The effects of various BM components on cell functions are mediated via cell surface receptors, like integrins and dystroglycan (Erickson and Couchman, 2000).

1.4 Transmembrane receptors:

Transmembrane receptors are necessary to induce migration, differentiation and fusion of myogenic cells as well as provide important cellular interactions between the actin cytoskeleton and the extracellular matrix in adult skeletal muscle. The two major transmembrane receptors expressed in skeletal muscle, which link laminin of the basement membrane to the actin cytoskeleton are the Dystrophin-Glycoprotein-Complex (DGC) and integrin α7β1.

1.4.1 Dystrophin-Glycoprotein-Complex (DGC):

The DGC is a multi-functional protein complex made up of membrane associated proteins and plays an important role in maintaining the integrity of the skeletal muscle fibre. This multi-subunit protein complex is comprised of structurally organised 3 distinct sub-complexes namely, the intracellular proteins, dystrophin, syntrophins, the sarcolemmal localised β-dystroglycan, sarcoglycans (α, β, γ and δ), sarcospan and the extracellular α-dystroglycan. Dystroglycan is a ubiquitously expressed large glycoprotein, which is distributed at the cell surface. It is a product of a single gene and the protein is further processed into two non- covalently linked sub-units called α -and β- dystroglycan. α- dystroglycan acts as a receptor for ECM components on the extacellular side, whereas β-dystroglycan is inserted into the plasma membrane where it binds to dystrophin inside the cell. Early studies demonstrate that dystroglycan plays an important role in BM formation of embryoid body; thus mice deficient for dystroglycan die early in development prior to gastrulation (Williamson et al., 1997).

Dystrophin binds to the actin cytoskeleton with its N-terminal end and with its C-terminal end to β-dystroglycan, which then links to the extracellular matrix by α-dystroglycan and laminin interaction (Durbeej and Campbell, 2002) thereby providing a link between the extracellular matrix and the actin cytoskeleton (Figure 1.6).

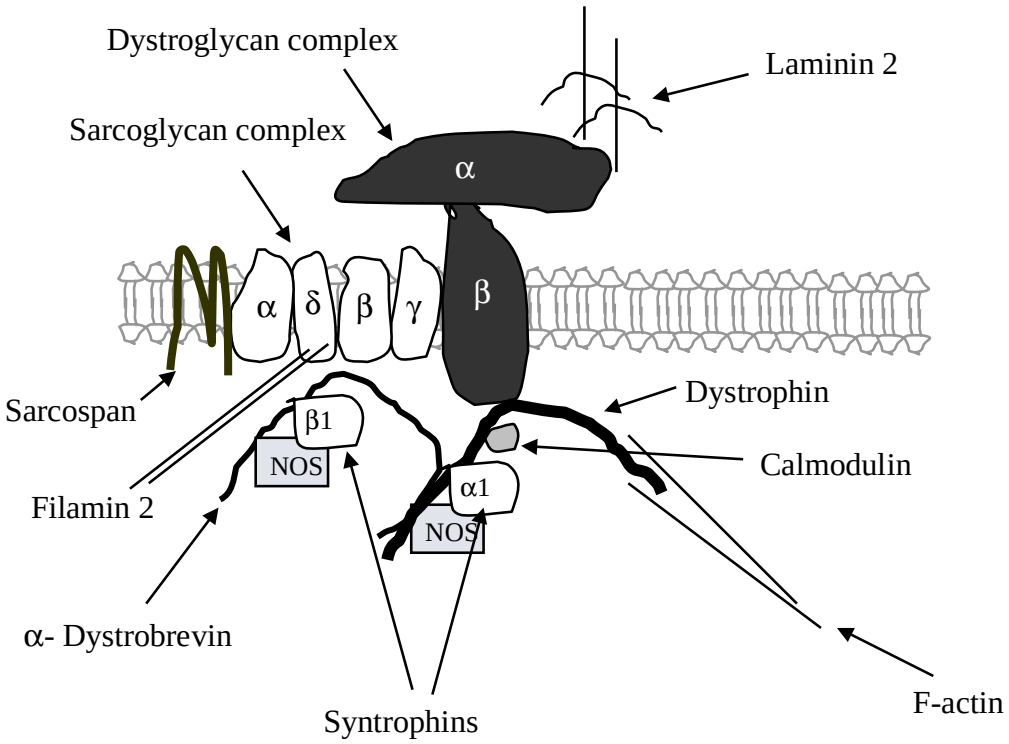

Figure1.6: The Dystrophin-Associated Protein Complex (DAPC). *This simplified cartoon represents the major components of the DGC, the extracellular laminin 211 ligand and intracellular binding partners. The DGC is made up of two subunits α and β. α-DG is located on the extracellular side of the membrane, where it binds to laminin-211 and the transmembrane -bound, β-DG. B-DG then binds intracellularly to dystrophin, linking DG to γ-actin. Associated with DG is the sarcoglycan complex, which is composed of multiple subunits. Other components include sarcospan, dystrobrevin, syntrophin, n-NOS and calmodulin.*

The DGC is critical in maintaining skeletal muscle. Mutations in the genes encoding components of DGC and the laminin α2 chain cause a class of hereditary myopathies, known as muscular dystrophy, characterised by muscle degeneration and regeneration, which is typically progressive and manifests in different severities depending upon the gene mutation.

1.4.2 Integrins:

Integrins constitute a large family of glycosylated heterodimeric transmembrane adhesion receptors mediating cell-cell, cell-matrix and cell-pathogen interactions. The name "integrin" comes from the "integrating" nature of these adhesions (Tamkun et al., 1986) as they integrate the cell's exterior (ECM) to the cell's interior (cytoskeleton). All integrins are αβ heterodimers. There are 8 known β subunits and 18 known α subunits that can associate to form 24 different integrins (Gullberg, and Lundgren-Akerlund, 2002). The β1 subunit is associated with at least 12 different α subunits to form the largest sub family of integrin (figure 1.7). The complexity is increased by the existence of several isoforms with alternatively spliced cytoplasmic domains (Altruda et al., 1990).

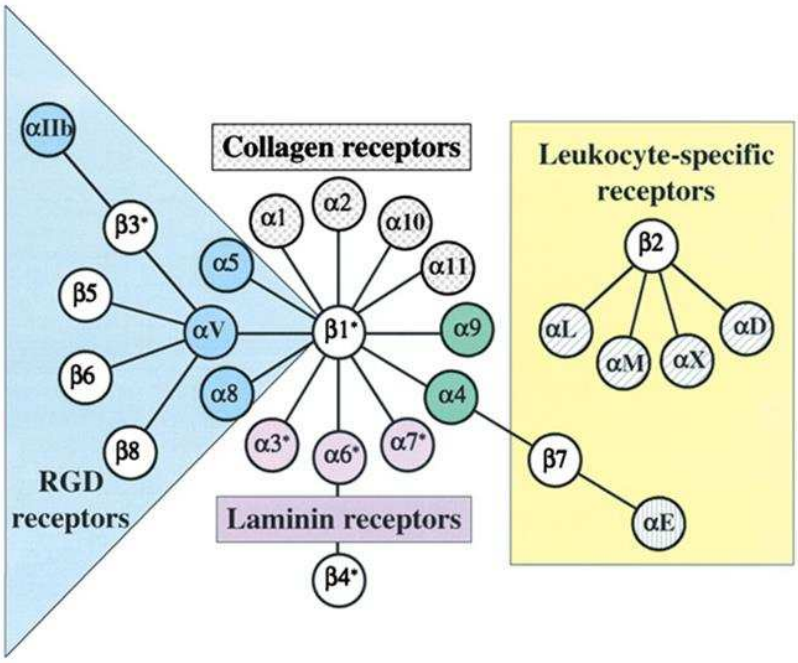

Figure 1.7: The integrin family. *Integrins consist of two subunits α and β. Together they form a heterodimer. 24 heterodimers are known to exist in vertebrates. Each heterodimer interacts with specific ligand. (Taken from Hynes, 2002)*

There are two intracellular splice variants known for the integrin β1 subunits in the mouse, namely β1A and β1D. They are also the most abundant form of β1 integrins in human (Baudoin et al., 1998). The β1A variant is ubiquitously present, while the β1D is restricted to skeletal and cardiac muscle (van der Flier et al., 1995; Zhidkova et al., 1995). The β1A subunit is expressed during primary myogenesis; it is then replaced by β1D during secondary myogenesis (Brancaccio et al., 1998).

1.4.2. 1 Integrin structure: the extracellular domains

The integrin α and β subunits show no homology to each other. The α subunits are 130-180 kD in size and β subunits are approximately 90 kD. Both subunits are in contact with each other via their N-terminal domains, which form globular head. This is the region at which the subunits interact with each other and with their ligands (Nermut, et al., 1988; Weisel et al., 1992) (Figure 1.8).

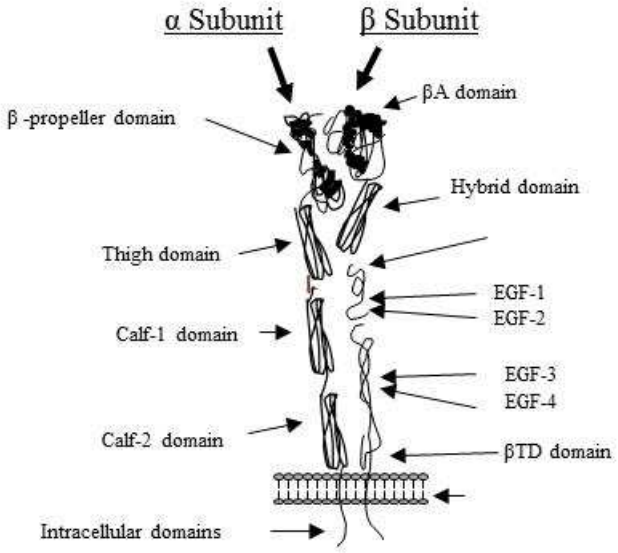

Figure 1.8: A Schematic and simplified portrayal of integrin α and β subunit domain structures. *Domains of the α subunit include, the β-propeller, three β-sandwich domains that make a 'thigh' domain and two similar domains forming the 'calf' module (Xiong et al., 2001). Within the β subunit there is a PSI domain, so termed because it is present in plexins, semaphorins and integrins (Bork et al., 1999), four epidermal growth factor domains and a β-tail domain.*

The globular head domain of the integrin is a region at which the subunits interact with each other and with their ligands (reviewed in Humphries, 2000). Ligand binding is complicated and requires an understanding of subunit structure. Ligand binding of integrins requires the presence of divalent cations. The way in which the α subunits contribute to the co-ordination of the cations divides them into two groups. This classification depends on the presence of an I-domain (Inserted domain) (Lee et al., 1995; Michishita and Arnaout, 1993)

The α subunits are structurally divided into two different groups, those with and those without an inserted "I'' domain (Lee et al., 1995). The domain is also referred to as the A-domain as it is homologous to the van Willebrand factor A domain (Arnaout et al., 1988; Corbi et al., 1987; Larson et al., 1989). A similar domain constitutes the globular head in the β subunit. The globular head of both types of α subunits is made up of seven repeated structures, which fold to form a seven-bladed β-propeller (Springer, 1997; Xiong et al., 2001), which is connected to a thigh and the calf-1 and calf-2 domains. Some of the β-propeller repeats assembles EF-hand like Ca^{2+} binding sites (Leitinger et al., 2000) (repeats 4-7 in non I domain α chains and repeats 5-7 in I domain α chains). A typical EF-hand repeat contains 12 amino acid residues, with oxygen containing residues at positions 1, 3, 5, 9 and 12 and these provide coordination sites for divalent cations (Strynadka and James, 1989). However, the EF-hand-like repeats in all integrin α subunits lack the coordination site at position 12, but still appear to be able to coordinate a cation (Gulino et al., 1992; D'Souza et al., 1991). The specific role of these sites has proven difficult to study as their mutation often leads to a lack of cell surface expression (Wilcox et al., 1995; Masumotp and Hemler, 1993). However, it has been shown that coordination at these sites may not be involved in the ability to bind ligand, but rather in the regulation of cell adhesion in a ligand binding-independent manner (Pujades et al., 1997). The Ca^{2+} binding to these sites allosterically affects the ligand binding (Humphries et al., 2003; Oxving and Springer, 1998). Half of the 18 known integrin α subunits have an inserted I domain. The α1, α2 α10 and α11 subunits associate with β1 subunit and form ECM-binding integrin. The αD, αM, αL, αX (β2 associated) and αE (β7 associated) mediate cell binding in cells of the immune system. The crystal structure of I domain from αM, αL, α1 and α2 revealed that the central β-sheet is surrounded by seven α-helices to form a Rossman fold (Emsley et al., 1997; Lee et al., 1995; Nolte et al., 1999; Qu and Leahy, 1995; Rich et al., 1999).

The extracellular domain of the β-subunit consists of an I domain (βI- domain) linked by a hybrid domain to the stalk region. The N-terminal also forms a separate domain called plexin-sempahorin-integrin (PSI) domain, which folds back from the βI domain to hybrid domain (Bork et al., 1999). The βI domain is involved in ligand binding. It consists of an Mg^{2+} coordinating MIDAS and a site adjacent to MIDAS (ADMIDAS) binding and inhibitory Ca^{2+} ion. βI domain is also involved in the folding of α-chain β-propeller. βI domain is responsible for the conformational changes by binding to the Mn2+ ion (Humphries et al., 2003). The β-chain cytoplasmic tail is longer than that of the α chain and is involved in the anchorage to cytoskeleton. The α subunits lacking an A domain lack the MIDAS, so an alternative method of metal ion co-ordination must be achieved. This is via the β-propeller domain and an I-like domain found in the β integrin subunit, as exemplified by the αVβ3 integrin crystal structure (Xiong et al., 2001). It seems that aromatic residues within the β-propeller of the αV interact with the β subunit to form an interface for cation co-ordination and therefore ligand binding (Xiong et al., 2001).

The two different groups of integrin α subunit (I-domain containing or not) also differ in that those not containing an I-domain (α3, α5, α6, α7, αv and αIIb) also have an endogenous proteolytic cleavage site, close to the transmembrane domain. These integrins exist as an N-terminal heavy chain and a 20-30kDa C-terminal light chain, held together by a disulfide bridge. Proteolytic cleavage is vital for the functional activation of cell surface receptors, adhesion molecules and extracellular matrix proteins (Seidah et al., 1998; Seidah and Chretien, 1997).

Limited investigation into the function of proteolytic cleavage in integrin α subunits has been carried out. Integrin α6 was expressed in the LoVo cell line, which expresses a mutated, non-functional form of the proteolytic cleavage enzyme Furin (Lehmann et al., 1996). The un-cleavable α6 integrin was able to associate with the β subunit and the attachment of these cells to laminin-1 was indistinguishable to cell lines expressing the cleaved form of integrin α6.

Similarly, mutation of the cleavage site of integrin αIIbβ3 did not affect cell surface expression or adhesion on fibrinogen (Kolodziej et al., 1991). In fact, the role of integrin α subunit cleavage has as yet, remained elusive. It has however been shown that disruption to the cleavage site of integrin α6 affected its inside-out signalling in

terms of affinity modulation by phorbol 12-myristate 13-acetate (Diamond and Springer 1994).

Integrins are major carriers of *N*-glycans and it is well known that cell surface carbohydrates contribute greatly to the interaction between a cell and its extracellular environment. This includes processes such as cell-cell communication, cell signalling, protein folding and stability. Both the α and β subunits of integrins are glycosylated. The α5β1 integrin is one of the best characterised integrins, it has been shown that *N*-glycans are a requirement for αβ dimerisation, proper integrin-matrix associations and probably lateral association of integrins with membrane associated proteins and glycolipids (Gu and Taniguchi 2004; Bellis 2004; Zheng and Hakomori 1994). Abnormal changes to N-glycosylation of integrins can modulate biological functions such as cell spreading and migration, which makes them of particular importance in disease, processes such as cancer (Dennis et al., 2002; Jasiulionis et al., 1996; Miyoshi et al., 1999).

The ligands that β1 integrins interact with are mostly components of the ECM and counter receptors on other cells. Integrins interact with defined recognition sites within their ligands. The first to be elucidated was Arg-Gly-Asp (RGD), present in fibronectin and vitronectin and recognised by α5β1, αIIbβ3 and αVβ3 integrins (Charo et al., 1990; D'Souza et al., 1988). RGD-reactive integrins are quite closely related and all contain α subunits that are without an I-domain and which are proteolytically cleaved. Within the group of laminin-recognising integrins two groups seem to have independently evolved. One recognises the E8 fragment containing the long arm of laminin (Gehlson et al., 1989) and is recognised by proteolytically processed α subunits, α3β1, α6β1 and α7β1. The other group recognises part of the short arm of the α chain in laminins, they have uncleaved α subunits with I domains and include α1β1 and α2β1 (Hall et al., 1990).

1.4.2.2 Integrin: intracellular domains

Ligand binding conveys a signal to the cell interior through the membrane spanning region and cytoplasmic portion of each chain within the dimer. Cytoplasmic tails are short in length and there is high sequence similarity between the different α and β cytoplasmic tails. The conveyance of an integrin-mediated signal involves the coordination of components of the cell cytoskeleton or associated signal transduction

molecules. The main difference between integrins and other adhesion receptors is their ability to regulate their signalling from the inside and the outside. Integrin modulation from within allows the cell to have some control over the ECM that surrounds it. The interaction of intracellular proteins with the cytoplasmic domains of the integrin dimer can regulate integrin function (Liu, Calderwood and Ginsburg, 2000). This could be by 'activating' them to increase their affinity for ligand (Schwartz, Schaller and Ginsberg, 1995). The interaction of the α and β cytoplasmic domains can also alter the affinity of the receptor (Lu, Takagi and Springer, 2001). It has been suggested that the receptors may be kept in a default low-affinity state, which may help to protect cells from opportunistic pathogens able to utilise the receptors (Hauck, 2002). It was suggested that the activation state of the integrin αVβ3 may be controlled by its extracellular conformation that a 'bent' inactive state may exist, where the globular head folds over to lie close to the cell membrane (Xiong et al., 2001; Beglova et al., 2002).

Ligand binding to integrins is associated with the clustering of integrins and the recruitment of actin filaments and signalling proteins (Hynes, 2002). The specialised complexes formed at the membrane are termed focal adhesions. The structures are dynamic and can dissociate and reform at different sites and this phenomenon is involved in processes such as wound healing and cell migration (Grose et al., 2002; Ballestrem et al., 2001). This provides an affinity independent mechanism of regulation through changes to integrin clustering and the diffusion rate of integrins within the membrane (Kim et al., 2004).

The correct localisation of integrins also requires a connection to the actin cytoskeleton via the integrin β1 cytoplasmic domain. This connection can be a direct or in-direct association of intermediary proteins including vinculin, talin, α-actinin, tensin and paxillin (reviewed in Brakebusch and Fassler, 2003). Mutations to the cytoplasmic domain of integrin β1, prevent the localisation of the heterodimer to focal adhesions, cause reduced ligand binding and impaired activation of downstream signalling molecules (Marcantonio et al., 1990; Hayashi et al., 1990; Solowska et al., 1989).

As integrin cytoplasmic domains have no detectable enzymatic activity, as well as providing an achor to the actin cytoskeleton, proteins binding the integrin β tails also regulate the bi-directional signalling mediated by integrins.

1.4.3: Bidirectional signalling of integrins

Integrins are bidirectional signalling molecule. Extracellular stimuli can induce intracellular signalling cascades (outside-in signalling) and intracellular stimuli can regulate extracellular changes (inside-out signalling). These will be discussed in detail below.

1.4.3 I Inside-out signalling

Integrins are expressed on the cell membrane in both inactive and active conformations. The active conformation of integrins is controlled by pathways that act on the interactions between the cytoplasmic tails of the α and β subunits (Constantin et al., 2000; Dustin and Springer, 1989; Lollo et al., 1993). In the absence of intracellular stimuli the cytoplasmic tails of the α and β subunits are bound together constraining the integrin in an inactive conformation. In this low affinity state the integrin assumes a bent conformation (Figure 1.9A) (Takagi et al., 2002). Binding of talin to the cytoplasmic tail of the β subunit leads to the separation of the α and β cytoplasmic tails (Tadokoro et al., 2003). This causes a separation of the transmembrane domains and the membrane proximal extracellular domain. This conformational change destabilises the interface between the headpiece and the tailpiece of integrins inducing a switch-blade like opening of the integrin into an extended, active conformation (Figure 1.9B) (Takagi et al., 2002). In the extended conformation integrins have a high- affinity towards their extracellular matrix ligands (Takagi et al., 2002). Active ligand-bound integrins then cluster on the cell membrane and, together with various cytoplasmic adaptor proteins, form complexes known as focal adhesions. Following the formation of focal adhesions, integrins modulate a vast array of intracellular changes.

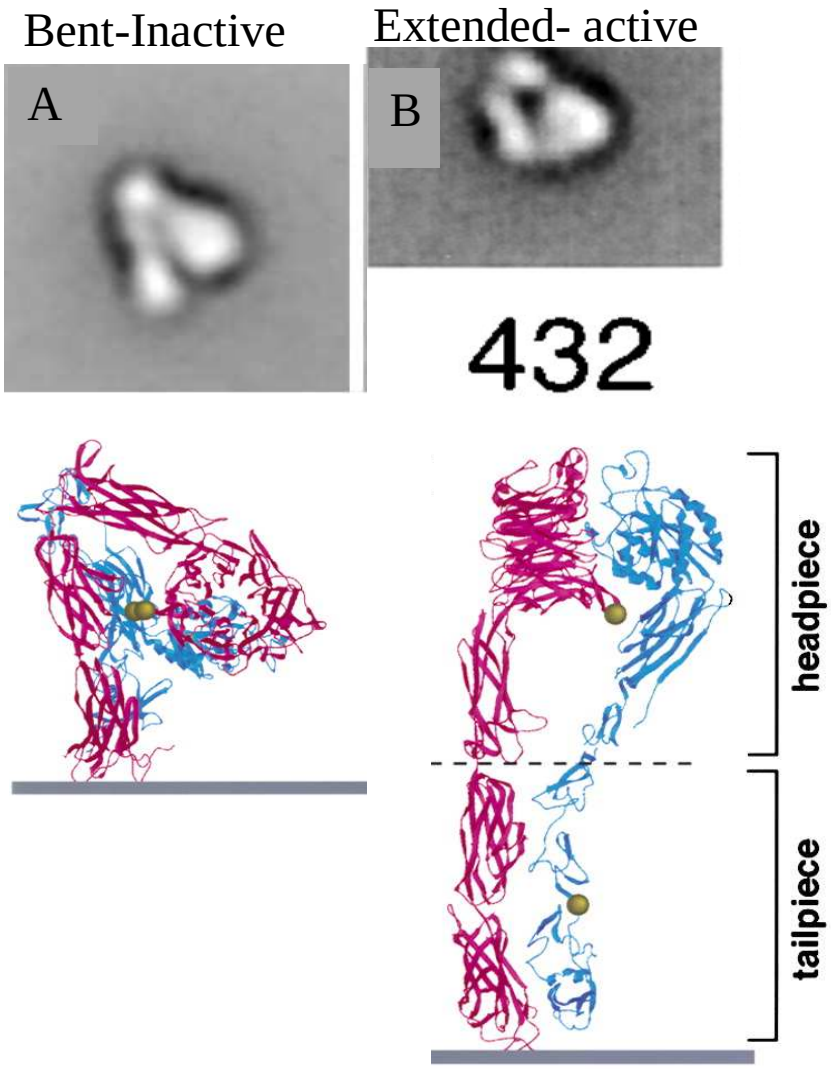

Figure 1.9: Inactive and extended integrin conformations. *Electron micrographs and ribbon diagrams of (A) bent/inactive and (B) extended/ active integrin conformations. Bending occurs at the junction between the tailpiece and the headpiece in the extracellular domains, corresponding to* α *position between the thigh and calf-1 domain of the a subunit and between I-EGF domains 1 and 2 in the* β *subunit (Modified from Takagi et al., 2002).*

1.4.3.II Outside-in signalling:

Approximately 150 different molecules have been shown to interact with integrins at focal adhesions, including growth factor receptors, kinases phosphatases, G protein regulators, proteases, actin modulators and multiple adaptor proteins (Zamir and Geiger, 2001). Integrin-mediated signalling is therefore a complex event, which is required to modulate a diverse array of cellular behaviours such as cell proliferation, cell survival, cell shape, cell polarity, cell migration, gene expression and differentiation. It is well established that signalling pathways rely on a cascade of phosphorylation events, however integrins do not contain any intrinsic kinase activity and therefore depend on kinases associated with their cytoplasmic tails. The two main kinases, which associate with the cytoplasmic tail of the β subunit and elicit downstream signalling effects are focal adhesion kinase (FAK) and integrin linked kinase (ILK). The importance of FAK and ILK has been established. Both are critical for development and their absence leads to embryonic lethality (IIic at al., 1995; Sakai et al., 2003). There are many additional binding proteins and downstream signalling pathways including membrane extension by the integrin-mediated dissociation of GTP-bound Rho-GTPases (Del Pozo et al., 2002) or the activation of Src-like kinases involved in pathways regulating microtubular re-organisation (Etienne-Manneville and Hall, 2001). Mitogenic signalling proteins can also be recruited including growth factor receptors (Miyamoto et al., 1996; Plopper et al., 1995), mitogen-activated protein kinase (MAPK), lipid second messengers and protein phosphatases (Miyaamoto et al 1995).

Most integrin heterodimers are expressed on a wide variety of cell types and most cells express several integrins. The wide variety of integrins and their ligands mean a cell can modulate its adhesiveness by changing the pattern of integrin expression. In addition, cells can even modulate the binding properties of the specific integrins they express (Elices and Hemler, 1989; Kirchhofer et al., 1990; Staatz et al., 1989).

1.5 Integrins during skeletal muscle development

Within adult mammalian skeletal muscle, members of the β1 family of integrins are expressed at areas important to muscle function. These include the costameres, neuromuscular junction (NMJ) (where the nerve meets the myofibre), the MTJ and the sarcolemma. Though their expression patterns at each of these sites vary depending on the stage of development. As described previously, myogenesis involves the migration of myoblasts to areas of muscle formation followed by their differentiation into adult muscle fibres. Regulation of this is controlled by cytokines, cell adhesion receptors and ECM components.

During and following the development of skeletal muscle the expression pattern of integrin subunits and their splice variants are tightly regulated (Figure 1.10). The predominant integrin subunits expressed in skeletal muscle are α4, α5, α6, α7, αv and β1. The integrin subunit α7 is alternatively spliced in both the cytoplasmic (α7A and α7B) and the extracellular (α7X1 and α7X2) domains (Collo et al., 1993; Song et al., 1993; Zober et al., 1993). Splicing of integrin β1 gives rise to two variants expressed in muscle β1A and β1D (van der Flier et al., 1995). The β1 integrins have been shown to be important at the specific step of plasma membrane breakdown and subsequent to this, in the assembly of the muscle fibre cytoskeleton (Schwander et al., 2003). By the time secondary myotubes have formed the integrin β1D cytoplasmic splice variant has replaced integrin β1A. Integrin β1A staining has disappeared from the sarcolemma of adult muscle fibres (Belkin et al., 1996). The β1D variant is specifically restricted to skeletal and cardiac muscle (van der Flier et al., 1995; Zhidkova, Belkin and Mayne, 1995) where it is enriched at sites of force transmission (Belkin et al., 1996; van der Flier et al., 1995). It is thought to provide a stronger connection at this site than the integrin β1A variant, and this has been exemplified *in vitro* by the improved cytoskeleton-ECM connection of non-muscle cells transfected with integrin β1D (Belkin et al., 1997).

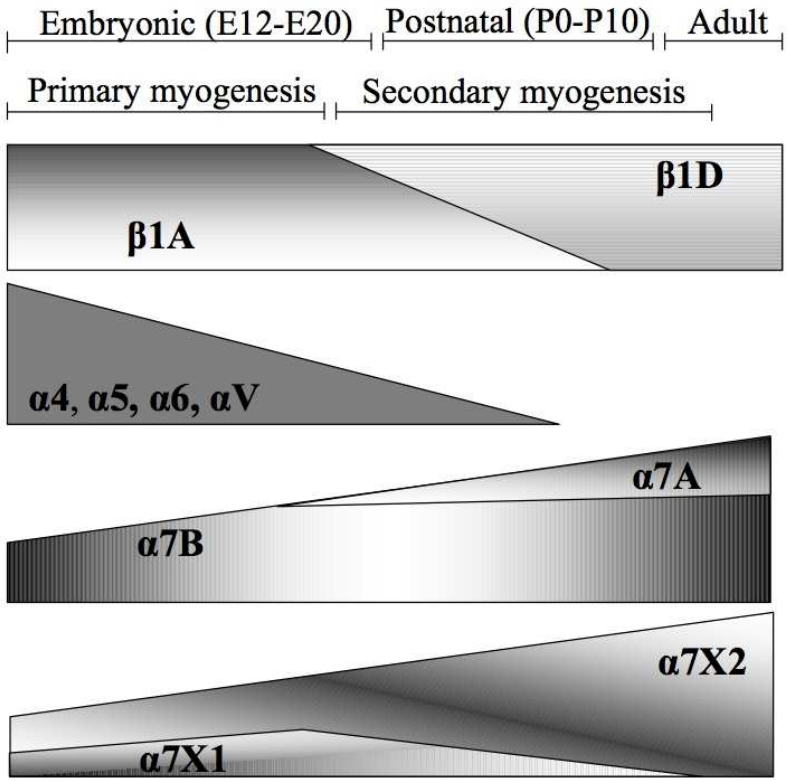

Figure 1.10: Integrin and extracellular matrix protein expression during myogenesis*. During primary myogenesis the integrin β1 splice variants β1A is predomintantly expressed while during the secondary myogenesis it was replaced by integrin β1D and remains predominantly expressed in adult skeletal muscle. Integrins α4, α5, α6 and αv are mainly expressed during primary myogenesis. Integrin α7 is expressed during primary myogenesis and is up-regulated at the onset of secondary myogenesis. The α7B variant is expressed both during primary and secondary myogenesis whereas α7A expression is induced at secondary myogenesis. The extracellular variant X1 and X2 are expressed during primary myogenesis. In the secondary myogenesis the expression of α7X1 decreases and is no longer seen in the adult. (From Rogers and Mayer, 2006)*

Despite the specific enrichment of integrin β1D at the myotendinous junction, the muscle specific knockout of integrin β1D, and replacement with integrin β1A showed no defect at this site, only a mild cardiac phenotype was seen. Yet, the two integrin β1 variants are clearly not functionally equivalent as the ubiquitous expression of integrin β1D resulted in embryonic lethality (Baudoin et al., 1998).

Crossing the integrin β1D knock-in mouse into a less penetrant genetic background attenuated the embryonic lethality and revealed low muscle mass at birth caused by impaired primary myogensis. Integrin β1D has subsequently been shown to

interfere with cell migration and proliferation, and this is in line with its onset of expression and the effect seen in the knock-in mouse model (Belkin and Retta, 1998; Gimond, Baudoin and Sonnenberg, 2000).

From the time of terminal differentiation and on into adult skeletal muscle, the level of α5 and α6 integrins has dropped significantly (Blaschuk and Holland, 1994; Boettiger et al., 1995; Bronner-Frase et al., 1992). The integrin α7 is restricted to skeletal and cardiac muscle and is strongly up regulated from terminal differentiation onwards (Song et al 1993; Yao et al., 1996). The α7β1D integrin is the only integrin expressed at the sarcolemma and MTJ, but at the NMJs the α7; α3 and αV integrin subunits are expressed (Figure 1.11)

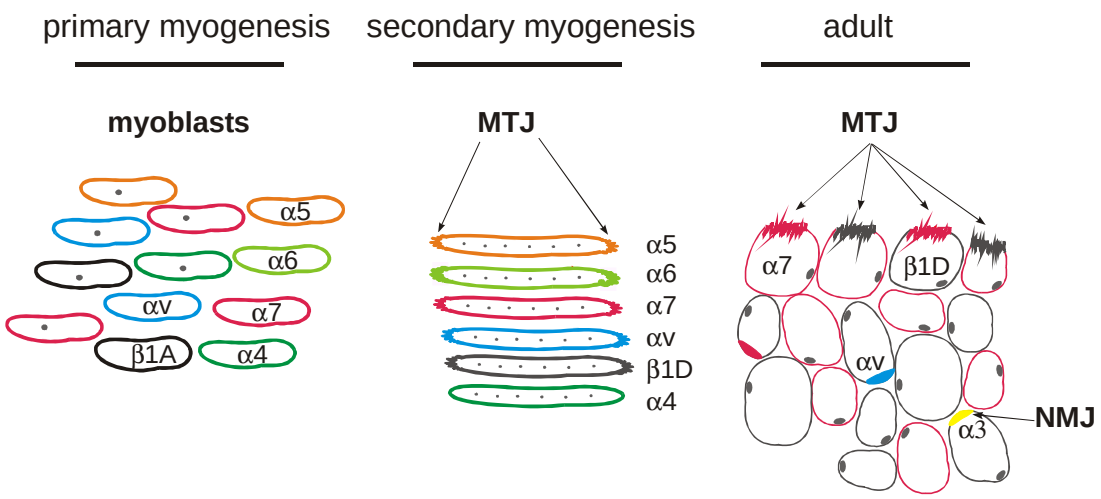

Figure 1.11: Schematic representation of integrin location during muscle development. *During the primary myogenesis integrins α4, α5, α6, α7, αv and are expressed β1A are present in the myoblast, which are then retained at the MTJ during the secondary myogenesis. However, in the adult skeletal muscle only integrin α7β1D is predominatly expressed at MTJ as well as at sarcolemmaof the muscle fibre. Integrin αv and α3 expression can be seen at NMJ along with expression of integrin α7 (Taken from Mayer, 2003)*

The changes in integrin expression occurring at the transition into adult muscle described above are numerous. It is therefore not surprising that the expression of their ligands also changes at this time. As described earlier, there is a switch from a fibronectin- rich ECM to a laminin-rich basement membrane during myogenesis. The expression pattern of integrin therefore fits with this pattern of ligand expression,

whereby integrin α5β1 dominates when fibronectin is present in the ECM and the switch to the laminin-rich basement membrane coincides with the increase of integrin α7β1.

It is unknown whether the changes to integrin expression cause the switch in ligand or vice versa, but it does however appear that the two are linked. Mice homozygous null for the laminin β2 chain express reduced amount of α7B at the MTJ and NMJ and in patients, while mice lacking the laminin α2 chain the presence of the α7β1 receptor at MTJs, NMJs and sarcolemma is also reduced (Vachon et al., 1997; Hodges et al., 1997).

1.5.1 Integrin α7 in skeletal muscle

α7β1 integrin is the most highly expressed integrin in adult skeletal muscle, where it localises at the sarcolemma, the NMJ and MTJ (Bao et al., 1993). This localisation implies its function in providing the terminal and peripheral cohesion that plays a role in muscle integrity, neuromuscular connectivity and force transmission. Integrin α7 is involved in many processes throughout the development of limb musculature including migration, proliferation and the connection of primary and secondary myotubes with the ECM (Yao et al., 1996; Crawley et al., 1997; Echtermeyer et al., 1996; Foster, Thompson and Kaufman 1987; Kaufman and Foster 1988) The role of integrin α7 seems more prominent in the adult as its expression is up-regulated at terminal differentiation and levels remain elevated throughout adulthood (Song et al., 1993; Yao et al., 1996).

Integrin α7β1 is functionally a diverse integrin because of the presence of different splice variants whose expression are temporally and spatially controlled. The α7 subunit has two major intracellular and two major extracellular splice variants. The intracellular variants are α7A and α7B (Figure 1.12) and they both differ in sequence, size and their phosphorylation (Collo et al., 1993).

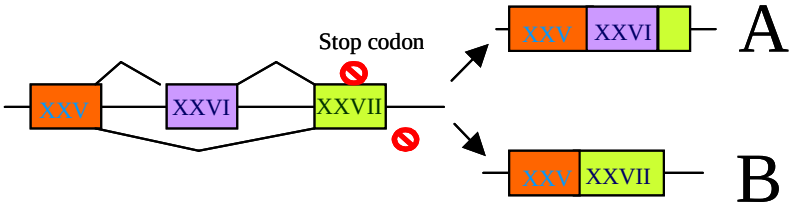

Figure 1.12: Alternative splicing of the integrin α7 intracellular domain. *The A variant is generated by splicing of exons XXV,XXVI and XXVII. The stop codon is located at base pair position 3536in exon XXVII. In the B variant exon XXV is followed by XXVII with skipping of exon XXVI, the reading frame shift now locates the stop codon to base pair position 3706 of exon XXVII.*

Integrin α7B is expressed in proliferating myoblasts and in the adult, whereas the A variant is induced specifically in skeletal muscle, upon terminal differentiation (Collo, Starr and Quaranta 1993; Ziober et al., 1997). However, the B variant remains the predominantly expressed variant. Both associate with the integrin β1D subunit in adult skeletal muscle (Belkin et al., 1996). The integrin α7B variant localises to the muscle fibre membrane and the MTJ, and staining for the integrin α7A variant is also seen at the MTJ (Hayashi et al., 1998; Velling et al., 1996; Cohn et al., 1999).

The α7B variant includes a serine/threonine protein kinase homology region, a putative actin-binding site and a receptor-like protein tyrosine phosphatase homology region (Song et al., 1993). But despite the apparent differences between the A and B variants, no functional differences have as yet been identified (Yao et al., 1996; Echtermeyer et al., 1996). A third cytoplasmic splice variant has also been identified namely the α7C variant. It is rat specific and exclusive variant to be expressed at rat sarcolemmal (Song et al., 1993).

There are two major extracellular variants described, the X1 and X2 (Figure 1.13) though other minor variants have also been described (Hodges and Kaufman 1996; Ziober et al., 1993).

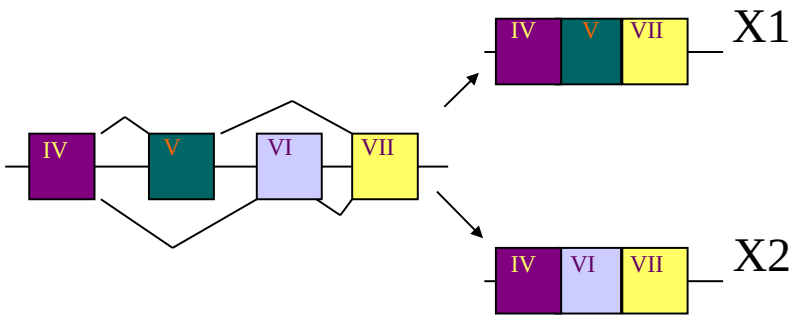

Figure 1.13: Alternative splicing within the extracellular domain. *The X1 variant contains exon IV, V and VII with exon VI skipped. The X2 variant contains exons IV, VI and VII with exon V skipped.*

In contrast to the cytoplasmic splice variants, only the α7X2 variant is found in adult skeletal muscle (Hodges and Kauffman 1996; Ziober, et al., 1993). The expression of these splice variants is also developmentally regulated (Figure 1.10). Both the α7X1 and α7X2 are expressed during primary myogenesis. In secondary myogenesis the expression of α7X1 decreases and is no longer seen in the adult.

The X1 and X2 variants are functionally distinct. The X2 variant has been shown to have a preference towards binding to laminin-111 whereas the X1 variant prefers to interact with laminin-411 (von der Mark et al., 2002) and it requires β1 activating monoclonal antibody to make X1 variant to bind laminin-111 (Ziober et al., 1997). However both X1 and X2 variants show equal affinity towards laminin-211.

Distinct functions within adult muscle fibres have been described for integrin α7 splice variants. Integrin α7 expression at the lateral surfaces of muscle fibres increases when adult muscle regenerates (Kaariainen et al., 2000). The expression of splice variants is regulated during this time so that in early regeneration the X1 and A variants are expressed whereas as the fibre is repaired the X2 and B variants again become predominant (Kaariainen et al., 2002).

Though it is seen that the α7β1 integrin plays an important and diverse role in muscle development, myogenesis occurs normally in its absence. This could be due to redundancy or overlap in function as using β1 inhibiting antibodies does disrupt the formation of myotubes in vitro (Menko and Boettiger 1987) and mice lacking β1 integrin specifically in muscle die immediately after birth having poorly developed muscle fibres (Schwander et al., 2003).

These findings highlight a fundamental difference between the α and β integrin subunit functions in the development of skeletal muscle. It appears that the α subunits are able to functionally compensate for each other or alternatively, have some redundancy in their functions. In contrast the integrin β1 subunit is vital to the development of muscle.

That is not to say that the absence of integrin α7 has no effect on skeletal muscle, as mice lacking the functional integrin α7 subunit develop a progressive muscular dystrophy (Mayer et al., 1997). Mice showed typical dystrophic symptoms in the soleus muscle such as variable muscle fibre size and centrally located nuclei. Also the MTJ where α7 integrin is normally concentrated was severely disrupted in the gastrocnemius (GC) and tibialis anterior (TA) muscles, where a high level of fibre necrosis was seen (Mayer et al., 1997). Whereas in a normal MTJ the muscle fibre folds to form interdigitations covered by a thin basement membrane, in the α7 null muscles this folding was greatly reduced and the normal sarcomere structure was disrupted.

At later stages the interdigitations of the muscle fibre were not visible at all and myofilaments had retracted from the sarcolemma. Most of these changes were specific to the α7 integrin absence as in *mdx* mice, in which dystrophin is lacking, the interdigitations remain and myofilaments do not retract from the sarcolemma. Also the basement membrane at the MTJ was doubled in thickness in integrin α7 null mice and its components were not localised normally (Miosge et al., 1999). In the wildtype controls nidogen-1, collagen type IV and the laminin α2 chain were only present in the basement membrane at the MTJs, yet in the α7 null MTJs nidogen-1 was found in the basement membrane but also in the muscle fibre cytoplasm and within the tendon. Both nidogen-1 and collagen type IV were increased as seen by immunogold labelling. The laminin α2 chain had become undetectable in the basement membrane and was found instead in the neighbouring matrix of the tendon. It seems that the integrin α7 is not a prerequisite of basement membrane assembly at the MTJ, as all the correct components were present, but that it is important to its maintenance

In Duchenne Muscular Dystrophy (DMD) patients and in *mdx* mice it was found that the expression of α7β1 integrin is up regulated (Cohn et al., 1999). In addition, the overexpression of α7β1 integrin in *mdx*/utr $^{-/-}$ double mutant mice that lack both dystrophin and its analogue utrophin leads to increased life span (Burkin et al., 2001).

This finding suggests that the integrin can physiologically compensate for the absence of the DGC and could be a potential therapeutic target for DMD.

1.5.2 Integrin α5 in skeletal muscle

α5β1 integrin goes through specific changes in distribution, activation and expression during myogenesis (Blaschuk et al., 1994). α5β1 and α6β1 are widely expressed during myogenesis and then down-regulated after myotube formation, but they are ligand opposing receptors, integrin α5 binds to fibronectin whlile integrin α6 is a laminin receptor and the reason they co-exist during myogenesis is not yet known. α5β1 has been shown to promote proliferation, while α6β1 has been shown to induce differentiation (Sastry et al., 1996).

Integrin α5β1 is a receptor for fibronectin which binds to the RGD region of fibronectin (Pytela et al., 1985). Studies carried out using various cell culture systems suggest the role of integrin α5β1 in many cellular processes. Integrin α5β1 is also important during embryonic development and its deficiency leads to embryonic lethality (Yang and Hynes, 1993). The effects seen are mesodermal, most prominently in the posterior region of the embryo, which is truncated, lacks a notochord and somites and has severely kinked neural tube. Integrin α5 knockout (KO) mice die before muscle differentiation begins; therefore the KO model does not shed any light on the role on integrin α5β1 in this process.

To study the function of integrin α5 by avoiding the embryonic lethality, chimeric mice were derived from integrin α5 -/- embryonic stem (ES) cell. Integrin α5 -/- ES cells were injected into wild type (WT) blastocysts to obtain α5 -/-, +/+ chimeric animals (Taverna et al., 1998). *In vitro,* neither α5-null ES cells nor α5-null myoblast showed any deficit in myogenesis and in chimeric mice, muscle with high proportion of α5- null cell could form (Taverna et al., 1998). This would initially suggest that integrin α5 is not required for primary or secondary myogenesis. However, further analysis of these mice revealed characteristics of muscular dystrophy with onset at late embryonic stages (Taverna et al., 1998). This could be explained by the fact that the muscle fibres are able to survive in α5-null chimeric mice by the fusion of -/- cells with WT myoblasts, which able to convey survival or anti-apoptotic signals and thus masking the absolute function of α5 integrin.

In the chimeric mice the expression of α5 integrin was shown to be greatly reduced, yet the expression of fibronectin remained unchanged in comparison with the wildtype muscles. Integrin α5 null cells assembled a fibronectin-rich matrix, formed focal contacts on fibronectin and even migrated on fibronectin-coated surfaces (Yang, Rayburn and Hynes, 1993). This implies that the assembly of the fibronectin-rich matrix, was achieved by compensation via other integrins. It has been shown that in the absence of integrin α5β1 both αVβ3 (Wennerberg et al., 1996; Wu et al., 1996) and activated integrin αIIbβ3 (Wu et al., 1995; Hughes et al., 1996) can direct fibronectin matrix assembly. Though it remains unclear as to whether such integrins would be expressed in muscle. It would therefore have been interesting to see if changes to the expression pattern of other integrin subunits were observed in muscle of the chimeric mice.

The reason for the degenerative changes observed in the muscle deficient in integrin α5 remains unclear and much more work in this field is required to fully understand the molecular defects behind it. Knocking out integrin α5 is embryonically lethal and conclusions drawn from the α5 -/- chimeric mice were limited. An ideal tool in the investigation of the role of integrin α5 during muscle development would be to generate a conditional knock out of integrin α5 where the deletion of integrin α5 is achieved by a muscle-specific promoter.

1.5.3 Association between integrins α7 and α5 during skeletal muscle development

In wildtype muscle integrins α5 and α7 are co-expressed at the MTJ up until postnatal day 5 and by postnatal day 10, α5 integrin expression is no longer seen at this site. In the absence of integrin α7 in the knock-out model, integrin β1D persists at the MTJ in the adult and is found to specifically co-localise with integrin α5 at this site. Integrin α5, was also the only α subunit to co-precipitate with the β1D integrin in the α7 deficient muscle (Nawrotzki et al., 2003).

The α5 integrin was shown to localise in place of α7 in the α7 lacking muscle. This data suggest that initial expression of both α5β1D and α7β1D integrins is followed by the down-regulation of α5β1D at the MTJ and the preservation of α7β1D. When the α7 subunit is absent in mutant muscles the down-regulation of the α5β1D integrin is not seen.

There is no transcriptional up-regulation of integrin α5 in the integrin α7 deficient muscle, in fact integrin α5 mRNA decreases by 3 weeks after birth in both

wildtype and α7-deficient muscle. The absence of integrin α7 is the cause of the integrin α5 persistence, as in MTJs of *mdx* muscles α5 integrin is not present and does not co-localise with integrin β1D (Nawrotzki et al., 2003). As the decrease in integrin α5 at the MTJs of normal muscle does not appear to be transcriptionally controlled, it is likely that the integrin α7 mediated displacement of integrin α5 will be complex.

The α5β1 integrin is a fibronectin receptor and its persistence at the MTJs of α7 integrin null muscles results in the deposition of fibronectin in the basement membranes of adult muscle fibres. It is thought that the α5β1-fibronectin link is inferior to the α7β1-laminin connection and results in muscle wasting seen in α7-deficient muscle (Nawrotzki et al., 2003). If this were the case, the disruption to the integrin α5-fibronectin link by integrin α7 and the setting up of the α7-laminin connection are vital to the integrity of wildtype adult muscle.

A negative co-cooperativity between integrin α7 and α5 subunits has been described, whereby α7β1 integrin is able to functionally inactivate the α5β1 integrin by the reduction of its surface expression and binding affinity (Tomatis et al., 1999). The binding affinity was defined as the ability of CHO cells to bind to a fibronectin matrix when α7 was overexpressed. This could be due to a simple competition between α subunits for integrin β1 binding, resulting in more α7β1 receptors than α5β1 and therefore lower fibronectin binding affinity.

The suggestion that the interaction of α5β1 and α7β1 is simply competitive could explain why the α5 subunit binds to β1D in the absence of integrin α7 in the knock out muscle. But, what it does not explain is why it is specifically the α5 integrin that co-localises with the β1D subunit at the MTJ. This is an especially interesting question when one considers that integrin α6 is also present in the muscle at this time. Integrin α6 is highly homologous to integrin α7 and its pairing with integrin β1 would create a laminin receptor.

The fact that integrin β1D is retained at the MTJ of integrin α7 deficient muscles further underlines its importance at this site. Despite the integrin α subunit that partners it, integrin β1D remains at the MTJ.

Perhaps the switch from integrin α5 to integrin α7 involves components binding the α or β cytoplasmic domains able to regulate activity or confirmation in a subunit specific manner. Proteins able to bind integrin cytoplasmic domains and regulate integrin α5β1 and α7β1 receptor function in muscle fibres could be of interest.

To investigate the relation between these both these integrins, it is important to design a tool by which the function and importance of integrin α7 is elucidated in integrin α5 deficient mice.

1.6 Muscular Dystrophies

As mentioned earlier, the high degree of muscle fibre specialisation and organisation makes muscle susceptible to the effect of mutations that lead to diseases of muscle wasting, termed the muscular dystrophies (MDs).

Muscular Dystrophies (MD) are a group of inherited disorders with clinical and molecular heterogeneity resulting in progressive muscle wasting (Cohn and Campbell, 2000). The highly organised and specialised structure of the muscle fibre makes it susceptible to the effects of mutations leading to congenital defects or late onset progressive muscle weakness. A previous study suggests that inherited or spontaneous mutations in approximately 100 different genes could potentially leads to MD. So far more than 40 genes have been identified causing various myopathies in both human and mice (Spence et al., 2002). The primary defects that cause the various myopathies identified in both man and mice highlight the importance of the myofibril-sarcolemma-basement membrane connection to muscle function.

As discussed before, the most important genes are those encoding transmembrane proteins such as dystrophin and integrins (Koenig et al., 1987; Mayer et al., 1997). Disruption of the link between the cytoskeleton and extracellular matrix makes the sarcolemma to lose its stability, which in turn renders the muscle fibres susceptible to necrosis (Cohn and Campbell, 2000). Similar to transmembrane protein mutation in their ligands also cause muscle-related disorders, for example mutation in the laminin α2 chain leads to congenital muscular dystrophy 1A (MDCIA) (Helbling-Leclerc et al., 1995). Less obvious candidates also exist, including cytoplasmic proteases, cytoplasmic proteins associated with organelles and sarcomeres and even nuclear membrane proteins, all of which are linked to diseases of muscle wasting (for reviews see Rando 2001; Spence et al., 2002).

The varying phenotypes and severities of different muscular dystrophies imply that some components of the anchorage link are more important than others, or perhaps that some can be compensated for more easily than others. The dual role of transmembrane proteins in mechanical linkage and signal transduction suggest they

would be very important to muscle fibre function and integrity, and this is confirmed by the severe muscular dystrophies occurring upon mutations in their genes.

The functional importance of the DGC in skeletal muscle is demonstrated by mutation of the human dystrophin gene as seen in Duchenne Muscular Dystrophy (DMD) and Becker muscular dystrophies (BMD) (Cohn and Campbell, 2000; Mayer et al., 1997). Mutations of the associated sarcoglycan family are observed in some limb-girdle muscular dystrophies (Bushby, 1999).

1.6.1 Duchenne Muscular Dystrophy

Duchenne muscular dystrophy (DMD) is an X-linked degenerative muscle disorder affecting about 1 in 3500 males. DMD is caused by mutations in the dystrophin gene (Kapsa et al., 2003). Dystrophin is a 427 kDa cytoskeleton protein which localises to the sarcolemma contributing 5% of sarcolemmal protein. In DMD the mutation of dystrophin leads to loss of functional protein thus leading to sarcolemmal instability and disruption of the DGC. In patients the clinical symptoms are not obvious until the age of 3-5 years when proximal muscle weakness is first observed leading to constant loss of muscle.

Clinical progression of the disease is confirmed by the onset of pseudohypertrophy of calf muscle and proximal limb muscle weakness, resulting in wheel-chair dependence by the age of 12. DMD patients suffer from respiratory complications due to weakness of intercostal muscles, which leads to premature death at early twenties. In some cases death may also be caused by cardiac dysfunction (Hoffman et al., 1987; Blake et al., 2002).

Normal skeletal muscle fibre is multinucleated with nuclei located at the periphery of the fibre. In diseased condition the muscle fibre undergoes cycles of degeneration and regeneration, which results in fibres with centrally located myonuclei. When the regenerative capacity of muscle is not adequate to the rate of damage then the muscle fibre is replaced by adipose and connective tissue resulting in pseudohypertrophy, which ultimately leads to muscle wasting.

1.6.2 Complexity of the disease phenotype

Certain characteristic pathological changes to skeletal muscle allow the categorisation of a muscular dystrophy, and these are present in DMD and the *mdx* mouse. The primary consequence of the genetic defect is degeneration of muscle fibres, but the extent of this varies between muscles, between muscle fibre types within muscles, at different ages and between species. In addition, various secondary consequences add to the disease phenotype such as an inflammatory cell response and chronic degeneration of tissue (characterised by the replacement of muscle tissue by adipose and connective tissues). To further complicate matters, it is difficult to separate some responses from a direct result of the primary defect and a secondary consequence of its effect. For example, fibre hypertrophy can be a direct consequence of the primary defect (Hardiman, 1994) or it can be a secondary response of one fibre to the degeneration of its neighbour.

Muscular dystrophy disease processes can be identified histologically in muscle cross sections. Degenerating fibres are often identified as a high concentration of nuclei or gaps in the tissue. Centrally located nuclei (CLN) mark a fibre, which has undergone repair, by the fusion of satellite cells (skeletal muscle stem cell) to the site of damage. In mice, once a fibre has been repaired the nuclei remains at the centre of the fibre. The percentage of fibres with centrally located nuclei is therefore an accumulative indication of the amount of damage and repair that has occurred in the muscle. However, it should be noted that every day wear and tear of muscle results in approximately 2% of normal muscle fibres having CLN.

1.6.3 Animal models available for study DMD:

Crucial to the study of DMD has been the *mdx* mouse, a naturally occurring genetic and biochemical model of the human disease (Stedman et al., 1991; Petrof et al., 1993). A point mutation in exon 23 of the dystrophin gene results in the disruption of the reading frame and therefore the absence of functional protein (Sicinski et al., 1989). The *mdx* mouse model has provided both insight into the disease pathology of DMD and a basis on which potential therapies can be tested. However, although both DMD patients and the *mdx* mouse have the same primary defect, the *mdx* mouse has a much less severe phenotype, with a later onset than seen in DMD and a normal life span. Histological analysis in *mdx* mice has shown similar features of muscle regeneration

such as centrally placed nuclei, necrosis, inflammation, loss of muscle fibre and accumulation of adipose tissue (Stedman et al., 1991). In the diaphragm the muscle fibre loss and collagen deposition is significant and the severity of the phenotype is comparable to human. Elsewhere, it appears that active regeneration is able to compensate for the repeated cycles of muscle degeneration. A phenotype more closely resembling that of the human one can be generated in mice lacking a combination of both utrophin (a dystrophin orthologue) and dystrophin (Grady et al., 1997) or integrin α7 and dystrophin (Guo et al 2006). The reasons for the species- specific differences remain unknown.

Overall the *mdx* mouse model is a very good tool for the studies of DMD. Other than *mdx*, there is a dog model available to study the DMD. The golden retriever dog model shows the closest similarity in phenotype to DMD patients and has a reduced life span. Keeping in mind the ease factor of maintenance, the *mdx* mouse remains the most popular mouse model.

1.7 Therapeutic strategies for DMD

Treatments able to slow the progression of DMD and improve quality of life do exist (van Deutekom and Ommen, 2003; Kapsa, Komberg and Byrne, 2003; Voisin and de la Porte, 2004; Tidball and Wehling-Henricks., 2004; Chakkalakal et al., 2005), but there is no cure. Routes that are currently being investigated can be classified into genetic, cell based and pharmacological. In people with DMD, corticossteroid (steroid) medication has been shown to improve muscle strength and function for six months to two years and slow down the process of muscle weakening. In addition, recent research has also shown that a creatine suppliments can help improve muscle strength in some people with MD.

The severity and prevalence of the disease means potential cures are being heavily investigated, but delivery methods and problems with immunogenicity have so far prevented the application of some of the most promising therapies (for recent review see Deconinck and Dan, 2007; Zhou et al., 2006; Engvall and Wewer, 2003).

1.7.1 Gene based therapy

If an alternative receptor, which is able to perform the same function as the DGC could be identified, many of the therapeutic setbacks could be avoided. Increasing levels of an endogenous alternative would avoid the problems of the large size of the dystrophin gene, the immunogenicity issues and delivery methods.

Utrophin is a member of the dystrophin-related protein family and an autosomal homologue of dystrophin, sharing both sequence and functional motif similarities with dystrophin (Tinsley et al., 1992; Pearce et al., 1993). It is speculated to be the foetal form of dystrophin, as its expression declines as dystrophin is up-regulated around birth (Clerk et al., 1993). There also appears to be functional redundancy in the adult between the two homologues. This is exemplified by the comparatively mild phenotypes of the *mdx* and utrophin-null mice as compared to the severe muscular dystrophy of the utrophin null-*mdx* double knockout (DKO) mouse (Deconinck et al., 1997). The DKO mouse has progressive muscle weakness, contractures, kyphoscoliosis and lethality within weeks of birth, in other words, a phenotype much more reminiscent of the human DMD disease, where there may be non-muscle effects contributing towards the adverse phenotype.

Further confirming its potential as an alternative to dystrophin are observations made in *mdx* mice, endogenous utrophin is redistributed to the sarcolemma and is expressed at high levels in regenerating muscle fibres (Khurana et al., 1991).

Indeed, the adenoviral delivery of utrophin did improve the *mdx* phenotype (Gilbert et al., 1999). It restored the histochemical staining pattern of the DGC, reduced the number of fibres with centrally located nuclei and made muscle fibre membranes impermeable to Evan's blue dye, indicative for improved muscle fibre membrane integrity. Similarly, in DKO mice, a marked decrease in CLN (from 80 to 12%) and fibre necrosis was seen on delivery of utrophin (Wakefield et al., 2000).

Transcriptional up-regulation of utrophin expression by glucocorticoids has been investigated with some success (Courdier-Fruh et al., 2002) and the search continues for small molecule pharmacological compounds that may also increase transcription.

Utrophin has shown potential as a candidate for the treatment of DMD. But the more candidates investigated, the higher the chance of finding a successful treatment. With this in mind, it is worth considering proteins, which may indirectly be able to improve dystrophic phenotypes. For example, Myostatin is a negative regulator of

muscle development and crossing myostatin null mice with *mdx* mice resulted in increased muscle mass and strength, with improved regeneration in the diaphragm (Wagner et al., 2002).

In terms of DMD, an additional candidate to be considered could be the integrin α7β1 receptor. Although the role of integrins in muscle function and development is less well documented, recent findings are revealing them as essential to the correct development and maintenance of adult muscle function. As mentioned before, like the DGC, integrin receptors are capable of forming extracellular - cytoskeletal connections through adaptor molecules that link their cytoplasmic tails to actin filaments (Liu, Calderwood and Ginsberg, 2000). Integrin α7β1 has been identified as a cellular receptor for laminin-111 (Kramer et al., 1991; von der Mark et al., 1991) and the α7 subunit is mainly expressed in skeletal and cardiac muscle (Song et al., 1992). In fact, its importance to skeletal muscle integrity is exemplified in mice with a targeted deletion of integrin α7, which develop a progressive muscular dystrophy (Mayer et al., 1997). Subsequently, human patients with previously unclassified myopathies were shown to have mutations in the integrin α7 gene (Hayashi et al., 1998).

These findings show the important role of integrin α7 in muscle fibre integrity, but of interest in this context are the changes that occur to integrin α7β1 levels in various muscular dystrophies. For example, in DMD patients and in the corresponding *mdx* model the level of integrin α7 is elevated (Vachon et al., 1997; Hodges et al., 1997). Also in dystroglycan-depleted chimeric mice increased amounts of integrin α7 have been observed (Cote, Moukhles and Carbonetto, 2002).

These natural elevations in the disease state make integrin α7 an obvious therapeutic target for further investigation and some studies have addressed this. In mice lacking dystrophin and its paralogue utrophin, transgenic overexpression of the integrin α7X2B splice variant increased life span and mobility (Burkin et al., 2005; Burkin et al 2001). Though, a seemingly contradictory outcome of this study showed no real improvement in the level of muscle degeneration (Burkin et al., 2005; Burkin et al 2001).

Encouraging results also came from a study involving transgenic overexpression of the ADAM12 metalloproteinase in mice. This resulted in elevated levels of integrin α7, and when it was overexpressed on the *mdx* background it resulted in an amelioration of the phenotype (Kronqvist et al., 2002; Moghadaszadeh et al., 2003).

These studies are by no means proof that integrin α7 could provide a therapeutic alternative to dystrophin, but they certainly highlight a promising avenue for further study. In this study I am exploring the idea of overexpressing integrin α7 in *mdx* mice, to demonstrate the capacity of integrin α7 splice variants to ameliorate the phenotype seen in these mice.

1.7.2 Cell based therapies

As discussed above, available therapies may improve the quality of life of patients, however, there is no definitive cure to date. Various stem cell-based strategies have been tested with no long-term success, but recently muscle-resident pericytes attracted attention for their potential to contribute to muscle regeneration.

Translational studies in the late 1970s and early 1980s first showed that donor myogenic cells can contribute to muscle regeneration (Watt et al., 1982; Blau et al., 1983; Morgan et al., 1988). It was not until the late 1980s that myoblast transplant was first used as a treatment in mdx mice (Partridge et al., 1989). After several more positive studies using both mouse and human myoblast, the first clinical trials were attempted to alleviate DMD in humans through cell transplantation (Negromi et al., 2006). Unfortunately, these efforts were largly ineffective. On the whole, there was a low level of donor cell incorporation, generally attributed to poor survival of transplanted cells or lack of dispersion from the injected site. As a result there was only minimal improvement in the recipients (Partridge et al., 1998; Peault et al., 2007). Although the cell based therapy approach has some limitations, there is still lot of potential which needs to be explored and thus we need to study the stem cell population not only from skeletal muscle but also from other sources which may contribute to muscle regeneration.

Canadian scientists McCulloch and Till first discovered the potential of stem cells by injecting bone marrow cells into the spleen of irradiated mice. They observed nodules arising from single bone marrow cells, which they speculated were stem cells (Siminovitch, McCulloch and Till, 1963). Stem cells are characterised by their ability to self-renew through cell division after being in a quiescent state. They also exhibit the capacity to differentiate into other lineages under certain physiological conditions and thus become tissue or organ- specific cells with special functions (Morrison et al 1997,Weissman 2000; Till and McCulloch 1961).

There are two categories of stem cells, embryonic stem cells and adult stem cells. Embryonic stem cells are present as the inner cell mass in blastocysts, at very early embryonic development. They are pluripotent and can form all the cell types from the three germ layers, endoderm, ectodem and mesoderm. On the other hand adult stem cells are active post nataly and are multipotent. There are adult stem cells unique for almost all tissues Relevant to my study here are the population of stem cells residing in skeletal muscle and the blood vessels surrounding the muscle fibre.

1.7.2.1 The Satellite Cell: the principal skeletal muscle stem cell

In the early 19th century it was claimed that multinucleated myofibres may be formed by the fusion of multiple mononucleated cells. The proof of which came in 1960s by a pair of scientists Bintliff and Walker. They performed a simple experiment on the mouse hind limb and demonstrated that following a muscle injury to the muscle, a pool of mononucleated cells assemble at the site of injury and these fuse together to form myofibres (Bintliff and Walker 1960). In 1961, based on observations of frog muscles under the electron microscope, Alexander Mauro provided the first description of the satellite cell (Mauro, 1961). He described a cell that, due to its small cytoplasmic volume, appeared indistinguishable from myonuclei except for the unique position that it occupied, 'wedged' between the plasma membrane and the basement membrane of the muscle fibre. These findings were verified by another paper of the same year that observed such a cell within muscle spindles (Katz, 1961).

Vertebrate skeletal muscle has a remarkable capacity for regeneration, following repeated or complete destruction of the tissue, and for this reason, it is the best-studied tissue in regenerative medicine in recent years (Gayraud-Morel et al., 2009). The stem cells that establish the muscle prenatally also give rise to a distinct lineage of quiescent muscle stem cells perinatally; these are the satellite cells (SC), which are now accepted as the principal regenerative cell type responsible for the post-natal growth, repair and regeneration of skeletal muscle (Gayraud-Morel et al., 2009). Muscle Satellite cells (MSCs) are a distinct, small population of myogenic precursor cells (MPCs) found in adult skeletal muscle. The primary role of these SCs is repair of a damaged myofibre upon injury (Relaix and Zammit, 2012). This small population of MPCs only contribute 2-7% of the total muscle nuclei and resides in the protected niche environment beneath the basal lamina but outside of sarcolemma of associated muscle fibres (Relaix et al., 2005). Stem cells give rise to myogenic precursor cells in adult muscle, which then

contribute to postnatal tissue growth and repair (Asakura, 2003; Seale, Asakura and Rudnicki , 2001). Stem cells reside in a highly specifialised niche, in close contact to the sarcolemma and beneath the BM, which surrounds the muscle fibre (Figure 1.14).

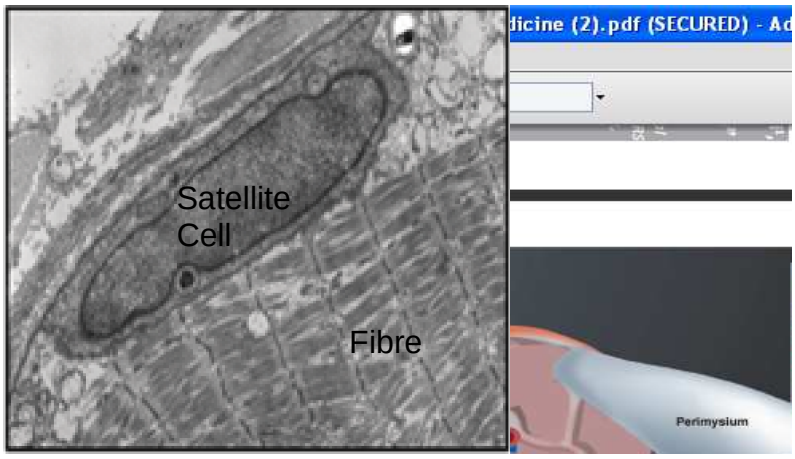

Figure 1.14: Satellite cell location and niche. *Satellite cells occupy a sub-laminar position in adult skeletal muscle. In the uninjured muscle fiber, the satellite cell is quiescent and rests in an indentation in the adult muscle fiber. The satellite cells can be distinguished from the myonuclei by a surrounding basal lamina. (Taken from Gayraud-Morel et al, 2009)*

The key protein determining the presence and myogenic determination of the SCs is the transcription factor Pax7, which appears to be crucial for maintenance of the SC population in the post-natal life (Seale et al., 2000). Further studies revealed that muscle of *Pax7*$^{-/-}$ mice contained a reduced number of SCs and exhibited impaired muscle regeneration, confirming its essential role in myogenesis (Oustanina et al., 2004) (Figure 1.15). Although Pax7 null mice die post-natally they do not show severe skeletal muscle pathology. This is likely due to the functional redundancy that Pax7 shares with its paralogue Pax3 (Relaix et al., 2004). Pax3 is expressed in the embryonic precursors of satellite cells. Accordingly, Pax3/Pax7 double-mutant mice die mid-gestation with no muscle development (Relaix et al., 2005).

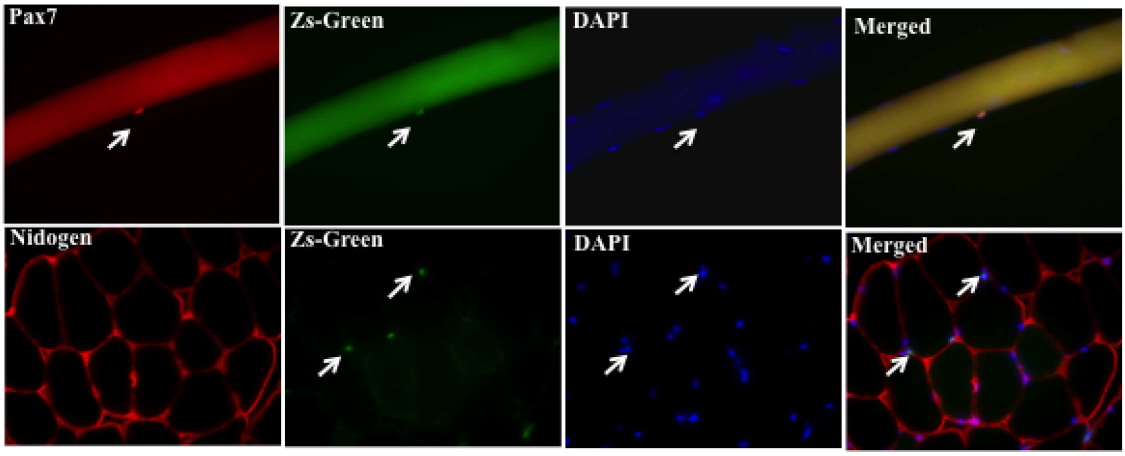

***Figure 1.15: The Satellite cell niche**. An isolated EDL myofibre from a wildtype Pax7-ZsGreen transgenic mouse, immunostained with Pax7 (Red) to identify SCs (Top row) which colocalise with Zs-green (fluorescent protein derived from Zoanthus Sp. reef coral 1) (green) of the transgene driven by the Pax7 promoter Zs-green-positive SCs are also readily identifiable in muscle sections of the GC muscle (bottom row) where nidogen staining (red) marks the basement membrane defining the exact location of SCs in the muscle fibre (Divekar D. and Mayer, U, unpublished results).*

MRFs are basic helix loop helix transcription factors. Myf5 is the first MRF expressed in the embryo and is critical for muscle determination (Ott et al., 1991; Buckingham, 1992). Upon entrance into the cell cycle adult satellite cells express a second MRF, MyoD (Beauchamp et al., 2000). MyoD is expressed throughout the proliferative phase before being down regulated upon differentiation (Figure 1.16) (Tajbakhsh & Buckingham, 2000).

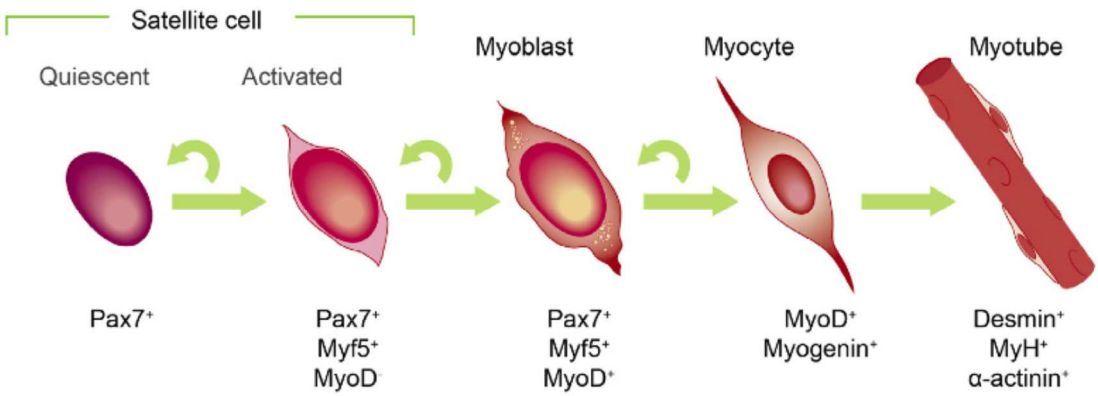

***Figure 1.16: Satellite cell differentiation during myogenesis**. Upon muscle fibre injury, satellite cells undergo differentiation and proliferation cycle. During this time they express myogenic differentiation markers like Myf5, MyoD and Myogenin. Pax7 expression begins during activation and then down regulated in later stages of differentiation. (Taken from McCullagh and Perlingeiro, 2014).*

Although Myf5 acts upstream of MyoD they share a degree of redundancy (Kassar- Duchossoy et al., 2004; Rudnicki et al., 1993) as individual deficiency did not result in impaired skeletal muscle formation, while Myf5/MyoD double knockout mice lack skeletal muscle completely and die soon after birth (Rudnicki et al., 1993). Myf5 and MyoD are critical determinants of the myogenic lineage and are indispensable for satellite cell specification and differentiation. MyoD null mice show a severe regeneration deficiency due to an inability of the satellite cells to differentiate and a failure of these cells to exit the cell cycle (Megeney et al., 1996; Sabourin et al., 1999; Yablonka-Reuveni et al., 1999). The majority of satellite cells down regulate MyoD and up-regulate the muscle specific transcription factor, and marker of differentiation Myogenin. Crucially however, a small minority of cells down-regulate MyoD, thus exit from the cell cycle, but re-express Pax7 returning to a quiescent, undifferentiated state. This is a good evidence to suggest that satellite cells are able to undergo self-renewal and maintain their own numbers (Zammit et al., 2004). In mature muscle, SCs are in quiescent state. However, in response to certain stimuli, such as myofibre necrosis as a result of trauma or damage, surviving SCs get activated and enter the cell cycle to proliferate. They generate new myoblasts, which proliferate, migrate to the site of injury and fuse with damaged myofibre, forming regenerated and functional myofibres. Following their activation in the first stage of this regeneration process, a subset of SC progeny return to the quiescent state in the process of self-renewal (Dahwan and Rando, 2005) (Figure1.17).

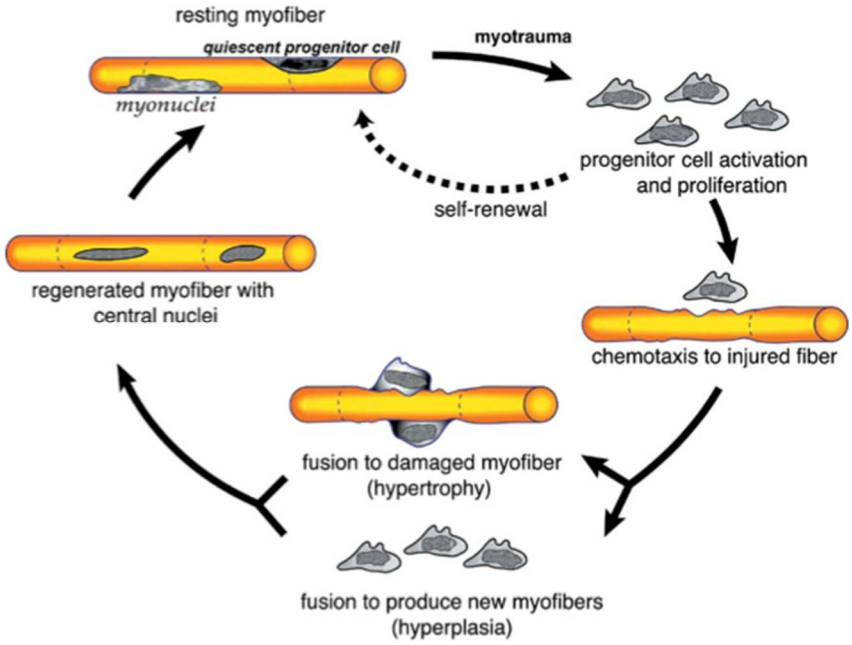

Figure 1.17: Satellite cell response to myotrauma. *Upon injury, satellite cells become activated and proliferate. Some of these satellite cells re-establish a quiescent cell pool through a process of self-renewal while others migrate to the site of damage and, depending on the severity of the injury, fuse to the existing myofiber or align and fuse to produce a new myofiber. (Taken from Hawke and Garry, 2001)*

Representing the principle endogenous cells with regenerative function in skeletal muscle and their great capacity for regeneration outlines satellite cells as the prime cell for therapies. Yet, by nature they exhibit a number of characteristics that limit their effectiveness. The number of possible SCs/myoblast division is limited. In humans, adult myoblast divide only 25-30 times, a number that has shown to decline with age and some diseases such as DMD. While a small minority of SCs is thought to withstand the aging process and retain the intrinsic capacity for regeneration (Collins et al., 2007), aged muscle displays a notable reduction in number and regenerative capacity of SCs. SCs also lack the ability to cross the muscle endothelium when delivered systemically. Even so intramuscular injections of SCs (110 injections per cm^2 of muscle surface) had some success (Skuk et al; 2007), the problem remains that the majority of injected cells are lost within the first day. Furthermore, *in vitro* expansion of SCs for transplantation has been shown to reduce their potency for differentiation *in vivo* (Dellavalle et al., 2007). Trials of myoblast transplantation in DMD patients enabled delivery of dystrophin and improved muscle strength, but the approach is still plagued by immune rejection, poor cell survival rates and limited spread of injected cells (Farini et al., 2009; Huard et al., 2003). For these reasons there has been a growing

interest in the field of developing alternative, more efficient cell-based therapies for conditions such as DMD.

1.7.3 Other resident skeletal muscle stem cells

It is established that the satellite cells are a source of myoblasts, but this does not answer whether satellite cells are the solely or just one of many sources for muscle myoblasts. Additionally, the source of the satellite cells themselves was until recently largely a mystery. There is evidence to suggest that satellite cells are not bona fide stem cells but rather muscle precursor cells themselves, renewed from another stem cell source.

Further evidence describes population of cells that are able to contribute to muscle regeneration. Ferrari et al. suggested in 1998 that bone marrow derived and skeletal muscle stem cells are of the same lineage. In transplantation experiments in immunocompromised mice, they demonstrated that genetically marked bone marrow derived cells migrated into degenerating areas, underwent myogenic differentiation and participated in the repair of the damaged fibers.

This data further suggested a potential role of genetically modified, bone marrow-derived myogenic progenitors to target therapeutic genes to muscle tissue, thus providing an alternative strategy for treatment of muscular dystrophies (Ferrari et al., 1998).

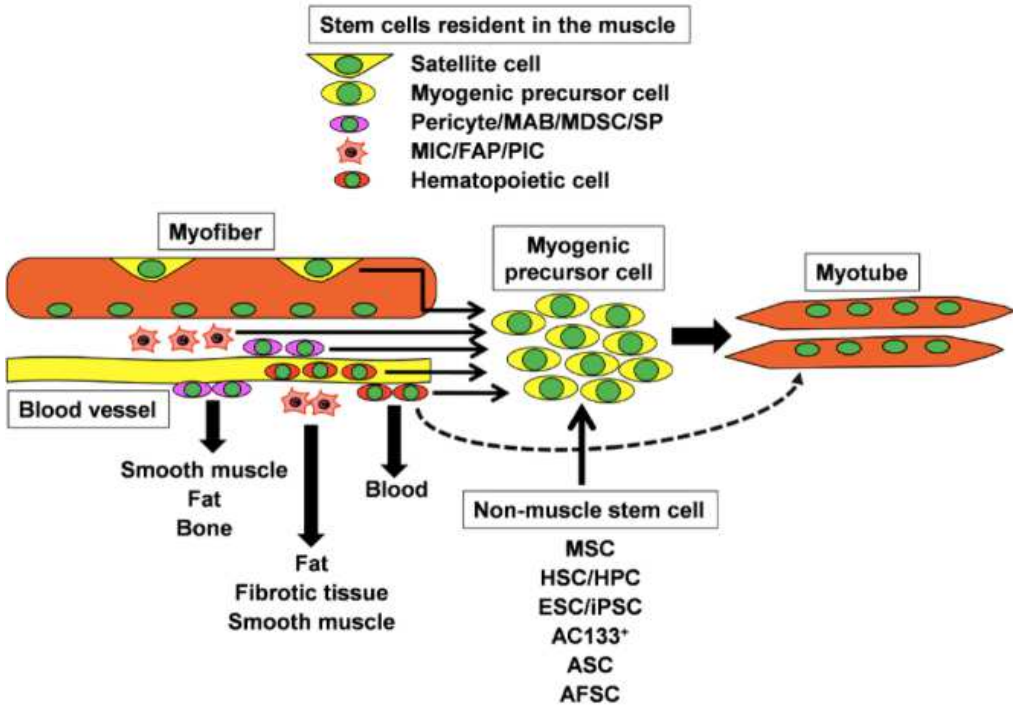

Figure 1.18: Other stem cell populations associated with skeletal muscle. *Skeletal muscle contains several types of cells with myogenic potential, including satellite cells, myogenic precursor cells, pericytes, mesoangioblasts (MAB), muscle-derived stem cells (MDSC), side population (SP) cells, muscle interstitial cells (MIC), fibro-adipogenic progenitor cells (FAP), Pw1+ interstitial cells (PIC) and hematopoietic cells. In addition, other non-muscle tissue-derived stem cells, including mesenchymal stem cells (MSC), hematopoietic stem cells/hematopoietic progenitor celsl (HSC/ HPC), embryonic stem cells/induced pluripotent stem cells (ESC/iPSC), AC133+, adipose-derived stem cells (ASC) and amnion fluid stem cells (AFSC) have been shown to be able to differentiate into myogenic cells, and thus these cells may be utilized for therapeutic stem cell transplantation (taken from Biressi and Asakura, 2012)*

In addition, experiments performed in 1999 underscored the remarkable capacity of adult skeletal muscle-derived cells. When injected into irradiated mice they contributed to all major blood lineages (Jackson, Mi and Goodell, 1999). Similar data were obtained by Gussoni et al. 1999, which indicated that intravenous injection of either normal haematopoietic stem cells or a novel population of muscle-derived stem cells into irradiated animals resulted in the reconstitution of the haematopoietic compartment of the transplanted recipients. In addition, it also revealed the incorporation of donor-derived nuclei into muscle, and the partial restoration of dystrophin expression in *mdx* muscle. These outcomes suggest that transplantation of stem cell populations, might provide an unanticipated avenue for treating muscular dystrophy as well as other diseases (Gussoni et al., 1999).

Apart from the bone marrow-derived cell population other cells of various origin, like dermal fibroblasts, mesangioblasts, and neural tube derived cells, have been a focus of investigation in the late 1990s. These stem cell-like populations have been shown to convert to the myogenic lineage after a period in culture and to contribute to muscle regeneration in the dystrophic mouse (Gibson et al., 1995; Saito et al., 1995; Tajbakhsh et al., 1994). More recently, it has been shown that a variety of circulating cells, including AC133-expressing cells and blood vessel-derived pericytes, when transplanted can contribute to muscle regeneration in *mdx* mice (Torrente et al., 2004, Sampaolesi et al., 2003, Dellavalle et al., 2007). These blood vessel associated cells attracted a lot of attention, due to evidence that suggests that they have mesenchymal stem cell-like properties and as such could be an easy accessible reserve cell population in the body. However, a detailed understanding of the identity and regulation of these progenitor cells as well as the final fate of their descendants is a crucial prerequisite for using and manipulating these cells in medical applications. There are many technical and practical challenges, which need to be overcome before they can be used to combat disease. For example, the method of cell extraction is crucially important to avoid any contaminating cells, which would make the results inconclusive. Furthermore, it is also vital to avoid any rejection from the donor cells from the host immune system. To overcome this obstacle most studies use the nude *mdx* mouse as a host model system.

1.7.3.1 Mesenchymal Stem Cells (MSCs)

Mesenchymal stem cells (MSCs) were first discovered in 1968 by the pioneering studies of Friedenstein. During *in vitro* culturing of hematopoatic stem cells (HSCs) it was discovered that there was a different type of cells in the bone marrow with a fibroblastic morphology. These cells could form colonies on the culture plate and were named as colony forming unit fibroblasts, CFU-F by Lanotte et al in 1981. Furthermore, they had the ability to generate cartilage, bone, muscle, tendon, ligament and fat (figure 1.19).

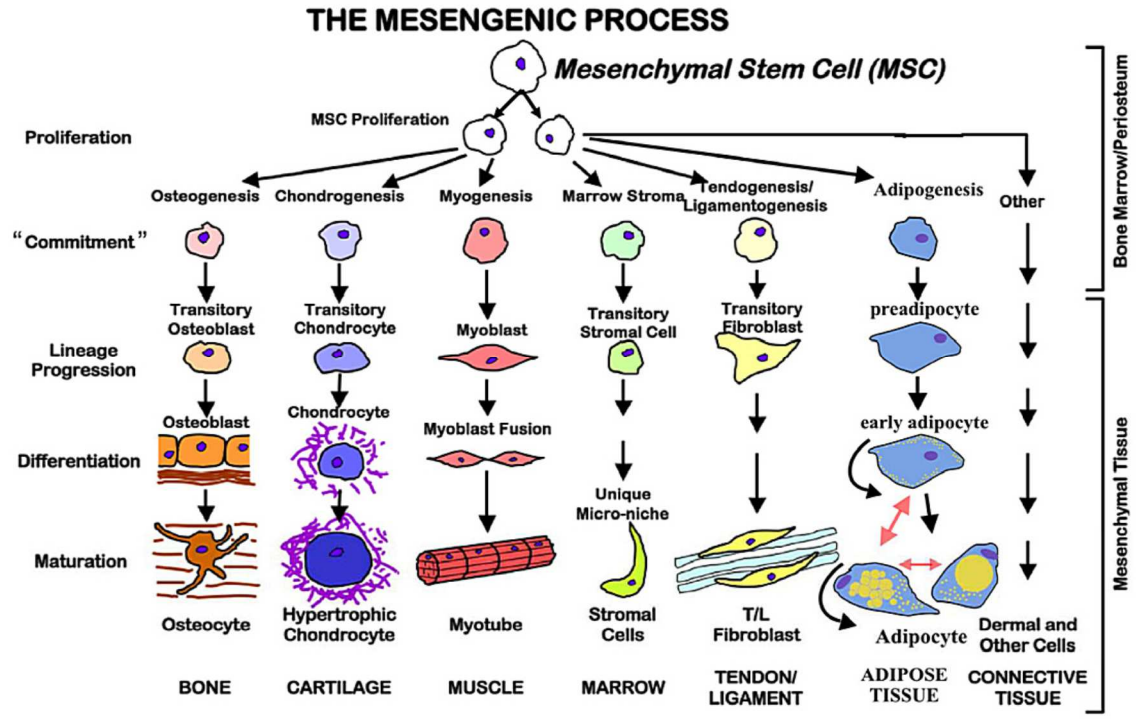

Figure 1.19: Mesenchymal Stem cells (MSCs) and their multilineage differentiation potential. *MSCs are capable of differentiating in multiple lineages displayed in the picture. Dependent on the stimuli provided in the medium they maintain the same differentiation capacity in vitro (taken from Bonfield and Caplan, 2010).*

Owen described them in 1988 as stromal cells due to their fibroblastic phenotype in 1988, but finally they were named MSCs by Caplan in 1991. Pittenger et al. performed the first experiments with MSCs from human bone marrow aspirates in 1999, and showed that they expressed CD29, CD90, CD71 and CD106 but were negative for CD45, CD14 and CD34. MSCs were also isolated from many other sources such as adipose tissue, umbilical cord blood, placenta and even from the dental pulp. However, MSCs from these sources differed in their CD marker expression. In 2006 the International Society for Cellular Therapy published a position paper by Dominici et al. and set the following features for MSCs. MSCs should be positive for CD73, CD90 and CD105, but be negative for CD19, CD34, CD45, CD11a and HLA-DR.

MSCs, chemokines and cytokines and their surface receptors were also shown to be important during inflammation and injury (da Silva Meirelles et al 2008). Inflammation at the injury site triggers a gradient of cytokines and chemokines, which mediates migration of MSCs to the injured site (Salem and Thiermann 2010). Especially CD44 was found to be important in homing of both mouse and human MSCs (Herrera et al., 2004; Sackstein et al., 2008). In addition, it was shown that CXCR4 and CD106 play an important role in the migration of MSCs (Segers et al., 2006; Shi et al., 2007; Hung et al., 2007).

MSCs are considered for cellular therapies for various reasons. Firstly, they can be isolated as a pure population due to the defined markers they express. Secondly, they can easily be cultured *in vitro* to obtain high numbers without loosing their properties. MSCs can migrate to the injured site *in vivo* and thus became a popular candidate in regenerative medicine and cellular therapies. Currently MSCs are being investigated extensively in clinical trials, mostly in the United States, Europe and East Asia studying their use in neurological, liver, bone, heart, graft versus host and some autoimmune diseases like diabetes and Crohn's disease.

1.7.3.2 Pericytes

Following their initial description by Charles Rouget in late 19th century, perivascular cells found in close association with capillaries were first referred to as 'Rouget cells' (Rouget 1873). They have since been given a variety of names including mural or vascular smooth muscle cells. The term pericyte (*peri*; around, *cyte*; cell) was introduced by Zimmerman in 1923 and remains the widely preferred idiom to denote these now extensively studied cells (Bergers and Song, 2005).

Pericytes (perivascular cells/ PVCs), microvascular mural cells, were originally identified for their primary function in angiogenesis. Formation of new blood vessels requires the mutual interaction of two cell types; endothelial cells which constitute the internal lining, and PVCs. They can be classified as microvasculature, or vascular smooth muscle cells in larger blood vessels; although this distinction is not absolute and there appears to be a continuum of pericyte-like phenotypes depending on morphology and location (Armulik, Abramsson and Betsholtz, 2005; Brachvogel et al., 2005). Capillaries and microvessels are enclosed by pericytes. The endothelial cells and pericytes associated in this way both synthesise and share the same basement membrane

within the microvasculature (Mandarino et al., 1993). Although different in location, pericytes reside in a distinct anatomical niche much like satellite cells (SC) (Figure 1.20).

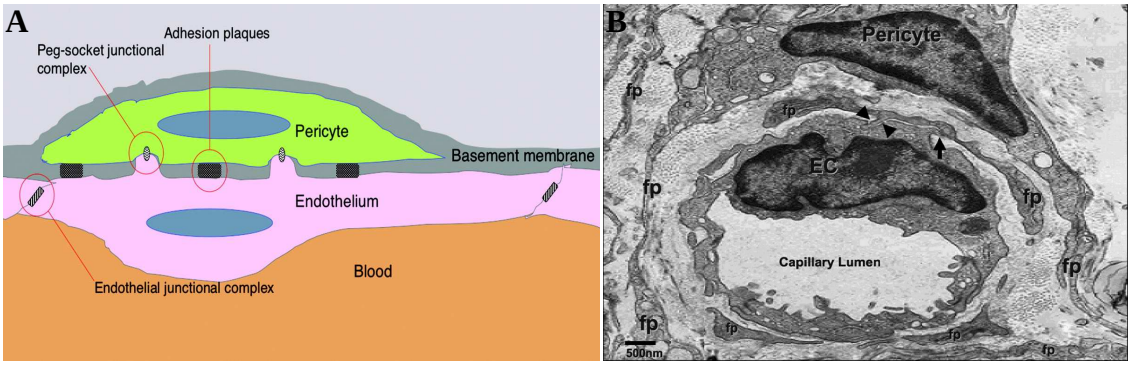

Figure 1.20: Interaction of Pericytes and endothelial cells in microvessels. *(A) Cartoon representing pericytes surrounded by a basement membrane establish direct contact with endothelial cells (taken from Armulik, Abramsson and Betsholtz, 2005), (B) Electron micrograph showing the close interaction between a pericyte and an endothelial cell (EC). Cytoplasmic foot processes (fp) surround and envelop the EC establishing intimate physical relationship between the Pericyte and EC allowing for crosstalk (Taken from Hayden et al., 2008).*

The reciprocal communication and interaction between the two is dependent on signaling through soluble factors such as platelet-derived growth factor (PDGF) and transforming growth factor β (TGF-β), in addition to physical contact mediated by adhesion plaques, integrin and peg/socket and gap junctions (Hirschi and D'Amore, 1996; Armulik et al., 2005).

Traditionally, perivascular cells are thought to act merely as scaffolding to stabilise blood vessels; but are now recognized to have an active role in vessel formation. They may sense the presence of angiogenic stimuli in the tissue, communicate via paracrine signaling to induce proliferation and differentiation of endothelial cells, deposit or degrade extracellular matrix and regulate blood vessel contractibility (Armulik, Abramsson and Betsholtz, 2005; Bergers and Song, 2005).

Despite extensive research the complex ontogeny and plasticity of pericytes is still incompletely understood and molecular markers remain controversial (Bergers and Song, 2005). Pericytes are thought to perform various functions throughout the body during different stages of development and a difference in morphology and distribution among vascular beds indicates adaptations for tissue-specific function. Furthermore, there is increasing evidence to suggest that pericytes are precursors for a number of

different cell types. They have been shown to differentiate into osteogenic, chondrogenic, adipogenic and myogenic lineages *in vitro* (Caplan, 2007; Farrington-Rock et al., 2004). A landmark publication by Crisan et al in 2008 denoted their close similarity to human mesenchymal stem cells (MSCs). This led to the provocative speculation that pericytes represents a population of MSCs and can contribute to tissue regeneration (Doherty et al., 1998; Caplan et al., 2008; 2011). Caplan et al. in 2008 even hypothesized that all MSCs are pericytes. This was further supported by studies showing that skin pericytes have MSC-like properties (Paquet-Fifield et al., 2009) Finally, Dellavelle et al showed in 2007 that perivascular cells from the microvasculature of human skeletal muscle are able to differentiate with high efficiency into myofibres *in vivo*, suggesting a potential option for DMD treatment.

Unfortunately, there is not a specific molecular marker with which pericytes can be defined without ambiguity and the lack of highly specific genetic tools for pericyte labeling limits the interpretation of FACS data and fate mapping (Armulik et al., 2011). There are a handful of markers that are commonly used for detection of pericytes, but they are not exclusive for them. Markers include the intracellular protein alpha smooth muscle actin (αSMA), NG2 proteoglycan, PDGFRβ, desmin and the regulator of G protein signaling-5 (RGS-5) (Bergers and Song, 2005). In addition, several mouse models have been generated in order to study and identify pericyte-like cells (Table 1.1).

Table 1.1: Available mouse models to study the pericyte.

Name	**Mouse model**	**Locus**	**Reference**
XlacZ4	Transgenic	Unknown	Tidhar et al., 2001
AP-Cre/LacZ	Knock-In	Alkaline Phosphatase	Cossu et al., 2001
Anxa5-LacZ	Knock-In	Anxa5-KI	Brachvogel et al., 2005
PDGFRβ-Cre/LacZ	Knock-In	PDGFRβ	Betsholtz et al., 2007

Of interest is the discovery that annexin A5 has recently been identified as a novel marker for pericytes (Brachvogel et al., 2001; 2003; 2005).

1.8 Annexins

Annexins represent a large family of calcium-dependent phospholipid-binding proteins, characterised by a unique architecture that allows their peripheral and reversible docking onto membranes. This family of structurally related proteins comprises over 500 different gene products expressed in most species. In vertebrates 12 annexin subfamilies have been identified (A1- A11 and A13) (Rescher and Gerke, 2004).

Annexin V (Anxa5) presents the prototype and has proved fundamental in the investigation and analysis of other members of the family (Liemann and Huber, 1997). First purified from chondrocytes as a potential receptor for collage type II (Mollenhauer and von der Mark, 1983), further studies demonstrated its ability to attach membranes through calcium-dependent binding of phospholipids (Huber et al., 1990; Rojas et al., 1990), what is also the hallmark for its ability to detect apoptotic cells, which present phosphatidylserine on their surface (Koopman et al., 1994). Anxa5 has been implicated in the mineralisation process during endochondral ossification (Kirsch et al., 2000; Brachvogel et al., 2001), and in membrane repair (Skrahina et al., 2008).

Most functions of Anxa5 have only been identified *in vitro.* However in 2003, an Anxa5-deficient mouse model has been generated, which showed that Anxa5 is specifically expressed in pericytes in development and the adult. (Brachvogel et al, 2003).

1.9 Aims

In order to develop successful strategies to ameliorate muscle wasting diseases and delay muscle loss with ageing, it is (1) critical to understand the function of all major skeletal muscle proteins and (2) potential new therapies need to be extensively tested. Although loss of integrin α7β1 has been shown to result in a congenital muscular dystrophy in mice and human, the function of integrins in skeletal muscle development and the adult is not well understood. Particularly the role of integrin α5β1, whose loss in chimeric mice led to dystrophic symptoms, and its relationship to integrin α7β1 remains elusive.

Objectives addressed in chapter 3: Integrin α5β1 in development and adult skeletal muscle

1. To investigate the role of integrin α5 in skeletal muscle

Knocking out integrin α5 is embryonically lethal and conclusions drawn from the α5 -/- chimeric mice were limited and therefore we aim to KO integrin α5 conditionally using Pax3 and HSA promoter driving expression of Cre recombinase.

2. To investigate the relationship between integrin α5 and α7 in skeletal muscle.

Integrin α7 displaces integrin α5 at the MTJ of developing muscle, suggesting a crosstalk between these two receptors exists. The mechanism for which is unknown. Revealing this mechanism will provide insight into the role and relationship of integrin α subunits in skeletal muscle development. To understand the relationship between integrin α5 and α7, we aim to study the double knockout (DKO) mice.

Objectives addressed in chapter 4: Could integrin α7β1 be a therapeutic target for DMD?

3. Could integrin α7 play a role in the ameliorating of dystrophic phenotype?

There is still not a successful therapy available to ameliorate myopathies. It is therefore necessary to continue research on identifying new therapeutic strategies or to improve current strategies. Integrin α7β1 has been suggested as potential therapeutic target for DMD as it is upregulated in DMD patients and in mdx mice.

This raises the following question, which we aim to answer by generating transgenic mice overexpressing integrin α7 intra and extra cellular splice variants.

- Is it possible to increase the levels of integrin α7 while maintaining the correct processing, localisation and function?
- Could the different integrin α7 splice variants have different abilities in improving the muscle phenotype seen in DMD?

Objectives addressed in chapter 5: Do pericytes contribute to skeletal muscle regeneration?

In recent years, pericytes attracted a lot of attention due to their mesenchymal stem cell-like properties and, more specifically, their potential to participate in muscle regeneration. Pericytes are a poorly defined cell population, and it is not clear whether these cells commit to the myogenic lineage when in contact with regenerating muscle, or whether there is a mutual relationship between pericytes and satellite cells, in which both cell types can adopt both phenotypes when exposed to stimuli provided by the environment. Understanding contribution of endogenous and exogenous pericytes to muscle regeneration is therefore pivotal in further defining pericytes and their relationship with satellite cells and to do so we aim

4. to generate the pericyte reporter mouse strain for cell lineage tracing

5. to transplant of labeled pericytes to follow the their fate in regenerating muscle

Chapter 2 Materials and Methods

2.1 Mouse lines

During this study we used different mouse models to investigate the role played by integrins and pericytes during the skeletal muscle regeneration. Some of the mouse stains were generated in the laboratory, while others were obtained from collaborators.

2.1.1 Integrin α7 overexpressing transgenic mouse line

Integrin α7 overexpressing strains were generated in our laboratory before the start of this study. In brief, integrin α subunit cDNAs had been generated in the laboratory from murine myoblast RNA by RT-PCR. The Human Skeletal α-actin (HSA) promoter element was added 5' to the integrin α7 cDNAs. After linearisation the DNA was injected into pronuclei of fertilised mouse embryos, these were transferred into the oviduct of pseudopregnant fosters mothers. Mice harbouring the transgene were detected by PCR using a sense primer (table 2.6) hybridising with the HSA promoter and antisense primers hybridising within the α subunit coding sequence and also cDNA specific primer pairs (table 2.6). The mice born following oocyte injection that were positive for the transgene were termed 'Founder' mice. Each Founder was backcrossed into the 129Sv wildtype strain. One positive offspring from this F1 generation was picked and crossed again with the 129Sv wildtype. The strain was then maintained by the crossing of subsequent generations with the 129Sv wildtype. Within a strain all mice are therefore heterozygous for the transgene, and every member is derived from a single 'F1 deriver' mouse. For each overexperssing integrin splice variant more than one stain were analysed according to the expression levels of the integrin overexpressed (Table 2.1) These transgenic mice were studied for the effect of overexpression of integrin on skeletal muscle and are discussed in chapter 4.

Table 2.1: Summary of Integrin α7 Splice Variant Overexpressing Transgenic Strains. Each construct corresponds extracellular splice variant and intracellular splice variant as shown. The various strains derived for each construct are named after the Founder mouse. An average relative level of overexpression/expression as compared to the wildtype is shown, the standard deviation for these values is found in Appendix 1. Strains crossed out in grey are those which were terminated as they did not overexpress the corresponding integrin α7 splice variant protein.

	1. Promoter	**2. Integrin α7 Extracellular Variant**	**3. Integrin α7 Intracellular Variant**	**4. Strain (Founder)**	**5. Integrin α7 Level**	**6. Integrin β1 Level**
Construct 1	HSA	X2	A	Susie	31.7	80.7
				Chris	33.2	80.7
				~~Tina~~	0	-
Construct 3	HSA	X1	A	Lydia	53.4	6.5
				Maria	164.8	19.9
				Judith	10.4	1.9
				Elke	19.0	1.6
Construct 5	HSA	X1	B	Xaver	20.4	9.3
				Karin	24.3	10.5
Construct 7	HSA	X2	B	Max	14.4	22.3
				Moritz	1.7	0.3
				Fritz	28.7	5.7
				~~Hans~~	0	-
				Babette	21.7	3.2

2.1.2 Integrin α7 overexpressing transgenic *mdx* mouse line

To investigate the role of integrin in muscle wasting disease like DMD, integrin α7 overexpressing mice were crossed with dystrophin-deficient *mdx* mice. The F2 generation was named *mdx*^{tg}. The four integrin α7 splice variant combinations were studied and documented in result chapter 4.

2.1.3 Integrin α5 conditional knockout mouse line

Integrin α5 conditional mice were a kind gift of Prof R.O Hynes (MIT, USA). The principal behind the homologous recombination and design of the targeting construct is included in chapter 3 (Figure 3.1). To study the role of integrin α5 during muscle development, heterozygous integrin α5 mice were crossed with mice, expressing Cre recombinase under the control of the HSA or the Pax3 promoter. The breeding strategy is explained in detail in chapter 3 (Figure 3.2). The outcome from these experiments is discussed in chapter 3.

2.1.4 Integrin α5/ α7 double knockout mouse line

In order to study the combined contribution of integrin α5 and α7 to muscle development Itga7 +/- mice were crossed with Itga5 +/- ^{Cre} mice to generate Itga7+/- // Itga5 +/-$^{Cre\ mice}$. Males from the F1 generation were then crossed with Itga7+/-// Itga5 FL/FL or Itga7 -/-// Itga5 FL/FL females to obtain Itga7 -/-// Itga5 FL/-^{Cre} mice for analysis.

2.1.5 Anaxa5 -Cre –KI mouse line

To investigate the role played by pericytes in muscle regeneration, we generated the Anxa5-Cre-KI mouse strain. Based on the previously generated Anxa5-LacZ fusion strain (Brachvogel 2001), the targeting construct for homologous recombination was designed in a way that activity of Cre- recombinase was controlled by the endogenous Anxa5 promoter.

2.1.6 Reporter mouse lines

For lineage tracing of pericytes, Anxa5-Cre-KI mice were crossed with ROSA26-EYFP and ROSA26-LacZ mice. ROSA-26-td-Tomato mice were used for *in vitro* labeling of pericytes using Adeno-Cre viral induction.

2.2 Molecular biology techniques

The general molecular biology methods used for Escherichia Coli (E. Coli) culture and preparation of competent cells, agarose gels and DNA extraction, precipitation, electrophoresis and digestion were all done according to Maniatis et al. (1982). Concentration of DNA was measured using NanoDrop. For preparation of large amounts/high quality plasmid DNA, the Quiafilter mini-, midi- and maxiprep kits (Qiagen) were used according to the manufacturer's protocols.

2.2.1 Bacterial growth

The competent E. coli strain DH5α was used to propagate plasmids. E. Coli were grown on sterile Luria and Bertani minimal medium (LB medium, Roth). All cultures were grown overnight at 37ºC, either on solid medium or shaken at 200rpm in liquid cultures. Selection for transformed bacteria was carried out in the presence of 100 µg/ml Ampicillin (Roche) unless otherwise stated.

2.2.2 Preparation of competent cells

For preparation of competent cells DH5α were plated on antibiotic free LB-agar plates and grown at 37°C overnight. A single colony was picked with a sterile toothpick and transferred to 2 ml LB media containing 0,02M $MgSO_4$ and 0,01M KCl in 15 ml polystyrene round bottom test tube (BD Falcone) and incubated in a shaker (200rpm) at 37°C overnight. The overnight culture was used to inoculate 100 ml of LB media containing 0,02M $MgSO_4$ and 0,01M KCl (1:100 dilution) in a 1000ml conical Erlenmeyer flask and left shaking at 37°C till at a wavelength of 600 nm an O.D. of approximately 0.3-0.55 was reached. The flask was left on ice with gentle shaking from time to time to prevent precipitation of the bacteria. The cells were then transferred to pre-cooled centrifugation bottles and were centrifuged at 6000 rpm for 10 min at 4°C in a pre-cooled centrifuge. The pellet was then re-suspended carefully in 50 ml of TFB-I (table 2.2) buffer taking care not to produce any air bubbles and was then centrifuged again same as above. The cells were then re-suspended again this time in 4 ml TFB-II (table 2.2) buffer and 100 µl aliquots were on a mixture of dry ice and acetone. The cells were then stored at -80°C and checked for competency at a later date. In general competency of 10^6 to 10^8 was achieved. When using these cells for transformations, each tube was split in two and transformations were done using 50 µl of competent cells.

Table 2.2: Composition of buffers used for preparation of competent cells. All solutions are made up in dH2O unless otherwise stated.

Reagent	**Composition**
TFB I buffer	30 mM K acetate, 50 mM Mn2Cl, 100 mM RbCl, 10 mM CaCl2, 15 % (v/v) Glycerine (pH 5.8), filter sterile
TFB II buffer	10 mM MOPS/NaOH (pH 7.0), 75 mM CaCl2, 10 mM RbCl, 15 % (v/v) Glycerine, filter sterile

2.2.3 Transformation of Plasmid DNA

Chemical competent DH5α E. Coli cells were thawed gently on ice. 50 µl was taken and transferred to a new tube to which 0.5 µl of plasmid DNA was added. The sample was then mixed by hand before incubating on ice for 30 minutes. Bacteria were then heat-shocked for 45 seconds 42ºC. Bacteria were then grown in 900 µl of LB broth without ampicillin for one hour at 37ºC with shaking and then plated onto an LB plate with ampicillin (100 µg/ml) and grown overnight at 37ºC. Single ampicillin resistant colonies were then picked using a sterile toothpick and incubated in 2 ml LB broth with ampicillin at 37ºC for 6-8 hours. For long term preservation of bacteria DMSO stocks were made by adding 20% DMSO to bacterial overnight cultures, snap frozen on dry ice and then stored at -80ºC. When appropriate, blue-white selection was performed at this stage by adding 40 µl of XGal (2% in DMF) and 40 µl of Isopropyl β-D-1-thiogalactopyranoside (IPTG) (100 mM) to the plates prior to plating.

2.2.4 Isolation of plasmid DNA by alkaline lysis

For isolation of plasmids, 2 ml LB media in a 15 ml Polystyrene round bottom test tube was inoculated after picking a single colony from an LB-agar plate and incubated overnight at 37°C in a shaker (200 rpm). The bacterial suspension was then transferred to a 1.5 ml eppendorf tube and centrifuged gently at 3000 rpm. Most of the media was removed and the remaining pellet was re-suspended in the residual media. TENS buffer (Table 2.3) was added at a volume of 300 µl followed by 150 µl of 3M Na-acetate/pH 5.2 and then mixed by inverting the tubes several times. The tubes were

then centrifuged at full speed (14,000 rpm) for 15 min and the supernatant was transferred to a new tube. Next, 900 µl of 100% ethanol was added and the tubes were stored at -20°C for 20 min followed by centrifugation for 20 min at full speed. The supernatant was discarded and the pellet was washed with 70% ethanol, air dried and re-suspended in 100 µl of TE buffer containing 0.1 mg/ml RNase.

Table 2.3: Composition of buffers used for plasmid isolation. All solutions are made up in dH_2O unless otherwise stated.

Reagent	**Composition**
TE buffer	10 mM Tris/HCl (pH 8.5), 1 mM EDTA (pH 8.0)
TENS buffer	10 mM Tris/HCl (pH 8.5), 1 mM EDTA (pH 8.0) ,1 M NaOH, 10 % SDS

2.2.5 Plasmid purification by Qiagen kit

A Qiagen plasmid purification midi kit was used for purification of plasmid DNA. Bacterial cultures were grown under the conditions stated above until reaching stationary growth phase, typically after 16 hours of incubation. Cells were then harvested by centrifugation (4000 rpm for 15 minutes at 4°C in a Beckman centrifuge with the rotor JA-25-50). The supernatant was discarded and the cell pellet carefully re-suspended in 4ml re-suspension buffer (P1). 100 µg/ml of RNase A was added to the buffer P1 prior to the re-suspension to prevent RNA contamination of purified plasmid DNA. 4 ml of lysis buffer (P2) was then added to the cell suspension, which was mixed gently to avoid the bacterial DNA contamination and then incubated at room temperature for 5 minutes. Following lysis, 4ml of pre cooled neutralisation buffer was added (P3), which was then gently mixed and incubated on ice for 20 minutes. Next, the solution was centrifuged (15000 RPM for 30minutes at 40 C in a Beckman centrifuge with the rotor JA 16-25), the supernatant was retained and the pellet discarded. The solution was then filtered through a damp tissue to remove any particulate material before passing over a Qiagen column, previously equilibrated with 4ml of buffer QBT. The plasmid DNA bound to the column was then washed twice with 10ml of medium salt buffer (QC). The plasmid DNA was then eluted with 5 ml of high salt buffer (QF)

and then precipitated by adding 3.5 ml of isopropanol. DNA was then recovered by centrifugation (at 15000 RPM for 30 minutes at 40 C in Beckman centrifuge with a rotor JA-16-25), which was then washed with 2 ml 70% ethanol. The solution was then centrifuged (at 15000 RPM for 10 minutes at 40 C in Beckman centrifuge with a rotor JA-16-25) and supernatant was carefully decanted off. The DNA pellet was allowed to dry before being dissolved in 200µl of filter sterilised TE buffer (Table 2.3).

2.2.6 DNA digestion by restriction enzymes

Digestions were made using Roche restriction enzymes with corresponding Roche buffers. For every 1 µg of DNA to be digested, 1 Unit of restriction enzyme was used. The ratio of enzyme to buffer was kept below 10% (v/v). All restriction digests were carried out at 37°C unless otherwise stated.

2.2.7 Agarose gel electrophoresis

DNA samples were mixed with 5x Orange G neutral loading dye (Table 2.4) and loaded onto a 0.6% agarose gel (made by diluting agarose in 1 X TAE buffer (Table 2.4). The gel was then run for approximately 40 minutes at a constant voltage of 150V. The DNA gel was then stained with 0.5-µg/ml ethidium bromide for 30 minutes and visualised using a UV trans-illuminator (UVP BioDocIt Systems)

Table 2.4: Composition of buffers used for DNA electrophoresis.

Reagent	**Composition**
50 X TAE buffer	40 mM Tris Acetate, 2 mM EDTA (pH 8.5)
DNA gel loading dye	50% (v/v) Glycerol, 1X TAE buffer, 0.5% (w/v) Orange G powder

2.2.8 Isolation of DNA fragment from agarose gels

For isolating DNA from agarose gel, the gel was run at 100 volts for ideal separation of restricted DNA fragments or PCR products. DNA was purified from agarose gel using the Gene-clean kit (MP-Biochemicals). After the gel was stained in Ethidium bromide, the desired size DNA was visualised under the UV hand lamp and cut out using a scalpel. It was then transferred in a pre-weighed eppendorf tube. Next, the amount of Nal was calculated according to the weight of the gel and was added to the eppendorf tube, which was then incubated in a thermo mixer at 55^0C for 5-10 minutes until the gel was completely dissolved. 5µl of glass beads were added to the gel solution, mixed and incubated on ice for 5 minutes with mixing regularly ensuring the glass beads stayed suspended. The solution was then centrifuged at 14000 rpm 10 seconds to recover the DNA bound to glass beads. The supernatant was decanted and the pellet was washed with 500µl of New wash buffer supplied with the kit. After re-suspension the solution was centrifuged at 14000 rpm for 10 seconds and the supernatant was discarded. The washing steps were repeated three times. The DNA pellet was dissolved in 10µl of ddH2O and incubated at 55^0C for 4 minutes to elute the DNA. The solution was then centrifuged at 14000 rpm 10 seconds to recover the DNA in the supernatant. The process was repeated one more time by adding 10µl of ddH_2O. The concentration of DNA was then measured with a NanoDrop.

2.2.9 Quantification of DNA

DNA concentration gel was measured by spectrophotometry using a NanoDrop. Briefly 1µl of TE buffer was used to create a zero value before DNA concentration and quality (OD_{260}/OD_{280} ratio) was determined for each sample.

2.2.10 Ligation of DNA fragment

For ligations, the Ready-To-Go kit (Amersham) was used; equal ratios of vector to insert (250-500 ng) were used in a final volume of 20 µl, with sticky-end ligations left for 30 minutes and blunt-end ligations for 45 minutes in a 16°C water bath which was maintained at constant temperature in the cold room. The ligated product was then used straight for transformation in competent E.Coli DH5α (2.2.3) or was frozen at -20°C for later use.

2.2.11 Phenol-chloroform extraction and ethanol precipitation of plasmid DNA

Equal volumes of phenol- chloroform were added to the plasmid DNA, vortexed and centrifuged at 14000 RPM for 2 minutes at room temperature (RT)). The upper layer (aqueous phase) was then collected into a fresh eppendorf before adding an equal volume of phenol and the centrifugation process was repeated. The upper layer was then transferred to a fresh eppendorf before an equal volume of chloroform was added and centrifuged. The upper aqueous layer was then treated with 1/10 volume of 3M sodium acetate and 2.5 volumes of absolute -20^0 C ethanol and incubated at -20^0 C for 20 minutes. The precipitated DNA was pelleted by centrifugation, washed with 70% ethanol and dissolved in an appropriate amount of TE buffer.

2.2.12 Cloning of PCR fragment into pUC18/19 vector

PCR products were cloned into pUC18 or pUC19 vectors using the Sure clone kit (Amersham). The PCR fragments were blunted using Klenow enzyme (Roche). This was achieved by adding 1 µl of Klenow fragment (5900 U/ml) to the DNA diluted in 1x blunt/kinase buffer and left at 37°C for 30 minutes after which the DNA was extracted by phenol-chloroform extractionThe PCR products were then separated on an agarose gel, cut and purified as described (2.2.7). The DNA was then cloned into linerarised and dephosporylated pUC18/19

2.2.13 Sequencing

Sequencing reactions were performed at TGAC at the John Innes Centre, Norwich. For plasmids <5kb in length 200ng and 500 ng of DNA for >5kb in length was sent for sequencing. Sequences were verified and aligned using the online tools Chromas and BLAST (NCBI).

2.3 Polymerase Chain Reaction (PCR)

2.3.1 Amplification of plasmid DNA fragment by PCR

700ng of plasmid DNA was amplified using the high-fidelity Taq polymerase (Roche) in total volume of 200µl. The reaction mixture was then divided in 4 tubes containing 50 µl each and subjected to the following PCR conditions.

Denaturation at 94°C for 2 min		
	94°C for 45sec	35 cycles
Annealing	at 55°C for 1 min	
Extension	at72°C for 1min/1kb + 3 seconds each cycle	
	72°C for10 min	
	4°C for 15 min	

PCR products were then separated on an agarose gel and purified with Gene Clean.

2.3.2 Genotyping of mouse tissue by PCR

Mouse ear biopsies were lysed (table 2.5) overnight at 55°C and 1:10 diluted for the PCR reaction according to table 2.6.

Table 2.5: Composition of lysis buffer used for mouse tail/ear biopsies.

Reagent	**Composition**
Proteinase K lysis buffer	0.1 M Tris/HCl, 0.2 M NaCl, 0.2 % (w/v) SDS, 5 mM EDTA, 0.1 mg/ml Proteinase K

Table 2.6: Master mix for genotyping by PCR.

Reagents	Concentration	Volume per reaction
Forward and Reverse primer mix	20 pM per primer	1µl
10x Buffer with detergent	100mM tris-HCL(pH 8.8 at 25°C), 500 mM KCl , 0.8% (v/v) Nonidet P40,15mM $MgCl_2^+$	5 µl
dNTPs	25µM	0.5 µl
TOD 1:10 diluted	Unknown	2 µl
Sterile H_2O (Fisher)	N/A	38.5 µl
Mouse DNA 1:10 diluted	Unknown	3 µl
Final Volume	-	50 µl

The standard touchdown programme used for genotyping is detailed below, followed by modifcations for itga5 mutant mice and mdx mice

a) Touchdown programme

Denaturation at 95°C for 5 min

95°C for 1 min

Annealing at 65°C for 1 min /minus one degree each cycle } 10cycles

Extension at72°C for 1 min

95°C for 1 min

55°C for 2 min } 30 cycles

72°C for 1 min

72°C for10 min

4°C for15 min

b) Itga5-specific programme

Denaturation at 95°C for 5 min		
	95°C for 45sec	30 cycles
Annealing	at 60°C for 45 sec	
Extension	at72°C for 1:30 min	
	72°C for10 min	
	4°C for 15 min	

c) mdx-specific programme

Denaturation at 95°C for 3 min		
	95°C for 45sec	40 cycles
Annealing	at 56°C for 45 sec	
Extension	at72°C for 1:30 min	
	72°C for10 min	
	4°C for 15 min	

Table 2.7: Oligonucleotides used for genotyping

Primer Number	Description	Sequence
1	A7 - 981.rev	CCA GAA TCG ATG GAG AAA CC
5	A7 - 3588.rev	GAT CGT CGA CTC TAG AAG ATG TTA GGC AGT GGC TGG
6	A7 3206.seq	CTC AGA GAT GCA TCC ACA GTG
7	A7 - 719.seq	TTC TGT GAG GGG CGC CCC CAG
12	HSA.seq	GCA CTA CCG AGG GGA ACC TG
13	MCK.seq	TCA CAC CCT GTA GGC TCC TC
43	A7.39.seq	GAG GGG TGC TGA GGT GAA AG
44	A7.264.rev	GCC GGT GGT AAG AAC AGT CC
64	Cre UM15B.rev	GAC GGA AAT CCA TCG CTC GAC CAG
65	Cre UM19B.seq	GAC ATG TTC AGG GAT CGC CAG GCG
95	HT030-dwn	GCA GGA TTT TAC TCT GTG GGC
96	HT031-wt/flox-up	TCC TCT GGC GTC CGG CCA A
97	HT032-ko-up	GAG GTT CTT CCA CTG CCT CCT A
98	HT038-neodwn	ACC GCT TCC TCG TGC TTT AC
82	AM p9427.seq	AAC TCA TCA AAT ATG CGT GTT AGT G
83	AM p260e.rev	GTC ACT CAG ATA GTT GAA GCC ATT TAG
84	AM p259e.rev	GTC ACT CAG ATA GTT GAA GCC ATT TAA
134	Anxa5-Int2.seq	TGG GGA GAG ACT TAG CCA AC
158	Anxa5-Int Ex3.rev	AATTAAACGTTACCCAAGCC
159	Anxa5-LacZ.rev	TGCGGGCCTCTTCGCTATTACG

Table 2.8: Oligonucleotides used for cloning

Primer Number	Description	Sequence
124	AnxA5-Cre-fus.rev	ATC AAT CGA TGA GTT GCT TC
125	AnxA5-Cre-fus.rev	GCT TGA TAT CGG TTA CAG TGT GAA TAG TAC TAC CCT TCC TTT CAC AGG CTA CGA TGC CCA AGA AGA AGA GGA AG
126	AnxA5-Ex6.rev	TGG CAC TGA GTT CTT CAG GTG
127	AnaxA5-Int5.Seq	CGT GAT GAT CGG TTT ATT GGC
131	Anxa5-int6.seq:	AGT TCT TAG AGG AGG CTT CAG GA
132	Anxa5-int6.rev	CTT GAT GCA CTG TGA AAT GGT TA
133	Anxa5-Ex3.rev	GAA GTC AGT CAC AGT GCC TC
134	Anxa5-Int2.seq	TGG GGA GAG ACT TAG CCA AC
135	Cre-A5KI.rev	CAT GTC CAT CAG GTT CTT GC
142	Anxa5-int6gPCR.rev	TGT CTC TTC TCT ATG CCT GCT TC
143	Anxa5KI-neopA.seq	GAG GAT TGG GAA GAC AAT AGC AG

2.4 Embryonic stem cells

After preparing 100 µg of high quality plasmid for each construct they were linearised using NotI and sent for transfection of embryonic stem cells at the transgenic core facility at Dresden, Germany. Mouse ES cells which were transfected with the targeting vector and selected on Neomycin were received in 96 well plates on dry ice and kept at 80°C. JM8N4 and 129Sv-derived R1 ES cells were used

2.5 DNA extraction and screening of targeted clones

For isolation of DNA the transfected ES cells were removed from -80°C and were thawed at 37°C for about 10 mins and transferred to 24 well plates containing feeder cells over night at 37°C, growth media was changed the following day. When confluent, cells were lysed with 500 µl PK lysis buffer and kept overnight at 37°C followed by addition of 500 µl isopropanol and plates were then left at 4°C for 4-6 hours for formation of the DNA precipitate. The visible precipitated DNA was transferred to 1.5 ml eppendorf tubes containing 100 µl sterile TE buffer (pH 8.0) using a sealed glass pipette and left at 55°C for 24 hrs to dissolve.

2.6 Southern blot analysis

2.6.1 DNA gel treatment and membrane transfer

Approximately 10µg of genomic DNA in TE buffer was digested overnight using the appropriate restriction enzyme in digestion buffer. The digested DNA was then separated on a 0.6% agarose gel, stained with ethidium bromide and viewed using UV light. The gels were then submerged in depurination buffer (Table 2.9) for 10 minutes. The solution was replaced with the denaturation buffer (Table 2.9). After 20 minutes fresh buffer was added for a further 20 minutes. The same was repeated with the neutralisation buffer (Table 2.9). The gels were then placed over 20xSSC saturated filter paper placed in solution and the DNA was transferred onto a nylon membrane (Hybond XL, GE healthcare) by vertical diffusion of the 20xSSC buffer through paper towels overnight. The DNA was then fixed to the membranes using freshly prepared 0.4N NaOH by placing them on saturated Whatman paper with the bound DNA facing upwards for 10 min. The membranes were then neutralised by transferring to 20xSSC (Table 2.9) for a further 10 min. For the membranes to be ready to use for radioactive labeling, they were heated at 55°C for 1-2 hours and kept at 4°C until use.

Table 2.9: Reagents used in southern blot analysis

Reagents	**Compositions**
Depurination buffer	0.25 M HCl
Denaturation buffer	0.5 M NaOH, 1 M NaCl
Neutralisation buffer	3 M NaCl, 0.5 M Tris/HCl (pH 7.4)
20X SSC	3 M NaCl, 0.3 M Na Citrate (pH 7.0)

2.6.2 Preparation of DNA probes

For screening of Anxa5-KI-Cre transfected ES cells 3 DNA probes were generated. Probe 1, (3' probe, Figure 5.4) was amplified by PCR with primers #126 and #127 (table 2.8) using plasmid pX1-E2-7. The 700bp Neo probe (Neomycin-specific) was obtained by restriction of plasmid pGem-NeoΔ-EcoRI plasmid with Pst I. The 870 bp probe 2 (5' probe, Figure 5.4) was obtained by restriction of plasmid pX3-EN-8-4 (#197) with BamHI.

2.6.3 Radioactive random labelling of DNA probes

50 ng of DNA fragment was labelled with 50 µCi α -dCTP32 using the "Prime it II" kit (Stratagene) according to the supplier's protocol, followed by purification using Illustra NICKTM columns (GE healthcare). The specific activity of 4 µl of the 400 µl elute was determined using a liquid scintillation counter (HIDEX). 2-3.10^6 cpm of labelled probe was denatured for 5 minutes at 95°C just before hybridization and kept on ice for 2 minutes

2.6.4. Hybridisation using radio-labeled probes

Nylon membranes containing DNA were placed into a hybridisation tube with the hybridised DNA facing inwards and prehybridised for 4-6 hrs at 42°C with 12.5 ml of pre-warmed hybridisation solution (Table 2.10) to which 100 µg/ml denatured salmon sperm DNA was added. The denatured radioactive probe was added with fresh hybridisation solution and incubated overnight at 37°C. The next day the membranes were washed at RT with washing solution (Table 2.10) for 10 min. A more stringent wash with pre-heated washing solution was carried out at 50°C depending on the radioactive signals picked up by a hand monitor and exposed to a BioMax MS-1 film (Kodak) together with an intensifying screen (Kodak) for amplification of the signal at -80°C

Table 2.10: Compositions of pre-hybridisation- hybridisation and washing buffer

Reagents	**Compositions**
20x SSPE buffer	3M NaCl, 0.2M NaH_2PO_4 x H_2O, 25mM Na_2EDTA, 65mM NaOH, ddH_20 (pH 7.4). sterilised by autoclaving
20 x SSC	3M Nacl, 0.3 M Na Citrate, H2O, pH 7.0
Washing buffer	2 X SSC in 0.1% SDS
Formamid buffer	Formamid (Sigma), 20x SSPE buffer, 10% SDS, 100 X Denhardt solution, ddH_20

2.7 Generation of chimeric mice from targeted ES cells

ES cells, which were identified as positive for homologous recombination were injected into host blastocysts and implanted into pseudo-pregnant foster mothers at the Transgenic Core Facility, Dresden, Germany.

2.8 Cardiotoxin (CTX) injection

Injury was performed by injecting 50µl of 10 µM CTX along the whole length of the TA muscle under general anaesthesia with isofluorane.

2.9 Dissection of mice

Mice were sacrificed by a schedule-1 method according to the Home office license guidelines. An incision was made over the hindlimbs (HL) to carefully remove the skin and expose the muscles of interest. Each muscle was individually isolated with the tendon and stretched on parafilm and secured with dissecting needles. It was then processed for post fixation in PFA or frozen for 1 minute in liquid nitrogen cooled isopentane.

For isolation of embryos, the pregnant female was sacrificed and embryos were separated and washed in PBS solution. The hind limbs of the embryos were either processed for cryo sectioning or for paraffin embedding. The diaphragms of the embryos were care fully dissected and processed for whole mount immunostaining.

2.10 Histology

2.10.1 Post fixation of tissue for cryo sectioning

Muscles were incubated in 2% PFA solution for 4 hours at 4^0C. The PFA solution was replaced by PBS (Table 2.11), and incubated overnight with regular changes. The next day PBS was replaced by 5% sucrose in PBS solution for 2-4 hours with regular changes and then replaced by 20% sucrose solution in PBS over night before freezing for cryo sectioning.

Table 2.11: Composition of Phosphate buffered Saline

Reagent	**Composition**
Phosphate buffered Saline 10x pH 7.4	1.37M NaCl, 27mM KCl, 100mM Na_2HPO_4, 18mM KH_2PO_4, 5mM $MgCl_2 \cdot 6H_2O$

2.10.2 Cryosectioning

Frozen tissues from mice were mounted with OCT to the specimen holder. The temperature of the sample was maintained at -24 while the blade temperature was maintained at -26 and 10µm thick sections were collected on TESPA (3'aminopropyl-triethoxy silane) coated slides. Every fifth section was collected onto an independent slide, which was used to obtain an overall representation of the muscle.

2.10.3 Preparation of Diaphragm for paraffin embedding

After isolating the diaphragms from Itga5cKO and control mice at post natal day 3 (P3), they were washed with PBS and were dehydrated through the series of increasing concentrations of ethanol at RT. At the beginning, the samples were immersed in 30% ethanol for 1-2 hours changing to 50% ethanol and finally to 70% ethanol. The diaphragms were stored in 70% ethanol until processed for paraffin embedding.

2.10.4 Paraffin embedding of diaphragms

Diaphragm which were stored in 70% ethanol were then placed in the plastic cassettes and set up in a tissue preparation machine (LEICA TP1020) on the pre set program.

90% ethanol	1 hr
95% ethanol	1 hr
100% ethanol	1/2 hr
100% ethanol	1/2 hour
100% ethanol	1/2 hour

Diaphragms were then cleared of any remaining ethanol by immersing in histoclear (Fisher) solution for 30 minutes and repeating it for 3 times before adding it to molten paraffin. Samples were then rotated through 3 metal containers containing molten paraffin at 65^0C. Once this process is over the diaphragms were embedded on embedding station (Microm EC350-2). All cassettes were placed in a wax bath in the embedding station and removed from their cassettes individually before placing into wax blocks. A mold was half filled with hot wax and the tissue was orientated within the wax and the base mould is placed on the cold plate to set. Paraffin blocks were stored at 4^0C before sectioning on microtome (Microm HM355S).

2.10.5 Microtome sectioning

To set up the microtome the machine is filled with dH_2O to warm to 40^0C small amount of "STA-ON", a tissue section adhesive from Surgipath was added to improve the tissue collection on the precoated slides. Paraffin block was placed on the pre cooled tissue holder before sectioning at 10-µm thicknesses. Slide was left to air dry before storing them at room temperature. Samples were then stained with Hematoxylin and Eosin dyes.

2.10.6 TESPA (3'aminopropyl-triethoxy silane) coating of the slides

Slides were pre-coated with the adhesive TESPA (Sigma) as described in Table 2.12. Slides were then dried at 55^0C and stored at RT until used.

Table 2.12: TESPA coating solutions

Reagents	**Incubation period**
Acetone	30 sec
2% TESPA in acetone	1 min
Acetone	Quick immersion
Acetone	Quick immersion
ddH_2O	Quick immersion

2.10.7 Hematoxylin and Eosin staining

Eosin Y (Sigma-Aldrich) was freshly prepared by making a 0.1% solution in distilled water and adding a few drops of glacial acetic acid; Mayer's hematoxylin (Merck) was 1:1 diluted with ddH_2O. Sections were submerged in freshly filtered hematoxylin for 3 minutes. The sections were then washed with cold running tap water for 10 minutes before they were submerged into freshly filtered eosin for 30 seconds to 1 minute before dehydration with increasing ethanol concentration. Samples were then treated twice in histoclear for 7 to 10 minutes and mounted using DPX (Fisher), protected with a cover slip and left to air dry for 15 to 20 minutes.

2.10.8 Oil Red O staining

Oil Red O staining was performed to confirm the deposition of adipose tissue in and around the muscle tissue. The stock solution was prepared by dissolving 300mg of Oil red O powder in 100mls of 60% isopropanol over night. The stock solution is stable for up to one year and sored at 4^0C until to be used for staining. The working solution was made by mixing 3 parts of Oil Red O stock solution with 2 parts of ddH_2O, which was then incubated at RT for 10 min. Working solution was then filtered through a 0.2µm filter before using it for staining. 10µm thin muscle sections were immersed in working solution of Oil Red O and incubated for 10-12 minutes at 60^0C before washing under the running tap water for 10 min. The slides were then rinsed with 60%isopropanol and mounted using Galvatol mounting medium.

2.10.9 X-gal staining for detection of LacZ

X-gal staining for β-galactosidase activity was used to detect expression of the LacZ fusion gene. X-gal staining was carried out on muscle sections of various thickness (10µm -20µm). Muscle sections were fixed for 30 minutes in fixation buffer (Table 2.13) before washing them in wash buffer (Table 2.13) for 15 minutes for 3 times. Fresh X-gal staining solution was prepared from core X-gal buffer (Table 2.13) by addition of X-gal stock solution at the concentration of 50mg/ml. the solution was filtered before use on the sections. Muscle sections were then incubated at 37^0C untill the LacZ staining was visible. Staining was stopped by washing the sections in wash buffer, before mounting with them with Gelvetol mounting medium.

Table 2.13: Reagents for X-gal staining

Reagents	**Compositons**
0.1 M Phosphate buffer	NaH_2PO_4, Na_2HPO_4, ddH_2O
Fixation buffer	5mM EGTA, 2mM $MgCl_2$, 0.2% glutaraldehyde, 0.1M phosphate buffer
Wash Buffer	2mM $MgCl_2$, 0.1M phosphate buffer
X-Gal core solution	2mM $MgCl_2$; 5mM K4Fe (CN) 6-3H_20, 5mM K3Fe (CN) 6-3H_2O, 0.1M phosphate buffer
X-gal Stock solution	500mg X-gal, 10 ml dimethylformamide

2.10.10 Immunohistochemistry

Sections were rehydrated in PBS for 10 minutes before fixing with 1% paraformaldehyde (PFA) (Sigma) in PBS for 10 minutes at room temperature in a humid chamber. Three washes of PBS with 0.1% Tween-20 (PBS-T) for 5 minutes were performed after the PFA fixation. Slides were then permeabilised in methanol at -20^{o}C for 8 minutes and then washed three times in PBS-T for 5 minutes. Non-specific binding was blocked using 5% Normal Goat Serum (NGS) (Invitrogen) diluted in PBS-T for 90 minutes at 37^{o}C in a humid chamber. Primary and secondary antibodies (Tables 2.14 (a) and (b)) were prepared and diluted in 2% NGS in PBS-T.

Table 2.14(a): Primary antibodies used for immunohistochemistry

Protein of interest	**Primary antibody**	**Dilution (in 2% NGS)**	**Manufacturer**
Nidogen	U13+ (anti-rabbit)	1:2000	In house
Laminin α2	LNα2	1:20	Sorokin
Integrin α7B	U12+ (anti-rabbit)	1:400	In house
Integrin α7B	U31+ (anti-rabbit)	1:400	In house
Integrin β1	U49+(anti-rabbit)	1:400	
Integrin β1D	U30+(anti-rabbit)	1:400	In house
Integrin α6	GOH3	1:10	In house
Integrin α5	CD49e	2.5µg/ml	Pharmingen
Integrin αv	CD51	5µg/ml	Pharmingen
Lectin	FITC	1:500	Sigma

Table 2.14(b) Secondary antibodies and nuclear stain used for immunohistochemistry

Secondary antibody	**Dilution (in 2% NGS)**	**Manufacturer**
Goat anti-rabbit Cy2	1:200	Jackons
alpha SMA- mouse mAb-Cy3	1:400	Sigma
Goat anti-rabbit Cy3	1:800	Jacksons
Goat anti-rat 647	1:200	Jackons

Nuclear Stain	**Dilution (2% NGS)**	**Manufacturer**
4- (Amidinophenyl)-6-indolecarbamidine dihydrochloride (DAPI)	1:500 (1µg/µl)	Sigma

2.10.11 Preparation of Gelvatol mounting medium

10ml solution of 0.1M KH2PO4.H2O was adjusted to 7.2 by addition of 0.1M $Na_2HPO_4.H_2O$. The resulting solution was then diluted 1:10 to make a 0.01M solution to which 20gms of Polyvinyl alcohol (Gelvatol, Type II. cold water soluble, Sigma P-1836) and 0.65gm of NaCl (0.14M) were added. The mixture was left on the stirrer to mix over night before adding 40ml of Glycerin (Sigma). Next day the mixture was transferred in two 50ml falcons and centrifuged at 14000rpm for 15 minutes. Supernatant was collected and anti-bleaching agent DABCO (Sigma) was added at the concentration of 25µg/ml. Syringes were filled with the Gelvetol avoiding the formation of air bubbles and were stored at -20^0C until used for mounting.

2.11 Microscopy

Immunostained cryosections were analysed with a Zeiss upright fluorescent microscope. Images were captured with a monochrome camera (Axiocam HR). H&E stained images were captured using the colour camera (AxioCam HRc, Zeiss) usingAxiovision software version 4.8.2.

2.12 Western blot analysis

2.12.1 Preparation of Muscle Lysates

GC (Gastrocnemius), TA (Tibialis Anterior), Sol (Soleus) and EDL (extensor Digitorum longous) muscles were dissected and snap frozen in liquid nitrogen and stored in -80 ºC. For preparation of muscle lysates, the tissue was immersed in 2ml pre-cooled RIPA buffer (Table 2.15) and homogenised on ice. Tissue lysates were centrifuged for 5 minutes at 14000rpm. The supernatant was centrifuged for a further 60 minutes at 35,000 rpm at 4°C. The protein concentration was quantified using the Pierce BCA Protein Assay kit using bovine serum albumin as a standard according to the supplier's protocol. The samples were then stored at -80 ºC.

Table 2.15: Reagents used for western blotting

Reagent	Components
Tris buffer saline (TBS) 10x pH 7.6	50mM Tris-Cl, 150mM NaCl
RIPA buffer 5x	100mM Tris (pH 7.4), 750mM NaCl, 5% NP40, 0.25% Triton-X 100 and 2.5% Na-Deoxycholate
Sample buffer 5x pH 6.8	5% SDS, 25% glycerine (v/v), 200nM Tris (v/v), and bromophenol blue
Running buffer 10x	1.92M glycine, 0.25M Tris, and 1% SDS diluted in ELGA water
Transfer buffer stock 10x pH 9.2	29.9g glycine, 58g Tris, and 3.7g SDS dissolved in ELGA water

2.12.2 Immunoblotting

20μg muscle lysates in 1x sample buffer were denatured at 95°C for 5 minutes. SDS-PAGE 5-15% or 8-18% gradient gels were used to separate samples at 200V under non-reducing, or reducing (8-18%) conditions by the addition of 5% β-mercapterethanol. Biorad broad range molecular range marker was used as standard. Transfer onto PVDF membranes was carried out in 10mM sodium borate overnight at 200mA at 4°C. Protein marker was identified by Ponceau S (2.5% Ponceau S in 5% Trichloroacetic Acid) staining. After blocking in 1x Sigma blocking Buffer B6429 (for quantification) or 2% NGS in PBS-T (all other), the appropriate affinity-purified polyclonal primary antibodies were applied at 1:1000 dilution in 1x Sigma block or 2% NGS PBS-T and incubated 1 hour at room temperature. Membranes were then washed three times in PBS-T and then incubated with IR-dye conjugated (for quantification blots) or goat anti-rabbit secondary antibodies conjugated to horseradish peroxidase (HRP) together with actin antibody as a loading control. Membranes were then washed two times with PBS-T and once in PBS. Protein bands were visualised with ECL using a CCD camera (LAS 1000, Fujifilms) or using the Odyssey Li-Cor scanner (for quantification).

Table: 2.16: Composition of gradient gels used during western blotting

		Separating Gel		Separating	Gel
Components	**Source**	**5% (ml)**	**15% (ml)**	**8% (ml)**	**18% (ml)**
ELGA water	Water polisher	16.9	6.9	13.9	3.9
30% acryl-bisacrylamide	BIO-RAD	5	15	8	18
Separating buffer 4x 1.5M Tris, 0.4% SDS pH8.8	In house	7.5	7.5	7.5	7.5
10% Ammonium persulfate	Melford	0.06	0.05	0.06	0.05
TEMED	Fisher Scientific	0.011	0.011	0.011	0.011

		Stacking gel	
Components	**Source**	**3% (ml)**	**4.5% (ml)**
ELGA water	Water polisher	13	12
30% acryl-bisacrylamide	BIO-RAD	2	3
Stacking buffer 4x 0.5 M Tris, 0.4% SDS pH 6.8	In house	5	5
10% Ammonium persulfate	Melford	0.05	0.05
TEMED	Fisher Scientific	0.010	0.010

2.12.3 Quantification of Immunoblot

Quantification of integrin α7, β1 and actin expression was calculated from immunoblots, using the Odyssey System. Two infrared fluorescent channels can be detected, meaning two target proteins can be detected simultaneously, in the same immunoblot. Actin was used in all cases as a loading control. For each sample, the fluorescence intensity of both the integrin α7/β1D and actin bands was measured by manually outlining the immunoblot band. The background was automatically subtracted from this measurement. All parameters were constant for all immunoblot band measurements. The integrin α7/β1D value was then divided by that of actin, to normalise any loading discrepancies. When quantifying overexpression for the transgenic strains, all (normalised) values for integrin α7/β1D were then divided by the (normalised) value of the wild type. This gave the wildtype value an assigned value of 1, and all overexpressing strains a fold increase from this value. Immunoblots samples were run for two mice from each strain and each was repeated at least three times and the average values were calculated.

2.12.4 Immunoprecipitation of muscle lysates

1mg of total protein extract was pre-cleared for 2 hours with 50µl of Protein Sepharose A (GE-Healthcare). The supernatant was used for precipitation with 5µL/500µL of the appropriate affinity purified rabbit polyclonal antibody in a total volume of 500µl 1X RIPA lysis buffer and left to rotate overnight. 50µl of Protein Sepharose A was added and incubated on a rotating wheel for 2 hours. Samples were briefly spun down and the supernatant discarded, the sepharose pellet was washed 3 times in 500µl 1X RIPA buffer and briefly centrifuged. After final washing the supernatant was removed using a Hamilton syringe and the antigen was eluted with 100µl freshly made treatment buffer. Samples were then denatured at 95°C for 5 minutes and 5µl of sample was run on 5-15% or 8-18% SDS-PAGE gradient gels. Remaining samples were then stored at -20 ºC after quick freezing on dry ice.

2.13 Animal maintenance

Mice were handled in accordance with Home office regulations. All mouse lines were kept under specific pathogen-free conditions in individually-ventilated cages and were routinely screened for common mouse pathogens. Mice were weaned and genders were separated around 3 to 4 weeks of age. At this stage, they were ear tagged, and ear biopsies were used for genotyping. Mice that were not needed where humanely culled by a schedule 1 method. For genotyping embryos, pregnant female mice were sacrificed by schedule 1 method and the embryos were removed and analysed for phenotype. The tail tissue from embryos was taken for genotyping by PCR.

2.14 Isolation of pericytes from mouse tissue

This technique was performed in collaboration with Dr Zhou. ROSA-td Tomato mice were dissected under dissecting microscope and tissues from muscle and peritoneum were carefully isolated and washed with sterile PBS several times. Tissue samples were then sliced in to small pieces before incubating in to Collagenase (Col type II, 3mg/ml) for 20 minutes. The tubes containing tissue were gently agitated after every 5 minutes to facilitate complete dissociation of the tissue by Col type II. Samples were mixed by passing through 5ml pipette before incubating for further 20 minutes. After this process, disintegrated tissues were passed through 40µm cell strainer and

centrifuged at 1600 rpm for 20 minutes. Supernatant was discarded and cell pellet was suspended in DMEM 10% FCS medium before culturing them on gelatin-coated plates overnight. Next morning cells were washed by PBS to remove the loose cells before changing medium and incubated further until 100% confluence. Medium was changed on daily basis.

2.15 Fluorescence Activated Cell Sorting (FACS)

This technique was performed in collaboration with Dr Zhou. Cells were grown on gelatin-coated plates until they reach confluence. Cell were then detached from the plates using 5mM EDTA before splitting them in two 15 ml falcons, one will serve as control for FACS staining. Cells were centrifuged at 1000 rpm for 4 minutes, supernatant was discarded and cells were resuspended in 5ml PBS with 5%FCS for further centrifugation. Cell pellet were then resuspended in 100µl PBS with 5%FCS. At this stage one set of cells were stained with varied cell surface markers (CD140b, CD31, CD45) conjugated with different fluorochroms, while second set was labeled with relevant IgG antibody to serve as a negative control. Cells were incubated for 45 min on ice with intermittent mixing before washing twice with 5ml of 5% FCS in PBS. Cells were resuspended in 5% FCS in PBS before sorting them on FACS machine (BD FACS Aria II).

Chapter 3

Integrin α5β1 in development and adult Skeletal Muscle

Integrin α5β1 deficiency leads to embryonic lethality before muscle development begins, due to mesodermal defects, most prominent in the posterior region of the embryo (Yang and Hynes, 1993). To study the function of integrin α5 in skeletal muscle we made use of conditional knockout (cKO) integrin α5 fl/fl and heterozygous integrin α5 +/- knockout mice in combination with Cre recombinase driven by the muscle specific promoters, Human α-Smooth muscle actin (HSA) and Pax3.

3.1 Generation of integrin α5 conditional knockout in skeletal muscle.

Integrin α5 mutant mice were a kind gift of Prof R.O Hynes (MIT, Boston, USA), which were generated in his laboratory with the gene targeting strategy described in figure 3.1.

To generate integrin α5 fl/fl (Itga5), the targeting vector was designed in such a way that exon 1 was flanked by two LoxP sites, while the neomycin cassette was flanked by two frt sites. After homologous recombination in ES cells mice heterozygous for the targeted allele were generated and then crossed with Flp deleter mice to excise the Neo cassette. These α5 fl/fl animals are normal and used for cross breeding with mice in which Cre is driven by a tissue specific promoter. In addition we obtained mice, which carried a null allele for integrin α5 (Itga5 +/-).

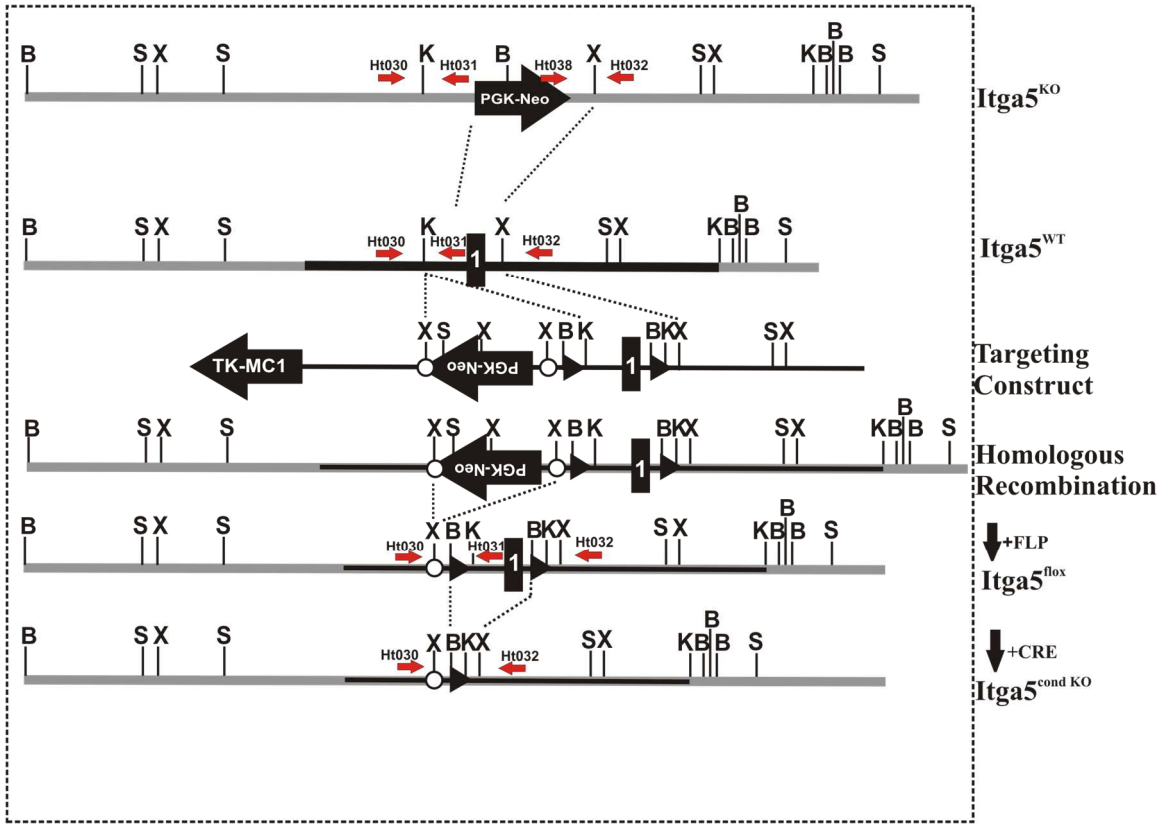

Figure 3.1: Design of the targeting vector for homologous recombination in integrin α5 mice. *Genomic organisation of the integrin α5 knockout (Itga5^{KO}) and Wildtype (Itga5^{WT}) alleles is shown in the first two constructs (top two). The targeting construct for the conditional integrin α5 knockout allele (middle) and the resulting targeted allele after homologous recombination (upper bottom) is shown. Mating with Flp recombinase transgenic mice removes the neomycin selection cassette located between frt sites (lower bottom). Breeding with Cre recombinase expressing mice will excise exon 1 which is flanked by two loxP sites, resulting in conditional loss of integrin α5 (Itga5$^{cond\ KO}$) (bottom last).*

3.1.1 Breeding strategies to generate integrin α5 conditional null mice

In order to understand the role of integrin α5 in skeletal muscle, we decided to delete integrin α5 specifically in skeletal muscle. To obtain these animals we crossed heterozygous Itga5$^{+/-}$ mice with animals expressing Cre recombinase under the control of HSA promoter (figure 3.2 A), which becomes active at embryonic day 9.5 (Asante, E.A., et al., 1993) and predominantly active in differentiating skeletal muscle (Miniou, P., et al., 1999). This created Itga5 $^{+/-\ HSA\text{-}Cre}$ mice, which were then crossed with Itga5 fl/fl females to obtain Itga5 fl/-$^{HSA\text{-}Cre}$ mice (figure 3.2 B).

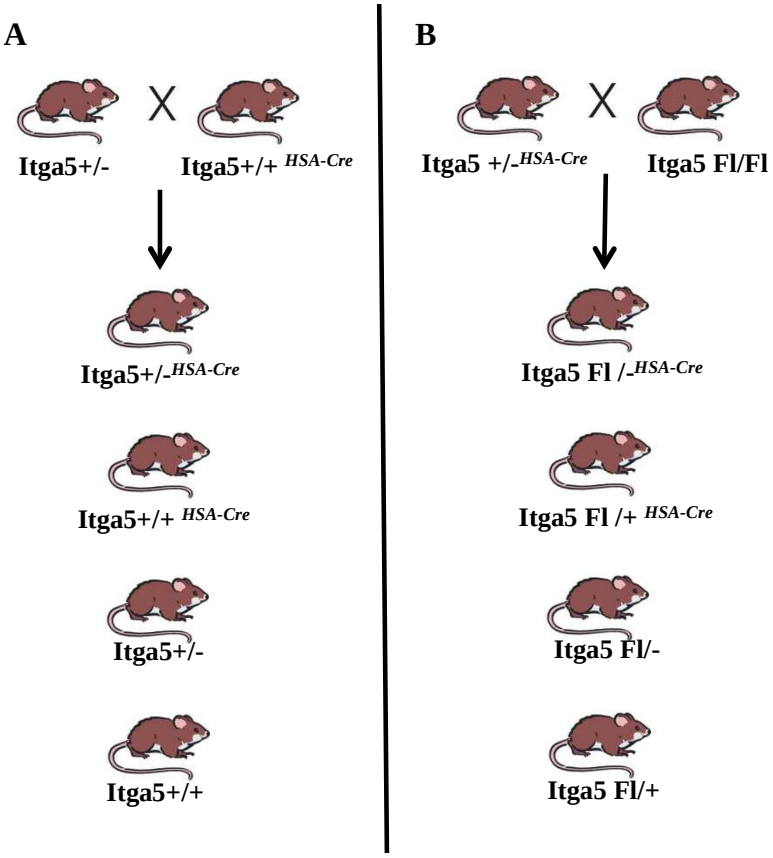

Figure 3.2: The breeding strategy applied to obtain Itga5 cKO mice. *(A) Itga5+/- mice were crossed with mice expressing Cre recombinase under the control of the HSA promoter to generate Itga5+/-$^{HSA\text{-}Cre}$ mice, which were then crossed (B) with Itga5 fl/fl mice to generate Itga5 fl/-$^{HSA\text{-}Cre}$ mice in which the expression of integrin α5 is knocked out in skeletal muscle.*

3.1.2 Genotyping by PCR analysis of integrin α5 cKO mice

Tail biopsies of the experimental mice were processed for preparing DNA lysates which were then used for genotyping by polymerase chain reaction (PCR) using primers HT030-dwn, HT031-wt/flox up, HT032-KO-up, HT038-Neo dwn (Table 2.7) and Figure 3.1). The primer combination HT032 and HT038 gave a 1KB band specific for the Itga5^{KO} allele. The combination of HT030 and HT031 primers resulted in a 550bp band for the WT allele in integrin α5 heterozygous animals but detected also the presence of the floxed allele (fl) by the appearance of a 700bp band. Finally, excision of exon 1 by Cre- recombinase was confirmed by the presence of a 500bp band, which was the product of the primer pair HT030 and HT032 (Figure 3.3). Cre-specific primers were used to confirm the presence of HSA-Cre.

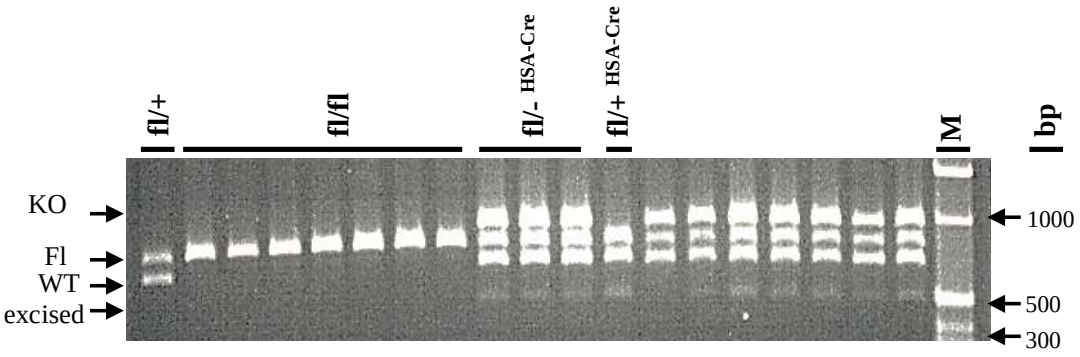

Figure 3.3: Genotyping of Itga5^{cKO} mice. *Genotyping was carried out by touchdown PCR programme using primers HT030, HT031, HT032 and HT038. "Fl" = Floxed allele (exon 1 of Itga5 flanked by 2 loxP sites), while "WT" = wild type allele, M= marker (1KB ladder). After Cre-mediated recombination, exon 1 was excised which was visualised as 500bp band in samples 9-11.*

We observed a 500bp band corresponding to excised allele, which is likely due to small amounts of muscle tissue present in the tail biopsies. We therefore decided to perform the PCR on the DNA samples obtained from individual muscle like GC, TA; Sol and EDL (figure 3.4). This allowed us to visualise the amount of excised Fl allele in individual muscles.

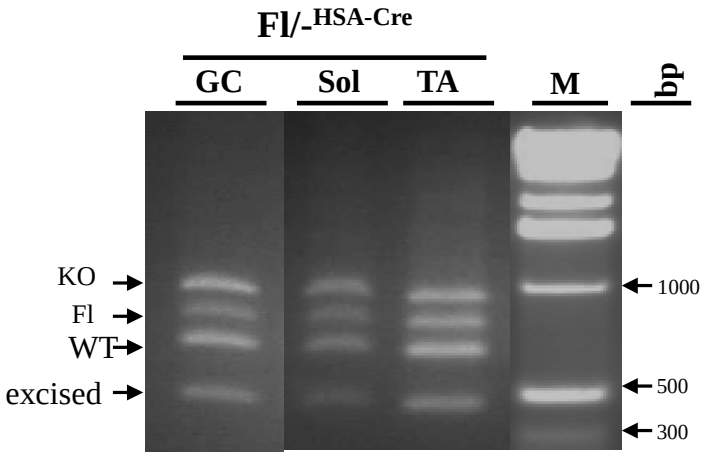

Figure 3.4: Representative PCR results from DNA isolated from individual muscle. *DNA was isolated from GA, TA and Sol muscle isolated from Itga5fl/-$^{HSA\text{-}Cre}$ mice and PCR was carried out using the specific primer combinations. The KO allele was identified as a 1000bp band while the floxed allele (FL) was observed at 700bp. The wild type allele (WT) gave a 550bp band while the excised allele showed at 500bp.*

The amount of excision was quantified by calculating the ratio of the intensity of the floxed and excised allele by Image J analysis software. There was almost 50% excision observed in all the muscle in Itga5 fl/-$^{HSA\text{-}Cre}$ mice. The representative table with the actual values obtained from Image J analysis is documented in table 1(Appendix I)

3.1.3 Histological analysis of adult integrin α5 $^{HSA\text{-}Cre}$ mice

Itga5 fl/-$^{HSA\text{-}Cre}$ mice were born at the Mendelian ratio, and were viable and fertile. There was no apparent abnormality. It was therefore crucial to determine the effects of integrin α5 deficiency in muscle. To answer this question skeletal muscle of integrin α5 cKO and control mice were analysed by histology. As controls we choose the following genotypes, Itga5 fl/+ $^{HSA\text{-}Cre}$, Itga5 fl/fl and Itga5 WT. Experimental mice were sacrificed at four weeks, three months and one year of age. Whole hind limbs (HL) were dissected and frozen for cryosectioning as described in materials and methods. Cryosections of 10µm of thickness were taken and analysed by Hematoxylin and Eosin (H&E) staining to visualise any signs of muscle damage. In addition we also analysed the diaphragm to observe any changes in phenotype.

Often early signs of muscle degeneration are visible at four weeks of age. However, muscle sections of 4-week-old Itga5fl/-$^{HSA\text{-}Cre}$ mice had no obvious signs of muscle damage when compared with Itga5fl/+$^{HSA\text{-}Cre}$ littermate controls (Figure 3.5). At

the age of three months the muscle phenotype did not change and the morphology of the muscles was comparable to that of controls. There was no obvious difference in muscle fibre diameter observed. However, we observed some centrally located nuclei (CLN) particularly in the GC muscle and therefore we decided to quantify the number of fibres with CLN in both Itga5^{cKO} and control mice. These experiments were repeated for three different sets of mice at four weeks and three months of age to eliminate any biological differences between individual mice.

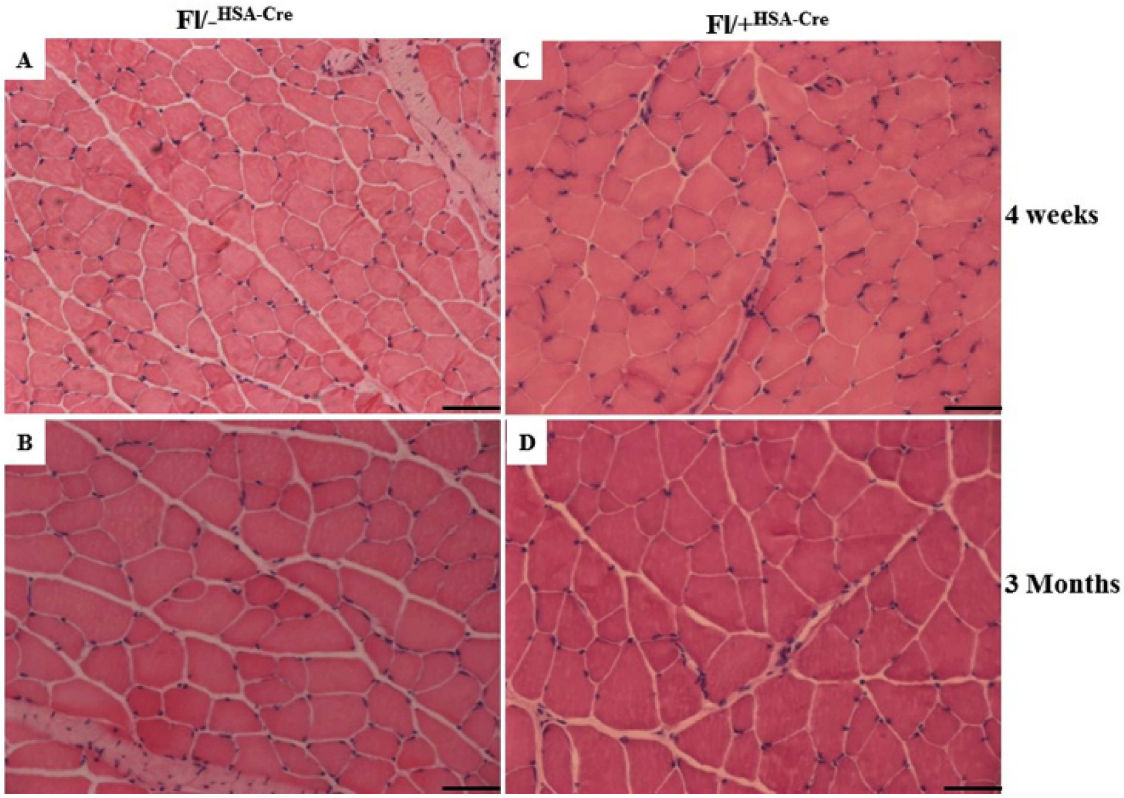

Figure 3.5: Representative images comparing muscle sections of Itga5 ^{cKO} and littermate controls: *H&E staining of 10µm cryosections of GC muscle reveled no major signs of muscle damage in Itga5 fl/-$^{HSA\text{-}Cre}$ mice at 4 weeks and 3 months of age (B, D) when compared with age matched Itga5 fl/+$^{HSA\text{-}Cre}$ mice (A, C). Bar, 50µm.*

The numbers of CLN were counted from sections, which were 100µm apart from each other. The mean of two values was then taken for statistical analysis. In GC muscle we observed a slight increase (0.8%) of fibres containing CLN compared to control mice (0.6%). However, there was no statistical significant difference between

both genotypes. In the TA and Sol muscles the number fibres with CLN (0.5%) was consistent in both sets of mice (Figure 3.6).

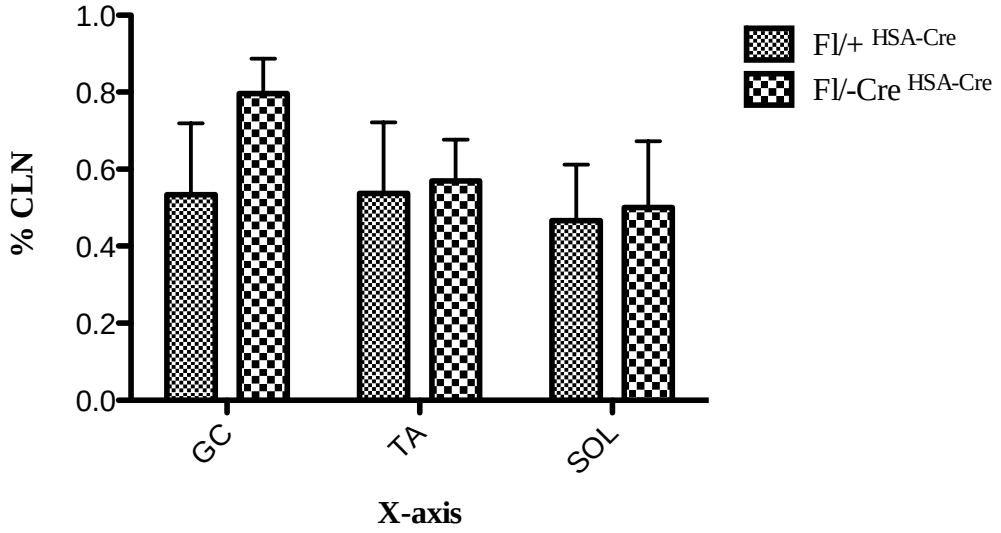

Figure 3.6: Graphical representations of fibres with CLN in Itga5^{cKO} and control mice. *Graph shows the percentage of fibres with CLN in GC, TA and Sol muscles of Itga5 fl/-$^{HSA\text{-}Cre}$ and fl/+$^{HSA\text{-}Cre}$ mice. n=3 and p=0.9451*

As there were nophenotypic abnormalities observed in young mice, we decided to analyse another cohort of integrin α5$^{HSA\text{-}cre}$ mice at 12 months of age. Surprisingly Itga5fl/-$^{HSA\text{-}Cre}$ mice showed some signs of muscle degeneration. H&E staining of the muscle cryosections of 12-month-old Itga5 fl/-$^{HSA\text{-}Cre}$ mice displayed centrally located nuclei and smaller fibre diameter when compared with age matched Itga5 fl/+$^{HSA\text{-}Cre}$ (Figure 3.7 A-F). Presence of calcification and fibrosis around the fibres was also prominent in muscle sections of some Itga5 fl/-$^{HSA\text{-}Cre}$ mice (Figure 3.7 C). However, these histological changes were prominent only at a localised area of the GC muscle and not apparent in any other HL muscles.

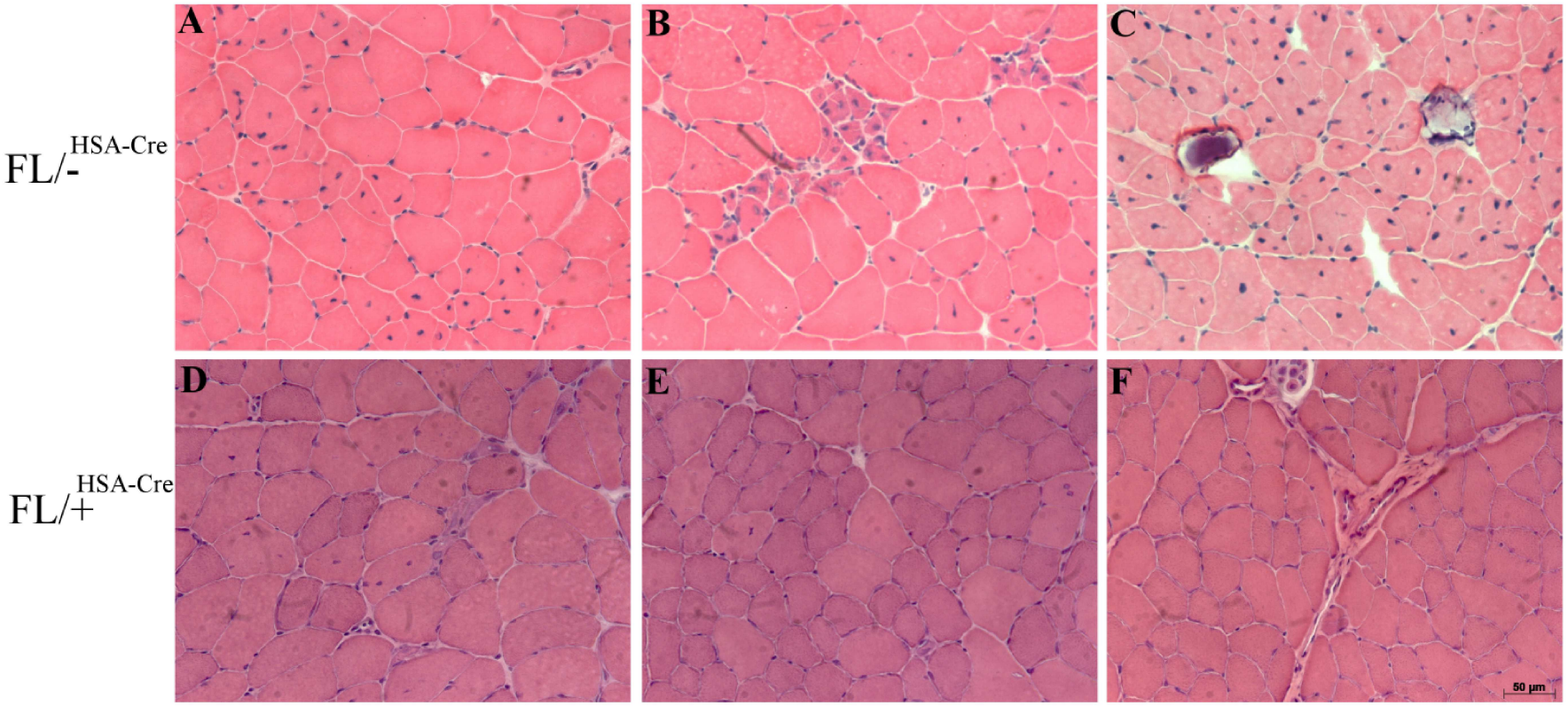

Figure 3.7: Representative images comparing muscle sections of Itga5 cKO and littermate controls. *H&E staining of 10µm cryosections of GC muscles revealed signs of the muscle regeneration in Itga5 fl/-HSA-Cre mice at 12months of age (A-C) when compared with age matched Itga5 fl/+HSA-Cre mice (D-F). Bar,50µm.*

3.2 Investigating the conditional loss of integrin α5 at early stage of muscle development

The results in adult mice can be due to either there is indeed no major muscle phenotype when integrin α5 is deleted when muscle differentiation occurs, or it is inefficiently deleted by Cre driven by the HSA promoter. Since integrin α5 is down-regulated after birth, between day5 and 10 postnatally (Blaschuk and Holland, 1994; Boettiger et al., 1995; Bronner-Fraser et al., 1992) but strongly present before, we decided to determine whether integrin α5 is efficiently deleted by Cre recombinase at early postnatal stages.

3.2.1 Histological analysis of newborn integrin α5 fl/- $^{HSA\text{-}Cre}$ mice

In order to evaluate the phenotype in newborn mice we generated postnatal day 3 (P3) mice through time mating. Plugged females were separated, monitored until they gave birth and pups were genotyped by PCR as described before. The HLs were frozen for cryosectioning and H&E staining was performed on tissue sections and analysed by microscopy.

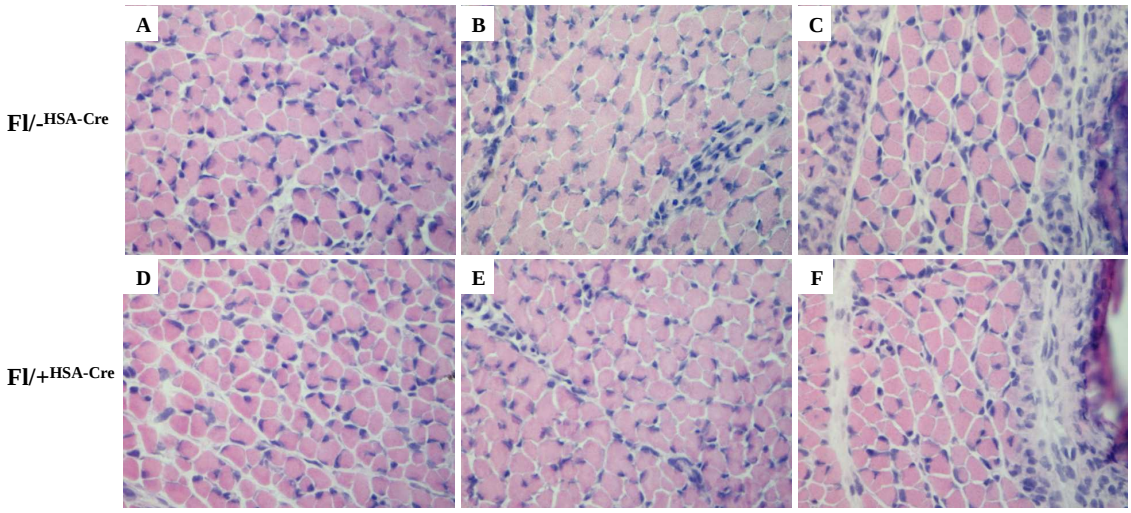

Figure 3.8: Representative images comparing muscle sections of Itga5^{cKO} and littermate controls: *H&E staining of 10μm cryosections of HL muscles revealed no signs of muscle damage in Itga5 fl/-$^{HSA\text{-}Cre}$ mice at postnatal day 3(P3)(A-C), when compared with age matched Itga5 fl/+$^{HSA\text{-}Cre}$ mice (D-F). Pictures were taken at x40 magnification.*

As expected, there were no signs of muscle degeneration in P3 Itga5 fl/-$^{HSA\text{-}Cre}$ mice, due to the loss of integrin α5. The structure of all the muscles including GC, TA, and Sol was normal and there were no gross abnormalities observed when compared with littermate controls. (Figure 3.8, A-F). To confirm the absence of integrin α5 in these mice we performed immunostaining on cryosections from Itga5^{cKO} and control mice (Figures 3.9-3.12).

By double-immunofluorescence analysis we stained for integrin α5 in combination with integrin α7B (Figure 3.9), αv (Figure 3.10), β1D (Figure 3.11) and α6 (figure 3.12) to observe if there was any change in the expression pattern of these integrin, because of the absence of integrin α5. All immunostainings were performed with secondary controls to avoid false positive results (data not shown). Immunostaining with integrin α5-specific antibodies on muscle sections of Itga5^{cKO} mice confirmed the absence of integrin α5, whereas we observed a strong staining for integrin α5 at the MTJ of control mice (Figure 3.9), indicating that integrin α5 had been efficiently deleted. Integrin α7B is strongly expressed at the MTJ but the expression level was not elevated in absence of integrin α5, when compared to control sections (Figure 3.9). Sections were also stained with integrin αv to analyse if there is any compensatory mechanism in place in the absence of integrin α5. However, it was difficult to draw a conclusion from these results as antibodies raised against murine αv are notoriously bad in immunostaining (Figure 3.10). Strong expression of integrin β1D was also observed at MTJ on both the Itga5 cKO and control mice (Figure 3.12).

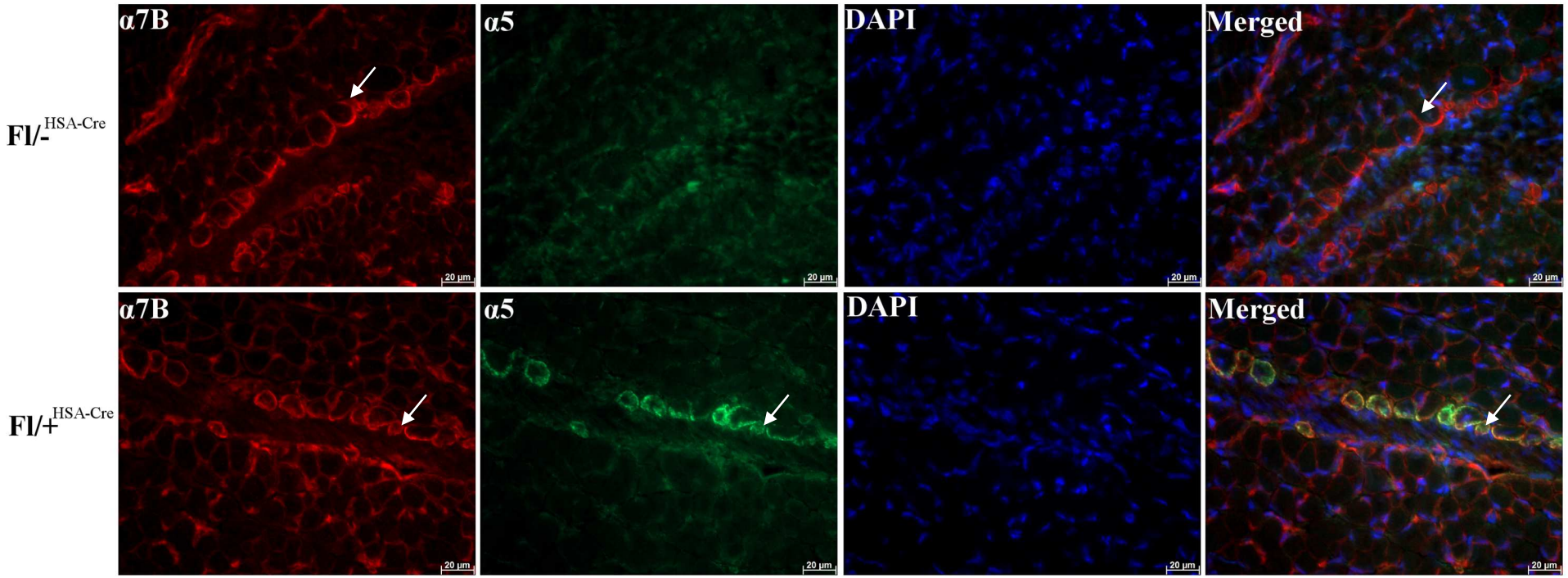

Figure 3.9: Representative images of immunostaining against integrins α7B and α5 in muscle sections of Itga5cKO and control mice. *Immunostaining of 10µm cryosections of HL muscles confirmed absence of integrin α5 expression in Itga5 fl/-HSA-Cre mice (top row) at P3, while integrin α5 is strongly evident at MTJs (white arrow) in Itga5 Fl/+HSA-Cre mice (bottom row). The expression of integrin α7B remained unchanged. Bars, 20µm.*

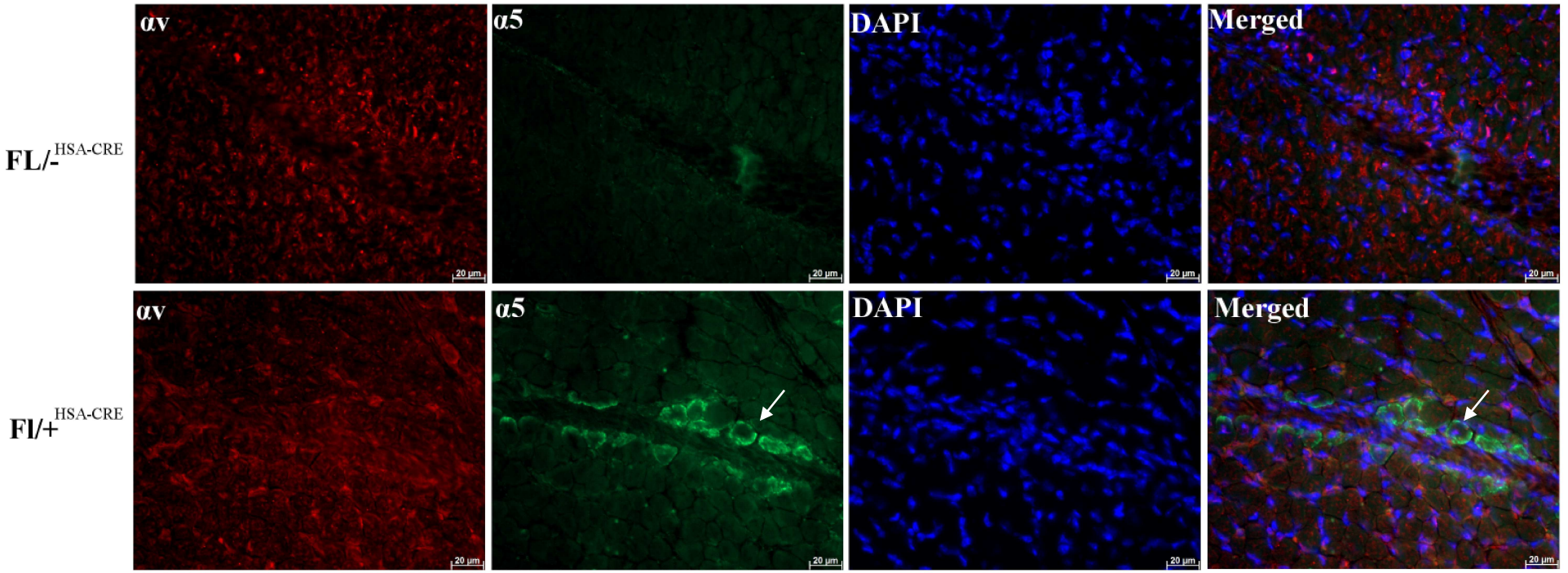

Figure 3.10: Representative images of immunostaining against integrins αv and α5 in muscle sections of Itga5cKO and control mice. *Immunostaining of 10µm cryosections of HL muscles confirmed integrin α5 expression in Itga5 Fl/+$^{HSA\text{-}Cre}$ mice (bottom row) at P3, while there was no evidence of expression of integrin α5 at MTJs (white arrow) in Itga5 Fl/-$^{HSA\text{-}Cre}$ mice (top row). The sections were co-stained with integrin αv. There was no difference in the staining pattern between the two genotypes. Bars, 20µm.*

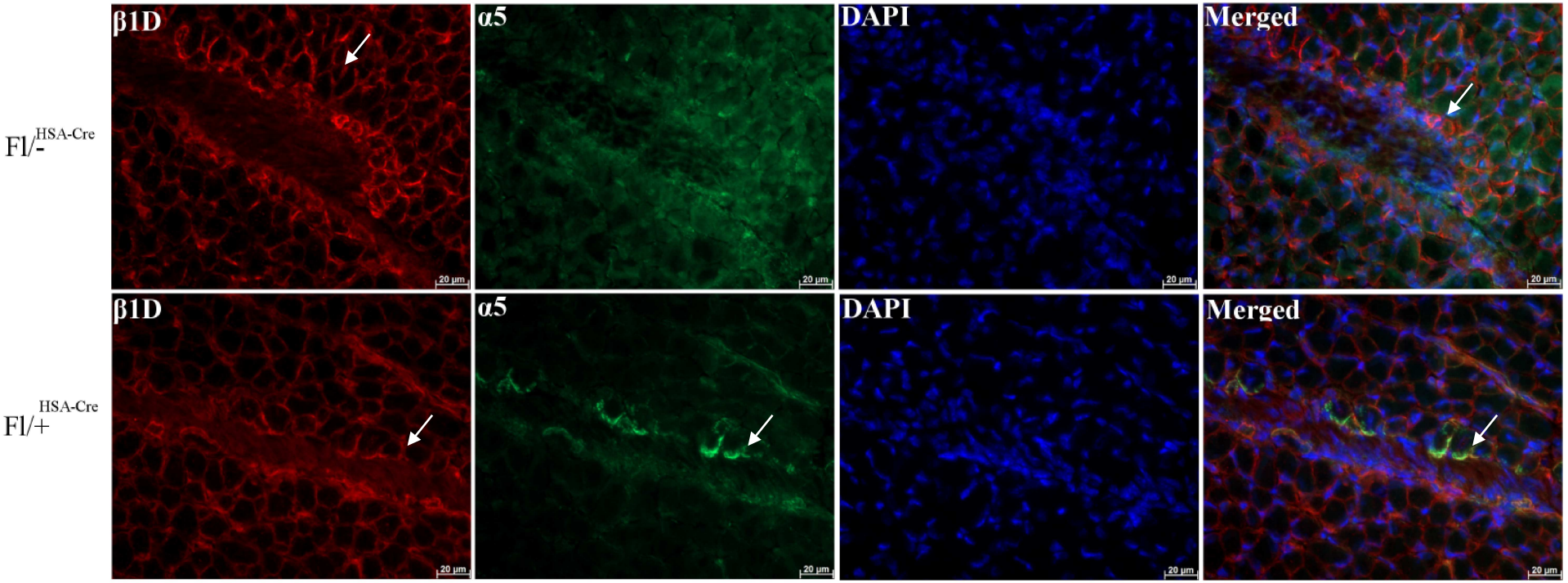

Figure 3.11: Representative images of immunostaining against integrins β1D and α5 in muscle sections of Itga5cKO and Itga5 control mice. *Immunostaining of 10µm sections of HL muscles confirmed presence of integrin α5 in Itga5 Fl/+$^{HSA\text{-}Cre}$ mice along with the strong expression of integrin β1D at MTJs (white arrow). The expression of integrin β1D was also strongly present at MTJs(white arrow) of Itga5 Fl/-$^{HSA\text{-}Cre}$ mice. Bars, 20µm.*

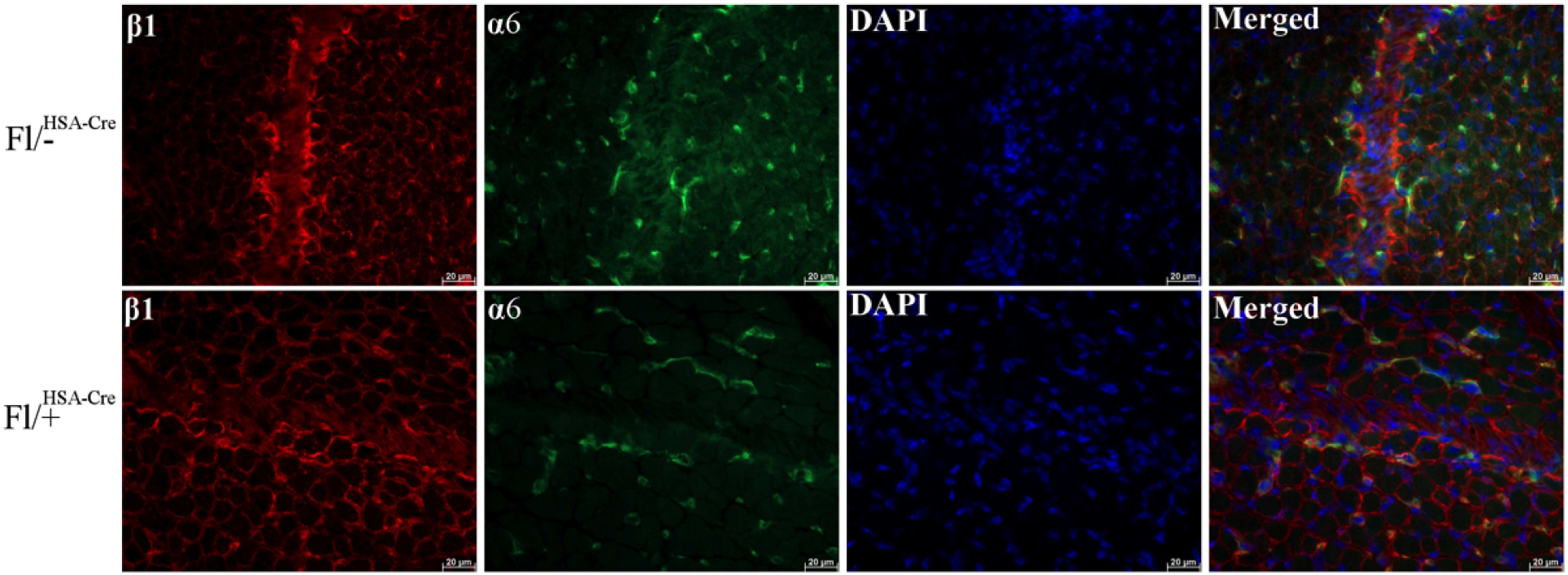

Figure 3.12: Representative images of immunostaining against integrins α6 and β1D in muscle sections of Itga5cKO and control mice. *Immunostaining of 10μm sections of HL muscles confirmed the presence of integrin α6 at capillaries and β1D at MtJs in Itga5 Fl/+$^{HSA\text{-}Cre}$ mice at MTJs, which was not different to cKO mice. Bars, 20μm.*

Integrin α6 is expressed in proliferating myoblasts during skeletal muscle development, but then down-regulated after myotube formation and completely lost in mice by P10 (Blaschuk and Holland, 1994; Nawrotzki et al., 2003). To visualise if there is any increase in expression of integrin α6 in integrin α5 cKO mice, we stained sections with antibodies against α6 and β1D (Figure 3.13). However, we did not see any difference in the expression of either α6 in the absence of integrin α5.

This data suggests that there was no compensatory mechanism by other integrins observed in the absence of integrin α5.

3.2.2 Histological analysis of adult diaphragm of integrin α5 $^{HSA\text{-}Cre}$ mice

In chimeric analysis of integrin α5-/- ES cells it was shown that the diaphragm was affected (Taverna et al., 1998). We therefore analysed the diaphragm from adult mice to look for any abnormalities. Diaphragms from the adult mice were processed for paraffin embedding and sectioning. 10µm thick sections were then subjected to H&E staining (figure 3.13).

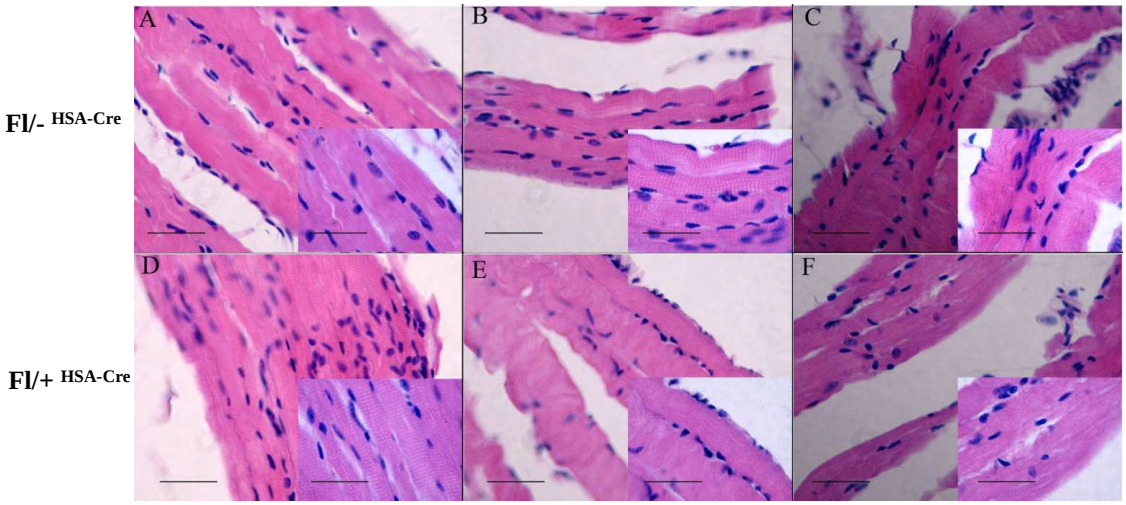

Figure 3.13: Histological analysis of diaphragms of Itga5^{cKO} and control mice. *H&E staining of diaphragms from Itga5fl/-$^{HSA\text{-}Cre}$ mice (A-C) showed no obvious phenotypic changes when compared with Itga5fl/+$^{HSA\text{-}Cre}$ mice (D-F). Bars, 25µm and 10µm for the inserts.*

This showed that there were no phenotypic abnormalities in the diaphragm of Itga5^{cKO} when compared with control mice. Fibres appeared normal and of similar size and nuclei were located at the edge of the fibres (Figure 3.13).

Results so far in to the analysis of integrin α5 conditional KO mice suggests that there was no obvious difference in the muscle phenotype when samples were compared at 4 weeks, 3 months and 6 months of age, but a mild dystrophic phenotype was observed at 12 months of age in the GC muscle. This made us think that there is a possibility that these mice when aged were unable to regenerate the muscle upon stress, suggesting a deficit in the function of regeneration.

3.3 Histological analysis of cardiotoxin (CTX) injected integrin α5 $^{HSA\text{-}Cre}$ mice

To examine the possibility of delayed regeneration in 12 months old integrin α5 conditional KO mice we decided to induce muscle regeneration using myotoxic agent. TA muscle of Itga5 fl/-$^{HSA\text{-}Cre}$ mice, and age matched littermate controls were injected with the myotoxic agent cardiotoxin (CTX) and regeneration capacity was analysed after cryosections were stained for H&E staining (Figure 3.14).

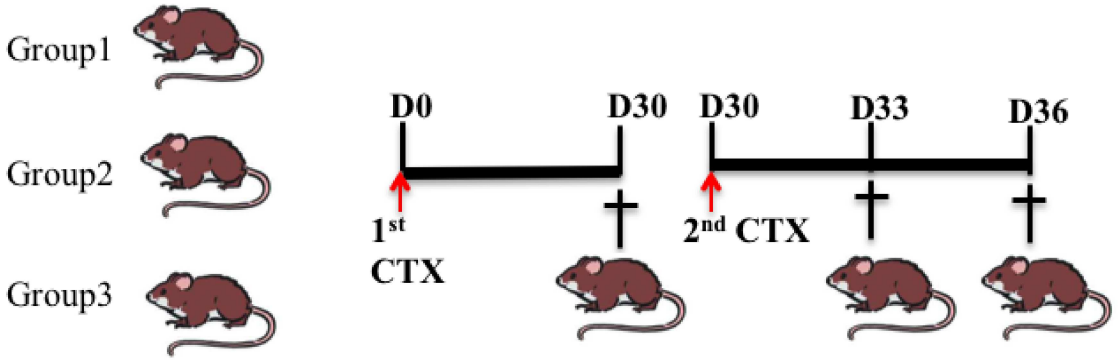

Figure 3.14: Schematic representation of the scheme followed for cardiotoxin (CTX) injections*. To identify the defect in regeneration Itga5^{cKO} and Itga5 control mice, CTX was injected at day 0 (D0) to mice in group 1, 2 and 3.. The muscle was left to recover for 30days. mice from group 1 were dissected and injured and non injured muscles were isolated. The mice from group 2 and 3 were further injected with second dose of CTX and dissected at day 33 (D33), day 36(D36).*

The muscle was left to recover for 30 days. The first set of Itga5 cKO and control mice were dissected at this stage and TA muscle was isolated for cryosectioning. The remaining sets of mice were injected a second time with CTX. The mice were then sacrificed at day 33 and 36 and the TA was isolated for cryosectioning. Cryosections from Itga5 fl/-$^{HSA\text{-}Cre}$ and Itga5 fl/+$^{HSA\text{-}Cre}$ TA muscle from day 30-36 were analysed by H&E staining (Figure 3.15).

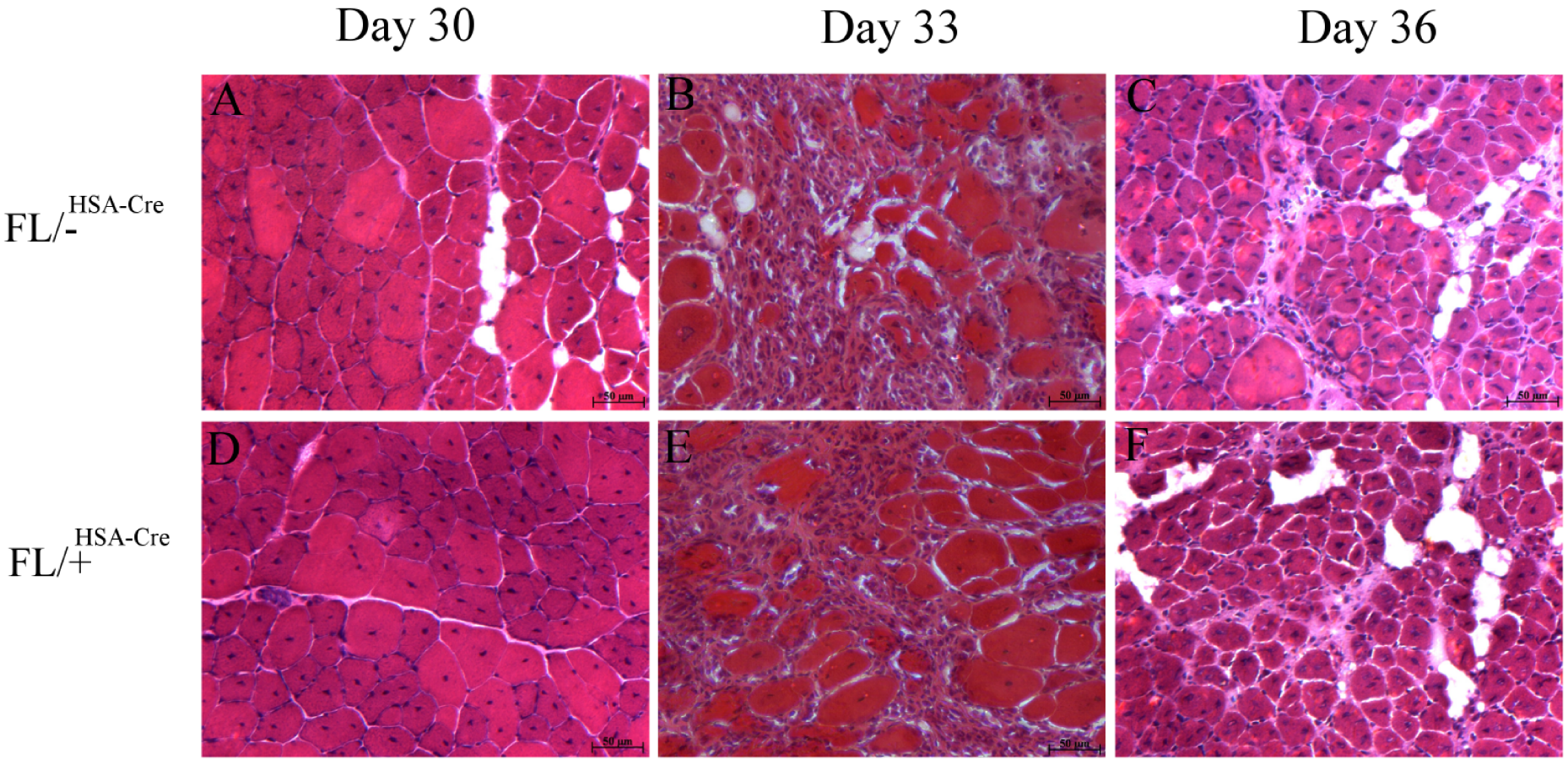

Figure 3.15: H&E staining of double injured Itga5 cKO and control TA muscles. *H&E staining of 10µm transverse sections of TA muscles injured with CTX revealed signs of muscle regeneration in Itga5 Fl/-$^{HSA\text{-}Cre}$ (A-C) and Itga5 Fl/+ $^{HSA\text{-}Cre}$ (D-F) mice. Day30 represents the time point after* the first dosage of CTX while Day33 and Day36 *represent day 3 and 6 after the second CTX administration. Bar, 50µm*

30 days (Day 30) after CTX injection the TA muscle of Itga5fl/-$^{HSA\text{-}Cre}$ mouse showed signs of regeneration with centrally located nuclei (CLN) (Figure 3.15 A) and was not significantly different to Itga5fl/+$^{HSA\text{-}Cre}$ injured TA muscle (Figure 3.15 D). The TA muscles of both Itga5^{cKO} and control mice displayed signs of dystrophy, such as fibrosis and smaller fibre diameter (Figure 3.15 B,C,E,F), but overall, there was no difference between the genotypes. However, we observed that there was possibly more fat deposited in cKO mice 30 days after the first CTX injection as compared to controls (Figure 3.15 A,D). These H&E results conclude that even there was a subtle difference between Itga5 cKO and control mice at day 30; there was no obvious difference in the phenotype of the muscle at day 33 and day36 when challenged twice with CTX injury. Data shown here is a representative from comparable regions from three injured muscles from both Itga5fl/-$^{HSA\text{-}Cre}$ and Itga5 fl/+$^{HSA\text{-}Cre}$ mice and thus we conclude that there was no obvious difference.

Replacement of myofibre by fat is a classical sign of muscular dystrophy. To confirm increased presence of fat we performed oil red O staining. The muscle sections from both Itga5 fl/-$^{HSA\text{-}Cre}$ and Itga5 fl/+$^{HSA\text{-}Cre}$ mice showed comparable staining for Oil red O three and six days after the second CTX injection (Figure 3.16 B,C,E,F), while, as seen before by H&E staining, increased fat deposition was apparent in cKO sections (Figure 3.16 A,D).

Consistent with the H&E results, the Oil red O staining also conclude that there is no obvious difference in regeneration between the Itga5 cKO and control mice.

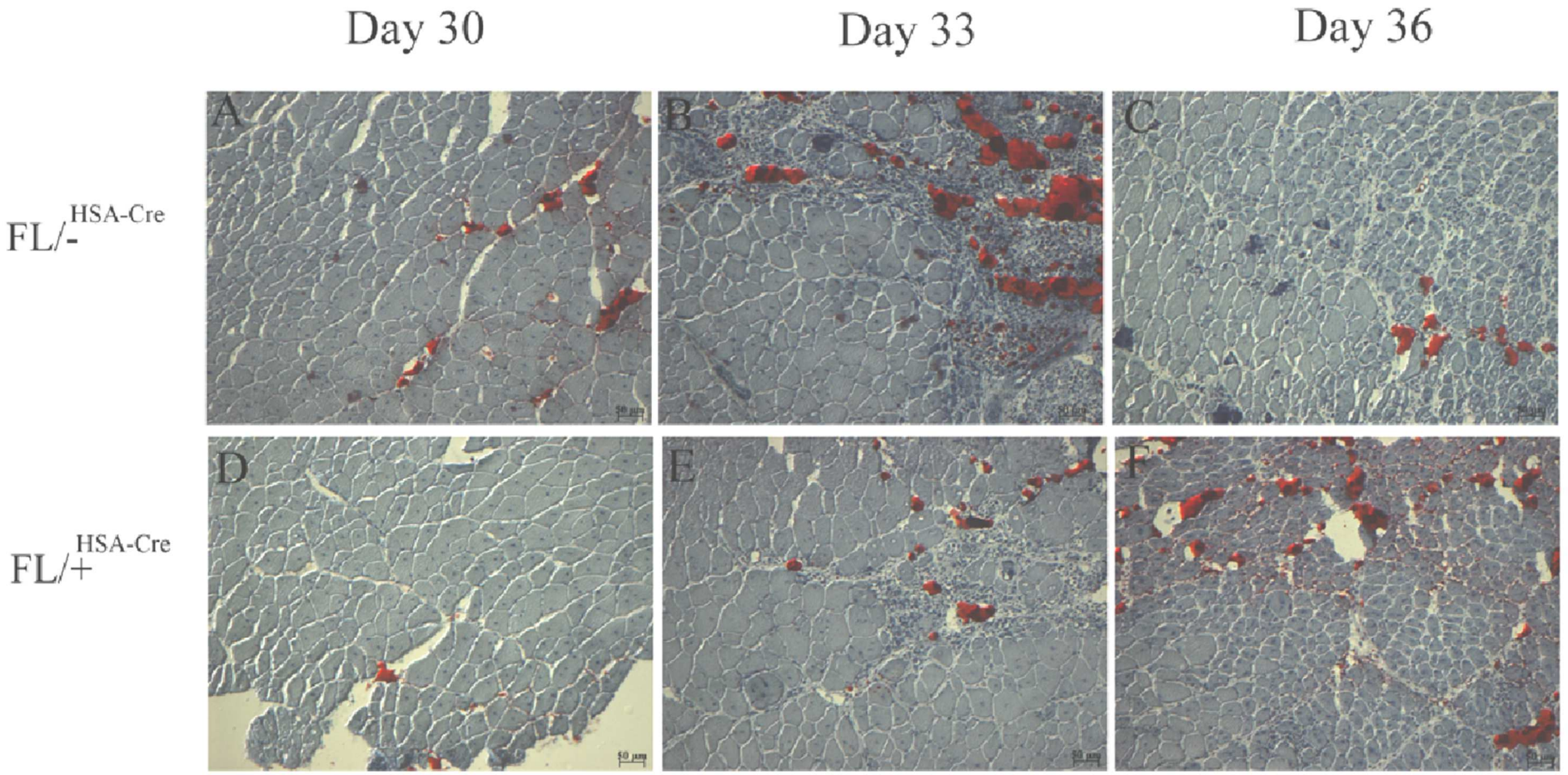

Figure 3.16: Oil Red O staining of muscle sections of Itga5 cKO and littermate controls. *Oil red O staining on 10µm cryosections of TA muscles injured twice show fat deposits in both genotypes (B,C,E,F) Day 30 after the first CTX injection cKO section (A) shower increased fat deposits as compared to controls (D). Bar, 50µm.*

Histological analysis of Itga5cKO mice so far suggests that the loss of integrin α5 under the HSA promoter is not a useful model to study the importance of integrin α5 in muscle development. It may be the case that, by the time HSA promoter is expressed, the expression of integrin α5 is already down regulated and very low amount of integrin α5 is present, which, after excision has no effect on later stages of muscle development. It is therefore necessary to knock down the expression of integrin α5 at very early stages of muscle development. This led us to consider the transcription factors, which are expressed at early embryonic stages of mouse development.

3.4 Conditional knockout of integrin α5 through the action of Pax3-Cre promoter

In mice, Pax3 expression initiates at E~8.5 (Goulding et al., 1991). Therefore we decided to cross breed Itga5 +/- mice with $Pax3^{Cre}$ mice, in which Cre had been inserted into Pax3 locus (Engleka, K.A., et al., 2005). Itga5 +/- $^{Pax3\text{-}Cre}$ males were mated with Itga5 fl/fl females to obtain Itga5 fl/-$^{Pax3\text{-}Cre}$ mice.

Genotyping of the F2 generation at weaning resulted in either fl/+, fl/- or fl/+$^{Pax3\text{-}Cre}$ mice, but no conditional KO. In total we genotyped 35 mice at 3 weeks of age, without obtaining Itga5 fl/-$^{Pax3\text{-}Cre}$ mice. We then suspected that the conditional loss of integrin α5 under Pax3-Cre expression is either embryonic or postnatal leathal. To investigate this further we decided to analyse embryos from time-mated females.

3.4.1 Isolation and visual observation of integrin α5 $^{Pax3\text{-}Cre}$ embryos

In order to determine the reason behind the premature death of integrin α5 $^{Pax3\text{-}Cre}$ mice, we analysed E18.5 embryos. The visual observation of these embryos showed a striking difference between the littermates. Genotyping confirmed a correlation between Itga5 fl/- $^{Pax3\text{-}Cre}$ genotype and posterior abnormalities. Itga5 fl/- $^{Pax3\text{-}Cre}$ embryos had a smaller (Figure 3.17 D) and curled tail compared to littermate controls (Figure 3.17 A, B). In addition the vertebral posture of embryos was strikingly different to controls (Figure 3.17 C).

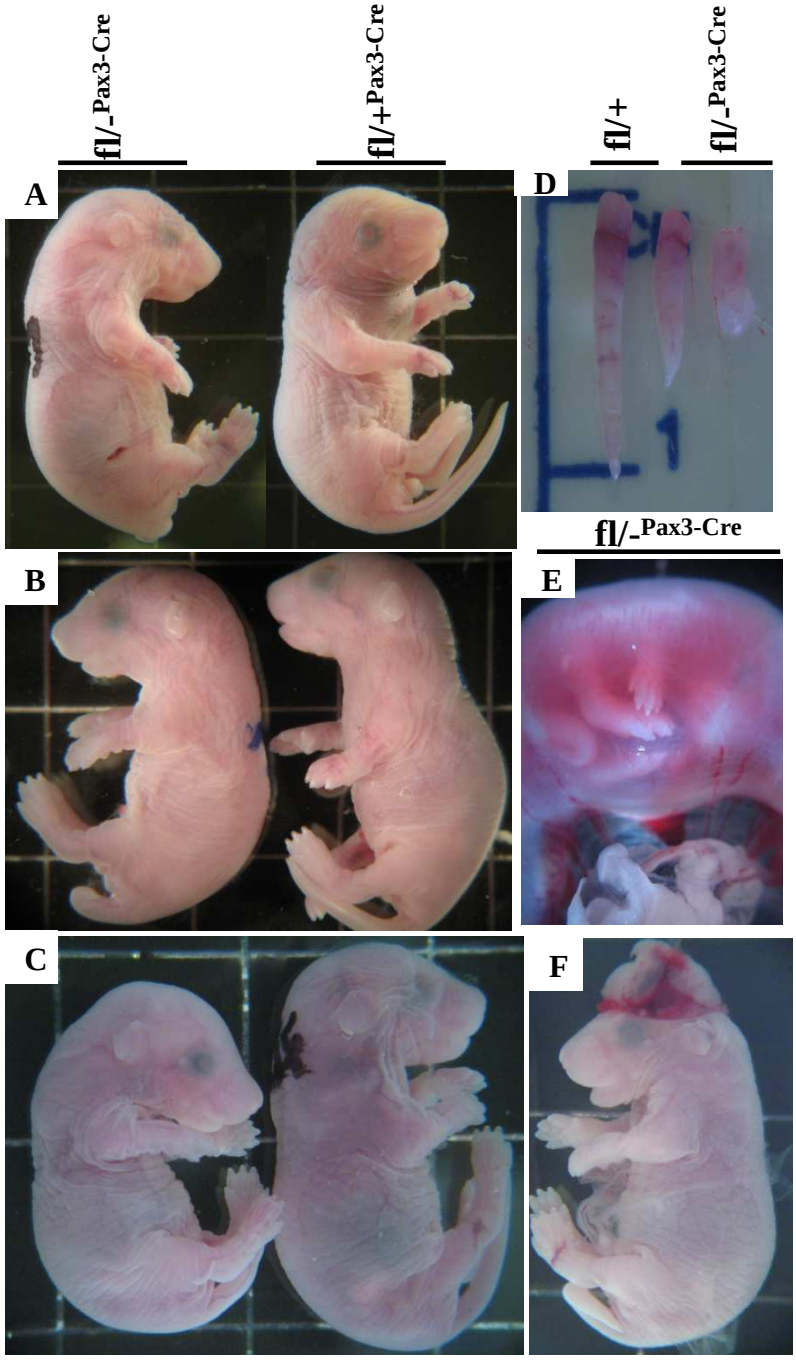

Figure 3.17: Representative images comparing E18.5 embryos of Itga5 cKO and control. *Embryos from Itga5 fl/-$^{Pax3\text{-}Cre}$ and Itga5 fl/+$^{Pax3\text{-}Cre}$ were analysed for any abnormalities at E18.5. A) Itga5 fl/-$^{Pax3\text{-}Cre}$ display a defect at the posterior end of the embryo characterised by a curled tail. B) Itga5 fl/+$^{Pax3\text{-}Cre}$ embryos have stretched HLs C) Itga5 fl/-$^{Pax3\text{-}Cre}$ embryos are considerably smaller and deformed. D) Variation of tail length, in Itga5 Fl/-$^{Pax3\text{-}Cre}$ embryos E) Blood-filled yolk sac in mutant embryos F) Some mutant embryos had exencephaly.*

We also observed that yolk sacs of Itga5 fl/-$^{Pax3\text{-}Cre}$ embryo were filled with blood (Figure 3.17 E), which could suggest a hemorrhage. We also noticed one embryo with exencephaly (Figure 3.17 F). Closer observations also revealed slight abnormalities with the limb structure. The Hind imb of integrin α5fl/- $^{Pax3\text{-}Cre}$ mice were similar in size and curved inwards while in controls they were well stretched (Figure 3.17 B). This observation corresponds with the published work of integrin α5KO mice (Yang and Hynes, 1993), where it has been shown that there were defects at the posterior trunk of the embryos between E8-10.5.These integrin α5 KO mice die at E10.5, unlike our conditional null integrin α5 mice, which survive until P2. To examine the reason behind the premature death of these mice we decided to isolate both hind limb and forelimb along with internal organs like heart, lung and diaphragm. Hind limb and forelimb were processed for cryosectioning, while heart, lung and diaphragms were processed for paraffin embedding.

3.4.2 Statistical analysis of of integrin α5 $^{Pax3\text{-}Cre}$ embryos

Statistical analysis for the Mendelian ratio from 104 embryos from crossing Itga5 +/-$^{Pax3\text{-}Cre}$ with Itga5 fl/fl mice between E18.5 and P2 showed that pubs are born at normal Mendelian ratio but none survived beyond P2.

Table 3.1: Statistical analysis of genotypes for the breeding pair Itga5 +/-$^{Pax3\text{-}Cre}$ X Itga5 Fl/Fl.

Genotype	**Expected %**	**Observed %**			
		E18.5	**E19.5**	**P1**	**P2**
Fl/-	**25%**	10 (15.625%)	4 (25%)	0 (0%)	5(27.77%)
Fl/-$^{Pax3\text{-}Cre}$	**25%**	15(23.4375%)	5(31.25%)	3(50%)	4(22.22%)
Fl/+	**25%**	18(28.125%)	3(18.75%)	1(16.66%)	6(33.33%)
Fl/+$^{Pax3\text{-}Cre}$	**25%**	21(32.8125%)	4(25%)	2(33.33%)	3(16.66%)
Total	**100%**	64 (100%)	16(100%)	6(100%)	18(100%)

3.4.3 Histological analysis of integrin α5 $^{Pax3\text{-}Cre}$ embryos

Cryosections from HLs and FLs from both Itga5 cKO and controls at E18.5 were analysed by H&E staining. The morphology of HL muscles TA, EDL and GC were similar to that of controls. There were no differences observed in FL muscles either. There was no direct evidence of any developmental defect in muscle sections of the cKO compared to control mice (Figure 3.18).

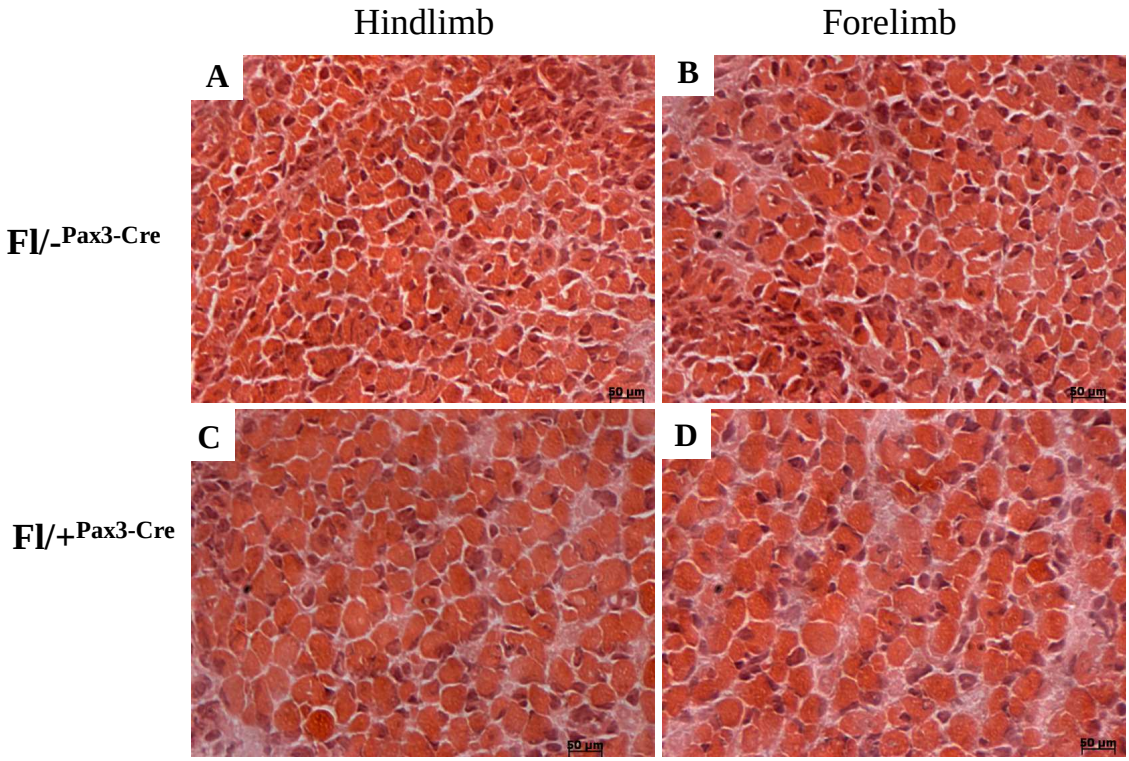

Figure 3.18: H&E staining of muscle sections of Itga5 cKO and control embryos: *H&E staining of 10µm cryosections from hindlimb and forelimb of Itga5 Fl/-$^{Pax3\text{-}Cre}$ (A,B) and Itga5 Fl/+$^{Pax3\text{-}Cre}$ (C,D) at E 18.5,embryos shows no striking difference in muscle morphology.. Bar, 50µm*

This data indicate that there is no specific muscle phenotype in the HL and FL muscles of integrin α5Fl/-$^{Pax3\text{-}Cre}$ embryos. At this stage we are unable to understand the reason behind the early death in conditional KO of integrin α5$^{Pax\text{-}Cre}$. As mentioned earlier, this project was a collaborative project with the team at MIT USA and we were limited to analyse the muscle phenotype as a possible neural crest phenotype was in the interest of our collaboration partner.

We then switched our focus of research on integrin α5/α7 double knockout (DKO) mice.

3.5 Generating integrin α5/α7 double knockout (DKO) mice

We first wanted to analyse whether half dosage of integrin α5 on a homozygous null background of integrin α7 worsened the phenotype. To do this we crossed hetero- or homozygous Itga7 mice with heterozygous Itga7 mice, which were heterozygous for Itga5 (Figure 3.19).

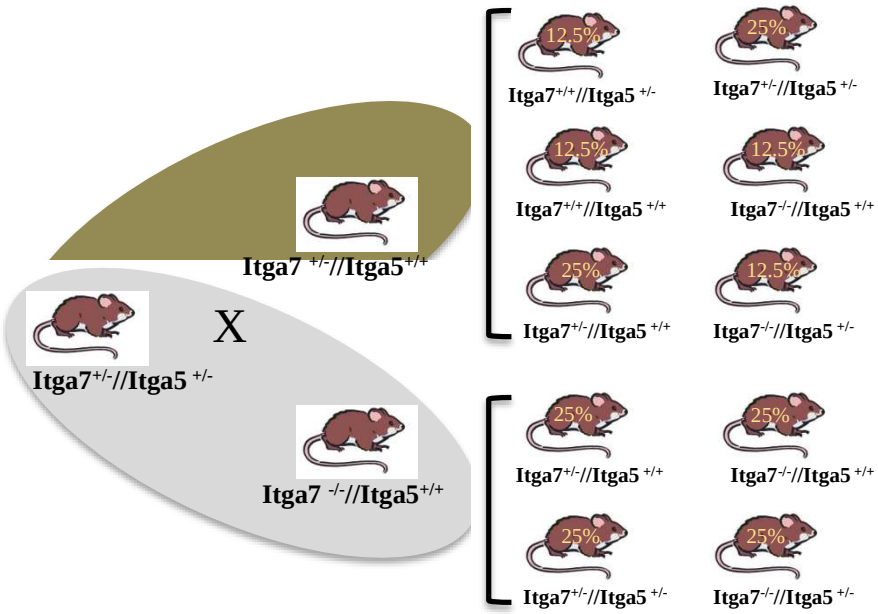

Figure 3.19: Breeding strategies to obtain α7-/-/α5+/- mice. *Hetero- or homozygous integrin α7 mice were bred with females heterozygous for bot integrin α7 and integrin α5. Resulting genotype combinations with the expected frequency is shown on the right.*

In figure 3.19 the expected genotypes are shown with at least 12.5% α7-/-/α5+/- mice. However, genotyping of more than 400 offspring failed to obtain any surviving adult mouse with Itga7$^{-/-}$ Itga5$^{+/-}$ genotype.

At the same time we started to generate a conditional KO of integrin α5 in combination with the α7 null allele. Therefore we designed another breeding strategy where Itga7+/-//Itga5+/-$^{HSA\text{-}Cre}$ mice were crossed with hetero- or homozygous Itga7 mice, homozygous floxed for Itga5 (figure 3.20).

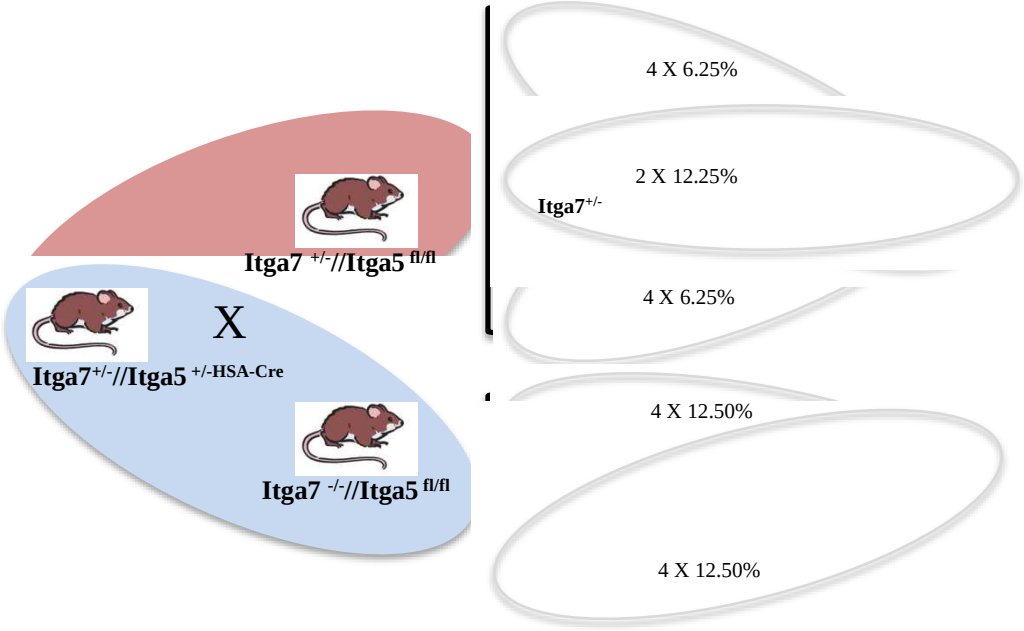

Figure 3.20: Breeding strategy to obtain α5/α7 DKO. *Integrin α7//α5 heterozygous mice carrying Cre recombinase gene were bred with integrin α7 heterozygous or homozygous females both floxed for the integrin α5 allele. Resulting combinations of genotypes with the expected frequency are shown on the right.*

Figure 3.20 displays all the possible combinations and the percentages of the expected genotypes. The most interesting genotype was Itga7-/-//Itga5 fl/-$^{HSA\text{-}Cre}$. However, as described above, we never obtained a surving mouse with this genotype, clearly indicating that half dosage of integrin α5 on an integrin α7 knockout results in embryonic lethality. We therefore decided to study these mice at very early stages of development.

In order to do so, we set up time matings and harvested embryos at E10.5. using the breeding strategy shown in figure 3.19. We identified embryos with the genotype Itga7-/-//Itga5+/-. These embryos were smaller than littermates and all had haemorrhages in the heads, along the spine and in intersomatic vessels. Some of these embryos were pale with very little blood visible.

3.5.1 Statistical analysis of the genotype from mice at embryonic day 10.5 (E10.5)

We genotyped 358 embryos to calculate percentages in agreement with the Mendelian ratio (Table 3.2) and the Chi square analysis between the last two groups (-/-//+/- Vs -/-//+/+) shows significant difference between the percentages of embryos with $p<0.01$.

Table 3.2: Statistical analysis of genotypes for the breeding pair Itga7$^{+/-}$//Itga5$^{+/-}$ X Itga7$^{+/-}$ or Itga7$^{-/-}$ //Itga5$^{+/+}$.

Genotype (Itga7//Itga5)	Number of embryos	Percentage expected	Percentage observed
+/-// +/+	95	25%	26.53%
+/+//+/-	60	12.5%	16.76%
+/-//+/-	110	25%	30.72%
+/+//+/+	39	12.5%	10.89%
-/-//+/-	19	12.5%	5.30%
-/-//+/+	35	12.5%	9.77%
Total	358	100%	100%

The analysis in table 3.2 suggests that there is a low frequency for embryos with null alleles for integrin α7 and only one allele for integrin α5, suggesting the importance of both integrins during developmental stages of the mice. According to the data shown in table 3.2, the highest percentage of embryos had at least one functional allele for both integrins, while only 19 out of 358 embryos were identified as Itga7-/-//Itga5+/-. This is still significantly lower than integrin α7 deficiency, for which it is known that 50% of the mutants die between E10.5-12.5, indicating that a more severe phenotype manifests when there is only half dosage of integrin α5 present.

3.6 Discussion

In this study we investigated the potential role of integrin α5 in skeletal muscle. Integrin α5 is known to be important during embryonic development and its deficiency causes death of the embryos at E10.5 due to defects in the development of mesodermal structures, mostly in the posterior part of the body (Yang et al., 1993). To study the function of integrin α5 in adulthood chimeric mice were derived from integrin α5 -/- embryonic stem (ES) cells (Taverna et al., 1998). These results. highlight the fact that the muscle fibres survive in α5-null chimeric mice by the fusion of -/- cells with WT myoblasts, suggesting that there is dosage effect of integrin α5, which is required for embryonic viability. In addition, their study indicates that α5 integrin is not essential for muscle development but necessary to maintain muscle fibre integrity (Taverna et al., 1998).

This is the only known *in vivo* study, which focused on the function of α5 integrin in skeletal muscle. However, the reason for the degenerative changes observed in the muscle deficient in integrin α5 remains unclear. To further investigate the involvement of integrin α5 in skeletal muscle development and maintenance we generated a muscle-specific KO of integrin α5.

3.6.1 Evaluating the outcome of integrin α5 conditional deletion in adult mice

The data suggests that loss of integrin α5 under the control of the HSA promoter had no adverse effect on the muscle phenotype. The mice at different developmental stages (4 weeks, 3 months and 6 months) displayed normal muscle fibre size and no phenotypic abnormalities when compared to age matched control mice. However, when we analysed older mice at the age of over 12 months, we saw signs of dystrophy in the HL muscle of Itga5 Fl/-$^{HSA\text{-}Cre}$ mice. We observed this phenotype in the GC muscle while other HL muscles showed normal muscle architecture. This could only be explained by the facts that firstly, integrin α5 is not efficiently deleted under the control of HSA-Cre system or secondly, there is a deficit in the regeneration process of Itga5 cKO mice.

To further investigate the first theory we decided to study Itga5 cKO and control mice at P3. Integrin α5 is highly expressed during the muscle development and its expression is down regulated after birth, between day5 and 10 post-natally (Blaschuk and Holland, 1994; Boettiger et al., 1995; Bronner-Fraser et al., 1992). Under the

control of the HSA promoter the deletion of integrin α5 was efficient as integrin α5 immunostaining was absent in the cKO but present in controls (figure 3.10, 3.11 and 3.12). It is also important to bear in mind that HSA promoter becomes active at embryonic day 9.5 (Asante, E.A., et al., 1993) and is predominantly active in differentiating skeletal muscle (Miniou, P., et al., 1999). It may be the case that by the time the HSA promoter becomes active, the expression of integrin α5 is already down regulated and very low amount of integrin α5 is present, which, after excision has no effect on later stages of muscle development. This would also explain normal regeneration seen after CTX injection, as Cre will only be expressed at differentiation during the regeneration cycle, while activated satellite cells and proliferating myoblasts will be positive for the integrin subunit. At this point we decided to divert our attention to a different promoter, which will allow the omission of integrin α5 at early stages of development.

3.6.2 Analysing the effects of loss of integrin α5 at early stages of muscle development

The Pax family of transcription factors plays an important role in the development of several organ systems. Pax3 was a choice of promoter as Pax3 is expressed in mice from E8 onwards (Goulding et al., 1991). Skeletal muscle arise from myogenic progenitor cells present in the somites of the embryo. Pax3 is also expressed in somites. The expression of Pax3 coincides with the earliest stages of somitogenesis, expressed in the dorsal region of new somite. After differentiation into sclerotome and dermomyotome, Pax3 expression is restricted to the dermomyotome that will then contribute to the formation of limb muscles and body wall (Epstein, 2000).

Pax3-Cre mice (Engleka, et al., 2005) were bred with Itga5 heterozygous mice and the resulting F1 generation males (Itga5+/- Pax3-Cre) were mated with Itga5 fl/fl females. Analysis of genotyping of the F2 generation at weaning resulted in fl/+, fl/- or fl/+$^{Pax3\text{-}Cre}$ genotype, but no conditional KO. This indicated that the conditional loss of integrin α5 under the control of the Pax3 promoter is embryonic or postnatal lethal.

To further investigate our findings we harvested embryos at E18.5, where we identified surviving embryos with conditional loss of integrin α5. We observed a

striking difference between the littermates. Itga5 cKO embryos were smaller and with posterior defects resulting in a curved spine and short or curled tails. Some embryos exhibited exencephaly, a defect in which the brain is completely exposed or protrudes through a defect in the cranial vault. As Pax3 is involved in neural crest specification during development (Monsoro-Burg et al., 1996)., this data indicates that integrin α5 has been deleted in the neural crest and the observed differences were the result of neural crest defects.

To conclude, our observations correspond with the published work of integrin α5KO mice (Yang and Hynes, 1993), where it has been shown that these were defects at the posterior trunk of the embryos between E8-10.5. The only difference was that some of our Itga5cKO mice were able to survive till P2. It will be interesting to study these mice to understand underlying defects. Our work was a joint collaboration between Hynes lab at MIT, USA. As a possible neural crest phenotype was in the interest of our collaborator, we did not further analyse the cause of the perinatal death of these mice and concentrated on the muscle phenotype in the conditional integrin α5 null mice.

In order to investigate if these Itga5cKO embryos exhibit a muscle phenotype, we analysed HL or FL muscle from these embryos. H&E staining of HL muscles revealed no obvious abnormalities between Itga5 fl/-$^{Pax3\text{-}Cre}$ and Itga5 fl/+$^{Pax3\text{-}Cre}$ muscles (Figure 3.18), suggesting that there is no skeletal muscle phenotype.

3.6.3 Studying skeletal muscle regeneration in Itga5 cKO and control mice

To test if there is a possible deficit in muscle regeneration in Itga5cKO mice, we induced artificial muscle regeneration by administration of CTX. Upon first CTX injection, the TA muscles from both Itga5 cKO and control mice revealed active regenerating fibres with CLN (Figure 3.15 A,D) when analysed 30 days post injury. However, there was some deposition of adipose tissue observed in Itga5 cKO muscle compared to controls (Figure 3.16 A,D). The muscle was given a second dose of CTX after 30 days of recovery and TA was analysed after day 33, and day 36. As expected at the peak of degeneration, TA muscle from both Itga5 cKO and control mice displayed massive infiltration of polymorphonuclear leukocytes. At day 36 TA muscle from Itga5

fl/-$^{HSA\text{-}Cre}$ and Itga5 fl/+$^{HSA\text{-}Cre}$ mice were regenerating muscle with some fat deposits (Figure 3.16).

Adipose tissue is necessary for muscle regeneration and appearance of it solely does not conclude the adverse phenotype. Due to time restrictions, we were able to analyse only one set of data and to draw the conclusion from this would not be appropriate. These experiments will need repetition on more sets of mice and it will be interesting to see what phenotype will be 15 days after the second CTX injection (Day 45).

3.6.4 Investigating the role of integrin α5 and α7 in skeletal muscle

From previous studies important insights have been gained into the pathological changes and molecular abnormalities associated with integrin α7-deficiency in mice (Mayer et al., 1997; Nawrotzki et al., 2003). The relationship between integrins α5 and α7 may be more specific than a simple competition as, despite the presence of integrin α6 and α3 in integrin α7 knockout muscle, only the integrin α5 co-precipitated with integrin β1D (Nawrotzki et al., 2003). Evidence suggests that the retention of integrin α5β1 and its ligand fibronectin at the MTJ precedes the onset of muscle wasting. It has been proposed that the α5β1/fibronectin link is inferior to that of the α7β1/laminin 2 link. This is potentially due to modifications in components of the junctional cytoskeleton, modulating signalling pathways downstream of integrins. By identifying signalling pathways active in myoblasts one will be able to study the role of integrin-mediated signalling (Figure 3.21).

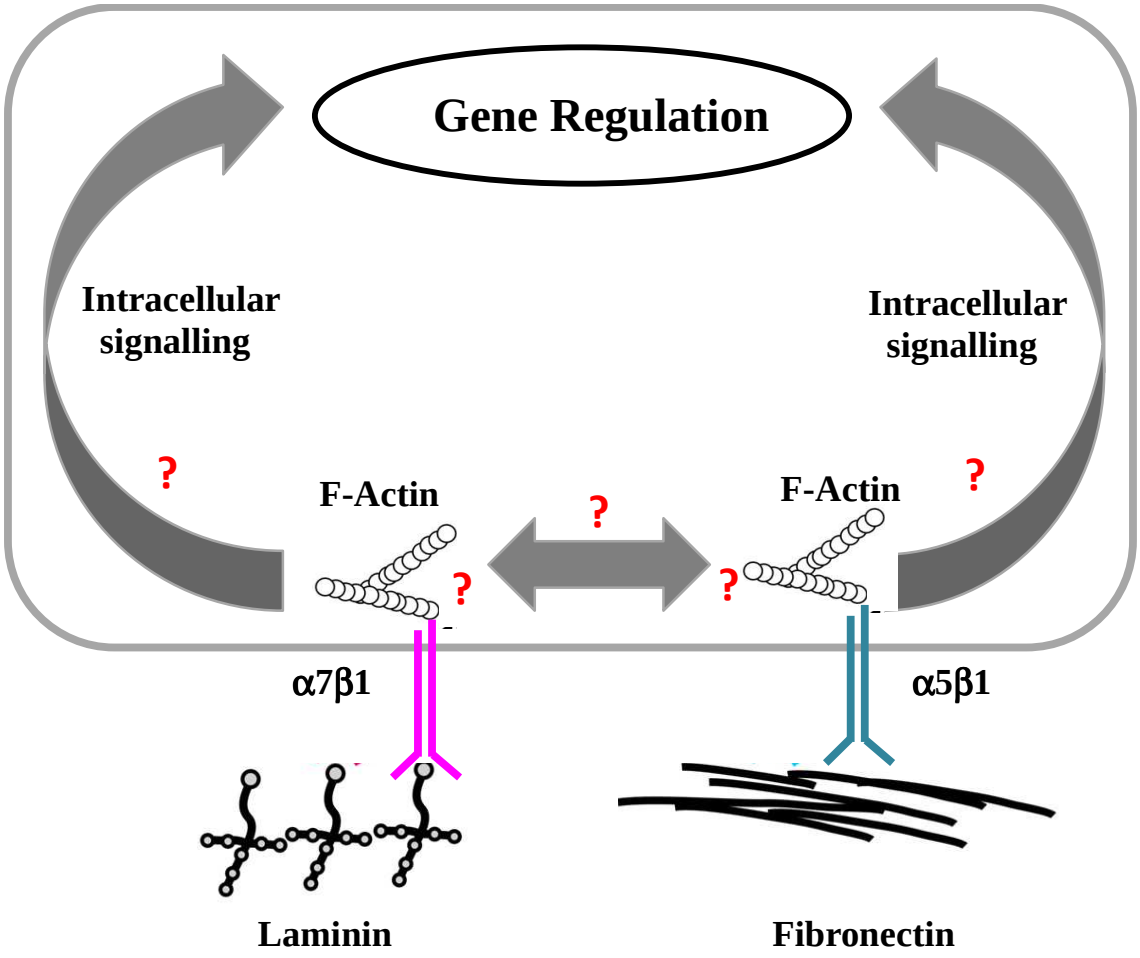

Figure 3.21 Schematic representation of integrin α7β1 and α5β1 interactions. *Diagram showing integin α7β1 and α5β1 connecting their respective ligands to the actin cytoskeleton. Exactly how they connect to the actin cytoskeleton and which intacellular signalling events they induce are unclear as is the cross talk mechanism, which occurs between the two receptors in skeletal muscle. (Modifided from Mayer 2003).*

The fact that the increase in integrin α5 does not appear proportional to the decrease in integrin α7 would further confirm the notion that the relationship between integrins α5 and α7 is more complex than a simple competition. To understand what drives the cross talk between these two transmembrane proteins, we decided to generate a double-knockout of both integrins in skeletal muscle.

3.6.5 Analysing the effect of DKO of integrin α7 and α5 on skeletal muscle.

As described in figure 3.19 we mated Itga7 mice with Itga5 heterozygous mice. The outcome of the F1 generation was somewhat surprising to our study. We were unable to see any surviving mice with the genotype of Itga7$^{-/-}$ Itga5$^{+/-}$. As described by Mayer et al in 1997, 50% of integrin α7 KO mice die during embryonic development, so this indicated a dosage effect of the integrin α5 for survival. At the same time we were working on generating a conditional KO of integrin α5 on an integrin α7 null background (refer to figure 3.20 for breeding strategy). Again, we did not obtain any viable pups with the genotype of Itga7-/-//Itga5 Fl/-$^{HSA\text{-}Cre}$. This supported our previous notion of a dosage effect of integrin α5, and that integrin α5 is a requirement for embryonic survival of integrin α7-deficient mice. To identify what had caused embryonic lethality with full penetrance we analysed embryos at E10.5 from the parents of the combinations of genotypes described in figure 3.19. Genotyping by PCR confirmed that the Itga7$^{-/-}$ Itga5$^{+/-}$ indeed is embryonically lethal. Many of these embryos were resorbed, but haemorrhages in most of these embryos indicate that death is caused by a defective vasculature.

During these experiments we also experienced a technical problem with the animal facility, because of which we had a very low success rate of females getting plugged. 50% of females, which were plugged, became never pregnant, and we also observed that a high number of wildtype embryos were resorbed. Due to all these technical difficulties and restricted time fame, we decided to discontinue the experiments related to investigating the phenotype of these Double Knock Out (DKO) embryos.

Chapter 4:

Could integrin α7β1 be a potential therapeutic target for DMD?

4.1 Characterisation of transgenic mice overexpressing integrin α7 splice variants

Integrin α7 plays an important role in muscle development and function (Song et al., 1993). The absence of integrin α7 leads to progressive muscular dystrophy, which was first described in mice as causing mild myopathy mainly in the Soleus muscle and affecting the MTJ (Mayer et al., 1997). Interest in integrin α7 has also arisen from its speculated potential to rescue the phenotype of DMD. Integrin α7β1 has been put forward as a promising candidate to treat DMD because it fulfills many of the functions of DGC, for example signal transduction, mechanical stability, it is a laminin receptor and it is naturally elevated in DMD. In addition, published data indicated prolonged lifespan of dystrophin/utrophin double mutant mice when the level of integrin α7 was increased (Burkin et al., 2005).

Integrin α7 is alternatively spliced in its intra- and extra-cellular domains and the expression of these splice variants is developmentally regulated. However, very little is known about the function of these different splice variants during skeletal muscle development or in their suitability to ameliorate the muscle phenotype seen in dystrophin deficient *mdx* mice. To investigate the function of these splice variants, transgenic mice were generated overexpressing all four integrin α7 splice variants in all their intra- and extracellular combinations. They will work as a tool to investigate the role of each α7 integrin splice variants in ameliorating the DMD phenotype by crossing each overexpressing transgenic mouse strain to *mdx* background.

4.1.1 Generation of integrin α7 splice variant overexpressing mice

Mice overexpressing integrin α7 were already generated in the Mayer lab using the strategy mentioned below.

Plasmid corresponding to the four possible α7 intracellular and extracellular splice variant combinations had already been generated. Constructs were prepared expressing each integrin α subunit under the control of Human Skeletal α-Actin (HSA) promoter (Figure 4.1).

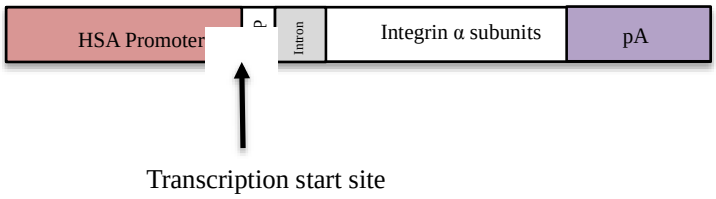

Figure 4.1: Integrin α subunit constructs under the control of HSA promoter*. Integrin α subunits were cloned into a cassette following the HSA (2239kB) promoter. Arrow marks the transcription start site. In addition the HSA construct contains an enhancer element (CAP) as well as a 5' UTR and a part of the first HSA intron to enhance expression. At the 3' end the PolyA sequence of bovine growth hormone is added*

The HSA promoter activity starts at embryonic day 9.5 and is predominately active in skeletal muscle (Chamberlain et al., 1985; Asante et al., 1992). Terminal differentiation is the end point of muscle development during which stage many changes occur in integrin expression. The HSA promoter is active prior to this process when cells terminally differentiate and thus the integrin expression induced via HSA promoter may have a significant effect on muscle development.

The various constructs were digested from their vectors, purified and injected into the pronuclei of fertilised oocytes. Oocytes were then implanted into pseudopregnant females. DNA was extracted from the tail tips of the offspring born and PCR amplification was carried out using primers specific for the HSA promoter region and the integrin α subunit cDNA. This identified offspring positive for the transgene.

Approximately 10% of the pups born after pronuclei injection were positive for the transgene. Each positive offspring is a so-called Founder Mouse, and each Founder

Mouse was named for ease of recognition. Because multiple copies of the DNA construct can integrate at random places within the genome after injection, the strains were established from a single mouse of the F1 generation. The Founder was therefore crossed with a wildtype mouse and one mouse from this subsequent F1 generation positive for the transgene was chosen to establish the entire strain. In this way, all mice within an established strain are heterozygous for the transgene and were originally derived from the same mouse and so, should have the same expression level. The whole strain was named after the Founder mouse for simplification.

4.1.2 Identifying protein overexpression in transgenic strains

In order to establish the founder strain the pups born after the pronuclei injections were identified for the presence of the transgene. The tail biopsies were taken and processed for genotyping by PCR. The offspring born were checked for the transgene using primers specific for HSA promoter region, as well as integrin α subunit cDNA. The PCR result confirmed the presence of the transgene for each positive offspring.

The number of strains established for each construct varied. This is because the number of positive offspring born from each injection varied, and some of the positive strains were terminated because they did not overexpress the protein. The integrin α7 splice variant overexpressing strains that were generated are summarised in Table 4.1.

Table 4.1. Summary of integrin α7 splice variant overexpressing transgenic strains. Each construct corresponds to a combination of extracellular and intracellular splice variant as shown. The various strains derived for each construct are named after the Founder mouse.

	1. Promoter	2. Integrin α7 Extracellular Variant	3. Integrin α7 Intracellular Variant	4. Strain (Founder)
Construct 1	HSA	X2	A	Susie
				Chris
Construct 3	HSA	X1	A	Lydia
				Maria
				Judith
				Elke
Construct 5	HSA	X1	B	Xaver
				Karin
Construct 7	HSA	X2	B	Max
				Moritz
				Fritz
				Babette

4.1.3 Identifying protein overexpression in transgenic strains

The integration of the transgene into the genome does not guarantee that the protein will be overexpressed; therefore not all positive offspring will overexpress the protein. To identify and quantify the integrin α7 splice variant overexpression, the mice were sacrificed and Gastrocnemius (GC) muscle was isolated. Protein extracts were prepared and separated by SDS-PAGE. After transfer to PVDF membranes the overexpression of the integrin α7 splice variants was compared to the wildtype by immunoblotting with antibodies specific for the intracellular A or B splice variants.

The GC muscle lysates from the α7X1A (Judith, Lydia, Maria and Elke) and α7X2A (Susie and Chris) were separated under the non-reducing condition on 5-15% gradient SDS-PAGE gels. The PVDF membranes were probed with α7A (U12+) antibody raised in rabbit. Immunoblots in figure 4.2 represents all strains that overexpress the integrin α7A intracellular splice variant and were further sub-divided into α7X1A overexpressing or α7X2A overexpressing strains.

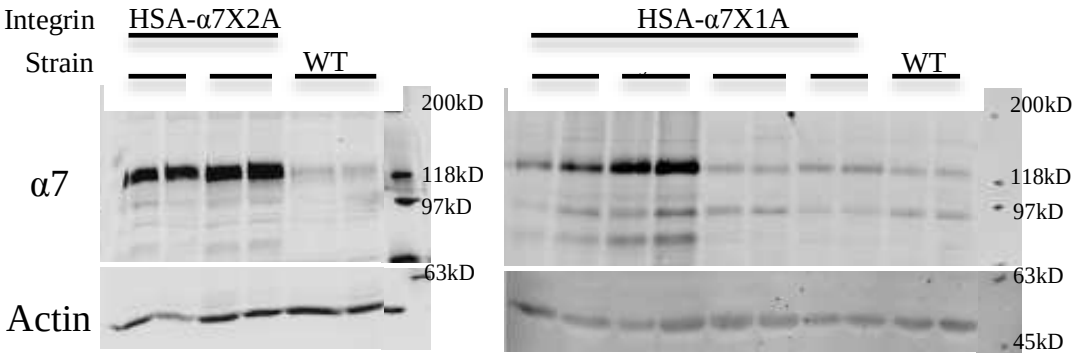

Figure 4.2: Integrin α7 levels in mice overexpressing integrin α7A splice variants. *Immunoblotting of GC muscle lysates identified strains overexpressing the integrin α7A under the control of HSA promoter. Strains were named for ease of recognition as shown. Two mice from each strain were analysed. 20μg of total protein from GC muscle lysate were run under non-reducing conditions by SDS-PAGE on 5-15% gels. Antibodies specific for intracellular α7A variant and actin were used for immunoblotting.*

The expression of integrin α7A was increased in all the overexpressing stains compared to wild type (Figure 4.2). The expression of the integrin α7A was difficult to visualise in wildtype muscle, as the level of the A variant was low in wildtype muscle. The level of overexpression varied between strains overexpressing α7X1A (Figure 4.2 right immunoblot) and α7X2A (Figure 4.2 left immunoblot). Variation in the level of overexpression was also apparent between strains expressing exactly the same construct. To take Lydia and Maria as an example, both overexpressing the α7X1A, yet Maria overexpresses less protein compared to Lydia.

Similarly, the GC muscle lysates from the α7X1B (Karin and Xaver) and α7X2B (Max, Moritz, Fritz and Babette) were separated under the non-reducing condition on 5-15% gradient SDS-PAGE gels. Immunoblots were probed with integrin α7B (U31+) specific antibody raised in rabbit (Figure 4.3). The protein levels of integrin α7B were elevated in all the stains overexpressing the integrin compared to the wild type.

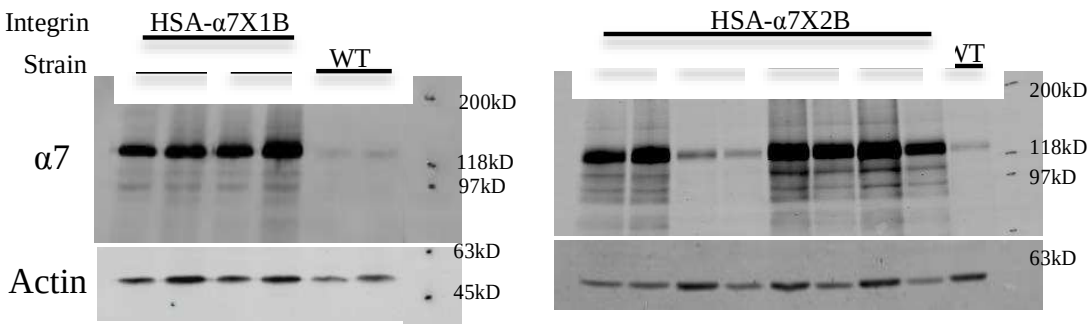

Figure 4.3: Integrin α7 levels in mice overexpressing integrin α7B splice variants. *Immunoblotting of GC muscle lysates of 3 months old mice overexpressing two α7X1B and four α7X2B overexpressing strains. Strains were named for ease of recognition as shown. 20μg of total protein was run under non-reducing conditions on 5-15% gradient SDS-PAGE gels. Antibodies specific for the intracellular integrin α7B variants and actin were used for immunoblotting.*

The level of overexpression was found to be similar between Xaver (α7X1B) and Karin (α7X1B) (Figure 4.3 left immunoblot), but variation was observed between strains overexpressing α7X2B. Max, Fritz and Babette were strongly expressing α7X2B compared to Moritz (Figure 4.3 right immunoblot).

It should be noted here that antibodies specific to the integrin extracellular splice variant X1 and X2 were not available and thus, only the blots with intracellular splice variants were feasible to do.

To conclude, integrin α7 splice variant overexpression was achieved in all the strains, but some variation was observed between the transgenic strains expressing the same integrin variant. For further study only one strain per mouse was selected with a similar expression pattern. Accordingly, Susie (α7X2A) and Lydia (α7X1A) were chosen from α7A overexpressing mice, while Xaver (α7X1B) and Babette (α7X2B) were selected from α7B overexpressing group. The fold expression was quantified for each strain.

4.1.4 Quantification of protein overexpression in integrin α7 transgenic strains

Integrin overexpression was quantified from immunoblots of muscle extracts probed with specific antibodies. However, when immunoblotting, instead of using ECL conjugated secondary antibodies, secondary antibodies conjugated to an Infra-Red Dye were used. The fluorescence generated from each immunoblot band was then quantified by a specialised scanner (Li-Cor Odyssey® scanner). Differences in immunoblot band intensity are often generated by experimental error, therefore it was necessary to normalise integrin expression to a protein remaining constant in all samples. Actin is a house keeping gene which was used to normalise the protein values obtained when the spice variants were over expressed compared to wildtype protein expression (Figure 4.3). The value assigned to each transgenic strain represents the fold increase in expression of the splice variant where the wildtype expression has been assigned the value of 1.

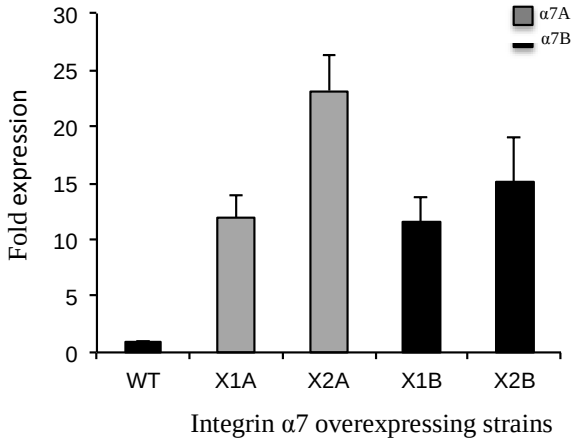

Figure 4.4: Quantification of integrin α7 splice variant overexpression*. The optical density of integrin α7 bands was determined using Odyssey sofware The relative expression level to the wildtype was calculated after normalisation to actin.*

The integrin α7A variants are overexpressed to a greater extent than the α7B variants compared to the respective intracellular splice variant in the wildtype (Figure 4.4). This could be due to the natural high level of expression of the integrin α7B variant while the endogenous α7A variant expression is low within adult muscle. It was essential to confirm that the sub-strain chosen for each strain has similar protein expression in each hindlimb muscles. Therefore lysates were prepared from GC, TA, *Soleus* (Sol) and *Extensor Digitorum Longus* (EDL) muscles and separated by SDS-

PAGE. After transfer to PVDF membrane the expression of integrin α7 was compared to wildtype by immunoblotting (Figure 4.5)

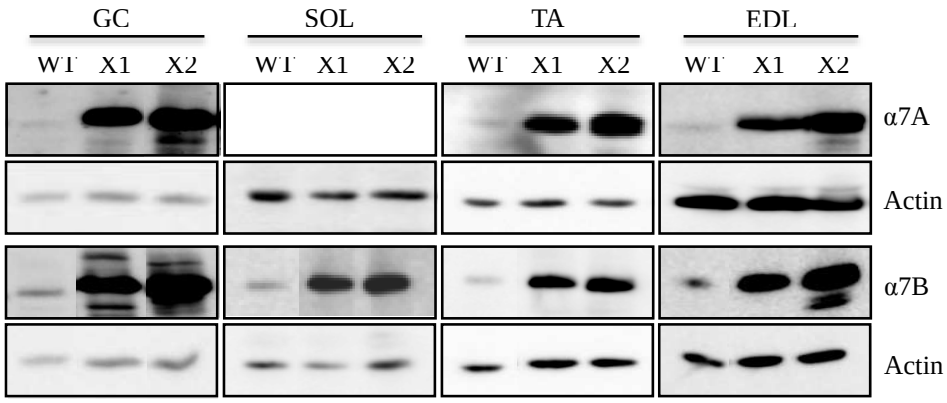

Figure 4.5: Integrin α7 levels in different muscles of transgenic mice. *Proteins were extracted from gastrocnemius (Gc), soleus (Sol), extensor digitorum longus (EDL) and tibialis anterior (TA) muscles of the 4 representative strains overexpressing α7A and α7B integrins. Immunoblots were probed with specific antibodies for each overexpressing integrin. Actin was used as a loading control. Top, α7X1A and α7X2A; Bottom, α7X1B and α7X2B. It is evident that the integrin level is increased at least 10fold as compared to WT and similar in all the muscles of each strain.*

The integrin level is increased at least 10fold in both α7A and α7B overexpressing mice as compared to wildtype and is similar in all four muscles analysed (Figure 4.5).

From the above results it is clear that the integrin α7 splice variant expression is elevated in the respective mice but it was important to see where in muscle the expression of these proteins is localized. To further confirm the localization of α7A and α7B immunofluorescence staining were performed on sections of the hindlimb (HL).

Mice were sacrificed at 3 months and HLs were dissected and cryo-embedded. Sections were cut at 10μm and stained with antibodies raised against the intracellular variants of integrin α7 (A or B) (Figure 4.6)

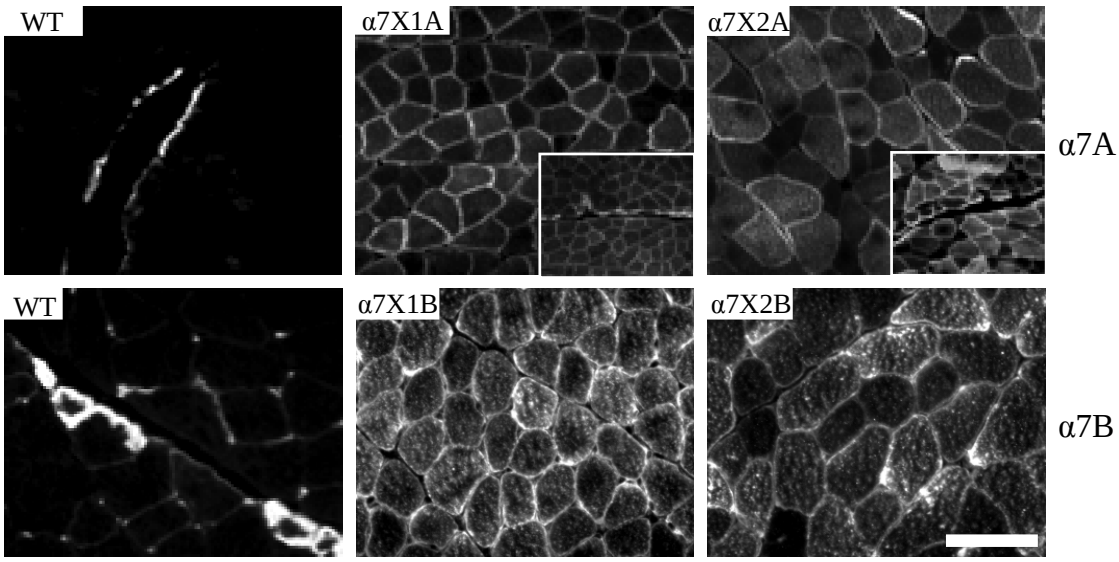

Figure 4.6: Localisation of integrin α7 splice variants in transgenic overexpressing mice. *Representative muscle sections taken from WT, integrin α7X1A, α7X2A, α7X1B and α7X2B transgenic mice were immunostained for integrin α7A and α7B. Integrin α7A is restricted to the MTJ in WT whereas it is additionally expressed at the sarcolemma and the sarcoplasm in integrin α7A transgenic mice. The inset (top row, middle and right) shows the expression of protein at MTJs in both α7A expressing strains. In WT, α7B is strongly expressed at the MTJ and a patchy staining of the sarcolemma is seen. In integrin α7B transgenic mice, α7B is strongly increased at the sarcolemma and is also found in the sarcoplasm. Bar, 50μm.*

In wild type muscle integrin α7A is expressed at the MTJ and can barely be seen at the sarcolemma. In the transgenic strain Lydia-α7X1A and Susie-α7X2A, very strong overexpression of the α7A intracellular variant is seen at the sarcolemma and in the sarcoplasm. In addition, the MTJs also displayed high level of expression of the protein. In the wild type, integrin α7B is also expressed at the MTJ but in contrast to the α7A intracellular variant is additionally expressed at the sarcolemma. In Xaver-α7X1B and Babette-α7X2B overexpression is also confirmed and integrin α7B expression is increased at the sarcolemma as well as in the sarcoplasm.

4.1.5 The effect of integrin overexpression on integrin β1

Integrins function as αβ heterodimers, so any increase in an integrin α7 splice variant will only be relevant if there is a concomitant increase in the functional heterodimer. To assess whether total integrin β1 increases when α7 is overexpressed, immunoblotting was repeated on the transgenic GC muscle lysates, with an antibody raised against the extracellular domain of integrin β1 (Figure 4.7 A-D).

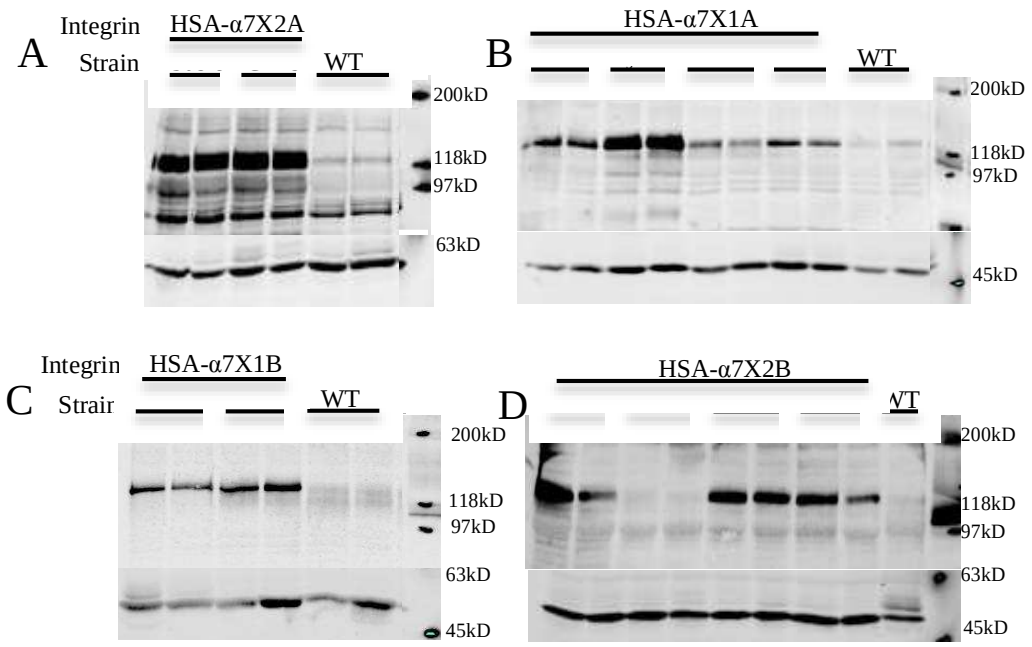

Figure 4.7 Integrin β1 expressions in integrin α7 splice variant overexpressing mouse strains. *20 μg of total protein from GC muscle lysates were separated under non-reducing conditions on 5-15% gels. Antibodies raised against the extracellular domain of integrin β1 and GAPDH were used for immunoblotting.*

The level of β1 varied widely between different strains. The level of integrin β1 increased slightly in transgenic mice compared to wild type controls. As shown in figure 4.7, Susie (α7X2A) and Chris (α7X2A) both display increased expression of β1 compared to Lydia (α7X1A), Elke (α7X1A), Maria (α7X1A) and Judith (α7X1A). The same is true for the strains expressing integrin α7B. Xaver and Karin (α7X1B) appeared to have lower expression of integrin β1 compared to Max, Moritz, Fritz and Babette (α7X2B).

The increased integrin β1 levels seen in strains overexpressing integrin α7 splice variants would infer that the amount of functional αβ integrin heterodimer is also increased. If this can be established then any effect of overexpression seen on muscle can be attributed to an increase in integrin α7β1 function, rather than a non-specific effect of protein overexpression. As the β1D variant is the predominant splice variant in adult skeletal muscle, heterodimer formation was investigated by immunoprecipitation of integrin β1D followed by immunoblotting for the overexpressed integrin α7 splice variant. This was carried out on a selection of transgenic strains (Figure 4.8). Polyclonal antibodies raised in the lab against the cytoplasmic domains of both integrin α7A and B and integrin β1D were used for precipitation. 1 mg of total protein was used from GC muscle lysates in all cases.

Figure 4.8: Analysis of integrin heterodimer formation in integrin α7 overexpressing strains. *Immunoprecipitation experiments were carried out using GC muscle lysates and 1mg of protein per strain. Strains were subdivided in to those expressing α7A and α7B integrin. (A) Strains overexpressing α7A variant. Integrin α7A was precipitated and samples were separated by SDS-PAGE under reducing conditions followed by immunoblottin for the precipitated integrin α7A (i) as a positive control. Reverse immunoprecipation with integrin β1D antibodies followed by immunoblotting for β1D (ii) or α7A (iii). An increase in αβ heterodimer formation is only seen in α7X2A overexpressing strains. (B) Strains overexpressing the integrin α7B intracellular variant.* ***i****. and* ***ii****. Immunoblotting for either α7B (i) or β1D (ii) was conducted in the strains overexpressing the α7B intracellular variant as a positive control for precipitation. The β1D precipitates were separated by SDS-PAGE and blotted for integrin α7B to determine the extent of heterodimerisation (iii). An increase in αβ heterodimer formation is only seen in α7X2B overexpressing strains*

As a positive control for this experiment, the integrin α7 splice variant being overexpressed was precipitated, separated by SDS-PAGE under reducing conditions and then immunoblotting for the precipitated variant was performed (Figure 4.8 Ai. and Bi.). Integrins were cleaved into their respective heavy and light chains on the blots by the reducing conditions as shown. As the α7A and α7B antibodies are both raised against the respective cytoplasmic domains, only the integrin α7 light chain (30kD) is recognised. Most of the overexpressed integrin α7 is correctly processed, however unprocessed integrin running at 120kD can also be seen on these blots. This is probably a result of the high level of integrin α7 overexpression exceeding the cells capabilities to process all of the integrin correctly, leaving some without a proteolytic cleavage site. These integrin β1D control blots confirm successful precipitation and the pattern of integrin α7 overexpression seen previously by direct immunoblotting.

The precipitation was repeated, this time using antibodies raised against the adult, muscle specific variant of integrin β1, integrin β1D (Figure 4.8 Aii. and Bii.). Samples were again run under reducing conditions and immunoblotting for integrin β1D was performed to confirm precipitation. βME reduction induces separation of the 150kDa IgG band into its heavy and light chains which prevents the integrin β1 bands from being obscured. However, this has the unfortunate effect that the peptide antibodies raised against β1A and β1D have a reduced affinity to their epitopes, the reason for which is unknown. This means that these blots confirm successful integrin β1 immunoprecipitation, but the subsequent integrin β1 immunoblotting of the reduced samples should not be relied on for comparisons of the level of integrin β1D between strains.

For this reason, integrin α7β1D heterodimerisation was investigated in the transgenic strains by blotting for the overexpressed integrin α7 splice variant on integrin β1D precipitates (Figure 4.8 Aiii. and Biii.), as the integrin α7 epitope is unaffected by reduction.

In the integrin α7A overexpressing strains (Figure 4.8 Aiii), integrin β1D precipitates were blotted using an antibody raised against integrin α7A. An increase in the amount of α7Aβ1D in all strains overexpressing the α7X2A variant was seen as compared to the wildtype. However, no increase in α7Aβ1D was seen in strains overexpressing the α7X1A variant.

Similarly, in strains overexpressing the α7B intracellular variant (Figure 4.8 Biii), an increase in α7Bβ1D was seen compared to the wildtype in the α7X2 overexpressing strains. Yet, the strains, which overexpress the α7X1, again show no increase in the level of integrin α7X1β1D as compared to the wildtype. This increase in dimerisation of integrin α7X2 with integrin β1D appears completely independent of the intracellular variant expressed or the level of integrin α7 overexpression. As even when very high overexpression of the α7X1 variant is achieved, as seen in for Lydia (α7X1A) no increase in α7β1D heterodimerisation is seen.

4.1.6 Analysis of integrin β1D expression

Overexpression of integrin α7 splice variants resulted in an increase in total integrin β1 which is relative to the extent of integrin α7 overexpression. Yet, only overexpression of the integrin α7X2 extracellular variant resulted in increased association with integrin β1D, the isoform of integrin β1 present in adult skeletal muscle. The levels of integrin β1D present in the muscle could not be reliably deduced from the immunoprecipitation experiments. Therefore, to investigate any changes to the levels of integrin β1D expression, GC muscle lysates were immunoblotted directly with antibodies specific to the integrin β1D intracellular variant (Figure 4.9).

Immunoblotting showed an increase in integrin β1D levels in strains overexpressing the integrin α7X2 extracellular variant in combination with either the A (Figure 4.9 A,B) or B intracellular variant (Figure 4.9 C,D). In stark contrast, strains overexpressing the integrin α7X1 extracellular variant either in combination with the A (Figure 4.9 B) or the B intracellular variant (Figure 4.9 C) showed no increase in integrin β1D.

Overexpression of the α7X2 extracellular splice variant resulted in an increase of the total level of integrin β1 and an increase in integrin β1D expression. As one would expect, this results in increased heterodimer formation. Although the overexpression of the X1 extracellular variant of integrin α7 resulted in an increase in the total amount of integrin β1, it did not result in increased levels of integrin β1D.

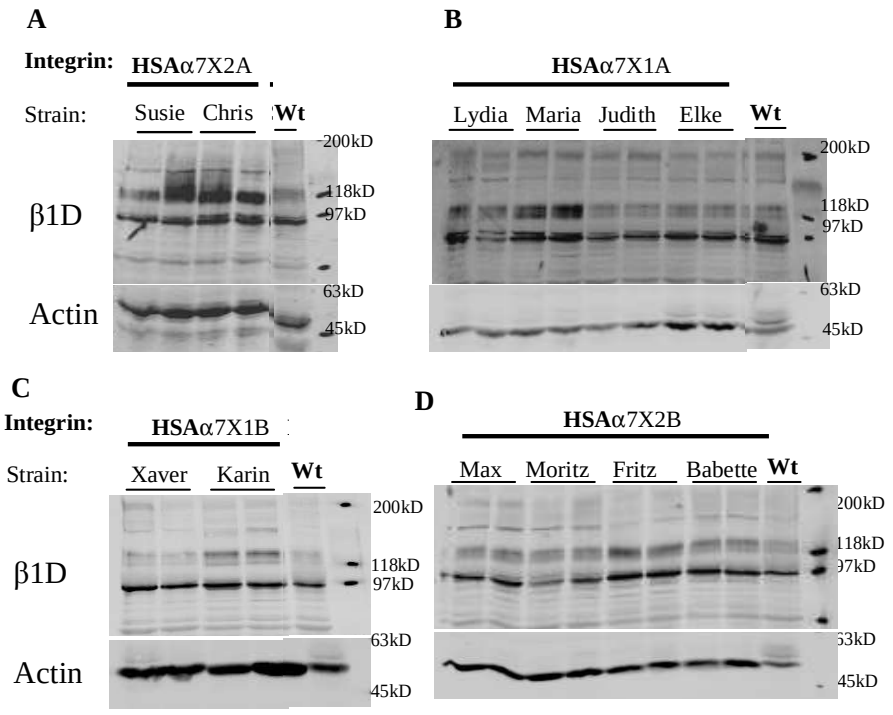

Figure 4.9: Analysis of integrin β1D expression in integrin α7 overexpressing mice. *Immunoblotting of GC muscle lysates were separated under non-reducing conditions by SDS-PAGE on 5-15% gels. Antibodies raised against the intracellular D variant of integrin β1 and actin were used for immunoblotting.*

The apparent lack of integrin β1D heterodimerisation with integrin α7X1 could be logically explained if this integrin α7 splice variant instead specifically dimerised with an alternative integrin β1 splice variant. Integrin β1A is expressed in muscle during myogenesis, but is replaced by the D variant on terminal differentiation. It is therefore not present at detectable levels in adult skeletal muscle. However, as the α7X1 is also predominantly expressed during myogenesis it is feasible that it may dimerise with integrin β1A.

To investigate this possibility, direct immunoblotting of the same GC lysates was carried out using a polyclonal antibody raised against integrin β1A. (Figure 4.10)

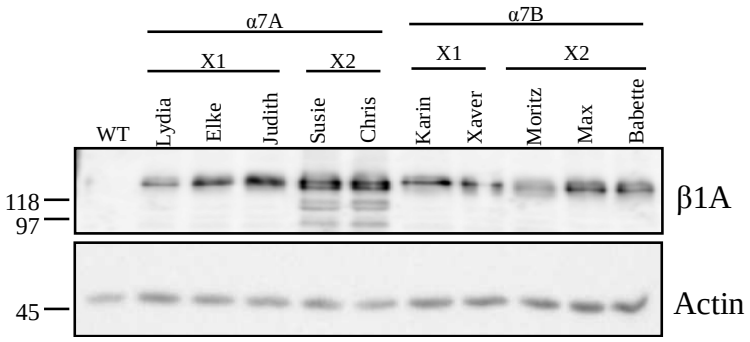

Figure 4.10: Analysis of integrin β1A expression in integrin α7 overexpressing mice. *Immunoblotting of GC muscle lysates were run under non-reducing conditions by SDS-PAGE on 5-15% gels. Antibodies raised against the intracellular A variant of integrin β1 and actin were used for immunoblotting.*

Overexpression of integrin α7 splice variants resulted in a slight increase in integrin β1A in the strains expressing X1 extracellular integrin variant when compared to wildtype controls. From the data it also seems that the mice overexpressing integrin α7X2 variant also display higher levels of expression of integrin β1A.

4.1.7 *In vivo* analysis of integrin β1D expression and effect of dimerisation

Heterodimer formation is a pre-requisite of cell surface expression. To further investigate integrin α7β1D heterodimer formation, immunostaining of muscle sections was performed. Mice were sacrificed at 3 months and hindlimbs were dissected and cryo-embedded. Sections were cut at 10μm and stained with antibodies raised against the extracellular part of integrin β1 or integrin β1D.

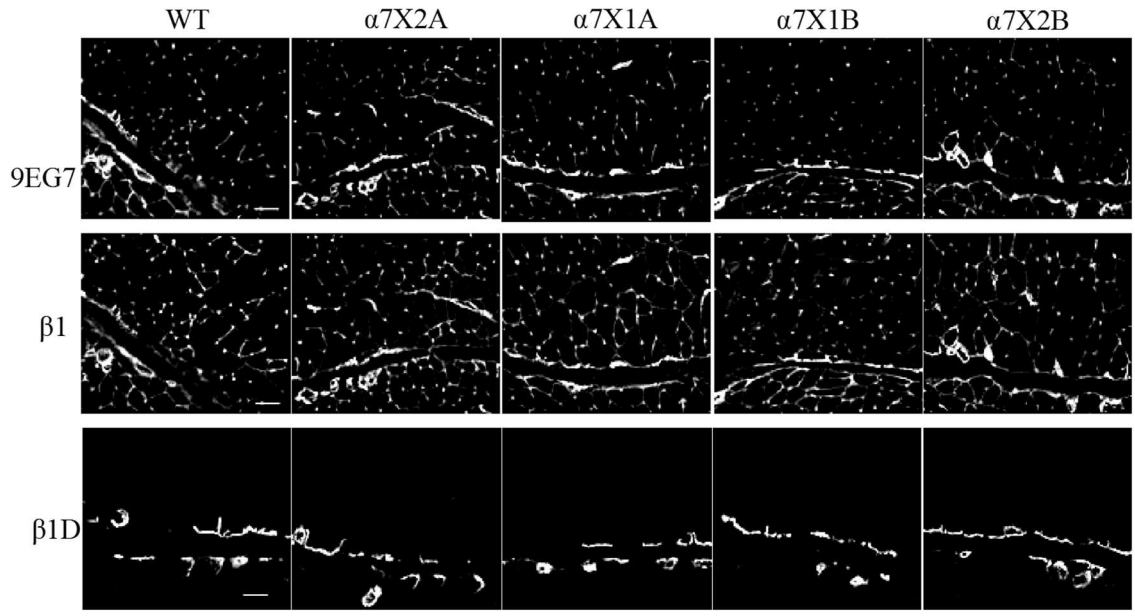

Figure 4.11: Expression of β1 subunit in transgenic muscle. *Muscle sections taken from WT, integrin α7X1A, X2A, X1B and X2B variant mice were stained for integrin β1 (CD29, clone 9EG7, Pharmingen, and polyclonal antibody against the extracellular domain and recognises activated form of integrin β1) and β1D (rabbit polyclonal) in comparable regions of the GC muscle. Bar, 100μm*

Integrin β1D is expressed at the MTJ of wildtype muscle and can also be seen, although weakly, at the sarcolemma (Figure 4.11 bottom row). In all four transgenic strains the staining pattern for β1D is similar to that seen in the wildtype. In contrast, β1staining is more intense and concentrated at the sarcolemma when the X2 variant is overexpressed, while the overexpression of the α7X1 variant results in an integrin β1 staining pattern similar to the wildtype.

In summary, only an increase in integrin α7X2 resulted in an increase in the amount of integrin β1D present (immunoblotting and staining) and in the formation of α7β1D integrin dimerisation (Figure 4.7 and 4.8). When integrin α7X1 is overexpressed, it is however localized to the MTJ and sarcolemma (Figure 4.11) suggesting it is able to heterodimerise with integrin β1. Yet, immunoprecipitation and immunoblotting would suggest this is not with integrin β1D. It may indicate that integrin β1A could be an alternative dimerisation partner for α7X1, but the mechanism behind their binding remains to be elucidated.

To conclude, increased expression of integrin α7X2 variant appears to cause increased β1 integrin expression, which could result in reduced sarcolemmal stability and therefore contribute to the phenotype observed in the α7X2 overexpressing mice (see below).

4.1.8 Muscle histology of transgenic strains overexpressing integrin α7

The role of integrin α7 splice variants in adult skeletal muscle is clearly intricate and complex. It is seen that association with integrin β1D is dependent on the extracellular splice variant expressed, and that localization and competition are dependent on the intracellular variant overexpressed. Of particular interest when considering this is whether these factors have any effect on the muscle itself. As one of the reasons these mice were generated was to investigate the potential of integrin α7 in rescuing the *mdx*/DMD phenotype.

To investigate the role of integrin α7β1 in skeletal muscle and its potential to rescue the phenotype in *mdx* mice, we first needed to understand muscle histology of the transgenic overexpressing strains. It is important to determine whether the overexpression of the individual splice variant of integrin α7 *in vivo* caused any phenotypic changes to the muscle tissue. To investigate the muscle histology, the mice were sacrificed at four weeks, three months and six months of age. The hindlimbs were dissected and cryo-embeded. 10 µm sections were cut and slides were stained for Haematoxylin and Eosin (H&E) staining. Four muscles representing a variation of muscle fiber types were studied for each strain, namely GC TA, EDL and Sol (Figure 4.12

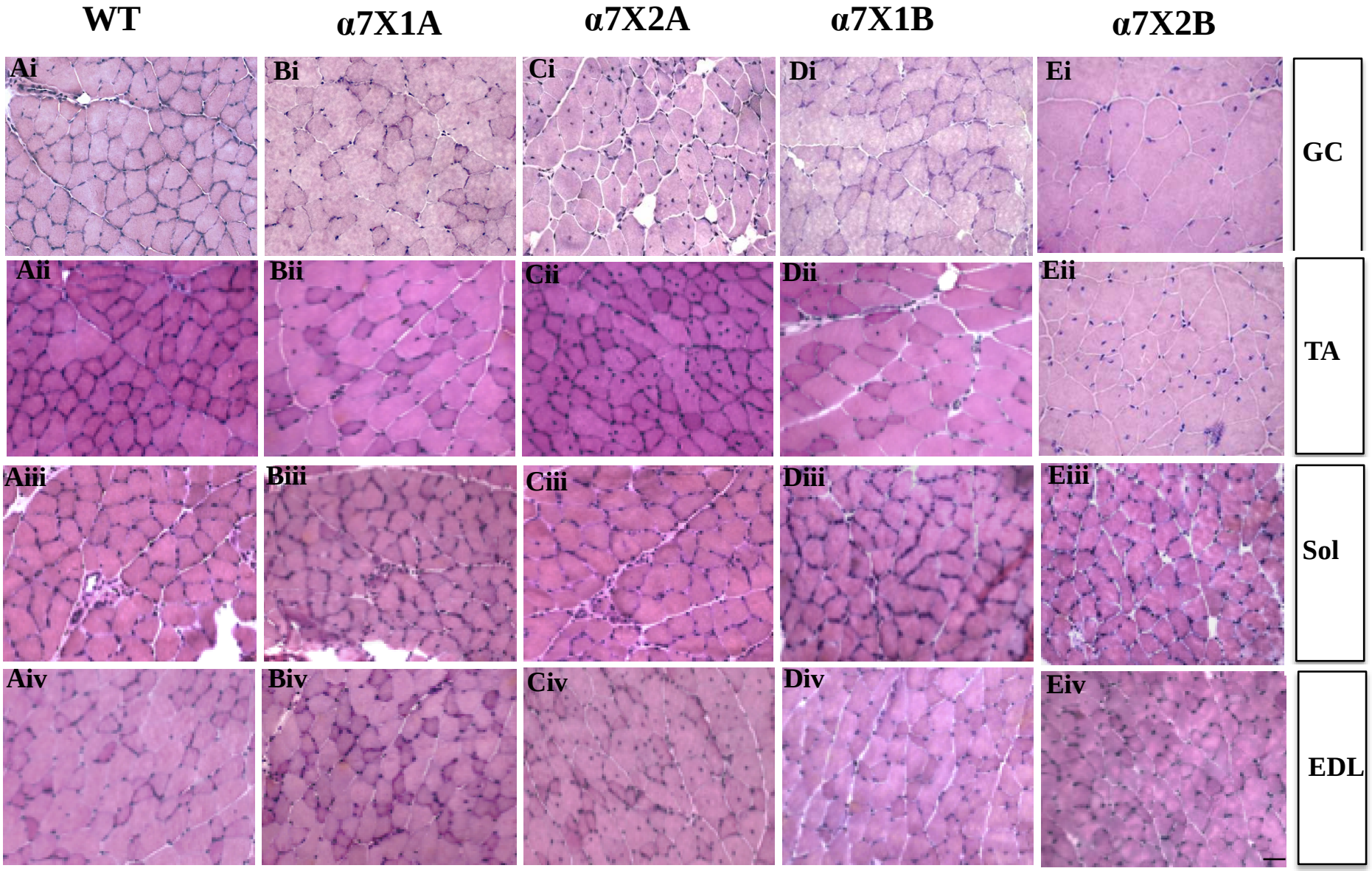
WT
α7X1A
α7X2A
α7X1B
α7X2B
Ai
Bi
Ci
Di
Ei
GC
Aii
Bii
Cii
Dii
Eii
TA
Aiii
Biii
Ciii
Diii
Eiii
Sol
Aiv
Biv
Civ
Div
Eiv
EDL

Figure 4.12: Histological analysis of integrin α7 overexpressing mice. *Representative muscle sections from wildtype and integrin α7X2A (Susie), α7X1A (Lydia), α7X1B (Xaver), and α7X2B (Babette) overexpressing mice at three months of age. Sections were stained with haematoxylin and eosin. Centrally located nuclei are marked with an asterisk. The soleus muscle is spared in all transgenic strains (lower panel). Bar, 20μm.*

In the wild type all muscle fibres are of similar diameter and all the nuclei are located at the edge of the fibre, close to the sarcolemma. In the muscle sections of the mice overexpressing integrin α7X1A and α7X1B (Lydia and Xaver), the muscle histology is almost similar to that of the wild type control. Muscle fibers are of similar diameter and all the nuclei are located at the edge of the fiber. A similar phenotype/genotype correlation was seen at four weeks and six months of age. Interestingly, H&E staining of transverse cryosections of mice overexpressing integrin α7X2A and α7X2B showed a myopathic phenotype. Large number of muscle fibers showed centrally located nuclei indicating that the muscle has undergone regeneration following degeneration. This suggests that overexpressing these two splice variants has actually caused damage to the muscle. Intriguingly, the soleus was protected in all the strains (figure 4.12). It seems that the Soleus has a specific protection with no centrally located nuclei present as seen in the GC, TA and EDL of either integrin α7X2A or α7X2B overexpressing strains.

4.1.9 Quantification of centrally located nuclei (CLN) in transgenic mice

H&E staining data indicated a clear phenotypic difference between the strains overexpressing the integrin α7X1 and X2 extracellular splice variants. To further investigate these differences, the number of centrally located nuclei (CLN) was quantified and this was carried out for three different age groups of mice in order to follow the progression of the disease phenotype. During muscle regeneration following the muscle injury, satellite cells of the muscle fibre become activated and enter the cell cycle. In order to repair the damaged muscle fibre, these SCs fuse with the muscle fibre and their nuclei can be seen at the centre of the fibre. The percentage of muscle fibres with CLN is used as an indicator of muscle damage.

Muscle sections at four weeks (fully developed muscle), three months (early-mid adult stage), and six months (adult stage) was analysed and compared to wildtype muscle at all ages. The number of muscle fibres was counted for CLN using the H&E images in IMAGE J software and the percentage of muscle fiber with CLN was calculated (Figure 4.13).

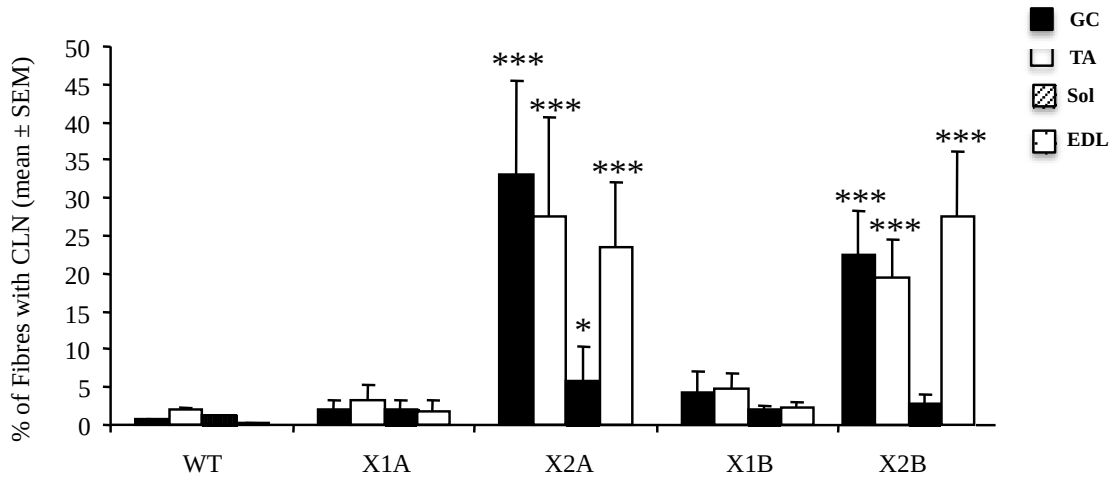

Figure 4.13 Quantification of CLN in integrin α7 transgenic mice. *The degree of de- and regeneration was assessed in H&E stained transverse sections of six-month-old Wildtype and transgenic mice. Data are expressed as % of fibers with centrally located nuclei. One-way ANOVA statistical analysis was performed in StatView 5 for Windows. Data are expressed in mean ± SE, *p<0.05; **p<0.01, ***p<0.001, ****p<0.0 001.*

Wildtype muscle usually has approximately 2% of fibres with centrally located nuclei. In all strains analysed, the GC, TA and EDL all had a very similar severity of phenotype. In strains overexpressing the integrin α7X1A (Lydia) and α7X1B (Xaver) the muscle phenotype did not differ from the wildtype (Figure 4.13). Muscle overexpressing the integrin α7X2A (Susie) and α7X2B (Babette), however, had an increase in the percentage of muscle fibres with centrally located nuclei.

Quantification of the percentage of muscle fibres with centrally located nuclei (CLN) of the GC, TA, EDL and Sol muscle confirms the difference in phenotype between the X1 and X2 overexpressing strains. As early as 4 weeks of age, strains overexpressing the X2 variant had between 5 and 15% of centrally located nuclei (data not shown). This phenotype gets progressively worse with age, whereby at 6 months of age approximately 35-40% of muscle fibres were affected (Figure 4.13). The percentage shown is an average from all mice analysed (four mice from each strain).

By 6 months of age an increase in muscle degeneration and regeneration can be seen in muscle overexpressing the integrin α7X2A subunit (Susie) and α7X2B subunit (Babette). In contrast, and as seen previously, α7X1 overexpressing strains showed less than 5% of muscle fibres with centrally located nuclei and are thus very similar to the histology observed in wildtype muscles.

Surprisingly, the Soleus muscle appeared to be protected and there was only a slight increase in centrally located nuclei for the integrin α7X2 overexpressing strains and this was true at all ages analysed (Figure 4.13 and data not shown). The percentage of CLN in the soleus muscle did not increase above 5%.

4.1.10 Summary of integrin α7 splice variant overexpressing strains

Strains were generated to overexpress integrin α7 splice variants. A large number of strains successfully overexpressed the splice variants and the HSA promoter provided substantial protein overexpression.

The overexpression of integrin α7 splice variants in transgenic mice models has revealed many significant differences between them. Integrin β1D preferentially heterodimerises with integrin α7X2 and not integrin α7X1. Increasing levels of integrin α7X2 in association with either intracellular splice variant resulted in increased integrin α7X2β1D and this caused a dystrophic phenotype. The dystrophic phenotype resulted in a considerable increase in muscle fibres with CLN, with the specific protection at the MTJ (data not shown) and soleus muscle. In contrast, completely normal muscle histology was seen on overexpression of the α7X1 extracellular splice variant. The phenotypic effect of integrin α7 splice variant overexpression was independent of the intracellular slice variant present

4.2 Investigating the effects of integrin α7 overexpression on *mdx* phenotype

To determine the contribution of integrin α7 splice variants in rescuing dystrophin deficiency, integrin α7 overexpressing mice were crossed with dystrophin-deficient *mdx* mice. Tail biopsies were taken from offspring to isolate the DNA for genotyping. PCR was performed using primers specific for the transgene and for *mdx.*

4.2.1 Integrin α7 splice variant's overexpression in *mdx* mice

To identify and quantify integrin expression in *mdx* transgenic (m^{Tg}) mice we sacrificed the mice and hindlimb muscles were isolated. Protein extracts were prepared from the largest muscle, GC and separated by SDS-PAGE (Figure 4.12). The immunoblots were probed with rabbit polyclonal antibodies specific for the integrin α7A, integrin α7B and integrin β1D. GAPDH was used as a loading control.

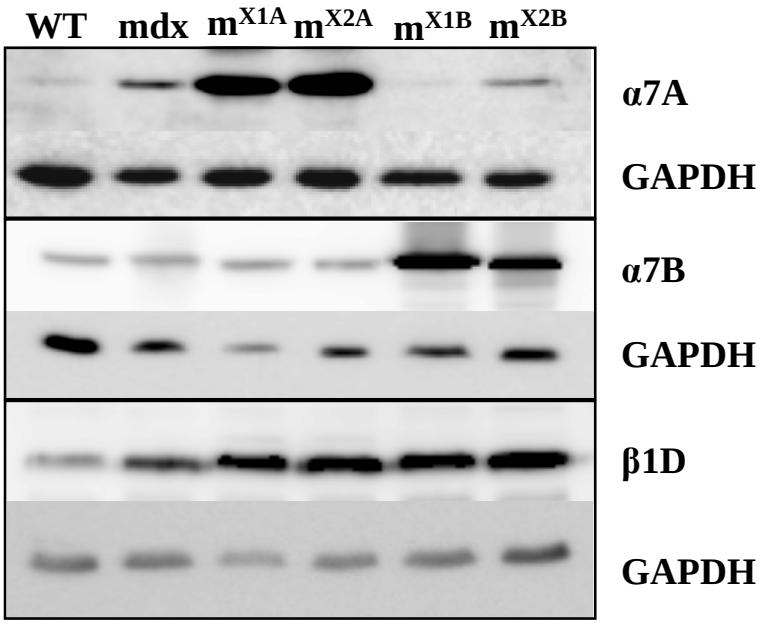

Figure 4.14: Integrin α7 splice variant expression in mdx mice*. Immunoblots of lysates from Gc muscle of mice overexpressing integrin α7X1A, α7X2A, α7X1B, α7X2B on the mdx background and WT muscle as control. At least 3 mice per splice variant were lysed in RIPA buffer and submitted to immunoblotting with rabbit polyclonal integrin antibodies. GAPDH detection was used as loading control.*

Integrin α7 splice variant overexpression was achieved in m^{tg}-Susie ($mdx^{\alpha 7X2A}$), m^{tg}-Lydia ($mdx^{\alpha 7X1A}$), m^{tg}-Xaver ($mdx^{\alpha 7X1B}$) and m^{tg}-Babette ($mdx^{\alpha 7X2B}$). Immunoblot clearly shows overexpression of integrin α7A in m^{tg}-Susie ($mdx^{\alpha 7X2A}$) and m^{tg}-Lydia ($mdx^{\alpha 7X1A}$) (Figure 4.14 top row) when compared to the wildtype and *mdx* littermate. Similarly in m^{tg}-Xaver ($mdx^{\alpha 7X1B}$) and m^{tg}-Babette ($mdx^{\alpha 7X2B}$) the expression of integrin α7B was shown to have increased (Figure 4.14 middle row) noticeably when compared against the controls. At the same time the heterodimer formation was analysed by probing the immunoblots with the antibody raised against β1D. The presence of the β1D protein in all the mdx^{tg} strains was confirmed by the appearance of a 150 kD band in all the analysed samples.

4.2.2 Protein quantification of alternative splice variants in $mdx^{\alpha 7tg}$ mice

An effect of the transgene on the endogenous alternative splice variant in transgenic mice was analysed by quantifying the protein levels of α7A in $mdx^{\alpha 7B}$ and of α7B in $mdx^{\alpha 7A}$ mice by Western blotting and immunostaining. The membranes were probed with rabbit polyclonal antibodies specific for integrin α7A, α7B and β1D.

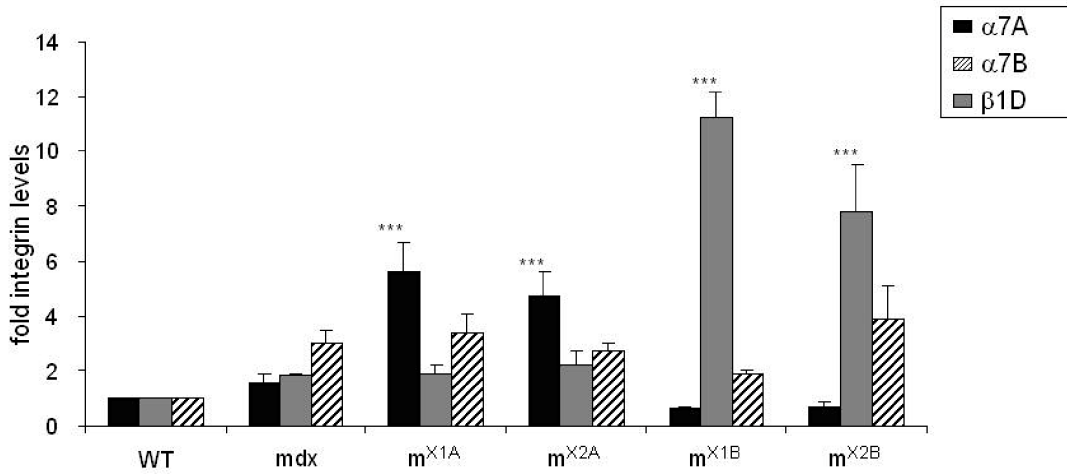

Figure 4.15: Quantification of integrin α7 splice variant overexpressionin mdx mice*. The optical density of integrin α7 bands was determined using ImageJ software. The relative expression level to the wildtype and mdx was calculated after normalisation to GAPDH.*

It was observed that the levels of α7A, α7B and β1D were increased by 1.5, 2.5 and 3 fold respectively in *mdx* mice, but were not significantly different from wildtype mice. As expected in *mdx*$^{\alpha 7tg}$ mice, integrin levels were increased by ~5fold for α7A and ~8- ~16fold for α7B as compared to wildtype mice (Figure 4.15). Different to the transgenic lines, the level of β1D was high in all transgenes and not only restricted to the α7X2 splice variants.

4.2.3 Muscle histology of *mdx* transgenic (*mdx*^{tg}) mice overexpressing integrin α7 splice variants

H&E staining of integrin α7 splice variant overexpressing mice suggested that mice expressing the extracellular X2 splice variant have a myopathic phenotype. It is therefore important to investigate the effect of α7 splice variant overexpression on *mdx* mice *in vivo*. In order to do this, mice were sacrificed at four weeks, three months and six months. The hind limbs were dissected and cryo-embedded. 10µm sections were cut and slides were stained for H&E staining. The GC muscle from *mdx* mice showed a typical dystrophic phenotype with fibrosis and many fibres containing CLN. The morphology of muscle sections from *mdx*$^{\alpha 7tg}$ mice is somewhat similar to *mdx* mice with many fibers undergone a degeneration-regeneration cycle. Interestingly, *mdx* mice expressing the α7X2 variant seemed to have larger areas of muscle damage compared to *mdx*$^{\alpha 7X1}$ mice in GC muscle. (Figure 4.16)

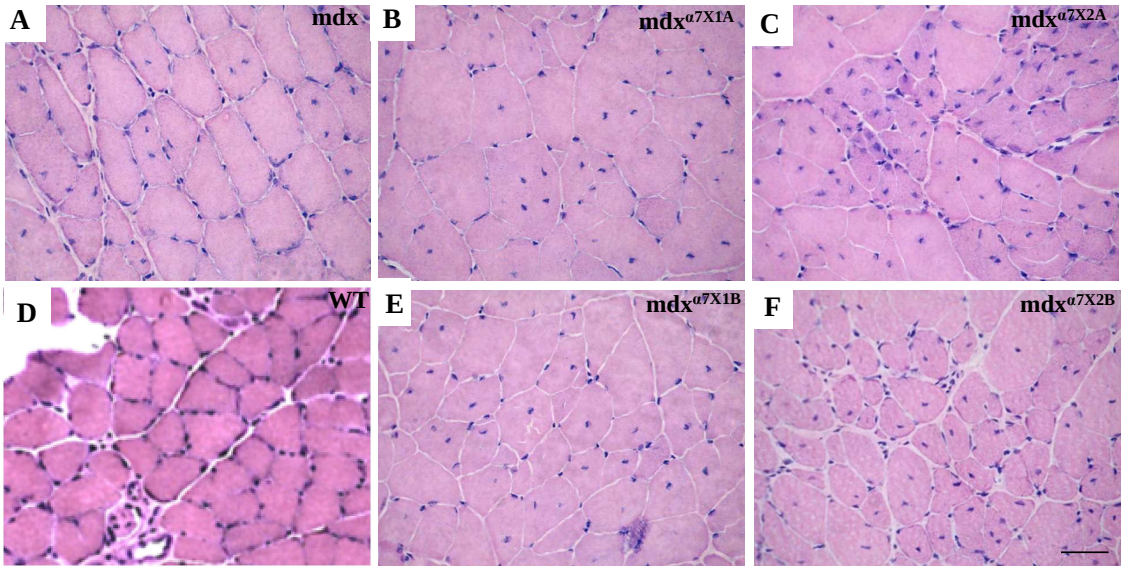

Figure 4.16: Histological analysis of integrin α7 overexpressing mdx mice. *H&E staining of 10 µm thick cryosections of GC muscle from WT (D) mdx (A) and integrin mdx$^{\alpha7X2A}$ (C), mdx$^{\alpha7X1A}$ (B), mdx$^{\alpha7X1B}$ (E), and mdx$^{\alpha7X2B}$ (F) overexpressing mice at three months of age reveals signs of muscle regeneration in mdx as well as m^{tg} mice. Appearance of CLN was pronounced in mdx$^{\alpha7X2B}$ and mdx$^{\alpha7X2A}$ muscle compared to mdx and WT mice. Bar 50µm*

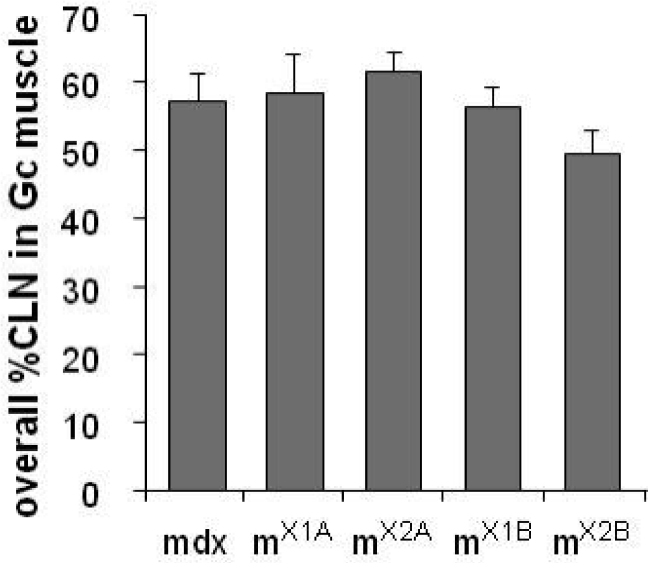

Figure 4.17: Quanification of fibres with CLN in mdx^{tg} mice. *Percentage of fibers with centrally located nuclei in GC muscles of mdx and mdx$^{\alpha7tg}$ mice. Areas of degeneration were excluded. Overall, the percentage of fibres with centrally located nuclei in GC muscle is not significantly modified by the overexpression of any integrin α7 splice variant in mdx mice.*

It was therefore important to count the percentage of fibers with CLN in GC muscle of *mdx* and *mdx*$^{\alpha 7tg}$ mice. Surprisingly, the overall percentage of fibres containing CLN in *mdx*$^{\alpha 7X2}$ was not significantly different compared to *mdx*$^{\alpha 7X1}$ and *mdx* mice. These results demonstrate that *mdx* mice expressing integrin α7 variants are not histologically different than *mdx* control mice (Figure 4.17).

In addition, immunostaining of muscle sections from *mdx*^{tg} mice for integrin α7 intracellular splice variant and the laminin α2 was performed. As shown in figure 4.18, this showed a strong staining of the respective overexpressed splice variant in muscle sections of *mdx*^{tg} mice at the sarcolemma (Figure 4.18 Bi, Ci, Di and Ei).

Closer inspection of the sections revealed the interesting finding that some of the muscle fibres overexpressing integrin α7 were actually protected against muscle damage. There were no CLN in most of the fibres expressing integrin α7X1A (Figure 4.18 Biii) and α7X1B (Figure 4.18 Diii). However, in α7X2A (Figure 4.18 Ciii) and α7X2B (figure 4.18 Eiii) muscle sections the ratio of overexpressing fibres with CLN was higher compared to α7X1A, α7X1B.

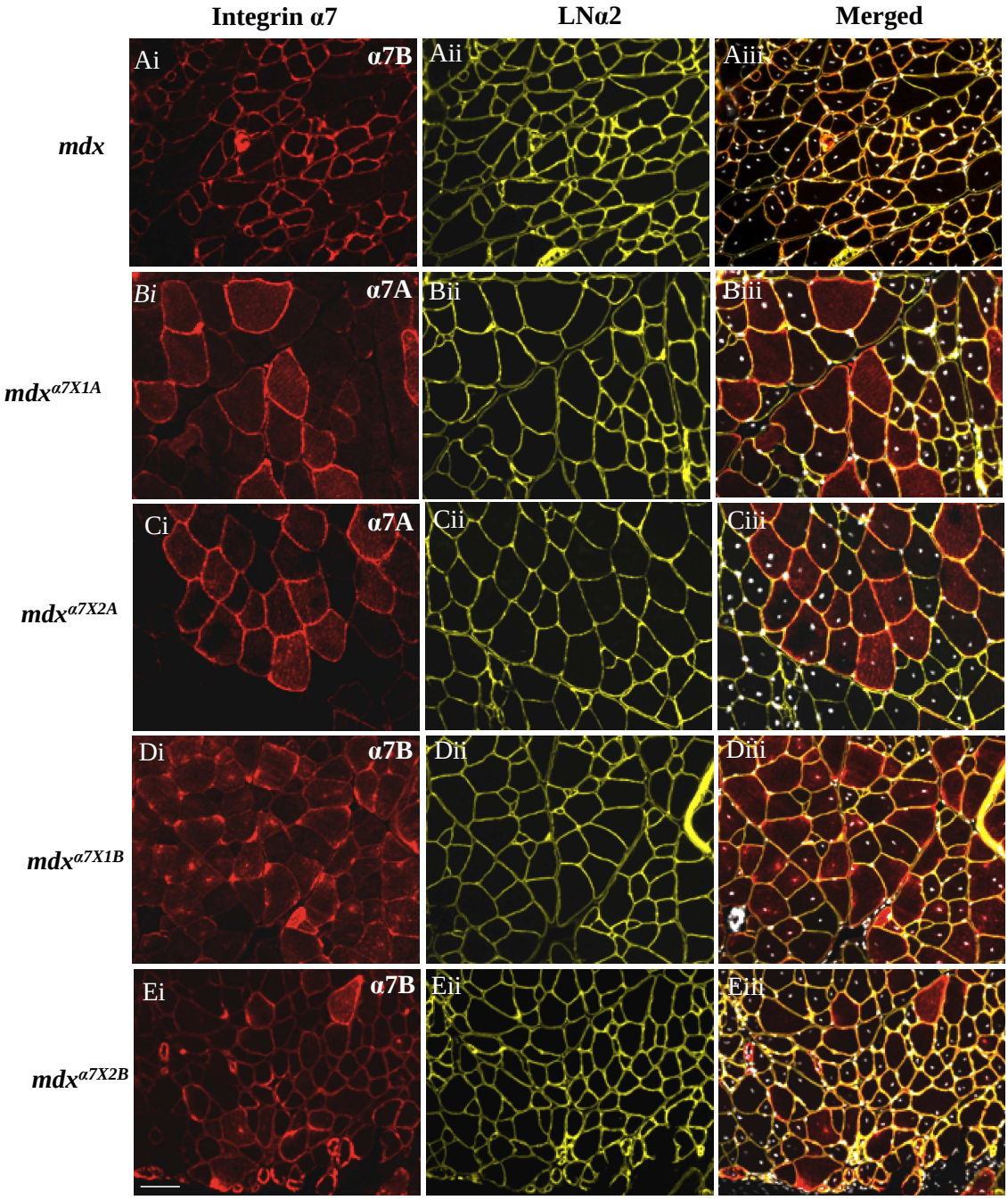

Figure 4.18: Investigating expression and localisation of integrin α7 splice variants in mdx^{tg} mice. *Representative muscle sections taken from mdx, mdx^{α7X1A}, mdx^{α7X2A}, mdx^{α7X1B} and mdx^{α7X2B} mice were immunostained for integrin α7A and α7B. Integrin α7A is restricted to the MTJs in mdx mice whereas it is additionally expressed at the sarcolemma and the sarcoplasm in transgenic mice. Integrin α7B is found at the sarcolemma and the sarcoplasm in mdx^{α7B} transgenic mice. Laminin α2 (LN α2 in yellow) stained the BM and DAPI was used to mark the nuclei (white). Pictures were taken at x20 magnification. Bar 50 μm*

4.2.4 Analysis of membrane damage in *mdx*$^{\alpha 7tg}$ mice using Evan's blue dye

After the H&E staining results it was clear that the muscles of *mdx*$^{\alpha 7X2}$ mice showed a more severe dystrophic phenotype compared to *mdx* and *mdx*$^{\alpha 7X1}$ mice. In *mdx* mice one of the dystrophic features is membrane damage, which can be detected with the help of Evans Blue Dye (EBD).

In order to evaluate the protection offered by each integrin α7 splice variant, *mdx*, *mdx*^{tg} and α7 transgenic mice were injected with EBD six hours prior to dissection. Mice were sacrificed and hindlimbs and diaphragms were isolated. Evans blue positive fibers were visualized and scanned at low magnification using the Odyssey machine (Li-Cor) (Figure 4.19) and at higher magnification using Zeiss Axioplan fluorescent microscope (data not shown).

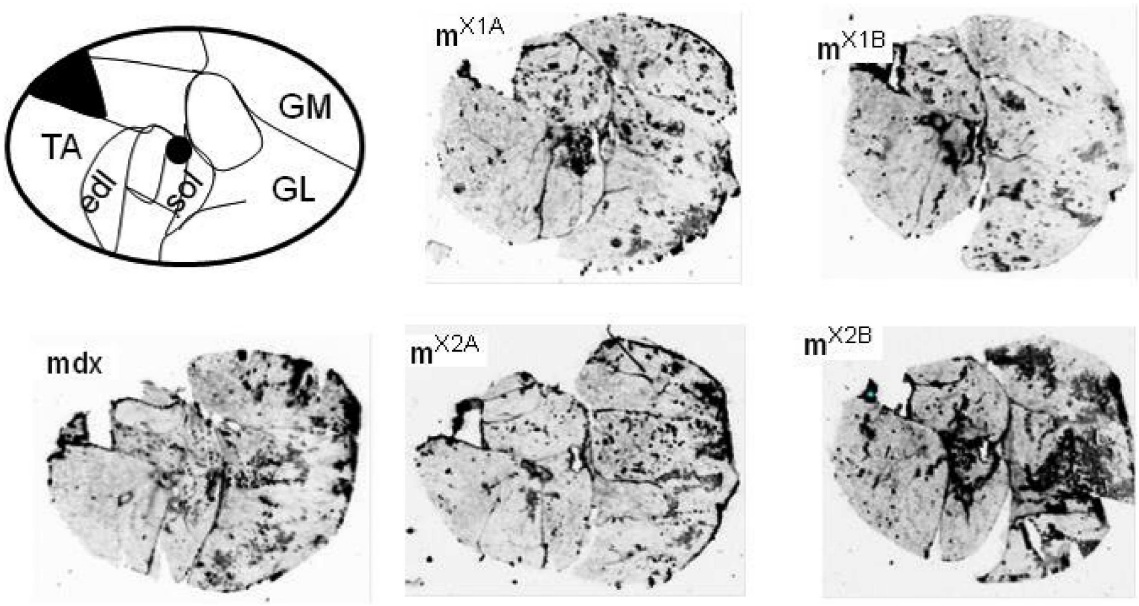

Figure 4.19: Membrane damage in mdx$^{\alpha 7tg}$ mice using Evan's blue dye. *Membrane damage was assessed by injection of Evan's Blue Dye. Hindlimbs were harvested from mdx and mdx$^{\alpha 7tg}$ mice, 6 hours post-injection and cryosections were scanned at 700nm using the Odyssey Imager (Li-Cor). Scanned images of the EBD injected hindlimbs show membrane damage in all muscles. mdx$^{\alpha 7X2B}$ sections show increased uptake of the dye.*

The α7 transgenic mice did not show any EBD uptake, while all *mdx*$^{\alpha 7tg}$ mice displayed signs of membrane damage. Some muscles were spared and in some muscles the morphology was improved compared to *mdx* muscles, most often in Peroneus. However, this result was variable between individuals of the same genotype. In order to evaluate if the α7 splice variants really improve the dystrophic phenotype of *mdx* mice, we analysed the most affected muscle, the GC. The scanned images of the hindlimb sections revealed that there is no difference in EBD incorporation in *mdx* and *mdx* $^{\alpha 7tg}$ mice (Figure 4.19). In fact *mdx* α7X2, especially *mdx*$^{\alpha 7X2B}$ mice had more areas of membrane damage compared to *mdx* and *mdx*$^{\alpha 7X1}$ transgenic mice. We therefore compared the diapharagms of *mdx* $^{\alpha 7X2A}$ with *mdx* and α7X2A transgenic mice (Figure 4.20).

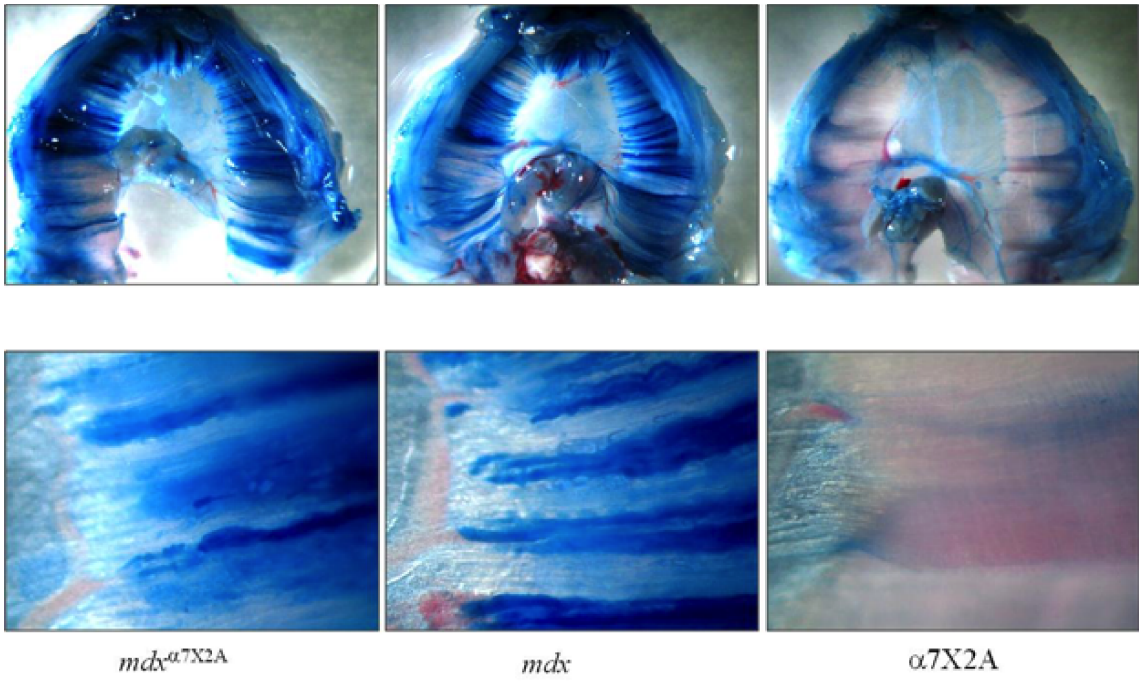

Figure 4.20: Membrane damage in diaphragms of mdx$^{\alpha 7tg}$ mice using Evan's blue dye. *Membrane damage in diaphragms of α7X2A, mdx and mdx$^{\alpha 7X2A}$ mice 6 hours post-injection with EBD. Fibres in the diaphragm of mdx$^{\alpha 7XA2}$ mice have more uptake of EBD compared to that dissected from mdx and α7X2A transgenic mice.*

It clearly shows that the fibres in the diaphragm of *mdx*$^{\alpha 7X2A}$ mice has more uptake of EBD compared to the diaphragm of *mdx mice.* α7X2A transgenic mice did not show any signs of membrane damage. Together, this data argue that overexpression of α7X2 variants worsen the phenotype of *mdx* mice. However, more work is need into analysis of the effect of α7X1 variants on muscle stability in *mdx* mice.

4.3 Discussion

Integrins play an important role during skeletal muscle development. The integrin α7β1 is the only β1 integrin present throughout the muscle development and adulthood, and deficiency of α7 leads to congenital myopathies in mice and human (Mayer, 1997, Hayashi et al, 1998). Integrin α7 share a similar function as the DGC by connecting the cytoskeleton to the extracellular matrix. Transgenic expression of the adult isoforms of integrin α7β1 has shown improvement of the phenotype in mice deficient in dystrophin and its analogue utrophin (Burkin et al, 2001). This data suggests that integrin α7β1 could play a role in ameliorating the phenotype caused by the dystrophin deficiency. However, integrin α7 expression is developmentally regulated and the complexity has increased with the existences of intra- and extracellular splice variants. In order to evaluate the importance of developmental splice variants of integrin α7, we generated transgenic mice overexpressing all four possible combinations of these splice variants. These mice were then crossed with the dystrophin deficient *mdx* mice to analyse the importance of integrin α7 overexpression.

4.3.1 Integrin α7 overexpression and its effect on muscle phenotype

Transgenic mice overexpressing integrin α7 splice variants were generated to provide insight into the possibility and efficiency of increasing integrin α7 splice variant protein expression *in vivo.* In addition, the mice were generated to compare the roles of the different integrin α7 splice variants. Offspring positive for each of the integrin α7 splice variant transgenes were born healthy and viable.

The expression of the transgene was controlled by the HSA promoter and thus expression will be specifically in skeletal muscle. Variation in the level of protein overexpression in the different transgenic strains is to be expected, as there is no control on where the transgene will integrate into the genome. In addition, although a measured amount of DNA is injected, the copy number of the transgene will vary between injections and therefore strains.

Protein overexpression was verified by immunoblotting and immunofluorence and then quantified. Integrin α7A and B transgenic mice showed a strong 10 fold increase in α7 expression and immunostaining results showed localization of the protein at MTJ and at the sarcolemma. There was also an ectopic presence of integrin in the

sarcoplasm, suggesting that the protein is produced in a larger mount than the cell is capable to translocate it to the sarcolemma.

4.3.2 Integrin β1D association with the integrin α7X2 variant

An increase in integrin α7 is only relevant if there is a concomitant increase in the integrin α7β1 heterodimer. Changes to integrin α7 and β1 splice variant expression in skeletal muscle have been documented (Song et al., 1992;Belkin et al., 1996; van der Flier et al., 1995; Song et al., 1993; Hodges and Kauffman, 1996; Collo , Starr and Quaranta, 1993; Ziober et al., 1993; Velling et al., 1996; von der Mark et al., 2002; Ziober, Chen and Kramer, 1997; Kaariainen et al., 2002) , but there has been no evidence to suggest that either of the β1 cytoplasmic splice variants has a specific preference for any of the α7 integrin isoforms in terms of heterodimer formation. It was therefore surprising to find that enhanced dimer formation with integrin β1D was only observed when the α7X2 splice variants were overexpressed. In addition, the total amount of integrin β1D present only increased when the α7X2 variant was overexpressed. In contrast, integrin β1D does not increase when integrin α7X1 variants are overexpressed.

This is even more surprising, when one considers that the integrin α7X2 specific association with integrin β1D is completely independent of whether the A or B intracellular variant is present. That is to say the extracellular domain of integrin α7 has a specificity for an intracellular domain of integrin β1.

The α7X2β1D splice variant-specific pairing is in line with the expression pattern of these two splice variants. Integrin α7X2 and integrin β1D are both the predominantly expressed isoforms of these two integrin subunits in adult skeletal muscle, so it makes sense that they would preferentially form a heterodimer.

The role of integrin α7X1 in adult muscle is less straightforward. Increasing the amount of the integrin α7X1 variant did not result in an increase in the α7X1β1D heterodimer, even though it is known that the α7X1 and β1D integrins can form a heterodimer (Yeh et al., 2003). Overexpressing the integrin α7X1 variant did result in an increase in the total amount of integrin β1 present. It was hypothesised that this could

be because the integrin α7X1 variant was forming an association with integrin β1A. Yet, levels of integrin β1A remained undetectable in the integrin α7X1 overexpressing muscle as for the wildtype. Possible explanations of this discrepancy include that the increase in integrin β1A was too slight to be detected by immunoblotting, or alternatively, the integrin β1A specific antibody is not as efficient as the integrin β1D antibody. A further reason to suggest that the lack of integrin β1A detection is a problem of the technique is the fact that integrin α7X1 is localised to the sarcolemma of transgenic muscle, and surface expression of integrins requires αβ heterodimerisation. In other words, integrin α7X1 must be associated with integrin β1 to be expressed at the sarcolemma, and as shown by the immunoprecipitation experiments this was not the integrin β1D variant. This phenomenon does require further investigation, perhaps if antibodies were unable to identify integrin β1A, in situ hybridisation could be employed to verify the presence or absence of the β1A subunit.

The splice variant specific pairing of integrin α7 and β1 is a significant indication that the integrin α7 splice variants clearly play very different roles in skeletal muscle. This may have implications for their potential use in the treatment of DMD.

4.3.3 Integrin α7 extracellular splice variants and their effect on adult muscle integrity

The integrin α7 transgenic mice were developed mainly to investigate the potential of integrin α7 to treat Duchenne Muscular Dystrophy. In the initial characterisation of the overexpressing mice, many interesting and unexpected findings were made, that even expressing these constructs on a wildtype background gave much insight into the functional differences of these α7 integrin splice variants. However, these findings may be different when the splice variants are expressed in the context of a muscular dystrophy, be it in the α7 integrin knock-out or the *mdx* mouse.

The most surprising finding was that the overexpression of the integrin α7X2 splice variant caused a muscular dystrophy, yet the overexpression of the α7X1 variant did not. In α7X2 integrin overexpressing mice, a progressive increase in the number of fibres with centrally located nuclei was seen, reaching up to 40% at 6 months of age. In stark contrast, the overexpression of the integrin α7X1 variant appeared to have no

detrimental effect on adult muscle integrity. The difference in phenotypes when extracellular variants are overexpressed is surprising as the integrin α7X2 variant is naturally the predominantly expressed isoform in adult skeletal muscle. The phenotype was also completely independent of the intracellular variant present.

It has previously been suggested that integrins α7X2 and β1D provide a strong connection to the ECM required in adult muscle (Belkin and Retta. 1998; Kaariainen et al., 1998). In contrast, integrins α7X1 and β1A are transiently co-expressed at the early stages of muscle regeneration following injury (Kaariainen et al., 2002). It may therefore be postulated that these integrins fullfil specific requirements of regenerating muscle by providing a weaker and more dynamic connection to the ECM. The fact that the integrin α7X1 and integrin β1D do not form a heterodimer in adult skeletal muscle makes sense when one considers the requirements placed on the ECM-cytoskeletal connection in adult muscle. An increase in this link could therefore result in a stiffened muscle, which is more susceptible to mechanically induced damage. Even though we observed an increase in the fibres with CLN in three months old α7X2 overexpressing mice, no fibres appeared positive for membrane damage when analyzed for EBD uptake. Also there was no sign of fibrosis, calcification or fat deposition in the analyzed muscle sections. These results point to the fact that the phenotype observed in α7X2 overexpressing mice is a result of contraction- induced damage.

Integrin α7 expression increases in regenerating muscle (Kaariainen et al., 2002). The proliferation and fusion of satellite cells (muscle stem cells) is a feature of muscle regeneration. Therefore, a simple explanation of the increase in centrally located nuclei seen would be that integrin α7X2B and α7X2A had specifically activated muscle proliferation. This does not seem to be the case because if satellite cells were continuously proliferating and fusing to existing muscle fibres, they would become hypertrophic and this was not observed. It therefore appears that the overexpression of integrin α7X2B and α7X2A has actually caused damage to the muscle resulting in degeneration, which was then followed by regeneration. The question is therefore why increasing the expression of the integrin α7X2 damages adult skeletal muscle whereas the α7X1 splice variant does not.

This question is complicated as the Soleus muscle and MTJs were protected from an α7X2 induced dystrophic phenotype. In the integrin α7 knockout mouse the only affected muscle was the Soleus muscle and there was also a severe phenotype at the MTJs (Mayer et al, 1997). The findings of this thesis therefore support this previous conclusion that these are the two sites at which integrin α7 is localised and concentrated and plays a vital and unique role. Therefore, perhaps the protection of these two sites is simply because they are in some way adapted to elevated levels of integrin α7.

There is further evidence to suggest that the study of the Soleus muscle in particular may provide important clues as to how integrin α7X2 expression could still have a potential role in a gene therapy treatment of DMD. The Soleus muscle is primarily made up of the oxidative slow-twitch type I and fast-twitch type IIa fibres and it has been known for many years that these fibre types are affected the least by the degenerative effects of Duchenne Muscular Dystrophy (Karpati, Carpenter and Prescott, 1988; Webster et al., 1988). In support of this notion, the increase in the proportion of 'slower' type IIA fibres seen in the ADR-*mdx* double mutant mice resulted in the improvement of muscle fibre integrity and *mdx* disease phenotype (Heimann et al., 1998; Kramer et al., 1998). It seems more than coincidental that there is a high level of integrin α7 in the Soleus muscle and that this muscle in particular is protected from DMD.

One could hypothesise that the integrin α7β1 complex and the DGC play very similar roles in skeletal muscle but at complimentary sites. The integrin α7β1 would reside at the sarcolemma of the soleus and all MTJs and the DGC at the sarcolemma of all other muscles. Transgenic overexpression of the integrin α7 at the sarcolemma would then cause a disruption to the DGC-laminin link causing a muscular dystrophy. In contrast as the integrin α7β1-laminin link is predominant at the MTJ and perhaps the sarcolemma of the Soleus, there is no disruption to the DGC and therefore no disease phenotype. However, this would still suggest that the integrin α7β1-laminin link is inferior to the DGC-laminin link as when it acts in its place a dystrophic phenotype is caused. In order to provide an insight into the effect of integrin α7β1-laminin link in the *mdx* mouse, when DGC function is lacking, we crossed the integrin α7 splice variant overexpressors with *mdx* mice.

4.3.4 Effect of integrin α7 overexpression on dystrophin deficient muscle

Dystrophin deficient mice were crossed with α7β1 overexpressing strains to study the potential of its splice variants in rescuing the dystrophic phenotype. Morphological analysis of *mdx*^{tg} mice revealed a more severe muscle phenotype compared with *mdx* mice when the X2 extracellular splice variant was present, which was pronounced in the GC muscle Similarly, EBD injected muscle sections showed more membrane damage in *mdx*$^{\alpha 7X2}$ mice compared to controls. GC was the muscle then chosen to calculate the fibres positive for the cytoplasmic α7 splice variants with or without the CLN. The overall proportion of CLN in GC was similar in *mdx* and *mdx*^{tg} muscle. Overexpression of α7 integrin splice variant made no difference in the proportion of the fibres with CLN and thus offers no protection against the disease.

In the previous study on *mdx*/utr $^{-/-}$ double mutant mice, it was shown that overexpression of integrin α7X2B rescued the phenotype observed (Burkin et al., 2001). This is conflicting with the results observed in this study. A possible explanation is that the *mdx*/utr double mutant mice display a more severe phenotype compared to dystrophin deficiency alone. It is also interesting to note that in the *mdx*/utr double mutant study the overexpression of α7X2B was controlled by the MCK promoter, which is activated during the differentiation from the myoblast to myotubes, and in mice only becomes active around birth. In the current study protein overexpression was driven by HSA promoter, which is active at a similar stage in muscle differentiation but already expressed at early stages of skeletal muscle development (Sassoon, Garner and Buckingham, 1998).

In our study, overexpression of α7X2 variant modified the structure of the muscles, but the s*oleus* which was protected in all WT α7 transgenic strains. An opposite effect has previously been observed in α7-/- mice in which the loss of integrin α7 causes myopathic changes mainly in the soleus (Hayashi et al., 1998 ;Mayer et al., 1997; Miosge et al., 1999). We have evidence that the integrin α7 subunit is predominantly expressed in type I and IIa, moderately in IId but not detectable by immunostaining in type IIb fibers (unpublished data). The slow-twitch soleus is naturally extremely rich in integrin α7. Increased amount of integrin does not perturb the integrity of the muscle; however its absence has dramatic consequences. Also overexpression of α7 showed no beneficial effect of integrin α7 trangenic expression in *mdx* mice *soleus*. This result differ from previous studies showing that integrin α7B

transgenic ADR/*mdx* mice induce a fibre-type switch from integrin α7B-non-expressing type IIb fibres into integrin α7B-expressing type IIa fibres, inducing an amelioration in the phenotype of these mice that exhibited less severe dystrophic symptoms than *mdx* mice (Heimann et al., 1998 ;Kramer et al..1998). This suggests that the absence of protection of the soleus in mdx in our study could be explained by the fact that transgenic expression of α7 did not cause any fibre-type switch. In transgenic mice overexpressing α7B (WT background), most of the fibres overexpressed the transgene. Fewer fibres are overexpressing the α7A transgene but there was no correlation between fibre-type and fibres which preferentially expressed α7 transgene. Although there was no obvious change in fibre type in most muscles, only the EDL occasionally expressed MHCI. In *mdx*^{tg}, no switch in fibre-type had been observed either; however, while 90% of the fibres are positive for α7B, α7A overexpression is restricted to type IIa/d fibres. (Webster et al., 1988).

4.4 Future work

The initial characterisation of the transgenic strains raised so many interesting findings that within this study there was not enough time to cross the transgenic overexpressing mice into the integrin α7 knockout mice. This next step will no doubt shed further light on whether the integrin α7X1 can improve the dystrophic phenotype.

The study of splice variant expression in the integrin α7 knockout mice will also be of interest, particularly for the study of the integrin α7X1 and A variants, whose role and function was difficult to define on the wildtype background. Perhaps this was due to the endogenous expression of integrin α7X2 and B, which masked the more subtle effects, the X1 and A variants likely have. It will also be of interest to see if there is any difference between the integrin α7 splice variants in their ability to rescue the MTJ/Soleus specific phenotype.

One aspect of integrin function that has received little attention is the mechanism by which splicing is controlled. Perhaps one very significant area of future study may lie in elucidating what factors control the spatial and temporal specific splicing of integrin α7 and β1 isoforms. It is for example known that extracellular signals can play a significant role in this (Weg-Remers et al., 2001;Xie and Black, 2001; Matter, Herrlich and Konig, 2002; Konig, Ponta and Herrlich, 1998). Ras, Protein Kinase C and Ca^{2+} / calmodulin-dependent pathways have all been implicated showing that splicing could indeed be controlled by extracellular signals and in response to changing physiologic conditions. Such elucidation may also bypass the need to overexpress protein; perhaps all that is required is to shift the balance of splice variants present. The foetal pattern of integrin expression, that is clearly specialised to the proliferative, regenerative and dynamic connections and signalling pathways that may be able to repair the damaged muscle. Furthermore, if the pathways specifically controlling integrin splicing could be elucidated, small molecule inhibitors/activators of the pathways could be used transiently and easily according to need and so avoiding the complications associated with a gene therapy treatment.

Chapter 5

Do pericytes contribute to skeletal muscle regeneration?

In recent years, several markers have been identified that define subpopulations of pericytes, like desmin, smooth-muscle-actin (α-SMA), NG2-proteoglycan (Ozerdem et al., 2001), PDGFR-β or the GTPase-activating protein RGS5 (Gerhardt and Betsholtz, 2003). It became also clear that pericytes and vascular smooth muscle cells are subsets of a continuum of vascular cells with phenotypic plasticity (Nehls and Drenckhahn, 1993). The lack of specific markers limited the analysis of pericytes, as pure cell populations could not easily be purified from tissues. In most studies, authentic pericytes had to be isolated from larger species to obtain sufficient cell numbers, by methods that used selective adhesiveness of cells to substrates (Hirschi and D'Amore, 1996).

Until recently, no adequate method was available to purify pericytes from mouse tissues, a prerequisite for using modern mouse genomics and proteomics. Therefore, we used a mouse model (Anxa5-LacZ), which will help us identify these cells through Anxa5 driven LacZ expression.

5.1 Analysis of Anxa5-LacZ reporter mouse

Anxa5-LacZ mice were generated in the laboratory of Dr Poschl by homologous recombination resulting in deletion of exon 4 and fusion of LacZ in frame with exon 3 (Figure 5.1) (Brachvogel et al., 2003). Deficiency of this protein causes no obvious phenotypes, likely due to compensation by other members of the protein family (Brachvogel et al., 2001; Brachvogel et al., 2003).

The Anxa5-LacZ gene was found to be intimately associated with the developing vasculature in the yolk sac and meningi from adult mice, but detailed analysis showed that the vascular Anxa5-LacZ expression is restricted to perivascular cells/pericytes in development and in the adult (Figure 5.2) (Brachvogel et al., 2005).

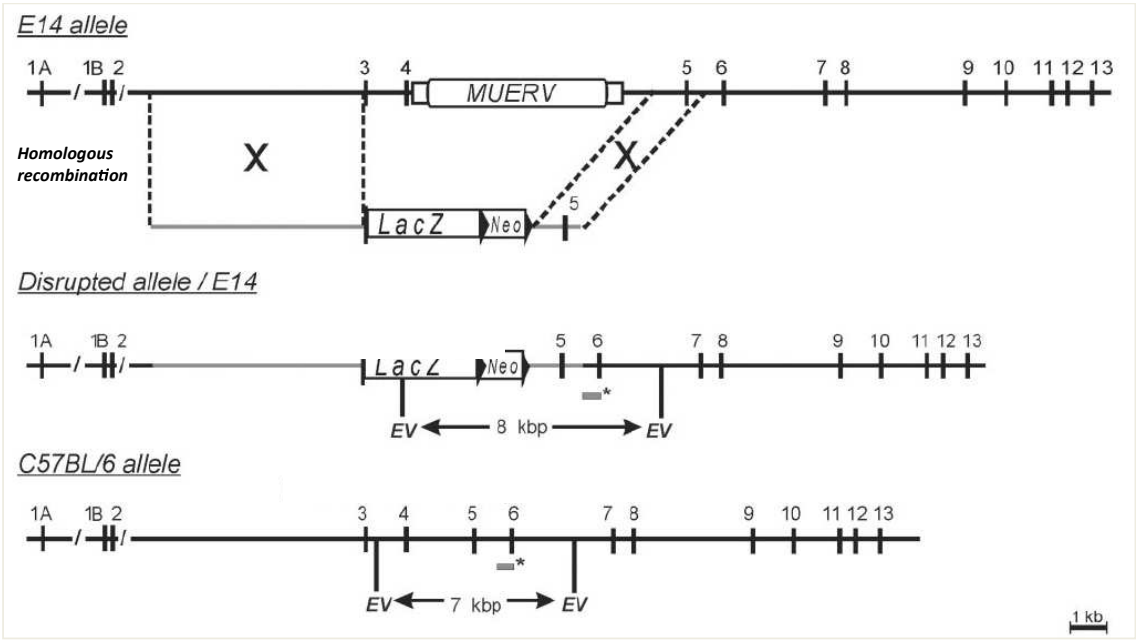

Figure 5.1: Strategy for the generation of Anxa5-LacZ reporter *mice The top picture shows the structure of the WT allele of Anxa5 gene in the 129SvJ (E14) genome with the integrated MuERV element (Rodriguez-Garcia et al., 1999). The top bottom picture shows the targeting construct. The mutated allele containing the LacZ reporter fused to exon 3 together with a neomycin resistance cassette, resulting in deletion of intron 3 and exon 4 after homologous recombination in ES cells is shown in the middle. The bottom shows the Anxa5 locus in C57Bl6 mice. Probe and resulting bands after Southern blotting are indicated in grey and exons are indicated by numbers. (Modified from Brachvogel et al., 2001)*

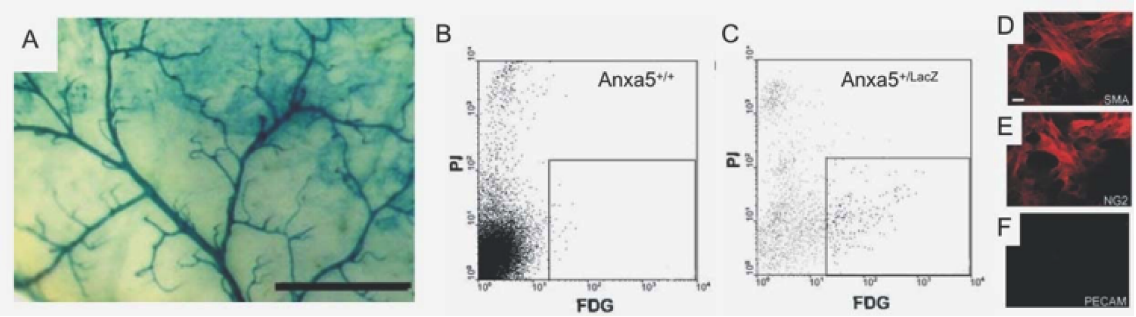

Figure 5.2: Characterisation of Anxa5-LacZ-positive perivascular cells. *(A) Anxa5-LacZ-positive pericytes are detected in meningi of Anxa-5-LacZ mice. (B,C) Cell sorting of cells from brain meningi of wild-type (Anxa5$^{+/+}$) and Anxa^{LacZ} mice after staining with the vital LacZ substrate FDG and PI. Vital FDG^{+}PI^{-} cells are shown in the square. (D-F) Isolated Anxa5^{LacZ} perivascular cells express α-smooth muscle actin (SMA), NG2 proteoglycan (NG2), but not endothelial- specific PECAM. (Brachvogel et al., 2005)*

This result was further confirmed by the co-expression of pericyte-specific markers (NG2 proteoglycan, PDGFR-β or α-SMA). The presence of the Anxa5-LacZ reporter enabled them to isolate pericytes from various mouse tissues by fluorescence-activated cell sorting (FACS) by detecting β-galactosidase activity with fluorescent substrates in vital cells (Figure 5.2) (Brachvogel et al., 2005). Using this method they were able to characterise mouse pericytes *in vitro* for differentiation behaviour and molecular signature (Brachvogel et al., 2007). Brachvogel et al (2003) also showed that the Anxa5-LacZ fusion gene is highly restricted to perivascular cells in embryonic and adult tissues. More importantly, isolated perivascular Anxa5-LacZ-positive cells express pericyte and stem cell-specific markers, differentiate into chondrogenic, osteogenic and adipogenic lineages and can be cultured for extended periods without undergoing senescence. In addition, in other studies, isolated pericytes were successfully used to ameliorate the muscular dystrophy phenotype in the golden retriever. Together, these results strongly suggest that pericytes could represent a novel source of mesenchymal stem cells and may contribute to repair processes in a variety of diseases.

5.2 Analysing the role of pericytes during skeletal muscle regeneration

Pericytes isolated from human muscle biopsy samples were recently shown to efficiently participate in muscle regeneration after intra-arterial injection into immuno-tolerant SCID-mdx mice, an animal model for human Duchenne muscular dystrophy (DMD) in which the dystrophin gene is mutated (Dellavalle et al., 2007). This has opened a promising area of stem cell-based therapies for DMD patients. However, although the differentiation potential of these cells has been well documented, the question still remains as to the fate of endogenous pericytes in the muscle tissue and whether or not they contribute to muscle regeneration. In order to address this question we crossed the Anxa5-LacZ reporter mice with dystropin deficient *mdx* mice, and compared staining for LacZ in muscle after the onset of muscle degeneration (Figure 5.3).

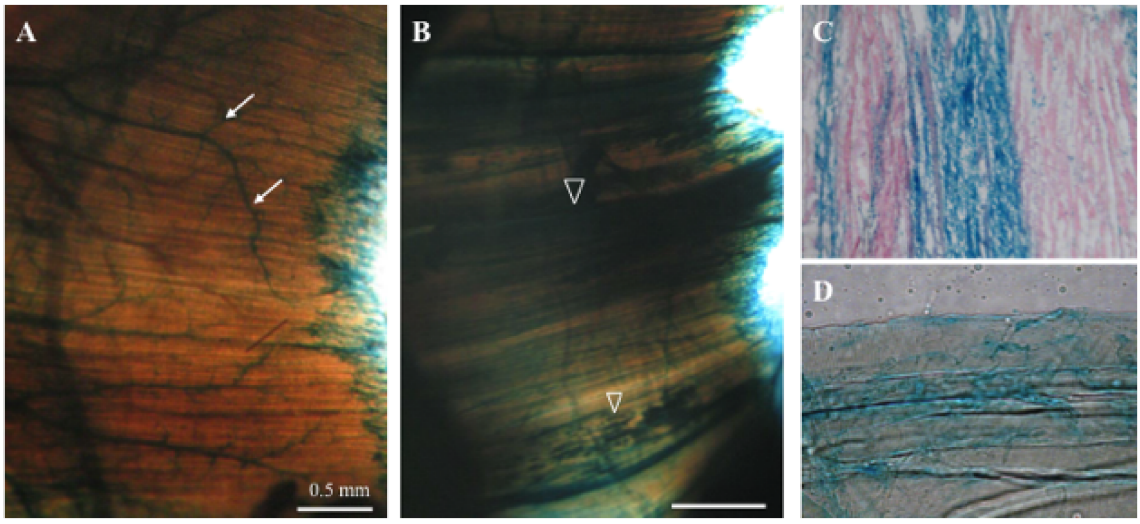

Figure 5.3: Localisation of Annexin V expressing cells in the diaphragm. *(A-B), Whole mount LacZ staining of the diaphragm highlights the vascular bed in wild-type-Anxa5-LacZ mice (A), and the stripe- like staining along the muscle fibres in mdx-Anxa5-LacZ mice (B). (C) Eosin-counterstained longitudinal section of LacZ-stained mdx-Anxa5-LacZ diaphragm showing the fibre-like dimension of the LacZ-positive cells. (D), Teased muscles fibres of LacZ-stained mdx-Anxa5-LacZ diaphragm showing a blue-stained fibre and positively labelled cells that are closely associated with unstained muscle fibres.*

Whole mount staining of the diaphragm marked the widespread vascular bed in the diaphragm of wild-type mice, heterozygous for the Anxa5 mutation. In contrast, a strong stripe-like staining parallel to the muscle fibres was observed in mdx-Anxa5-LacZ mice, which was more prominent than the blood vessel-associated staining (Figure 5.3 A and B). Sectioning of diaphragm muscles further confirmed these results, but it remained unclear whether or not LacZ-positive staining associated with muscles fibres (Figure 5.3 C). We therefore analysed enzymatically and mechanically teased muscle fibres. Some blue-stained fibres were obvious next to unlabeled muscle fibres, suggesting that endogenous pericytes participate in muscle regeneration. However, some cells that closely associated with the muscle fibres were also LacZ positive, yet, their identity still remains elusive (Figure 5.3 D).

To further investigate the process of regeneration, HL muscle sections were also analysed by immunofluorescence, using antibodies against nidogen-1, α-Smooth Muscle Acitn (α-SMA) and DAPI (Figure 5.4).

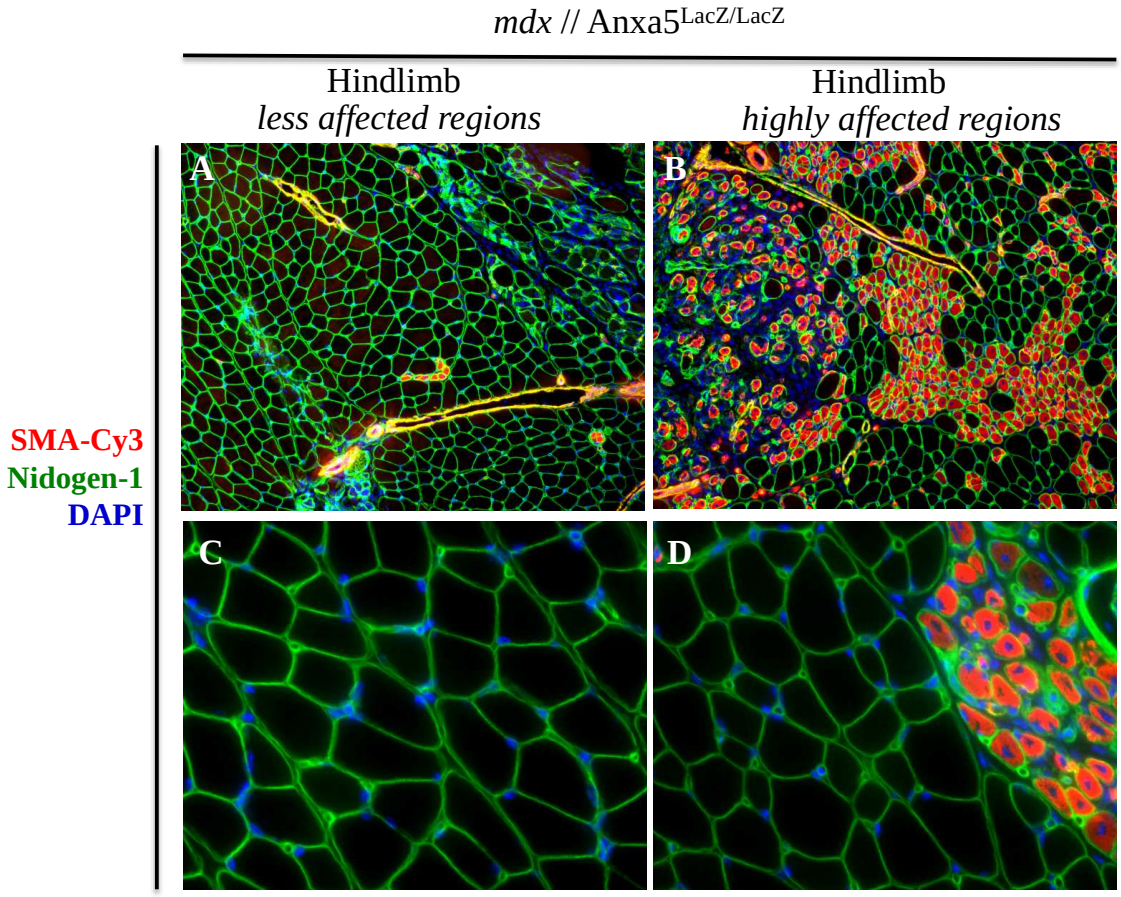

Figure 5.4: Immunofluorescence staining of muscle sections from mdx/Anxa5-Lacz mice. *HL sections of mdx-Anxa5$^{LacZ/LacZ}$ mice display varied staining pattern of α-SMA at affected region of the HL muscle. Pictures A and B were taken at x10 magnification while C and D were taken at x20 magnification showing a closer view of the affected and non affected regions of HL muscle.*

Immunofluorescence results from the HL muscle of mdx-Anxa5$^{LacZ/LacZ}$ mice confirm the extent of regeneration that has occurred in some regions of HL muscles. Affected regions of the muscle shows a strong staining of α-SMA within the fibres particularly the smallest, still growing fibres (Figure 5.4 B and D), suggesting the likelyhood for this protein in muscle regeneration, likely for the fusion of myoblasts and formation of early myotube structure and organisation (Springer, Ozawa and Blau, 2002). Nidogen-1 labeled the basement membrane, while DAPI marked the nuclei.

Although these results from LacZ staining are very intriguing, we may have in addition missed cell populations into which pericytes potentially differentiated as the Anxa5 promoter could have been turned off in these cells.

This preliminary data suggested a potential role of pericytes during muscle regeneration. But the Anxa5-LacZ mouse model has some limitations such as the LacZ

staining can only be done by histological analysis and thus prevent some information about the role of pericytes in tissue remodelling. In addition LacZ activity is only expressed when Anxa5 promoter is active and therefore when Anxa5 promoter is repressed in pericyte descendants, we may miss the identification cells into which pericytes differentiate and thus cannot lineage trace the descendants.

To address these concerns we generated a mouse model where Cre recombinase gene is fused in frame with the Anxa5 promoter in the mouse genome. This mouse strain will allow us to activate the expression of any reporter gene in pericytes and any descendants can then be identified thereafter. To generate the pericyte reporter mouse, we first designed the strategy to engineer the Anxa5-Cre targeting vector. After homologous recombination in ES cells the mouse strain was established and crossed with the ROSA-26 reporter mouse strain to address the overarching aim of the project, which is to define the cell fate of pericytes in tissue regeneration.

5.3 Generation of targeting vector for Anxa5-Cre knock-in mouse

To generate Anxa5-Cre-Knock-in mice we first designed a targeting vector to create a knock-in allele in which Cre recombinase activity will be controlled by the endogenous Anxa5 promoter (Figure 5.5). Several laboratories had tried to generate an Anxa5 mutant mouse strain but failed due to the existence of a murine endogenous retrovector (MuERV) in intron 4 of the Anxa5 gene in the 129Sv strain, which is commonly used for homologous recombination in embryonic stem (ES) cells but absent in the C57BL/6 genome (Figure 5.1) (Brachvogel et al., 2003 and Rodriguez-Garcia et al., 1999). We therefore used existing plasmids, which were previously used to generate the Anxa5-LacZ strain (Brachvogel et al., 2003). We fused part of Anax5 intron 2 and exon 3 with the sequence for Cre recombinase, including a nuclear localisation sequence (Cre-NLS) (Appendix II) by designing specific primers 124 and 125 (table 2.7). This PCR fragment was then cloned into Anax5-X3-EV/BHI plasmid cut with ClaI and EcoRV (Appendix II) in order to combine the rest of exon 3 of the Anax5 gene (Figure 5.5). Exon 5 and the phosphoglycerate kinase neomycin (PGK-Neo) resistance cassette were then cloned into the Sal I / Kpn I restriction sites. The PGK-Neo cassette was flanked by two Frt sites and was inserted downstream of the Cre recombinase cassette (Figure 5.5). The selection cassette was removed from heterozygous mice by breeding with mice expressing Flp recombinase (Figure 5.5). By this way we avoided the negative impact of the PGK promoter on the regulation of the Anxa5 promoter driving Cre recombinase activity.

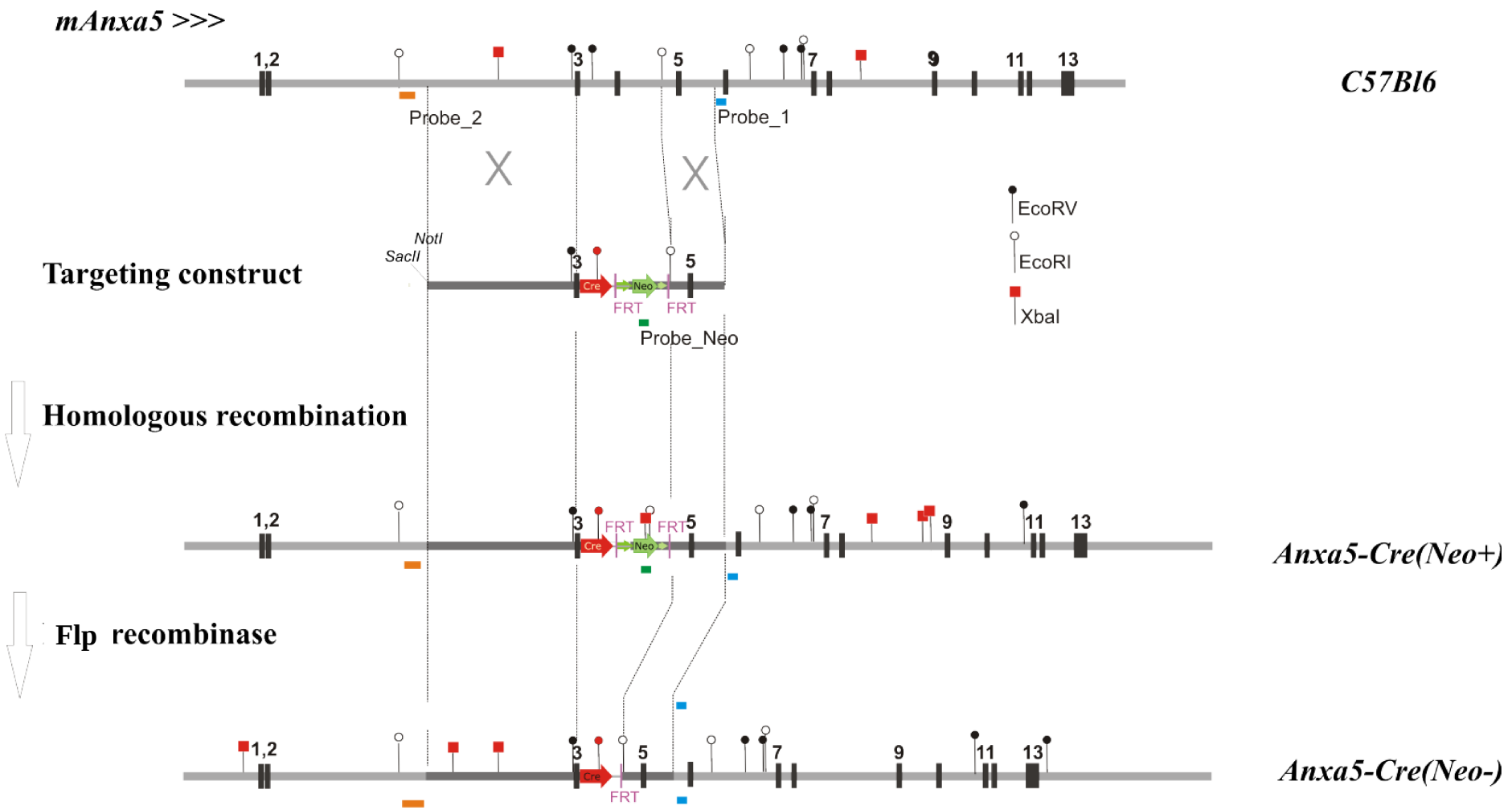
mAnxa5 >>>
1,2
3
5
7
9
11
13
C57Bl6
Probe_2
Probe_1
X
X
EcoRV
EcoRI
XbaI
NotI
SacII
Targeting construct
Cre
Neo
FRT
FRT
Probe_Neo
Homologous recombination
Anxa5-Cre(Neo+)
Flp recombinase
Anxa5-Cre(Neo-)

Figure 5.5: Strategy for the Anxa5-Cre knock-in targeting vector. *Partial genomic organisation of the Anxa5 gene in the C57BL/6 genome and the targeting vector (middle) and the resulting targeted allele after homologous recombination is shown. Mating with hACTB-FlpO transgenic mice removes the neomycin selection cassette located between frt sites (lower bottom). The 5'- probe (Probe 1 in blue), Neo probe (Green) and 3' probe (Probe 2 in Orange) were used for Southern blotting (explained in figure 5.5). Main restriction sites are indicated by symbols, Neo:PGK-neomycin cassette.*

5.3.1 Embryonic stem cell transfection

100 µg of the targeting vector was linearised with the restriction enzyme Not I and purified by phenol/chloroform and ethanol precipitation. The precipitated DNA was washed once more with 70% ethanol and dissolved in TE buffer. Transfection of ES cells was then performed at the transgenic core facility in Dresden, Germany and the positive clones were picked, expanded and sent to us to isolate genomic DNA. To identify the clones in which the homologous recombination has occurred, Southern blotting after Eco RV restriction was performed.

5.3.2 Screening of the targeted allele by Southern blot

Homologous recombination occurs between identical sequences of the targeting vector and genomic DNA. To screen for homologous recombination we designed three DNA probes for Southern blotting after restriction digestion (Figure 5.6).

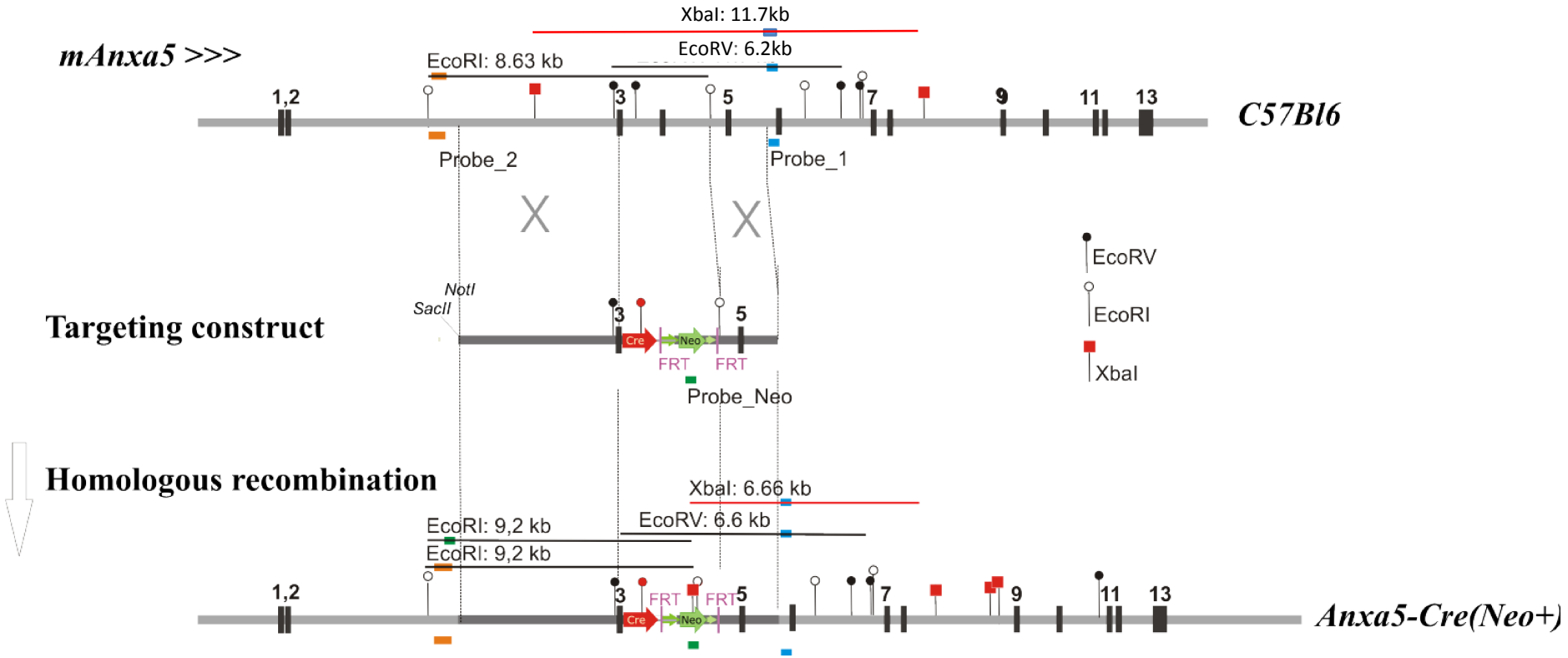

Figure 5.6: Relative positions of the probes designed for Southern blotting. *5' probe (Probe 1 in blue) was designed outside the arms of homology and will generate 11.7kb or 6.6 kb band in the WT or mutated alleles, respectively, after EcoRV and XbaI digestion. The Neo Probe (indicated in green) was designed to span the region associated with the Neo cassette, and generates a 9.2kb band in the mutated allele only after EcoRI restriction. The 3' probe (Probe 2, orange), also designed to bind outside the arms of homology generates a 8.63kb or 9.2kb band in the WT or mutated alleles, respectively, after EcoRI restriction.*

The 3'-probe (Probe 1 in blue, Figure 5.6) was designed to hybridise outside of the targeting vector to distinguish between homologous recombination and random insertion. When genomic DNA is digested with EcoRV, probe 1 will hybridise to a 6.6 kb band in C57 BL/6 genomic DNA when homologous recombination has taken place, whereas in the non-targeted allele it hybridises to a 6.2 kb fragment (Figure 5.6). This initial screening identified 16 ES cell clones for homologous recombination. These selective ES cell clones were further tested with Probe 1 after restriction digestion with XbaI and resulted in a 11.7kb fragment in the WT while in the targeted allele the fragment was reduced to 6.6kb (Figure 5.7). To exclude additional random insertion of the targeting vector, neomycin was used as internal probe (Neo probe) for Southern blotting after EcoRI digestion and resulted in a single band of 9.2kb. A 5' probe (probe 2, Figure 5.7), was also designed to prove correct homologous recombination on either side of the targeting vector. This probe hybridised upstream of the inserted EcoRI restriction site for detection of homologous recombination on the long arm of homology resulting in a 9.2 kb fragment after EcoRI digestion of genomic DNA, representing homologous recombination and a 8.6kb fragment in the WT allele. The design and by which method the probes were prepared and checked on C57 BL/6 genomic DNA is discussed in materials and methods.

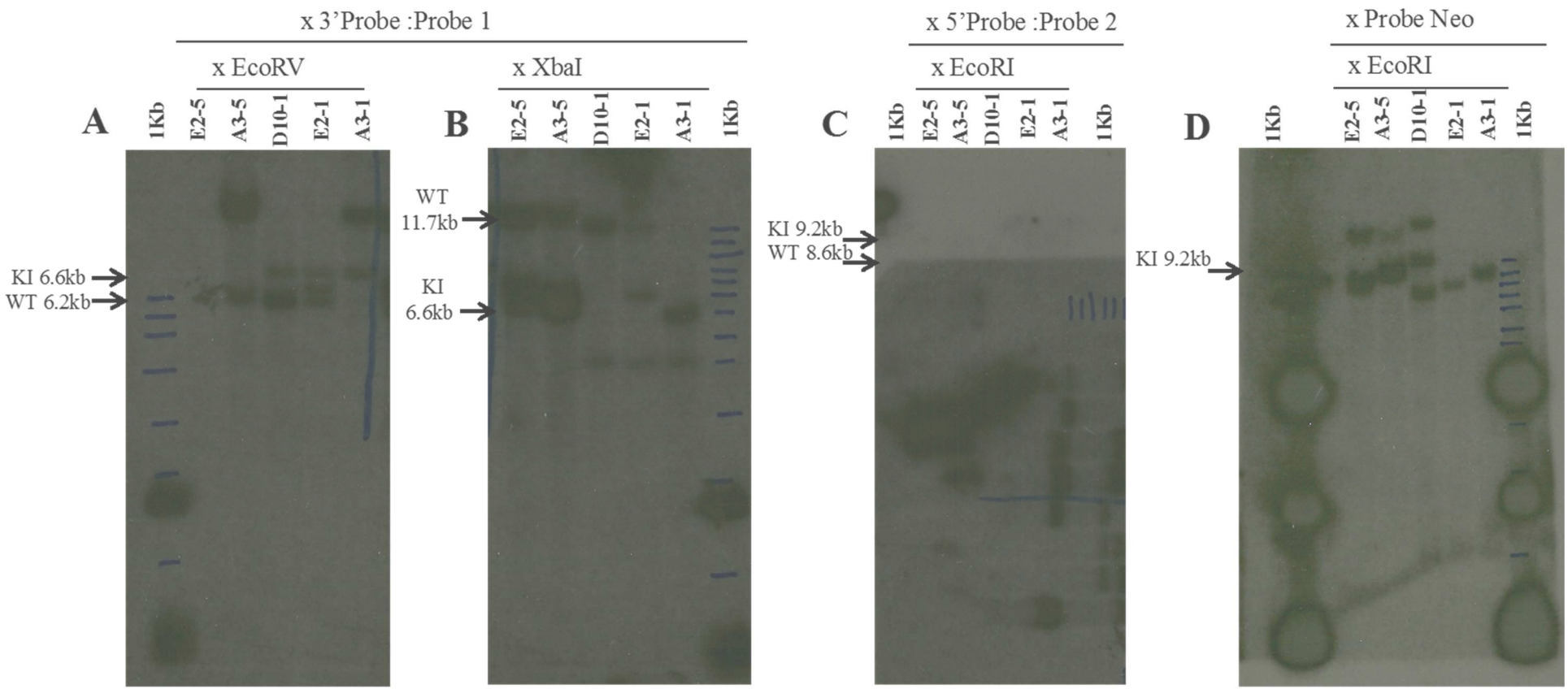

Figure 5.7: Southern blot analysis of the ES cell clones. *A) and B) represents the blots hybridised with the 3' probe (Probe 1-indicated in blue in figure 5.5) after restriction digestion with EcoRV or XbaI, respectively. After EcoRV digestion 6.6Kb fragment and 6.2Kb fragments were obtained representing KI and WT allele. Similarly restriction with XbaI resulted in 6.6Kb fragment for KI allele while 11.7 Kb for WT allele. C) Represents the blot hybridised with the 5' probe (Probe 2- indicated in orange in figure 5.5resulting in 9.2 Kb fragment for KI allele and 8.6 Kb fragment for WT allele. while D) represents the blot hybridised with the Probe Neo (indicated in green in figure 5.5).*

5.3.3 Screening the targeted allele by PCR

After the initial screening of ES cells by Southern hybridisation, 12 clones were selected and analysed by PCR using primers designed to amplify the regions were Cre recombinase had been inserted. Two different sets of primer combinations were used to test these clones for the presence of the neomycin cassette and for homologous recombination (Figure 5.8). The primer combination 142/143 was to screen for homologous recombination with primer 142 being located outside the targeting vector, while 143 being specific for neomycin. The primer combination 133/134/135 was to amplify fragments located within the targeting vector and which differentiate between the mutated and the WT alleles, resulting in a 453bp and a 344 bp band for the mutated and WT allele, respectively (Figure 5.8 C). Primer combination 142/143 resulted in the identification of 3 clones from C57 BL/6 ES cells, which were previously recognised as being positive by Southern blotting.

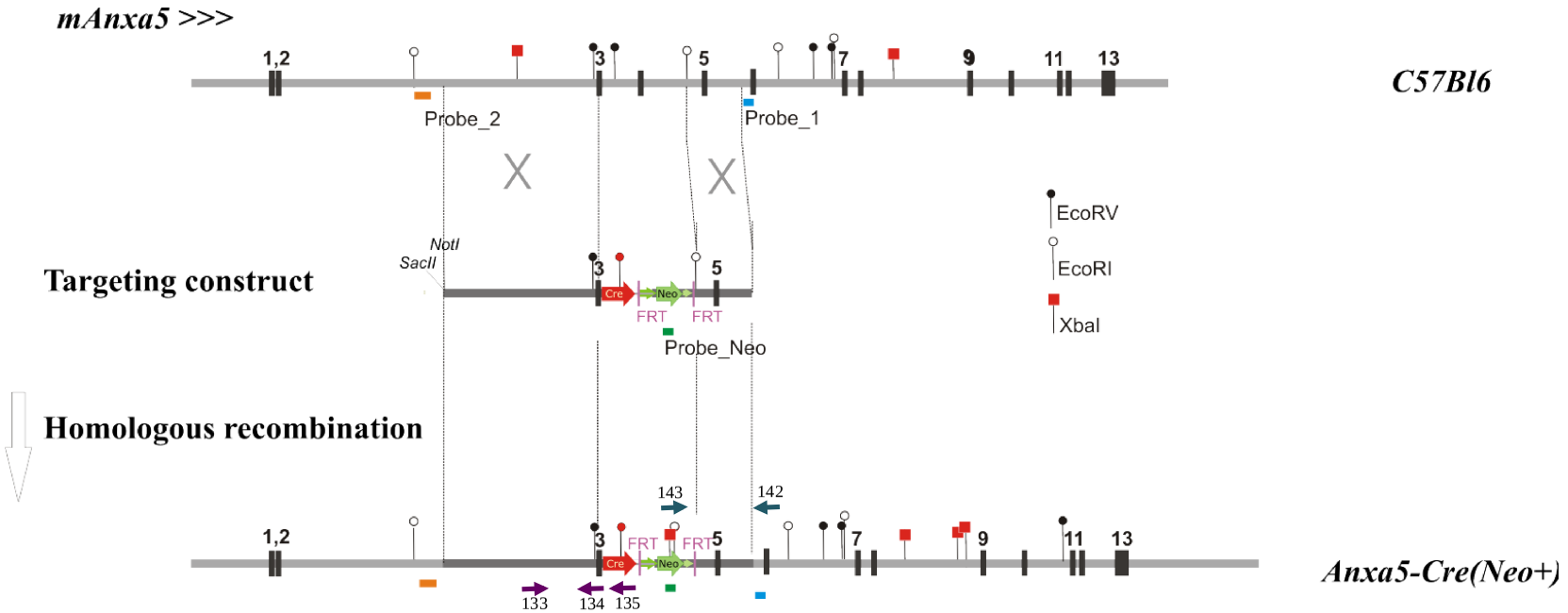
mAnxa5 >>>
1,2
3
5
7
9
11
13
C57Bl6
Probe_2
Probe_1
Targeting construct
NotI
SacII
Cre
Neo
FRT
FRT
Probe_Neo
EcoRV
EcoRI
XbaI
Homologous recombination
143
142
133
134
135
Anxa5-Cre(Neo+)

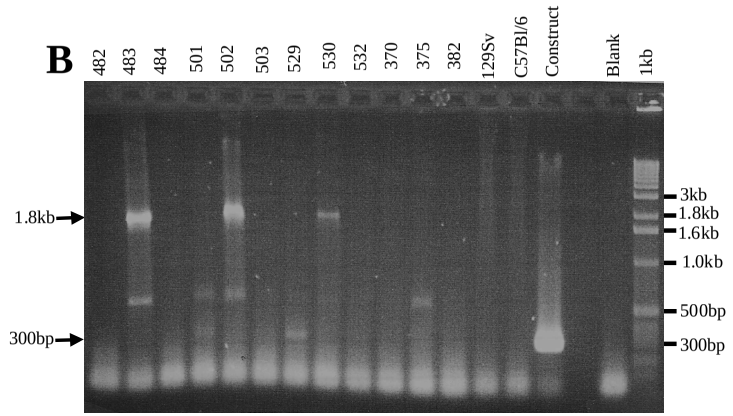
B
482
483
484
501
502
503
529
530
532
370
375
382
129Sv
C57Bl/6
Construct
Blank
1kb
1.8kb
300bp
3kb
1.8kb
1.6kb
1.0kb
500bp
300bp

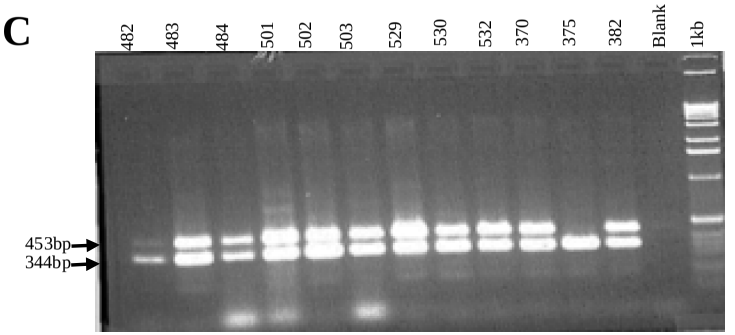
C
482
483
484
501
502
503
529
530
532
370
375
382
Blank
1kb
453bp
344bp

Figure 5.8: PCR analysis of ES cell clones. *A) Represents the WT construct (top), targeting vector (middle) and targeted construct (bottom) with the relative position of primers 142, 143 (blue), 133, 134 and 135 (indicated in purple). B) Represents the DNA gel after the PCR amplification with primer combination 142x143, resulting in 1.8kb fragment in the targeted allele. Plasmid DNA of the targeting vector was used positive control resulting in a 300bp fragment, while genomic DNA from 129Sv and C57BL/6 mice did not produce any fragment. C) Represents the DNA gel after PCR amplification with primers 133x134x135 resulting in a 453bp fragment for the targeted allele and a 344bp fragment for the WT allele. Only the positive ES cell clones are labelled as well as control DNA and 1kb ladder.*

5.3.4 Generation of the Anxa5-Cre-knock-in mouse strain

The heterozygous C57 BL/6 ES cell clones were injected into albino C57BL/6 blastocysts. The resulting male chimeras were mated with C57 BL/6 females, which were transgenic for recently generated Flpo recombinase (Flpo) (Kranz et al., 2010). With this crossing we combined germline transmission of the Anax5-Cre knock-in and germline excision of the neomycin cassette located between two Frt sites. The correct genotypes were confirmed by PCR analysis with primers specific for the individual allele (Figure 5.8). Anxa5-KI-Cre mice were then maintained as a breeding pair for further experiments

5.4 Investigating the fate of pericytes during skeletal muscle regeneration

As discussed previously there are limitations of using the Anxa5-LacZ mouse model to study muscle regeneration and thus to detect the potential fate of pericytes in muscle regeneration a marker is needed, which is independent of muscle specific down-regulation. To resolve this issue, we decided to focus on two main strategies by which it is possible to study the progeny of pericytes during muscle regeneration.

1) Use of ROSA26 reporter strain: In this approach the Anxa5-mediated expression of Cre recombinase mediated activation of ROSA26 reporter gene expression.
2) Use of isolated pericytes: Using muscle regeneration as a model, we isolated pericytes from skeletal muscle and the peritoneum from homozygous ROSA26-tdTomato reporter strain to compare their signature and their potential to contribute to muscle regeneration. The activation of tomato gene expression was achieved by *in vitro* transduction via an Adeno virus expressing Cre recombinase. Pericytes isolated from these mice induced angiogenic differentiation of endothelial cells, but also retained stem cell-like properties *in vitro*.

5.4.1 Analysis of the Anxa5-Cre-KI: ROSA26-LacZ mouse strain

To generate mice in which the expression of LacZ is conditionally regulated, we crossed the Anxa5-Cre-KI mice with the ROSA26-LacZ reporter strain. In these mice Cre recombinase leads to excision of the stop cassette flanked by two LoxP sites preceeding the LacZ reporter gene (Figure 5.9).

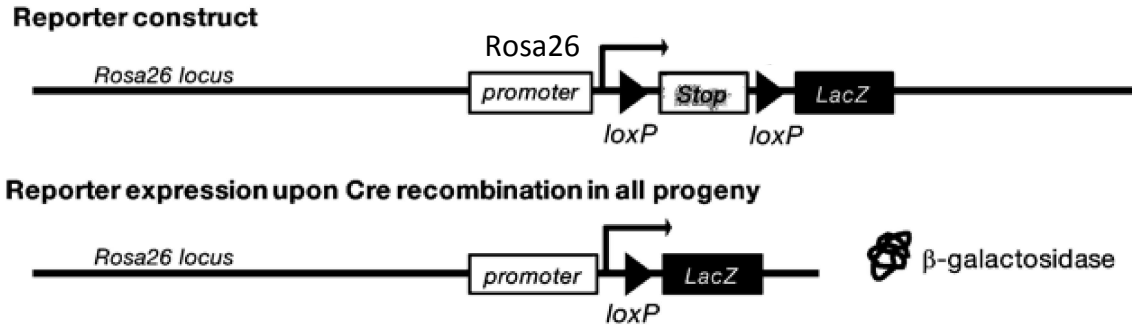

Figure 5.9: Schematic representation of ROSA26-LacZ reporter cassette for lineage tracing*. In the ROSA26-LacZ reporter mouse, a stop cassette flanked by loxP sites was inserted just downstream of the transcription start site at the ubiquitously expressed ROSA26 locus, but before the reporter gene. When intact, this cassette prevents expression of β -galactosidase (β-gal) from the downstream LacZ coding sequence. The stop cassette is excised upon exposure to Cre recombinase, which mediates recombination between the LoxP sites, thus permitting expression of the lacZ reporter. All progeny derived from these parent cells will carry this mutation and be marked by β-gal expression that can be detected by microscopy in tissue sections. (Modified from Kretzschmar and Watt, 2012).*

This will allow the ROSA26 promoter to drive the expression of the LacZ reporter gene. The expression of β-gal will be present in cells, in which the Anxa5 promoter is active and all their decendants, allowing us to lineage trace Anxa5 positive pericytes.

To analyse the β-gal activity in the muscle tissue in Anxa5$^{+/Cre}$//ROSA-LacZ mice, three months old mice were sacrificed and TA muscle was isolated and processed for cryosectioning. 20µm sections of TA muscle were then fixed with glutaraldehyde and processed for X-gal staining. Anxa5$^{LacZ/LacZ}$ mice were used as a control and TA muscle sections from these mice were stained with X-gal in parallel (Figure 5.10).

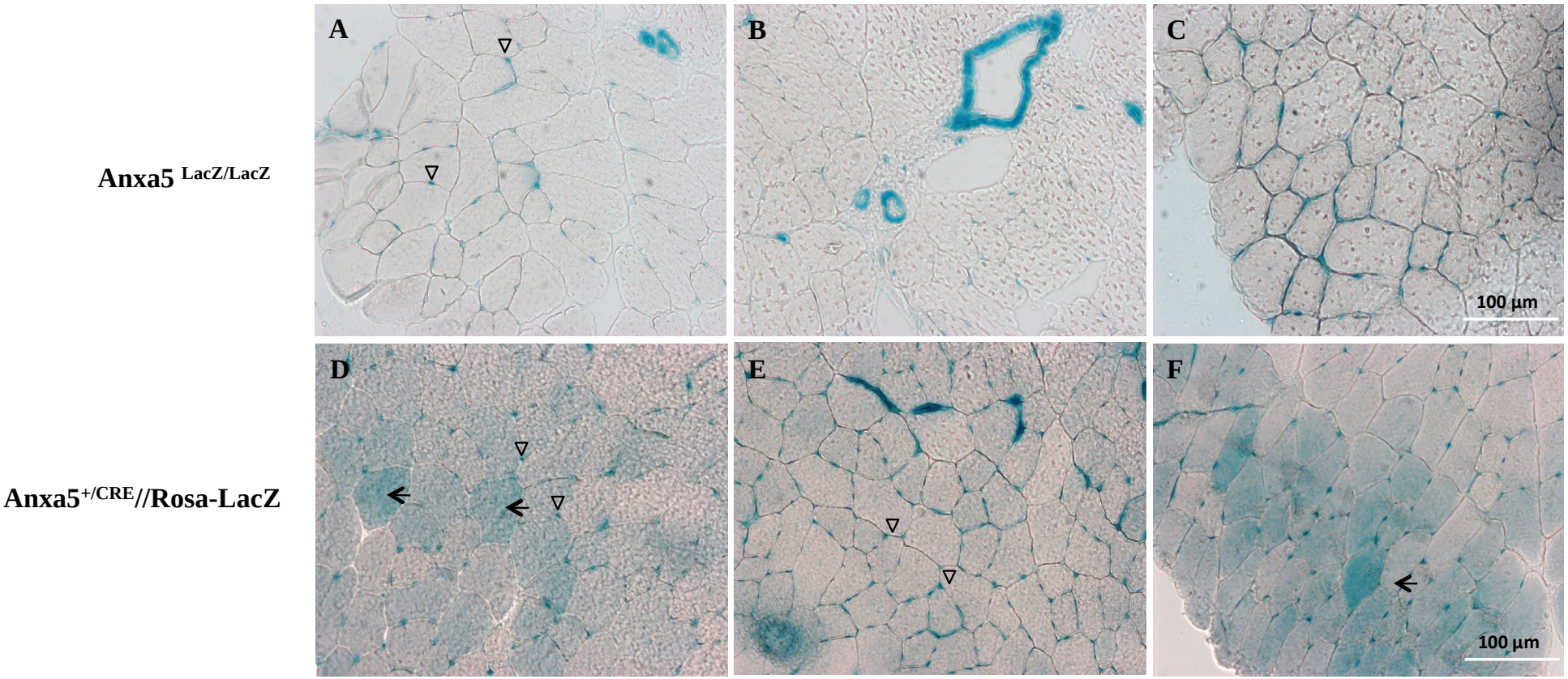

Figure 5.10: Representative images of muscle sections from Anxa5-Cre//ROSA-LacZ and Anxa5-LacZ mice: *20 um sections of TA muscle from both Anxa5$^{+/Cre}$//ROSA-LacZ (A-C) and Anxa5$^{LacZ/LacZ}$ (D-E) were fixed with glutaraldehyde and stained with X-gal substrate. All LacZ positive cells are associated with blood vessels, which are indicated with small triangles in figure A, D and E. We also observed entire myofibres staining blue (D and F indicated by arrowheads). Bars, 100µm.*

Anxa5$^{+/Cre}$//ROSA-Lacz mice displayed strong X-gal staining throughout the muscle section (Figure 5.10 D-E). All the blood vessels around the fibres were stained blue and some fibres showed intense staining of X-gal (Figure 5.10 D and F). However, the TA muscle sections of the control Anxa5$^{LacZ/LacZ}$ mice showed only certain areas of X-gal positive blood vessels (Figure 5.10 A-C). The intensity of the X-gal staining was also weak compared to the conditional KI strain. This may be because in Anxa5-LacZ mice Anxa5 promoter drives the expression of LacZ gene, whose expression varies in development. On the other hand, LacZ expression is conditionally activated in Anxa5$^{+/Cre}$//ROSA-LacZ mice thereby labelling all pericytes and their decendants with the LacZ marker.

In addition, whole mount staining of the diaphragms of Anxa5$^{+/Cre}$//ROSA-LacZ and Anxa5-LacZ mice was performed. Similarly to the TA muscle, LacZ activity was found in blood vessels of the diaphragm of both mice, but the intensity of the stain varied. Anxa5-LacZ mice displayed weaker X-gal stain compared to Anxa5$^{+/Cre}$//ROSA-LacZ mice (data not shown). In addition in conditionally activated Anxa5$^{+/Cre}$//ROSA-LacZ mice, some of the fibres close to the blood vessels stained positive for X-gal.

This data suggests that the conditional activation of the LacZ gene was successful and was able to mark pericytes, thus suitable to trace their fate. In order to verify that these pericytes contribute to muscle regeneration we decided to induce muscle regeneration in Anxa5$^{+/Cre}$//ROSA-LacZ and Anxa5 $^{LacZ/LacZ}$ mice. This was done by intramuscular injections of the mytotoxic agent cardiotoxin (CTX). TA muscles from three-month-old Anxa5$^{+/Cre}$//ROSA-LacZ and Anxa5 $^{LacZ/LacZ}$ mice were injected with 50µl of 10µM CTX and left to recover for 10 days before dissection. The contralateral non-injected muscle served as negative control (Figure-5.11).

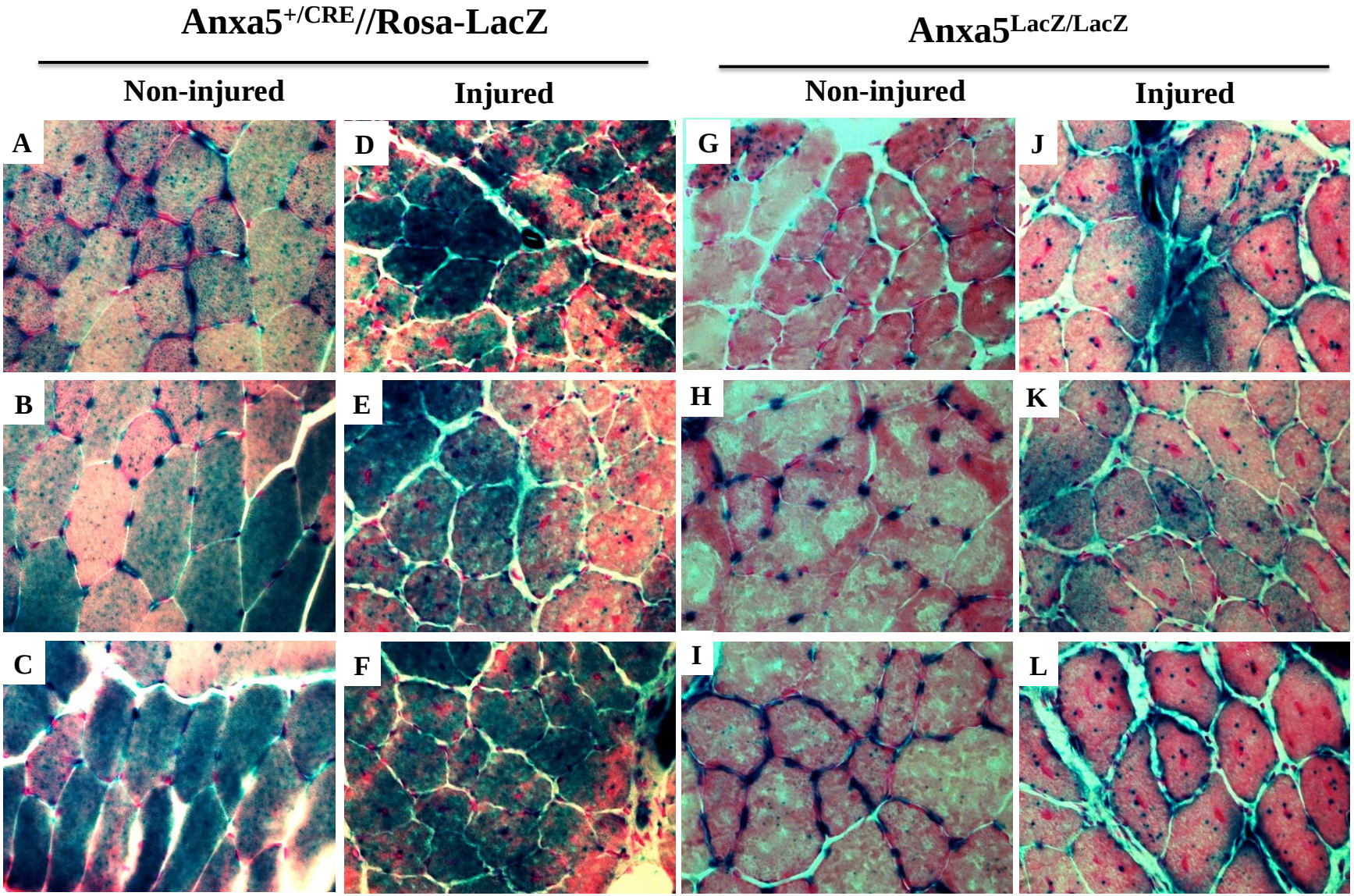
Anxa5+/CRE//Rosa-LacZ
Anxa5LacZ/LacZ
Non-injured
Injured
Non-injured
Injured
A
B
C
D
E
F
G
H
I
J
K
L

Figure 5.11: Representative images of muscle sections from Anxa5$^{+/Cre}$//ROSA-LacZ and Anxa5 $^{LacZ/LacZ}$ mice. *Cryosections from TA muscle of Anxa5$^{+/Cre}$//ROSA-LacZ and Anxa5 $^{LacZ/LacZ}$ mice were stained with LacZ and nuclear red. A-C and G-I represents the non-injected TA while D-F and J-L represents CTX injected side from Anxa5$^{+/Cre}$//ROSA-LacZ and Anxa5 $^{LacZ/LacZ}$ mice, respectively. The intensity of the LacZ stain is largely evident in Anxa5$^{+/Cre}$//ROSA-LacZ muscle tissue when comaped with Anxa5 $^{LacZ/LacZ}$ tissue. 40x magnification.*

10 days after the injury, muscles were dissected and processed for cryosectioning which were then analysed for LacZ staining. Nuclear red staining was used to mark the nuclei (Figure 5.11 A-L).

From figure 5.11 it was clear that there was a difference between the LacZ staining of the muscle sections from Anxa5$^{+/Cre}$//ROSA-LacZ and Anxa5 $^{LacZ/LacZ}$ mice. As seen before (Figure 5.10), in the non-injured muscle from Anxa5$^{+/Cre}$//ROSA-LacZ mice many fibres were seen with cells at the pericyte location marked with LacZ (Figure 5.11 A-C). The same was true in Anxa5 $^{LacZ/LacZ}$ mice but the LacZ staining was much weaker in some areas (Figure 5.11G). In Anxa5$^{+/Cre}$//ROSA-LacZ mice we also observed many fibres stained for LacZ and most of them were at the periphery of the muscle section. On the other hand control mice did not show any signs of LacZ stain inside the myofibre (Figure 5.11 G-I).

The CTX injected muscle sections from Anxa5$^{+/Cre}$//ROSA-LacZ displayed regenerating fibres with CLN marked by nuclear red stain. These myofibres were strongly stained with LacZ, indicating a possible fusion of pericytes with the fibre during muscle repair. In contrast in Anxa5 $^{LacZ/LacZ}$ muscle sections weak patchy blue staining was evident inside the regenerating fibres. Some LacZ staining was also observed around the blood vessels of non-injured muscle sections.

In addition to the LacZ staining we also stained the 20 μm of CTX injected TA muscle with PECAM 1, α-SMA and Nidogen (figure 5.12). PECAM 1 stainins endothelial cells thus identifing the location of capillaries□ □Affected regions of the muscle shows strong staining of α- SMA within the fibres. Nidogen antibody was used to highlight the basementmembrane thus identifing the fibres.

Anxa5$^{+/CRE}$//Rosa-LacZ _TA muscle_Injured with CTX

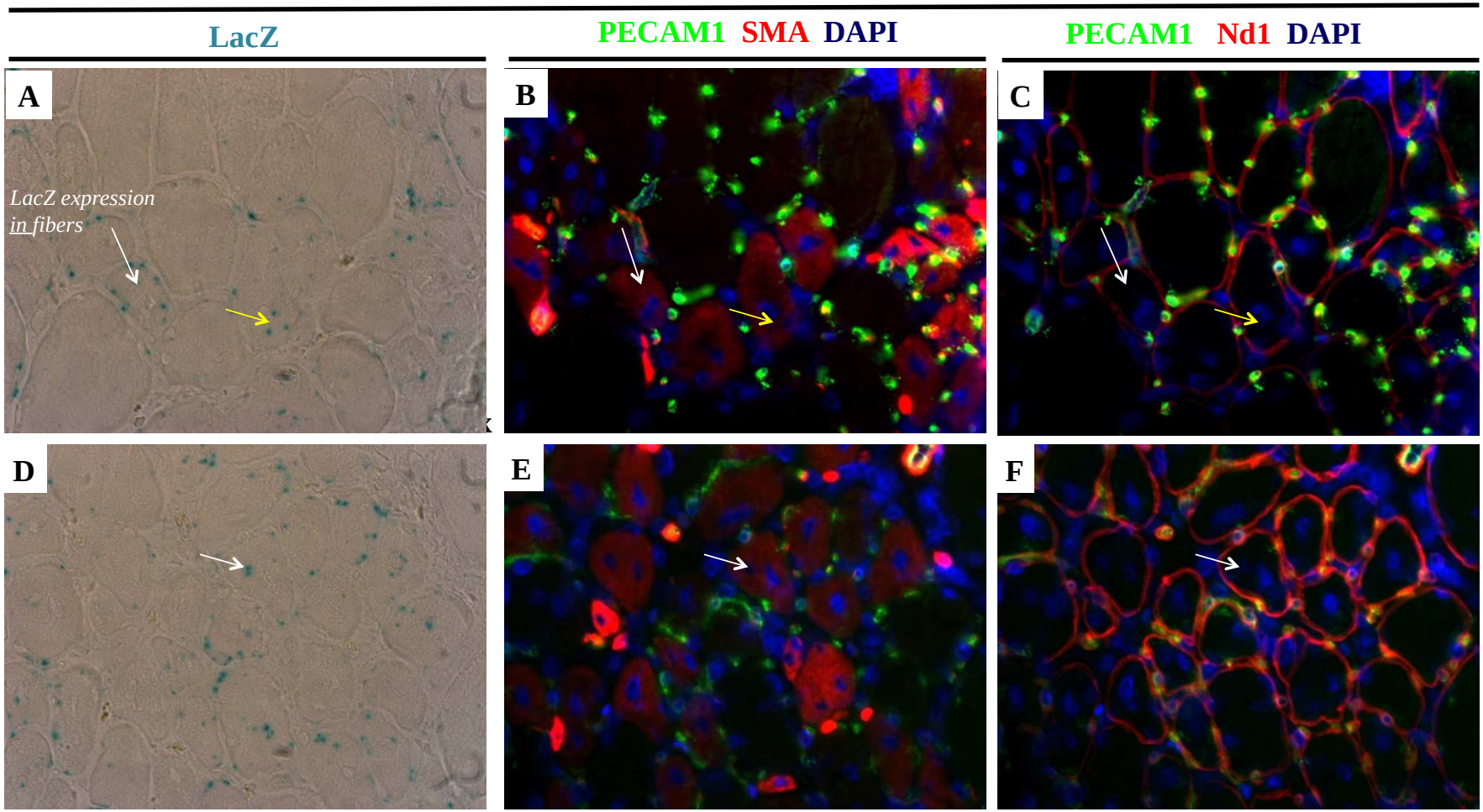

Figure 5.12: Representative images of muscle sections from Anxa5-Cre//ROSA-LacZ mice: *20 μm sections of TA muscle from Anxa5$^{+/Cre}$//ROSA-LacZ were fixed with glutaraldehyde and stained with X-gal substrate (A and D). All LacZ positive cells are associated with blood vessels, which are indicated with white arrow in A and D, Additionally the LacZ staining was observed at nuclear position in fibres with CLN (A and D , yellow arrow).The sections were further stained by PECAM 1 and α-SMA (B and E) to locate the capillaries and the CTX injured sites respectively. The basement membrane was stained by nidogen (Nd1) antibody (C and F). Dapi was used as nuclear stain (B, C, E and F). Pictures were taken at x40 magnification.*

To conclude the data from LacZ staining from Anxa5$^{+/Cre}$//ROSA-LacZ and Anxa5 $^{LacZ/LacZ}$ mice suggests that there is a difference in the LacZ staining. To overcome the limitations from LacZ staining and to trace pericytes using a fluorescent marker, we made use of other reporter stains. We therefore crossed Anxa5-Cre-KI mice with ROSA26-EYFP and ROSA26-tdTomato reporter strains.

5.4.2 Analysis of the Anxa5-Cre-KI: ROSA26-EYFP mouse strain

To expand our possibilities to lineage trace pericytes we made use of the ROSA26-EYFP strain (Shrinivas et al., 2001), made available by Dr S.Shrinivas from the University of Oxford. The mouse strain was generated using homologous recombination using a targeting vector into ROSA26 locus.

This strain has been successfully used in many high-profile publications for lineage tracing of precursor cells and long-term tracking of their progeny and shown to be useful for localisation of YFP in tissues and unbiased isolation of cells through FACS analysis (Schwarz et al., 2008**;** Rivers et al., 2008; Kuang et al.,, 2007; Geoffroy and Raineteau, 2007;Clayton et al., 2007). We then crossed Rosa26-EYFP mice with Anxa5-Cre mice to generate Anxa5-Cre-EYFP mice, which should express YFP in Anxa5 positive pericytes and its descendants.

First, we isolated pericytes from muscle and peritoneum tissue and sorted them by FACS analysis (figure 5.13) to enrich the CD140b+/YFP+/CD31- pericyte population. CD140b, also known as PDGFRβ and is expressed by pericytes as a surface marker, while CD31 is a cell surface marker expressed by endothelial cells.

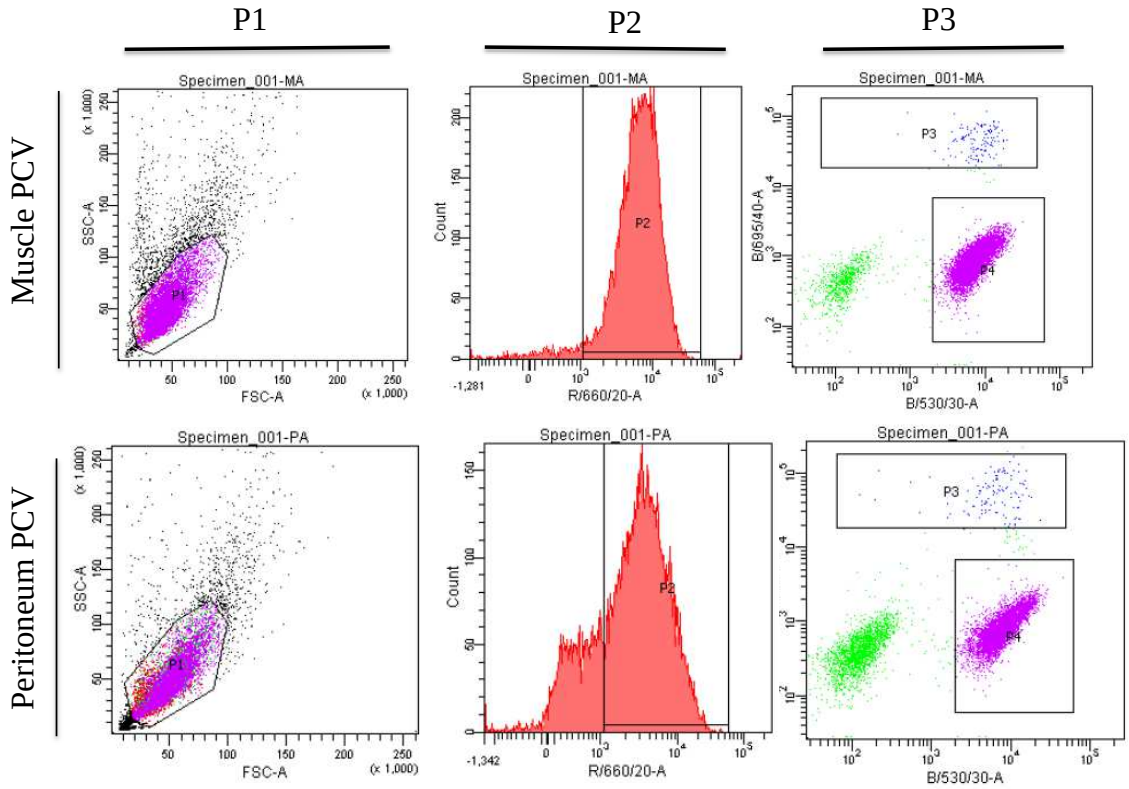

Figure 5.13: FACS sorting of pericytes isolated from muscle and peritoneum of ROSA26-EYFP mice. *Cells from muscle and peritoneum were labeled with CD140b and CD31 before loaded into sorting machine. P1 indicates vital cell population from debris. P2 shows CD140b positive population of P1, which was further enriched by P4 gating (Cd31-/YFP+) to isolate the final pericyte population P3 (CD140+/YFP+/CD31-)*

The isolated YFP+ pericytes could be easily identified in FACS analysis and maintained the marker for more than 10 passages. The isolated PVCs from peritoneum and muscle were co-cultured with HUVEC (Human Vascular Endothelial Cells) and showed pro-angiogenic effects compared to HUVEC mono culture in a 3D tube formation assay in collagen gel (Data from Dr Zhou, not shown). These EYFP+ pericytes stained positive for several tested PVC markers but the YFP signal was too weak to be detected by epifluorescence. We therefore used the much stronger tandem dimer tomato ROSA26, which expresses a strong red fluorescent signal (Madisen et al, 2010).

5.4.3 Analysis of Anxa5-Cre-KI- ROSA26-td-Tomato mouse strain

We crossed the Anxa5-Cre-KI mice with ROSA26-tdTomato mice. Offspring showed a very strong expression of td-Tomato and the specificity of the expression was hard to define. The entire mouse appeared red and we were unable to use these mice for any experiments to elucidate the role of pericytes in muscle regeneration. We therefore focused our attention on inverse strategy, in which we isolated pericytes from ROSA26-tdTomato silent mice and activated expression of the Tomato gene by *in vitro* induction of Cre recombinase via viral delivery.

5.4.4 Approach 2: Transplantation study

5.4.4.1 Efficiency of pericytes in skeletal muscle regeneration

In order to study the role played by pericytes in muscle regeneration, we decided to transplant Tomato-positive pericytes isolated from muscle and peritoneum. The expected outcome from these experiments is summarised in figure 5.14. These experiments were carried out in collaboration with Dr. E. Poschl and Dr. Z. Zhou

For the isolation of pericytes they used a silent ROSA-td-Tomato mice in which the expression of Tomato gene is inactive. Upon the *in vitro* induction of Adeno-Cre virus, these cells were expressing the fluorescent marker.

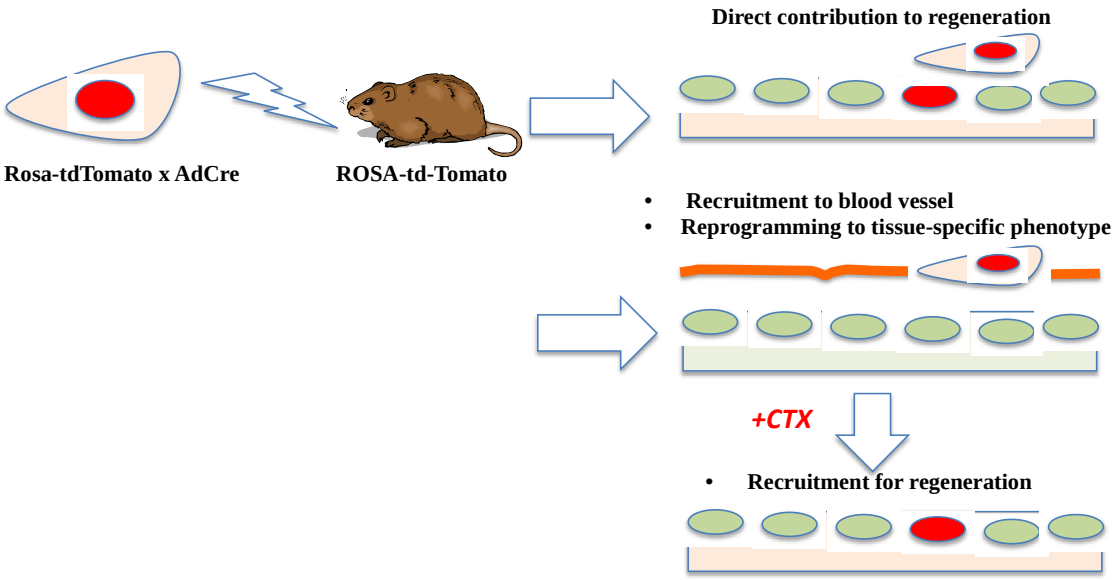

Figure 5.14: Schematic representation of the expected outcome from transplantation experiments. Silent *ROSA-td-Tomato mice were injected with cells expressing td-tomato after being transduced with Adeno-Cre virus. The cells could contribute to muscle regeneration and find their niche in the blood vessels. Upon the cardiotoxin (CTX) induced muscle regeneration, it is expected to see the recruitment of these pericytes to regenerated fibres.*

Before these cells can be injected in to the mouse hindlimb muscles, FACS was used to isolate a pure pericyte population (Figure 5.14 A-C). These cells were then varified for expression of specific markers.

5.4.4.2 FACS analysis of PVC isolated from muscle and peritoneum tissue

Pericytes were isolated from muscle and peritoneum of ROSA26-tdTomato -/- mouse. The cells were then cultured as described in methods and maintained in 100% confluence. These cells were then sorted using FACS for CD140B+, CD45-, CD31- (Figure 5.15). The P1 population was gated to distinguish between the real cell population and debris (Figure 5.15 A) which was further gated against CD140B, CD45 and CD31 as shown in the histograms (Figure 5.15 B). A clear peak of the cells positive for CD140B was evident in the histograms in both muscle and peritoneum cell population. P3 population was gated against CD140b, CD31, suggesting this is a pure pericyte population expressing pdgfr-β.

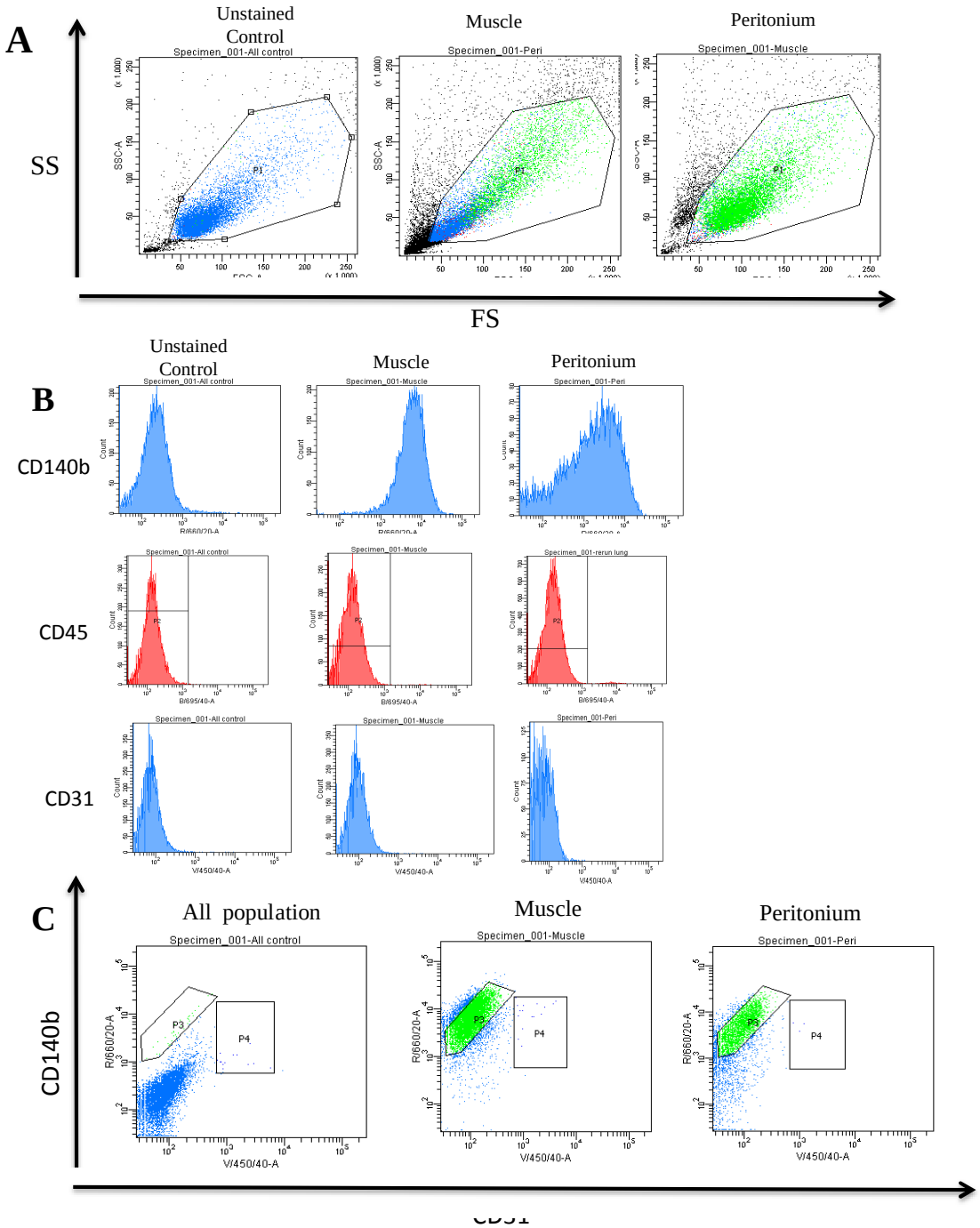

Figure 5.15: FACS sorting for pericyte populations. *Pericytes (CD140b+/CD31-/CD45-) were isolated from muscle and peritoneum from ROSA-td-Tomato mice. A) Shows the gating strategy (P1) to distinguish between the cell population and debris. B) Shows the histogram for the cells stained for CD140b (top row), CD45 (middle row) and CD31 (bottom row). P2, CD45 negative population was gated for further sorting. C) P3, CD140b+ and CD31- population were isolated from both muscle and peritoneum. (In collaboration with Dr Zhou and Dr Poschl.)*

To avoid immune rejection red-labeled pericytes were injected in the hindlimb TA muscle of congenic ROSA26tdTomato mice. To elucidate the role played by pericytes in muscle regeneration, we injected cardiotoxin (CTX) into the TA muscle 20 days after cells had been transplanted. This time point had been determined in initial experiments to be best for obtaining Tomato-positive pericytes in capillaries. The non-injected TA muscle from the contralateral side was used as a control. The scheme of the experiment is detailed in figure 5.16.

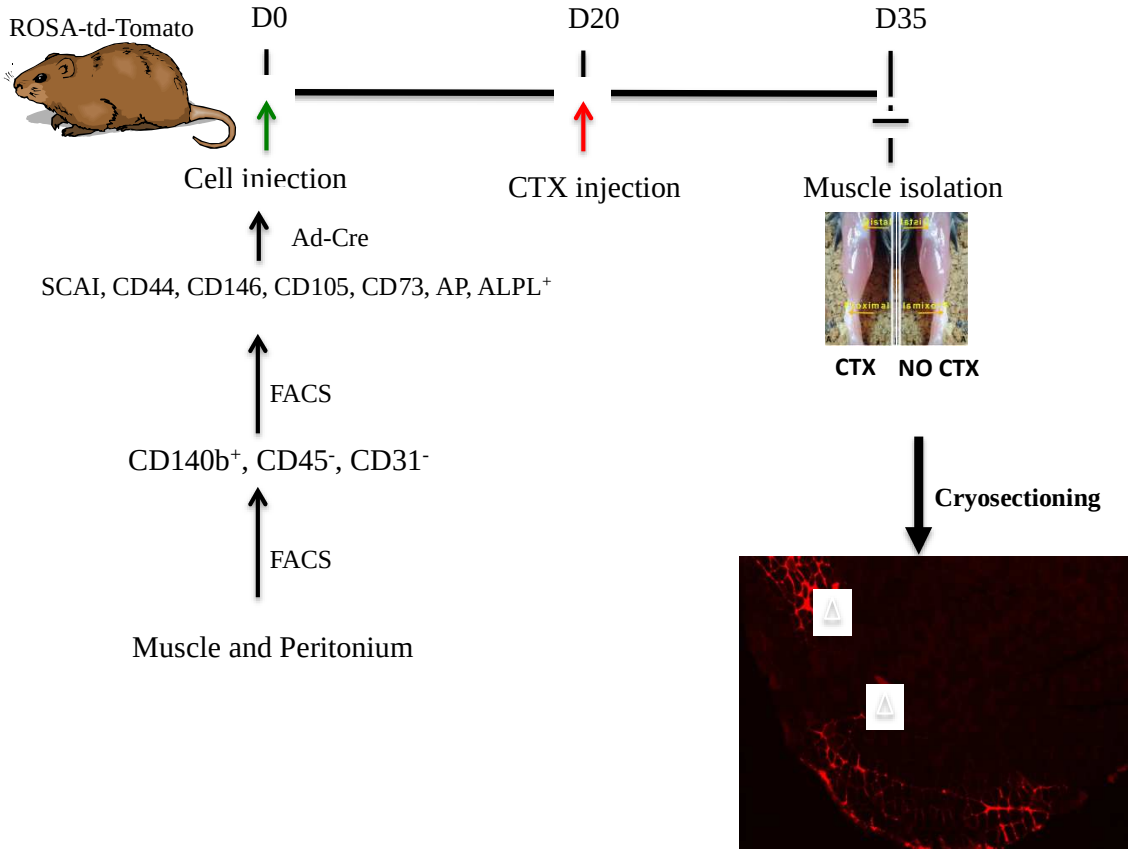

Figure 5.16: Transplantation scheme for injecting cells in silent ROSA-td-Tomato mice: *Cells were isolated from muscle and peritoneum of ROSA-td-Tomato mice and FACS sorted for various pericyte-specific markers. These cells were then transduced with Adeno-Cre (Ad-Cre) virus before injecting in the TA muscle. Muscle injury by CTX was carried out on day 20 post transplantation and mice were sacrificed on day 35. TA muscle from injured and non-injured side was isolated and processed for cryosectioning showing pericytes labeled by td-Tomato (indicated by while triangles).*

15 days post CTX injection, TA muscles were dissected and 10μm thick cryosections were stained with Lectin to highlight endothelial cells, and DAPI (Figure 5.17).

Tomato-labeled muscle fibres were present in sections injected with muscle (Figure 5.17-Ai, Aiii and Bi, Biii) and peritoneum-derived (Figure 5.17-Ci, Ciii Di, Diii) pericytes both in non-injured and injured TA muscle. Even though the injection site is not visible after 35 days, one could see the spread of these tomato-labeled muscle pericytes is along the path of injection (Figure 5.17-Ai). The same was true on the injured side (Figure 5.17-Bi). In addition, these pericytes were found to be located in blood vessels and capillaries as evidenced by lectin staining (Figure 5.17 Aii and Bii). In the injured side some fibres had CLN (Figure 5.17 Biv) but none of them was strongly positive for Tomato. On the other hand there were few tomato positive fibres with CLN visible in the injured side when peritoneal-derived pericytes were injected (Figure 5.17 Div). The distribution of tomato-positive fibres in the non-injured side was similar when compared with section from TA muscle transplanted with muscle pericytes (Figure 5.17 Ci). Co-localisation with lectin staining was also evident in both injured and non-injured muscles injected with peritoneal pericytes, indicating their presence in capillaries (Figure 5.17 Di).

This data indicate that both muscle- and peritoneum-derived pericytes can contribute to muscle regeneration. However, there was still the possibility that the pericyte populations still contained other myogenic cells.

.

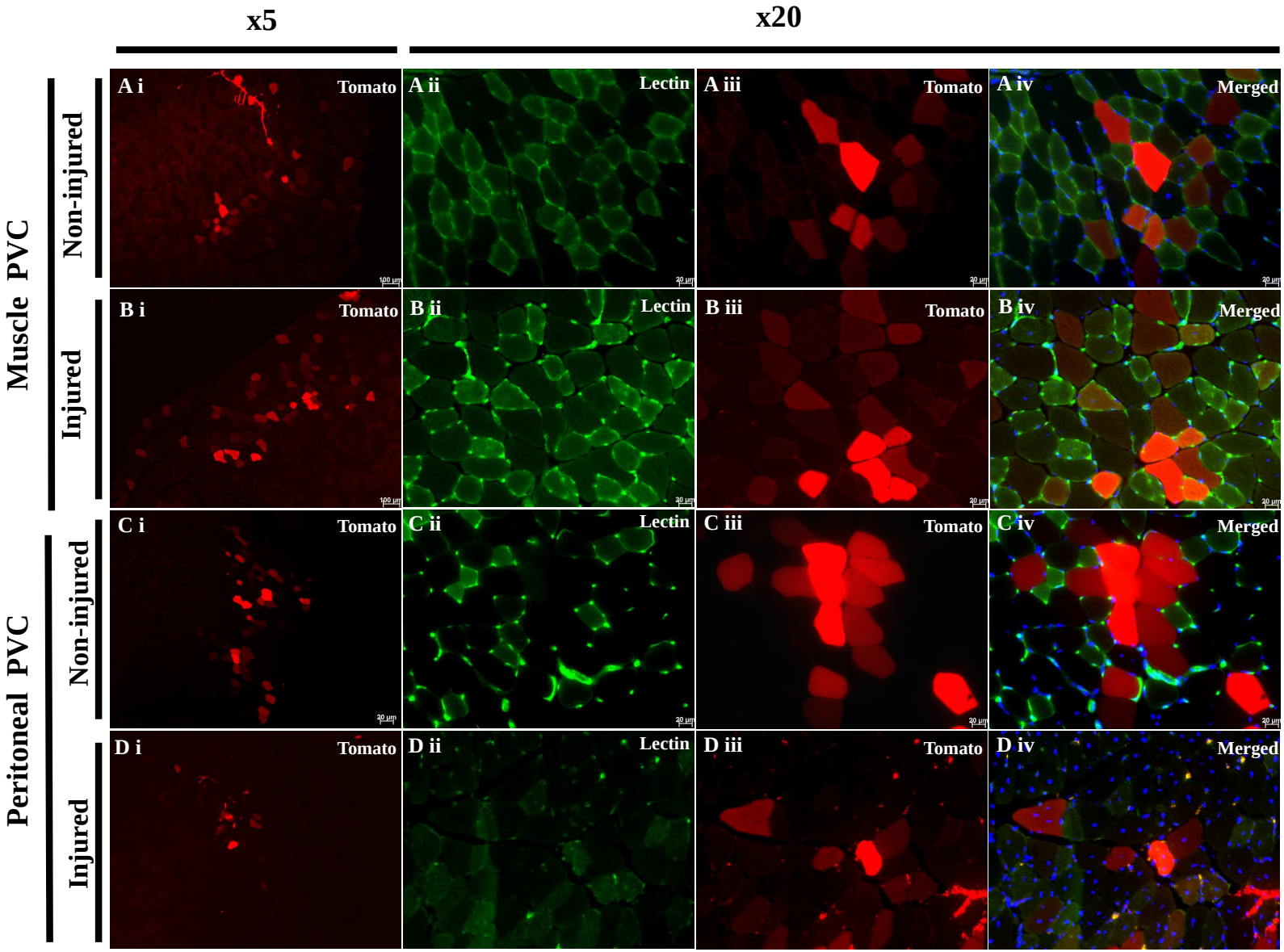
x5
x20
Muscle PVC
Non-injured
Injured
Peritoneal PVC
Non-injured
Injured
A i
Tomato
A ii
Lectin
A iii
Tomato
A iv
Merged
B i
Tomato
B ii
Lectin
B iii
Tomato
B iv
Merged
C i
Tomato
C ii
Lectin
C iii
Tomato
C iv
Merged
D i
Tomato
D ii
Lectin
D iii
Tomato
D iv
Merged

Figure 5.17: Localisation of transplantated tomato-labelled pericytes in the TA muscle of ROSA-tdTomato mice. *TA muscles of ROSA26-tdTomato mice were injected with tomato-labelled pericytes isolated from either muscle (Ai- Aiv and Bi- B iv) or peritoneum (Ci-Civ and Di-Div). In each mouse one TA was injured with CTX, while the other TA served as a non-injured control. Tomato-labelled pericytes are visible in red, Lectin BS1 staining in green marks the pericyte location in capillaries, while DAPI (blue) marks the nuclei. Scale bars, 100µm (A-Di), 20µm (Aii-Div).*

Previously, Dellavalle et al. (2011) described that the tissue non-specific alkaline phosphatase ALPL is specifically expressed by a subset of vessel-associated cells in skeletal muscle, but not in myogenic cells and myofibres. They generated an inducible Alkaline Phosphatase CreERT2 mouse strain with which they could show that these ALPL-positive pericytes are distinct from endothelial and satellite cells. In addition, they showed evidence that these ALPL-positive pericytes contribute to muscle regenerating. We therefore decided to FACS sort our muscle- and peritoneum-derived pericytes with ALPL, to exclude a possible contamination of our initial cell population with myogenic cells.

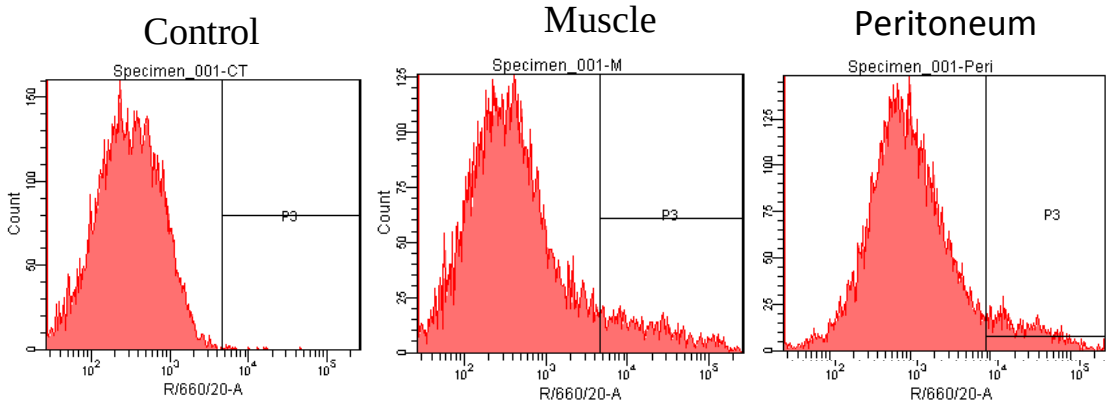

Figure 5.18: ALPL FACS sorting of pericytes isolated from muscle and peritoneum.*CD140b+/CD45-/CD31- pericytes were isolated as before. These cells then labelled with ALPL and sorted according to gate P3 to separate the ALPL-positive population.*

FACS sorting demonstrated that around 10-20% of our pericyte populations were positive for ALPL (Figure 5.18). These cells were then injected intramuscularly into the TA muscle of ROSA26-tdTomato mice as described in figure 5.16. Cryosections from the isolated muscles were immunostained with Lectin BS1 and DAPI while tomato positive fibres were visualised in the red channel (Figure 5.19).

The immunostaining data from the muscle sections of ROSA26-td Tomato -/- mice transplanted with muscle or peritoneum PVCs additionally sorted for ALPL (Figure 5.19) gave a similar result as before seen with the non-ALPL-sorted pericyte populations (Figure 5.17). Sections from the injured and non-injured side showed Tomato-positive fibres with varying intensity. Interestingly, most fibres that were positive for tomato also showed co-localisation of Tomato with lectin BS1-positive endothelial cells in capillaries, though this is difficult to see due to the intensity of the signal inside the muscle fibres (Figure 5.19 Aii-Div). In some cases a spider web-like structure of Tomato-positive blood vessels was visible (Figure 5.19 Ciii, Diii). In sections from the injured sides Tomato-positive fibres that had CLN were visible, indicating that pericytes had fused with the regenerating fibre (Figure 5.19 Biv)

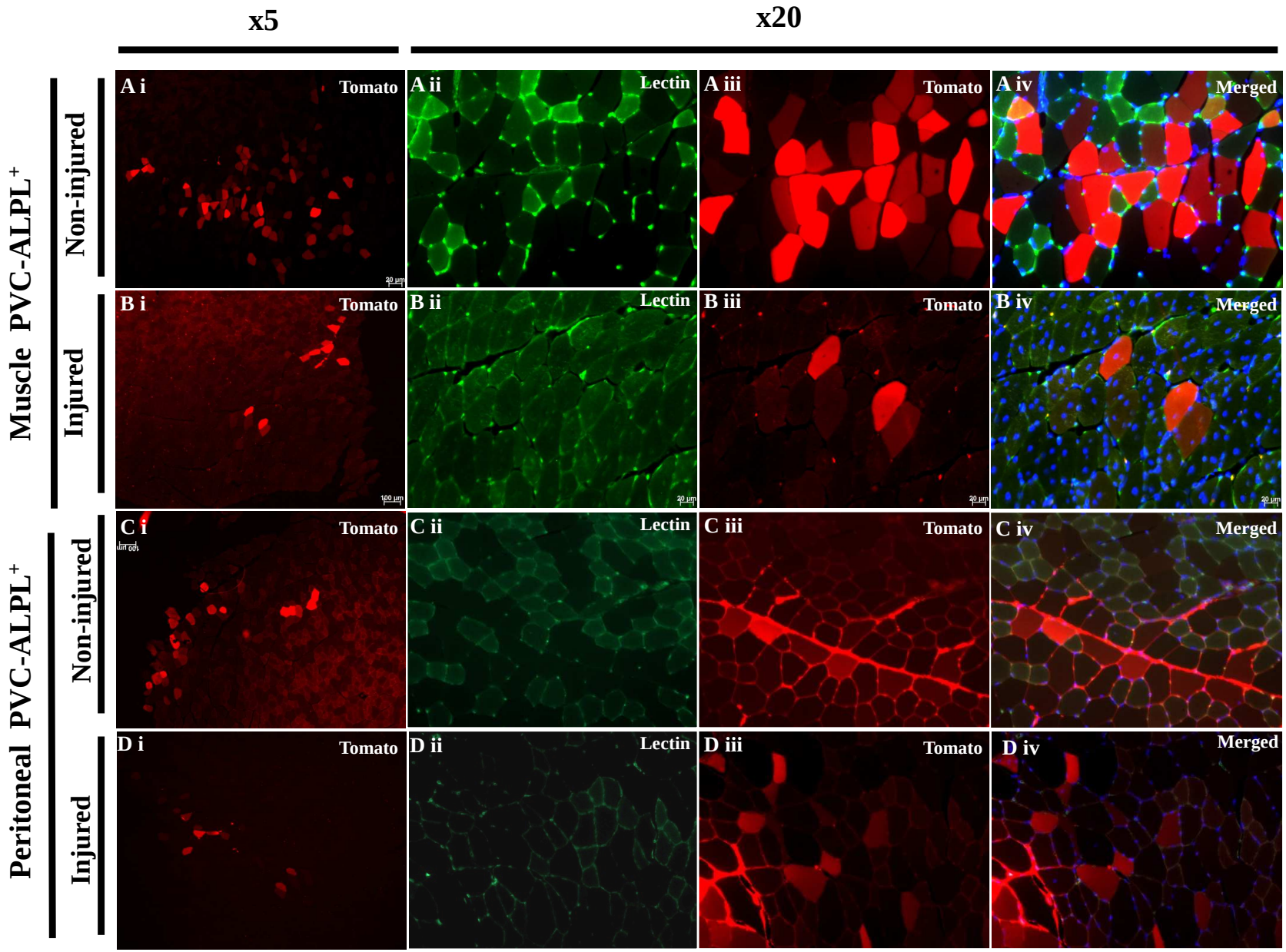
x5
x20
Muscle PVC-ALPL+
Non-injured
Injured
Peritoneal PVC-ALPL+
Non-injured
Injured
A i
Tomato
A ii
Lectin
A iii
Tomato
A iv
Merged
B i
Tomato
B ii
Lectin
B iii
Tomato
B iv
Merged
C i
Tomato
C ii
Lectin
C iii
Tomato
C iv
Merged
D i
Tomato
D ii
Lectin
D iii
Tomato
D iv
Merged

Figure 5.19: Localisation of transplanted ALPL-sorted tomato-labelled pericytes in the TA muscle of ROSA-tdTomato mice. *TA muscles of ROSA26-tdTomato mice were injected with ALPL-positive tomato-labelled pericytes isolated from either muscle (Ai- Aiv and Bi- B iv) or peritoneum (Ci-Civ and Di-Div). In each mouse one TA was injured with CTX and the other served as a non-injured control. Tomato-labelled pericytes are in red, lectin BS1 staining in green marks the pericyte location in capillaries, while DAPI (blue) marks the nuclei. Scale bars, 100µm (A-Di), 20µm (Aii-Div).*

5.5 Discussion

Pericytes are essential constituents of blood vessels and act as important regulators of vessel development, stabilisation and contractility. It has been suggested that pericytes and vascular smooth muscle cells (vSMCs) are phenotypic subtypes of a continuous perivascular cell (PVC) population that may have the capacity to give rise to each other (Brachvogel et al., 2005). It has been demonstrated that these PVCs constitute a population of mesenchymal stem cells (MSCs) associated with the vasculature (Brachvogel et al., 2005) and with the ability to differentiate in to chondrocytes, osteoblasts and adipocytes. Additionally, pericytes show myogenic potential distinct from satellite cells (Dellavalle et al., 2007), however, the contribution of PVCs to tissue and repair in situ remains uncertain. With an increased interest in the field of these PVCs, the process of studying and understanding the complexity of this versatile and intriguing cell types has just begun.

5.5.1 Perivascular cells and mesenchymal stem cells

As there has been a remarkable increase in knowledge in the field of stem cell biology in the past decade, much effort has been devoted to understand the molecular mechanisms that regulate adult stem cells, or the stem cell/progenitor cells derived from adult bone marrow (BMSCs), and developing ways to exploit their potential for therapies. The notion that PVCs are recruited from stromal cells (where MSCs were originally isolated from) by mutual contacts with endothelial cells has been indicated in several studies (Caplan et al., 2008; 2011; Crisan et al., 2008). In this study we tried to answer some of the basic questions regarding the role of these PVCs.

5.5.2 Anxa5-based reporter mouse models to identify perivascular cells

While there are still many unanswered questions about pericytes today, several techniques were developed and additional cellular markers identified that now allow isolation of PVCs and *in vivo* studies in mice. Markers like α-SMA, NG2 proteoglycan, desmin and pdgfr-β are now regularly used to identify populations of perivascular cells *in vitro and in vivo* (Bergers and Song, 2005), but the most significant of all appears to be that of the annexin A5 protein that has proved pivotal in increasing the detection, isolation and characterisation of these cells (Brachvogel et al., 2003; 2005; 2007). In this study, we provide additional support that highlights this protein as a distinct marker

of pericytes. Through use of the Anxa5-LacZ mouse model developed by Brachvogel et al., 2005, we have been able to visualise and observe the distribution of pericytes through detection of LacZ expression. The mouse model has proved fundamental in identifying the distribution of pericyte-like cells along and in close association with the microvasculature of postnatal tissue. In our study we made use of the Anxa5-LacZ mouse model to study the role of pericytes during muscle regeneration by crossing them with *mdx* mice, a mouse model for DMD. Our data clearly shows a close relationship between regenerating fibres and the PVC population, which are wrapped around the blood vessels close to the fibre (Figure 5.3 C and D)

The Anxa5-LacZ model has been instrumental in increasing our knowledge of pericytes. A large body of evidence further indicates that all mesenchymal stem cells (MSCs) are pericytes (Caplan, 2008). Adult mammalian bone marrow has been shown to harbor not one but two discrete adult stem cell lines. While the hematopoietic stem cells generated in the bone marrow responsible for maintaining life long production of blood cells are certainly well characterised, the biological characteristics and properties of the second bone marrow resident population of stem cell are much less understood. This lack of understanding has been compounded, until relatively recently, by the shortage of specific antibody reagents to facilitate the isolation and enrichment of these mesenchymal stem cells (Short et al., 2004). In 2003 Baddoo et al., used a combination of plastic adherence and *in vitro* culture to establish a bone marrow stromal cell culture. They then removed any contaminating hematopoietic cells by negative selection using antibodies to a number of hematopoietic-specific antigens. The remaining stromal cells were shown to exibit osteogenic, adipogenic, and chondrogenic differentiation potential *in vitro* and expressed no markers of hematopoietic or vascular endothelial cells (Baddoo et al., 2003). They did however, express SCA1, much like a candidate osteoprogenitor population in mouse bone marrow as demonstrated by Falla et al., back in 1993 (Falla et al., 1993). Most recently in 2007, Brachvogel et al., demonstrated that a population of Anxa5-LacZ^{+} PVC isolated from mouse meningeal vasculature expressed SCA1- and it is now a common marker used for the characterisation and purification of mesenchymal stem cells.

For many in the field it is still remains to be unequivocally proven that all MSCs are in fact pericytes. Certainly, all pericytes are not MSCs; it has been documented that, while pericytes do not differentiate into hematopoietic or neural cell in adults, the vasculature/perivascular location of hematopoietic and neural stem cells in early foetal tissue implies that other stem cells too inhabit the perivascular niche (Caplan, 2008; Hirschi and D'amore, 1996). But unfortunately, while there still remains much to discover about the complex ontogeny and function of pericytes, the proposal that all pericytes are MSCs will continue to be a somewhat open question rather than a proven statement. Nonetheless, advances such as the Anax5-LacZ and the Anxa5-Cre//ROSA26-LacZ models give hope that we may be able to provide a definite answer to this question in the future.

5.5.3 Role of pericytes as myogenic precursors

In regards to in situ functions of pericytes several doubts still remain. The most topical enquiring is into the potential contribution of these cells to tissue repair and regeneration, through their differentiation into various lineages (Caplan, 2008; Crisan et al., 2008). Our study had in mind the specific role of pericytes as myogenic precursors, and aimed to uncover any intimation towards the involvement of these perivascular cells giving rise to the muscle lineages in skeletal muscle regeneration. Our data suggests that there is a direct involvement of pericytes in myofibre regeneration. In *mdx*//Anxa5-LacZ muscle sections the α-SMA positive cells were evident inside the regenerating fibres indicating the location of pericytes. But this piece of data alone does not support that pericytes are a stem cell population, which can contribute to muscle repair. To support our findings we generated the Anxa5-Cre-KI mouse model, which provided us a tool to follow the fate of these pericytes during muscle regeneration in combination with various reporter strains such as ROSA26-LacZ and ROSA26-td-Tomato. Preliminary data from our experiments on Anxa5-ROSA26-LacZ mice (Figure 5.9 and 5.10) suggests that LacZ-positive pericytes or pericyte-like cells have contributed to muscle regeneration, which was evident by strong LacZ staining inside fibres with CLN. To further investigate these findings it was necessary to lineage trace this stem cell like population. This led us to our hypothesis described in figure 5.19, where we propose the possibility of these cells to differentiate into a different lineage even after committed to one cell lineage due to their phenotypic plasticity. A feature

that distinguishes the MSC from that of the hematopoietic stem cell lineage is that differentiation pathways are not strictly delineated, since even apparently fully differentiated cells from a given lineage have the potential to convert into another lineage.

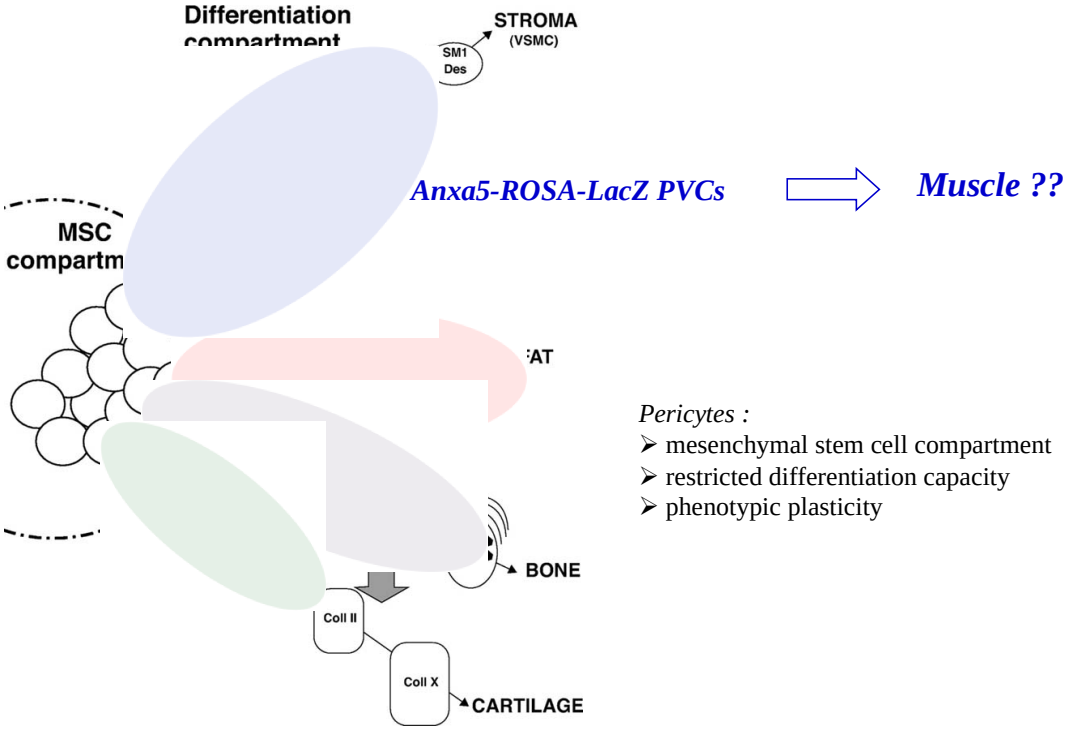

Figure 5.20: The mesenchymal stem cell system. *Factors shown at the exit of the MSC compartment are those used in (osteogenic, chondrogenic, and adipogenic) or compatible with (VSMC differentiation) culture conditions. Double arrows indicate plasticity. The potential sequence of events occurring in the MSC compartment is shown.(Modified from Dennis & Charbord ,2002)*

Potential sequence of events occurring in the MSC compartment is shown in Abbreviations: MSC = mesenchymal stem cell; TGF□β = transforming growth factor□β; PDGF = platelet□derived growth factor; ASMA = α□smooth muscle actin; TSP□1 = thrombospondin□1; EDa^{+}FN = fibronectin comprising the EDa domain; 1E12 = smooth muscle α□actinin recognized by the 1E12 monoclonal antibody; h1Calp = h1□calponin; hCald = h□caldesmon; mV = metavinculin; SM1 = SM myosin heavy chain of 204 kDa; Des = desmin; Dex = dexamethasone; IBMX = isobutylmethylxanthine; IM = indomethacine; β□gp = beta□ glycerophosphate; aP = ascorbate□2□phosphate; NRO = Nile red O stain; vK = von Kossa stain; Coll = collagen I

At the same time we also realised the limitation of using the Anxa5-Cre-Ki mouse model. One major drawback of this model is that, after somatic differentiation all decendants will be labeled with the reporter gene. To avoid this dilemma we have tried to develop an inducible Cre mouse model, Anxa5-Cre-ERT2. In order to do so we designed the targeting construct and transfected ES cells. Unfortunately, we failed to get any homologous recombination in ES cells twice. During the same time Dellavalle et al., used the ALPL-Cre-ERT2 mouse model (Dellavalle et al., 2011). Their data

suggested that ALPL-positive pericytes, but not endothelial cells, fuse with developing myofibres and enter the satellite cell compartment during unperturbed postnatal development. This contribution increased significantly during acute injury or in chronically regenerating dystrophic muscle. This data indicates that pericytes, resident in small vessels of skeletal muscle, contribute to muscle growth and regeneration during postnatal life.

To further investigate the involvement of pericytes as a stem cell we decided to follow an inverse approach. Instead of using the inducible Cre system *in vivo*, we isolated and purified perivascular cells from tdTomato reporter mice and induced reporter expression *in vitro* by viral delivery of Cre recombinase.

5.5.4 Investigating the contribution of pericytes in regenerating muscle by transplantation experiments

To investigate the potential of pericytes as a stem cell population we isolated and purified pericytes from ROSA-td-Tomato mice in which the expression of Tomato is silent and induced reporter expression *in vitro* by transduction with Adeno-Cre virus. Our data indicates that the isolated pericytes population from muscle and peritonium contributed to muscle regeneration. After intramuscular injection of these pericytes in ROSA26-tdTomato congenic mice we observed many fibres in regenerating areas expressing td-Tomato indicating the possible fusion of pericytes with the regenerating fibre. The intensity of the expression varied between fibres. This can be explained by a possible dilution effect when pericytes fuse with pre-existing fibres, as the reporter has a cytoplasmic location. Surprisingly in non-injured muscle we found more Tomato-positive fibres. This can be explained by several possibilites. Firstly, there are more pericytes surviving in the un-injured situation, and, as there is still constant homeostasis in skeletal muscle up to six months of age (G. Kardon, personal communication) more pericytes could be recruited to the muscle fibres. Secondly, there could have been a possible carry over of the virus. To address this issue we injected these pericytes in WT C57/BL6 mice (Figure 5.21). If there was an issue of carrying the virus over then muscle cells, which became infected should turn red in the ROSA26 reporter stain, but not in C57/BL6 mice.

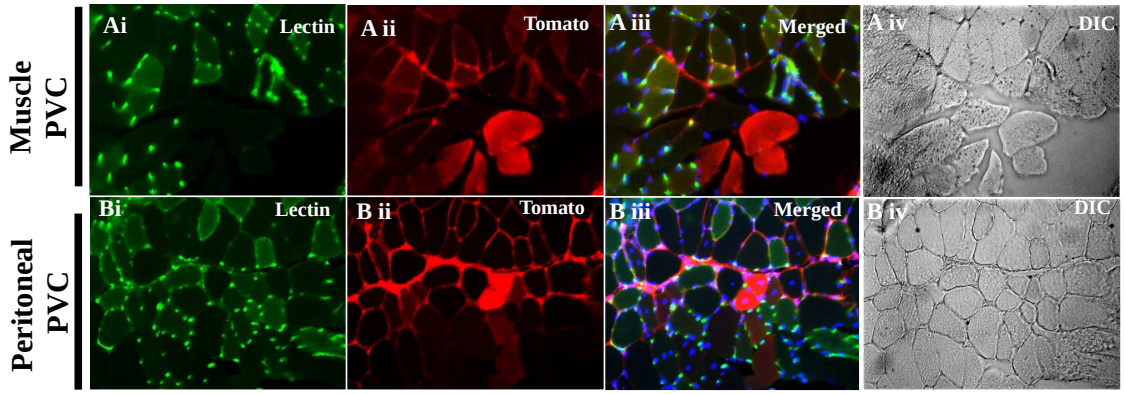

Figure 5.21: Transplantation of Tomato-labelled pericytes into TA muscle of C57BL/6 mice. *TA muscles of C57BL/6 mice were injected with Tomato- labelled pericytes isolated from either muscle (Ai- Aiv) or peritoneum (Bi-Biv). Tomato expression is in red, endothelial cells marked with lectin BS1 in green, DAPI in blue to mark nuclei. Images were taken at x20 magnification.*

From these immunostaining results it was evident that Tomato-positive pericytes from both muscle and peritoneum were in fact able to fuse with muscle fibres (Figure 5.21 Aii and Bii). Tomato-positive spider web-like structures along the blood vessels were again visible, identical to the results when we used the ROSA26-tdTomato mouse strain. Some fibres were positive for Tomato and had also CLN (Figure 5.21 Biii). These regenerating fibres were not due to induced injury, but normal wear and tear of the muscle. Together, our data showed unequivocally that the presence of red fibres was not due to viral contamination of our pericytes.

These findings support the hypothesis that in response to focal injury pericytes are activated and released from their position on the vascular tube to migrate/proliferate to the site of injury and contribute to the regeneration process. Support for this hypothesis is the fact that degradation products of extracellular matrix (ECM) proteins are chemotactic for progenitor cells, and pericytes show strong migration towards both papain and pepsin digested ECM (Crisan et al., 2008; Reing et al., 2008).

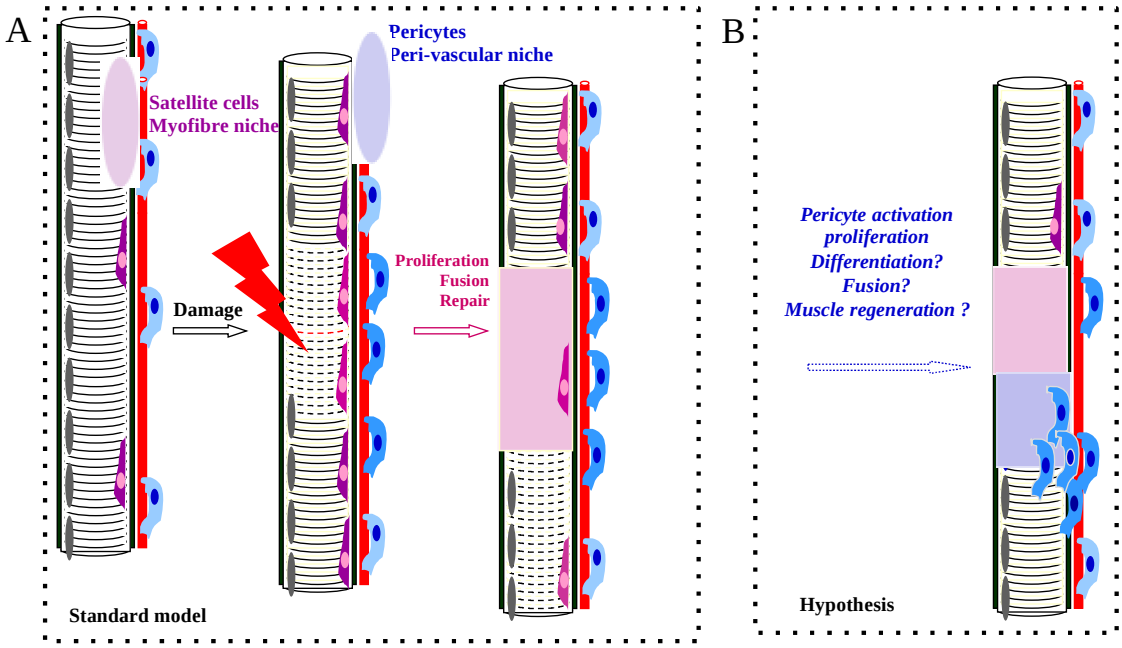

Figure 5.22: Schematic representation of proposed hypothesis: *A) Indicates the involvement of satellite cells (pink) in muscle regeneration upon activation. The pericytes are shown in blue wrapped arround the blood vessels surrounding the myofibre. B) Demonstrates the proposed role of pericytes (blue) to become activated and fuse with the muscle fibre, leading to regeneration.*

Based on the results shown in this study we propose the working hypothesis, which is displayed in figure 5.22. The schematic representation of a well-known standard model of muscle regeneration can be seen in figure 5.22, where the role of the satellite cells in regeneration is shown. Alternatively, the model (Figure 5.22 B) shows the involvement of pericytes in myofibre regeneration. As therapy by isolated myoblasts is considered to be insufficient to rescue damaged muscle (Tedesco et al., 2010), isolated pericytes may become a potential therapy for muscle disease.

In our study we have shown that annexin A5 is a distinct and significant marker for pericyte cells resident in the vasculature. It has been clearly demonstrated that pericyte-like stem cells can differentiate into myogenic lineages (Dellavalle et al., 2007), and our results further support that notion by showing that not only pericytes isolated from skeletal muscle but also from the peritoneum can contribute to skeletal muscle repair. Whether pericytes from all tissues are similar in their molecular signature and their contribution to muscle regeneration remains open.

Chapter 6 Summary

Major players in maintaining the muscle integrity during development and in adult skeletal muscle are integrins. Presented in this thesis is the initial characterisation and investigation of the use of transgenic mice overexpressing integrin α7 splice variants and the conditional KO of integrin α5 in muscle. These mice were generated with the eventual aim to increase the knowledge and understanding of the role of integrins in adult and developing muscle and their potential role in in muscle wasting disease.

The loss of integrins from skeletal muscle has been shown to result in muscle wasting diseases, but for the first time it has been presented that an increase in integrin α subunits can also cause a dystrophic phenotype in adult skeletal muscle. The onset and progression of this phenotype varies between different locations within muscle and correlates with the level of the integrin α subunit expression and the specific alternative splice variant of the subunit.

Increasing the levels of integrin α7 results in an increase in the level of integrin β1 and integrin α7 splice variants can compete with each other for integrin β1 association to a certain extent, but there are controls in place to ensure that the specific localisation and therefore function of certain receptor combinations are preserved.

To elucidate the function of integrin α5 in skeletal muscle, it is important to knock down the expression of Itga5 gene. Knocking out integrin α5 is embryonically lethal and conclusions drawn from the α5 -/- chimeric mice were limited. An ideal tool in the investigation of the role of integrin α5 during muscle development would be to generate a conditional knock out of integrin α5 where, the expression of Cre is driven by a muscle-specific promoter. Here we have shown that knocking down integrin α5 conditionally by the HSA-Cre promoter does not lead to a muscular dystrophy, however, loss of integrin α5 during development using Pax3-Cre system, does cause posterior defect in the embryo at E18.5.

Integrin α5 is vital to skeletal muscle development and has a close relationship with integrin α7 (Yao et al., 1996; Taverna et al., 1998; Nawrotzki et al in 2003). In normal postnatal muscle integrin α5β1 expression is detected at MTJs, which is then switched by presence of integrin α7β1 two weeks after birth. However, the observations made by Nawrotzki et al in 2003, suggests that in integrin α7-deficient muscles, the expression of integrin α5β1D persists into adulthood. This leads to the accumulation of fibronectin in place of laminin at the junctional basement membrane of the muscle fibre. This link between α5β1D/fibronectin is inferior to the α7β1D/ laminin link at the normal MTJ, and this possible gain-of-function phenotype could be leading to the onset of muscle wasting in α7-deficient mice.

Here we have shown the effect of loss of both the integrins by breeding integrin α7 heterozygous or homozygous mice with integrin α5 heterozygous mice to generate integrin α7KO mice carrying only one allele of integrin α5. To our surprise none of these mice survived the postnatal stage and analysis of embryos at E10.5 suggests that these is an dosage effect of integrin α5 which is needed in order to compensate the effect of loss of integrin α7 at early stages of development and there is a possible role of these integrins in vascular development.

Apart from gene therapy the stem cell based therapies are getting more interest in the field of regenerative medicine. For muscle related diseases, the potential candidates are stem cell population from muscle itself called, satellite cells (SCs), yet by nature they exhibit a number of characteristics that limit their effectiveness as discussed before. In 2007, Dallavalle et al demonstrated other cell types, which behave like stem cell populations and have the capacity to differentiate into skeletal muscle. One such stem cell population included in this study is the cells associated with the microvasculature of skeletal muscle.

Of particular relevance as a promising candidate for future cell therapy, pericytes may represent as embryonic mesangioblst present after birth, but by disparity do not express the endothelial markers found in these cells. In addition, they have a number of unequivocal characteristics that distinguish them from SCs, including a different anatomical niche and growth requirements. Unlike SCs, they do not express mitogenic factors such as Pax7, Myf5 and MyoD (Kassar-Duchossoy et al., 2004; 2005) until terminal

differentiation, but instead express a number of other markers. In recent years, several markers have been identified that define subpopulations of pericytes, like desmin, smooth-muscle-actin (α-SMA), NG2-proteoglycan (Ozerdem et al., 2001), PDGFR-β or the GTPase-activating protein RGS5 (Gerhardt and Betsholtz, 2003) and non tissue-specific alkaline phosphatase (ALPL). By this it became also clear that pericytes and vascular smooth muscle cells are subsets of a continuum of vascular cells with phenotypic plasticity (Nehls and Drenckhahn, 1993). The lack of specific markers limited the analysis of pericytes, as pure cell populations could not easily be purified from tissues. Until recently, no adequate method was available to purify pericytes from mouse tissues, a prerequisite for using modern mouse genomics and proteomics. Therefore, we used a mouse model (Anxa5-LacZ), which helped us to identify these cells with the help of Anxa5 driven LacZ expression. Anxa5-LacZ fusion reporter mice have been shown to be a valuable tool for the identification, isolation and characterisation of perivascular cells/pericytes from tissues (Brachvogel et al., 2003; 2005; 2007). However, LacZ staining can only be done by traditional static histological analysis, and therefore lacks any information about the dynamics of pericytes in tissue remodelling. Additionally, it is very likely that the Anxa5 promoter is not active in pericyte descendants and so we may miss the identification of cells into which pericytes differentiate. In this study we demonstrate the potential fate of the pericytes in muscle regeneration by generating conditional KI mice (Anxa5-Cre-KI).

Dallavalle et al proposed these pericyte-derived cells as a second myogenic precursor present within postnatal skeletal muscle, distinct from SCs yet similar myogenic potency (Dallavalle et al., 2007). In this study we demonstrate the potential fate of the pericytes in muscle regeneration by transplanting fluorescently labeled pericytes into the TA muscle of congenic mice. Upon muscle injury we were able to trace the lineage of these transplanted cell and have shown here that these cell do contribute towards new myofibre formation by fusing with the regenerating fibres.

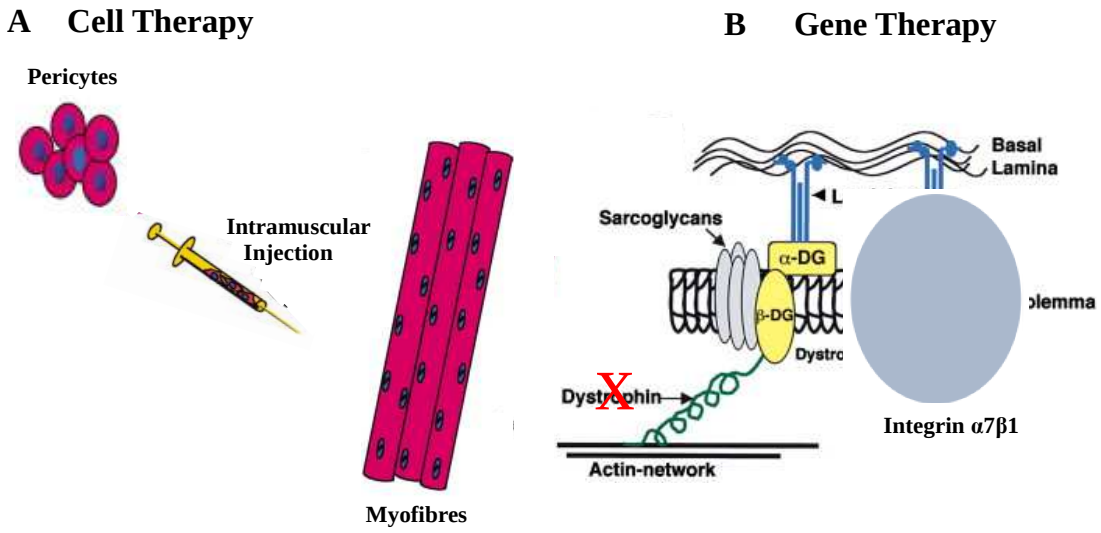

Figure 6.1 Therapeutic possibilities for Duchenne Muscular Dystrophy. *(A) Intramuscular injection of fluorescently labeled pericytes, isolated from muscle or peritoneum in order to follow the fate of these cells during muscle regeneration. (B) A schematic representation of the dystrophin/glycoprotein complex and the integrin/laminin-mediated attachment of muscle cells to the surrounding extracellular matrix. Upregulation of integrin α7 may compensate for the functional loss of dystrophin (Modified from Seale, Asakura and Rudnicki, 2001)*

Over all in this study we tried to evaluate possible therapies for DMD. As explained above the integrin α7β1 would be a candidate for gene therapy (Figure 6.1), but as discussed in the results chapter it might not be effective as seen in mdx mice. While on the other hand pericytes could be a potential option for cell-based therapy (figure 6.1).

References

Alberts, B., Johnson, J., Lewis, J.,Raff, M., Roberts, K., Walters, P. 2002. Molecular biology of the cell.

Allikian, M.J., A.A. Hack, S. Mewborn, U. Mayer, and E.M. McNally. 2004. Genetic compensation for sarcoglycan loss by integrin alpha7beta1 in muscle. *J Cell Sci*. 117:3821-3830.

Altruda, F., P. Cervella, G. Tarone, C. Botta, F. Balzac, G. Stefanuto, and L. Silengo. 1990. A human integrin β1 subunit with a unique cytoplasmic domain generated by alternative mRNA processing. *Gene*. 95:261-266.

Anderson, J.L., S.I. Head, and J.W. Morley. 2005. Synaptic plasticity in the dy2J mouse model of laminin [alpha]2-deficient congenital muscular dystrophy. *Brain Research*. 1042:23-28.

Armulik, A., A. Abramsson, and C. Betsholtz. 2005. Endothelial/pericyte interactions. *Circ Res*. 97:512-523.

Armulik, A., G. Genove, and C. Betsholtz. 2011. Pericytes: developmental, physiological, and pathological perspectives, problems, and promises. *Dev Cell*. 21:193-215.

Arnaout, M.A. 2002. Integrin structure: new twists and turns in dynamic cell adhesion. *Immunol Rev*. 186:125-140.

Arnaout, M.A., B. Mahalingam, and J.P. Xiong. 2005. Integrin structure, allostery, and bidirectional signaling. *Annual Review of Cell and Developmental Biology*. 21:381-410.

Asakura, A. 2003. Stem cells in adult skeletal muscle. *Trends Cardiovasc Med*. 13:123-128.

Ballestrem, C., B. Hinz, B.A. Imhof, and B. Wehrle-Haller. 2001. Marching at the front and dragging behind: differential alphaVbeta3-integrin turnover regulates focal adhesion behavior. *J Cell Biol*. 155:1319-1332.

Bao, Z.Z., M. Lakonishok, S. Kaufman, and A.F. Horwitz. 1993. Alpha 7 beta 1 integrin is a component of the myotendinous junction on skeletal muscle. *J Cell Sci*. 106 (Pt 2):579-589.

Baudoin, C., M.J. Goumans, C. Mummery, and A. Sonnenberg. 1998. Knockout and knockin of the beta1 exon D define distinct roles for integrin splice variants in heart function and embryonic development. *Genes Dev*. 12:1202-1216.

Beauchamp, J.R., L. Heslop, D.S. Yu, S. Tajbakhsh, R.G. Kelly, A. Wernig, M.E. Buckingham, T.A. Partridge, and P.S. Zammit. 2000. Expression of CD34 and Myf5 defines the majority of quiescent adult skeletal muscle satellite cells. *J Cell Biol*. 151:1221-1234.

Beglova, N., S.C. Blacklow, J. Takagi, and T.A. Springer. 2002. Cysteine-rich module structure reveals a fulcrum for integrin rearrangement upon activation. *Nature structural biology*. 9:282-287.

Belkin, A.M., and S.F. Retta. 1998. β1D Integrin Inhibits Cell Cycle Progression in Normal Myoblasts and Fibroblasts. *Journal of Biological Chemistry*. 273:15234-15240.

Belkin, A.M., S.F. Retta, O.Y. Pletjushkina, F. Balzac, L. Silengo, R. Fassler, V.E. Koteliansky, K. Burridge, and G. Tarone. 1997. Muscle beta1D integrin reinforces the cytoskeleton-matrix link: modulation of integrin adhesive function by alternative splicing. *J Cell Biol*. 139:1583-1595.

Belkin, A.M., N.I. Zhidkova, F. Balzac, F. Altruda, D. Tomatis, A. Maier, G. Tarone, V.E. Koteliansky, and K. Burridge. 1996. Beta 1D integrin displaces the beta 1A isoform in striated muscles: localization at junctional structures and signaling potential in nonmuscle cells. *J Cell Biol*. 132:211-226.

Bellis, S.L. 2004. Variant glycosylation: an underappreciated regulatory mechanism for beta1 integrins. *Biochim Biophys Acta*. 1663:52-60.

Benchaouir, R., M. Meregalli, A. Farini, G. D'Antona, M. Belicchi, A. Goyenvalle, M. Battistelli, N. Bresolin, R. Bottinelli, L. Garcia, and Y. Torrente. 2007. Restoration of Human Dystrophin Following Transplantation of Exon-Skipping-Engineered DMD Patient Stem Cells into Dystrophic Mice. *Cell Stem Cell*. 1:646-657.

Bergers, G., and S. Song. 2005. The role of pericytes in blood-vessel formation and maintenance. *Neuro-oncology*. 7:452-464.

Bi, Y., D. Ehirchiou, T.M. Kilts, C.A. Inkson, M.C. Embree, W. Sonoyama, L. Li, A.I. Leet, B.M. Seo, L. Zhang, S. Shi, and M.F. Young. 2007. Identification of tendon stem/progenitor cells and the role of the extracellular matrix in their niche. *Nat Med*.

Bintliff, S.W., B. E. 1960. Radioautographic study of skeletal muscle regeneration. *American Journal of Anatomy*. 106:233-246.

Biressi, S., and A. Asakura. 2012. Satellite Cells and the Universe of Adult Muscle Stem Cells. *Journal of stem cell research & therapy*. Suppl 11.

Blake, D.J., A. Weir, S.E. Newey, and K.E. Davies. 2002. Function and genetics of dystrophin and dystrophin-related proteins in muscle. *Physiol Rev*. 82:291-329.

Blankinship, M.J., P. Gregorevic, and J.S. Chamberlain. 2006. Gene therapy strategies for Duchenne muscular dystrophy utilizing recombinant adeno-associated virus vectors. *Mol Ther*. 13:241-249.

Blaschuk, K.L., and P.C. Holland. 1994. The regulation of alpha 5 beta 1 integrin expression in human muscle cells. *Dev Biol*. 164:475-483.

Blau, H.M., C. Webster, C.P. Chiu, S. Guttman, and F. Chandler. 1983. Differentiation properties of pure populations of human dystrophic muscle cells. *Exp Cell Res*. 144:495-503.

Boettiger, D., M. Enomoto-Iwamoto, H.Y. Yoon, U. Hofer, A.S. Menko, and R. Chiquet-Ehrismann. 1995. Regulation of integrin alpha 5 beta 1 affinity during myogenic differentiation. *Dev Biol*. 169:261-272.

Bonfield, T.L., and A.I. Caplan. 2010. Adult mesenchymal stem cells: an innovative therapeutic for lung diseases. *Discovery medicine*. 9:337-345.

Boppart, M.D., D.J. Burkin, and S.J. Kaufman. 2006. Alpha7beta1-integrin regulates mechanotransduction and prevents skeletal muscle injury. *Am J Physiol Cell Physiol*. 290:C1660-1665.

Bork, P., T. Doerks, T.A. Springer, and B. Snel. 1999. Domains in plexins: links to integrins and transcription factors. *Trends Biochem Sci*. 24:261-263.

Brachvogel, B., J. Dikschas, H. Moch, H. Welzel, K. von der Mark, C. Hofmann, and E. Pöschl. 2003. Annexin A5 Is Not Essential for Skeletal Development. *Molecular and Cellular Biology*. 23:2907-2913.

Brachvogel, B., H. Moch, F. Pausch, U. Schlotzer-Schrehardt, C. Hofmann, R. Hallmann, K. von der Mark, T. Winkler, and E. Poschl. 2005. Perivascular cells expressing annexin A5 define a novel mesenchymal stem cell-like population with the capacity to differentiate into multiple mesenchymal lineages. *Development*. 132:2657-2668.

Brachvogel, B., F. Pausch, P. Farlie, U. Gaipl, J. Etich, Z. Zhou, T. Cameron, K. von der Mark, J.F. Bateman, and E. Pöschl. 2007. Isolated Anxa5+/Sca-1+ perivascular cells from mouse meningeal vasculature retain their perivascular phenotype in vitro and in vivo. *Experimental Cell Research*. 313:2730-2743.

Brachvogel, B., H. Welzel, H. Moch, K. von der Mark, C. Hofmann, and E. Poschl. 2001. Sequential expression of annexin A5 in the vasculature and skeletal elements during mouse development. *Mech Dev*. 109:389-393.

Brakebusch, C., and R. Fassler. 2003. The integrin-actin connection, an eternal love affair. *EMBO J*. 22:2324-2333.

Brancaccio, A. 2003. The origin of dystrophin-glycoprotein complex(DGC)-related muscular dystrophies: the need for protection against an ancestral pathogen? *Ital J Biochem*. 52:68-71.

Bronner-Fraser, M., M. Artinger, J. Muschler, and A.F. Horwitz. 1992. Developmentally regulated expression of alpha 6 integrin in avian embryos. *Development*. 115:197-211.

Buckingham, M. 1992. Making muscle in mammals. *Trends in genetics : TIG*. 8:144-148.

Burkin, D.J., M. Gu, B.L. Hodges, J.T. Campanelli, and S.J. Kaufman. 1998. A functional role for specific spliced variants of the alpha7beta1 integrin in acetylcholine receptor clustering. *J Cell Biol*. 143:1067-1075.

Burkin, D.J., and S.J. Kaufman. 1999. The alpha7beta1 integrin in muscle development and disease. *Cell Tissue Res*. 296:183-190.

Burkin, D.J., G.Q. Wallace, D.J. Milner, E.J. Chaney, J.A. Mulligan, and S.J. Kaufman. 2005. Transgenic expression of {alpha}7{beta}1 integrin maintains muscle integrity, increases regenerative capacity, promotes hypertrophy, and reduces cardiomyopathy in dystrophic mice. *Am J Pathol*. 166:253-263.

Burkin, D.J., G.Q. Wallace, K.J. Nicol, D.J. Kaufman, and S.J. Kaufman. 2001. Enhanced expression of the alpha 7 beta 1 integrin reduces muscular dystrophy and restores viability in dystrophic mice. *J Cell Biol*. 152:1207-1218.

Bushby, K.M. 1999. The limb-girdle muscular dystrophies-multiple genes, multiple mechanisms. *Hum Mol Genet*. 8:1875-1882.

Bushby, K.M.D. 1999. Making sense of the limb-girdle muscular dystrophies. *Brain*. 122:1403-1420.

Caplan, A.I. 1991. Mesenchymal stem cells. *Journal of orthopaedic research : official publication of the Orthopaedic Research Society*. 9:641-650.

Caplan, A.I. 2007. Adult mesenchymal stem cells for tissue engineering versus regenerative medicine. *J Cell Physiol*. 213:341-347.

Caplan, A.I. 2008. All MSCs are pericytes? *Cell Stem Cell*. 3:229-230.

Caplan, A.I., and D. Correa. 2011. The MSC: an injury drugstore. *Cell Stem Cell*. 9:11-15.

Chakkalakal, J.V., J. Thompson, R.J. Parks, and B.J. Jasmin. 2005. Molecular, cellular, and

pharmacological therapies for Duchenne/Becker muscular dystrophies. *FASEB J*. 19:880-891.

Charo, I.F., L. Nannizzi, J.W. Smith, and D.A. Cheresh. 1990. The vitronectin receptor alpha v beta 3 binds fibronectin and acts in concert with alpha 5 beta 1 in promoting cellular attachment and spreading on fibronectin. *J Cell Biol*. 111:2795-2800.

Clerk, A., G.E. Morris, V. Dubowitz, K.E. Davies, and C.A. Sewry. 1993. Dystrophin-related protein, utrophin, in normal and dystrophic human fetal skeletal muscle. *The Histochemical journal*. 25:554-561.

Cohn, R.D., and K.P. Campbell. 2000. Molecular basis of muscular dystrophies. *Muscle & Nerve*. 23:1456-1471.

Cohn, R.D., U. Mayer, G. Saher, R. Herrmann, A. van der Flier, A. Sonnenberg, L. Sorokin, and T. Voit. 1999. Secondary reduction of alpha7B integrin in laminin alpha2 deficient congenital muscular dystrophy supports an additional transmembrane link in skeletal muscle. *J Neurol Sci*. 163:140-152.

Collins, C.A. 2006. Satellite cell self-renewal. *Curr Opin Pharmacol*. 6:301-306.

Collins, C.A., I. Olsen, P.S. Zammit, L. Heslop, A. Petrie, T.A. Partridge, and J.E. Morgan. 2005. Stem cell function, self-renewal, and behavioral heterogeneity of cells from the adult muscle satellite cell niche. *Cell*. 122:289-301.

Collins, C.A., P.S. Zammit, A.P. Ruiz, J.E. Morgan, and T.A. Partridge. 2007. A population of myogenic stem cells that survives skeletal muscle aging. *Stem Cells*. 25:885-894.

Collo, G., L. Starr, and V. Quaranta. 1993. A new isoform of the laminin receptor integrin alpha 7 beta 1 is developmentally regulated in skeletal muscle. *Journal of Biological Chemistry*. 268:19019-19024.

Cote, P.D., H. Moukhles, and S. Carbonetto. 2002. Dystroglycan is not required for localization of dystrophin, syntrophin, and neuronal nitric-oxide synthase at the sarcolemma but regulates integrin alpha 7B expression and caveolin-3 distribution. *J Biol Chem*. 277:4672-4679.

Cote, P.D., H. Moukhles, M. Lindenbaum, and S. Carbonetto. 1999. Chimaeric mice deficient in dystroglycans develop muscular dystrophy and have disrupted myoneural synapses. *Nat Genet*. 23:338-342.

Courdier-Fruh, I., L. Barman, A. Briguet, and T. Meier. 2002. Glucocorticoid-mediated regulation

of utrophin levels in human muscle fibers. *Neuromuscular disorders : NMD*. 12 Suppl 1:S95-104.

Crawley, S., E.M. Farrell, W. Wang, M. Gu, H.Y. Huang, V. Huynh, B.L. Hodges, D.N. Cooper, and S.J. Kaufman. 1997. The alpha7beta1 integrin mediates adhesion and migration of skeletal myoblasts on laminin. *Exp Cell Res*. 235:274-286.

Crisan, M., S. Yap, L. Casteilla, C.W. Chen, M. Corselli, T.S. Park, G. Andriolo, B. Sun, B. Zheng, L. Zhang, C. Norotte, P.N. Teng, J. Traas, R. Schugar, B.M. Deasy, S. Badylak, H.J. Buhring, J.P. Giacobino, L. Lazzari, J. Huard, and B. Peault. 2008. A perivascular origin for mesenchymal stem cells in multiple human organs. *Cell Stem Cell*. 3:301-313.

D'Souza, S.E., M.H. Ginsberg, T.A. Burke, S.C. Lam, and E.F. Plow. 1988. Localization of an Arg-Gly-Asp recognition site within an integrin adhesion receptor. *Science*. 242:91-93.

D'Souza, S.E., M.H. Ginsberg, G.R. Matsueda, and E.F. Plow. 1991. A discrete sequence in a platelet integrin is involved in ligand recognition. *Nature*. 350:66-68.

da Silva Meirelles, L., A.I. Caplan, and N.B. Nardi. 2008. In search of the in vivo identity of mesenchymal stem cells. *Stem Cells*. 26:2287-2299.

Deconinck, A.E., J.A. Rafael, J.A. Skinner, S.C. Brown, A.C. Potter, L. Metzinger, D.J. Watt, J.G. Dickson, J.M. Tinsley, and K.E. Davies. 1997. Utrophin-dystrophin-deficient mice as a model for Duchenne muscular dystrophy. *Cell*. 90:717-727.

Dedhar, S. 2000. Cell-substrate interactions and signaling through ILK. *Curr Opin Cell Biol*. 12:250-256.

Del Pozo, M.A., W.B. Kiosses, N.B. Alderson, N. Meller, K.M. Hahn, and M.A. Schwartz. 2002. Integrins regulate GTP-Rac localized effector interactions through dissociation of Rho-GDI. *Nat Cell Biol*. 4:232-239.

Dellavalle, A., M. Sampaolesi, R. Tonlorenzi, E. Tagliafico, B. Sacchetti, L. Perani, A. Innocenzi, B.G. Galvez, G. Messina, R. Morosetti, S. Li, M. Belicchi, G. Peretti, J.S. Chamberlain, W.E. Wright, Y. Torrente, S. Ferrari, P. Bianco, and G. Cossu. 2007. Pericytes of human skeletal muscle are myogenic precursors distinct from satellite cells. *Nat Cell Biol*. 9:255-267.

Dennis, J.W., J. Pawling, P. Cheung, E. Partridge, and M. Demetriou. 2002. UDP-N-acetylglucosamine:alpha-6-D-mannoside beta1,6 N-acetylglucosaminyltransferase V (Mgat5) deficient mice. *Biochim Biophys Acta*. 1573:414-422.

Dhawan, J., and T.A. Rando. 2005. Stem cells in postnatal myogenesis: molecular mechanisms of satellite cell quiescence, activation and replenishment. *Trends Cell Biol*. 15:666-673.

Diamond, M.S., and T.A. Springer. 1994. The dynamic regulation of integrin adhesiveness. *Current biology : CB*. 4:506-517.

Doherty, M.J., B.A. Ashton, S. Walsh, J.N. Beresford, M.E. Grant, and A.E. Canfield. 1998. Vascular pericytes express osteogenic potential in vitro and in vivo. *Journal of bone and mineral research : the official journal of the American Society for Bone and Mineral Research*. 13:828-838.

Doherty, M.J., B.A. Ashton, S. Walsh, J.N. Beresford, M.E. Grant, and A.E. Canfield. 1998. Vascular pericytes express osteogenic potential in vitro and in vivo. *Journal of bone and mineral research : the official journal of the American Society for Bone and Mineral Research*. 13:828-838.

Dominici, M., K. Le Blanc, I. Mueller, I. Slaper-Cortenbach, F. Marini, D. Krause, R. Deans, A. Keating, D. Prockop, and E. Horwitz. 2006. Minimal criteria for defining multipotent mesenchymal stromal cells. The International Society for Cellular Therapy position statement. *Cytotherapy*. 8:315-317.

Durbeej, M., and K.P. Campbell. 2002. Muscular dystrophies involving the dystrophin-glycoprotein complex: an overview of current mouse models. *Curr Opin Genet Dev*. 12:349-361.

Echtermeyer, F., S. Schober, E. Poschl, H. von der Mark, and K. von der Mark. 1996. Specific induction of cell motility on laminin by alpha 7 integrin. *J Biol Chem*. 271:2071-2075.

Emsley, J., S.L. King, J.M. Bergelson, and R.C. Liddington. 1997. Crystal Structure of the I Domain from Integrin α2β1. *Journal of Biological Chemistry*. 272:28512-28517.

Engvall, E. 1995. Structure and function of basement membranes. *Int J Dev Biol*. 39:781-787.

Engvall, E., and U.M. Wewer. 2003. The new frontier in muscular dystrophy research: booster genes. *FASEB J*. 17:1579-1584.

Erickson, A.C., and J.R. Couchman. 2000. Still More Complexity in Mammalian Basement Membranes. *Journal of Histochemistry & Cytochemistry*. 48:1291-1306.

Ervasti, J.M., K. Ohlendieck, S.D. Kahl, M.G. Gaver, and K.P. Campbell. 1990. Deficiency of a glycoprotein component of the dystrophin complex in dystrophic muscle. *Nature*. 345:315-319.

Farini, A., P. Razini, S. Erratico, Y. Torrente, and M. Meregalli. 2009. Cell based therapy for Duchenne muscular dystrophy. *J Cell Physiol*. 221:526-534.

Farrington-Rock, C., N.J. Crofts, M.J. Doherty, B.A. Ashton, C. Griffin-Jones, and A.E. Canfield. 2004. Chondrogenic and Adipogenic Potential of Microvascular Pericytes. *Circulation*. 110:2226-2232.

Fässler, R., and M. Meyer. 1995. Consequences of lack of beta 1 integrin gene expression in mice. *Genes & Development*. 9:1896-1908.

Fong, P.Y., P.R. Turner, W.F. Denetclaw, and R.A. Steinhardt. 1990. Increased activity of calcium leak channels in myotubes of Duchenne human and mdx mouse origin. *Science*. 250:673-676.

Foster, R.F., J.M. Thompson, and S.J. Kaufman. 1987. A laminin substrate promotes myogenesis in rat skeletal muscle cultures: analysis of replication and development using antidesmin and anti-BrdUrd monoclonal antibodies. *Dev Biol*. 122:11-20.

Francis, S.E., K.L. Goh, K. Hodivala-Dilke, B.L. Bader, M. Stark, D. Davidson, and R.O. Hynes. 2002. Central Roles of {alpha}5{beta}1 Integrin and Fibronectin in Vascular Development in Mouse Embryos and Embryoid Bodies. *Arterioscler Thromb Vasc Biol*. 22:927-933.

Friedenstein, A.J., R.K. Chailakhjan, and K.S. Lalykina. 1970. The development of fibroblast colonies in monolayer cultures of guinea-pig bone marrow and spleen cells. *Cell and tissue kinetics*. 3:393-403.

Friedenstein, A.J., K.V. Petrakova, A.I. Kurolesova, and G.P. Frolova. 1968. Heterotopic of bone marrow. Analysis of precursor cells for osteogenic and hematopoietic tissues. *Transplantation*. 6:230-247.

Gaipl, U.S., L.E. Munoz, F. Rodel, F. Pausch, B. Frey, B. Brachvogel, K. von der Mark, and E. Poschl. 2007. Modulation of the immune system by dying cells and the phosphatidylserine-ligand annexin A5. *Autoimmunity*. 40:254-259.

Gardiner, N.J., P. Fernyhough, D.R. Tomlinson, U. Mayer, H. von der Mark, and C.H. Streuli. 2005. Alpha7 integrin mediates neurite outgrowth of distinct populations of adult sensory neurons. *Mol Cell Neurosci*. 28:229-240.

Gayraud-Morel, B., F. Chretien, and S. Tajbakhsh. 2009. Skeletal muscle as a paradigm for regenerative biology and medicine. *Regenerative medicine*. 4:293-319.

George, E.L., E.N. Georges-Labouesse, R.S. Patel-King, H. Rayburn, and R.O. Hynes. 1993. Defects in mesoderm, neural tube and vascular development in mouse embryos lacking fibronectin. *Development*. 119:1079-1091.

Gerhardt, H., and C. Betsholtz. 2003. Endothelial-pericyte interactions in angiogenesis. *Cell Tissue Res*. 314:15-23.

Gibson, A.J., J. Karasinski, J. Relvas, J. Moss, T.G. Sherratt, P.N. Strong, and D.J. Watt. 1995. Dermal fibroblasts convert to a myogenic lineage in mdx mouse muscle. *J Cell Sci*. 108 (Pt 1):207-214.

Gilbert, R., J. Nalbantoglu, B.J. Petrof, S. Ebihara, G.H. Guibinga, J.M. Tinsley, A. Kamen, B. Massie, K.E. Davies, and G. Karpati. 1999. Adenovirus-mediated utrophin gene transfer mitigates the dystrophic phenotype of mdx mouse muscles. *Human gene therapy*. 10:1299-1310.

Gimond, C., C. Baudoin, and A. Sonnenberg. 2000. Defects in adhesion and migration, but not in proliferation and differentiation, of embryonic stem cells upon replacement of integrin subunit beta1A by beta1D. *Differentiation*. 66:93-105.

Goh, K.L., J.T. Yang, and R.O. Hynes. 1997. Mesodermal defects and cranial neural crest apoptosis in alpha5 integrin-null embryos. *Development*. 124:4309-4319.

Grady, R.M., H. Teng, M.C. Nichol, J.C. Cunningham, R.S. Wilkinson, and J.R. Sanes. 1997. Skeletal and cardiac myopathies in mice lacking utrophin and dystrophin: a model for Duchenne muscular dystrophy. *Cell*. 90:729-738.

Grose, R., C. Hutter, W. Bloch, I. Thorey, F.M. Watt, R. Fassler, C. Brakebusch, and S. Werner. 2002. A crucial role of beta 1 integrins for keratinocyte migration in vitro and during cutaneous wound repair. *Development*. 129:2303-2315.

Grounds, M.D. 1991. Towards understanding skeletal muscle regeneration. *Pathology, research and practice*. 187:1-22.

Gu, J., and N. Taniguchi. 2004. Regulation of integrin functions by N-glycans. *Glycoconjugate journal*. 21:9-15.

Gulino, D., C. Boudignon, L.Y. Zhang, E. Concord, M.J. Rabiet, and G. Marguerie. 1992. Ca(2+)-binding properties of the platelet glycoprotein IIb ligand-interacting domain. *J Biol Chem*.

267:1001-1007.

Gullberg, D., C.F. Tiger, and T. Velling. 1999. Laminins during muscle development and in muscular dystrophies. *Cell Mol Life Sci*. 56:442-460.

Gullberg, D., T. Velling, L. Lohikangas, and C.F. Tiger. 1998. Integrins during muscle development and in muscular dystrophies. *Front Biosci*. 3:D1039-1050.

Gullberg, D.E., and E. Lundgren-Ã…kerlund. 2002. Collagen-binding I domain integrins - what do they do? *Progress in Histochemistry and Cytochemistry*. 37:3-54.

Guo, C., M. Willem, A. Werner, G. Raivich, M. Emerson, L. Neyses, and U. Mayer. 2006. Absence of alpha7 integrin in dystrophin-deficient mice causes a myopathy similar to Duchenne muscular dystrophy. *Hum Mol Genet*. 15:989-998.

Gussoni, E., Y. Soneoka, C.D. Strickland, E.A. Buzney, M.K. Khan, A.F. Flint, L.M. Kunkel, and R.C. Mulligan. 1999. Dystrophin expression in the mdx mouse restored by stem cell transplantation. *Nature*. 401:390-394.

Gussoni, E., Y. Soneoka, C.D. Strickland, E.A. Buzney, M.K. Khan, A.F. Flint, L.M. Kunkel, and R.C. Mulligan. 1999. Dystrophin expression in the mdx mouse restored by stem cell transplantation. *Nature*. 401:390-394.

Haider, S.R., W. Wang, and S.J. Kaufman. 1994. SV40 T Antigen Inhibits Expression of MyoD and Myogenin, Up-Regulates Myf-5, but Does Not Affect Early Expression of Desmin or [alpha]7 Integrin during Muscle Development. *Experimental Cell Research*. 210:278-286.

Hall, D.E., L.F. Reichardt, E. Crowley, B. Holley, H. Moezzi, A. Sonnenberg, and C.H. Damsky. 1990. The alpha 1/beta 1 and alpha 6/beta 1 integrin heterodimers mediate cell attachment to distinct sites on laminin. *J Cell Biol*. 110:2175-2184.

Hardiman, O. 1994. Dystrophin deficiency, altered cell signalling and fibre hypertrophy. *Neuromuscular disorders : NMD*. 4:305-315.

Hauck, C.R. 2002. Cell adhesion receptors - signaling capacity and exploitation by bacterial pathogens. *Medical microbiology and immunology*. 191:55-62.

Hawke, T.J., D.J. Atkinson, S.B. Kanatous, P.F. van der Ven, S.C. Goetsch, and D.J. Garry. 2007. Xin, an actin binding protein, is expressed within muscle satellite cells and newly regenerated skeletal muscle fibres. *Am J Physiol Cell Physiol*.

Hawke, T.J., and D.J. Garry. 2001. Myogenic satellite cells: physiology to molecular biology. *Journal of applied physiology (Bethesda, Md. : 1985)*. 91:534-551.

Hayashi, Y., M.K. Furue, T. Okamoto, K. Ohnuma, Y. Myoishi, Y. Fukuhara, T. Abe, J.D. Sato, R.I. Hata, and M. Asashima. 2007. Integrins Regulate Mouse Embryonic Stem Cell Self-Renewal. *Stem Cells*.

Hayashi, Y., B. Haimovich, A. Reszka, D. Boettiger, and A. Horwitz. 1990. Expression and function of chicken integrin beta 1 subunit and its cytoplasmic domain mutants in mouse NIH 3T3 cells. *J Cell Biol*. 110:175-184.

Hayashi, Y.K., F.L. Chou, E. Engvall, M. Ogawa, C. Matsuda, S. Hirabayashi, K. Yokochi, B.L. Ziober, R.H. Kramer, S.J. Kaufman, E. Ozawa, Y. Goto, I. Nonaka, T. Tsukahara, J.Z. Wang, E.P. Hoffman, and K. Arahata. 1998. Mutations in the integrin alpha7 gene cause congenital myopathy. *Nat Genet*. 19:94-97.

Hayden, M.R., P.R. Karuparthi, J. Habibi, G. Lastra, K. Patel, C. Wasekar, C.M. Manrique, U. Ozerdem, S. Stas, and J.R. Sowers. 2008. Ultrastructure of islet microcirculation, pericytes and the islet exocrine interface in the HIP rat model of diabetes. *Experimental biology and medicine (Maywood, N.J.)*. 233:1109-1123.

Helbling-Leclerc, A., X. Zhang, H. Topaloglu, C. Cruaud, F. Tesson, J. Weissenbach, F.M. Tome, K. Schwartz, M. Fardeau, K. Tryggvason, and et al. 1995. Mutations in the laminin alpha 2-chain gene (LAMA2) cause merosin-deficient congenital muscular dystrophy. *Nat Genet*. 11:216-218.

Herrera, M.B., B. Bussolati, S. Bruno, V. Fonsato, G.M. Romanazzi, and G. Camussi. 2004. Mesenchymal stem cells contribute to the renal repair of acute tubular epithelial injury. *International journal of molecular medicine*. 14:1035-1041.

Hirsch, E., D. Gullberg, F. Balzac, F. Altruda, L. Silengo, and G. Tarone. 1994. Alpha v integrin subunit is predominantly located in nervous tissue and skeletal muscle during mouse development. *Dev Dyn*. 201:108-120.

Hirsch, E., L. Lohikangas, D. Gullberg, S. Johansson, and R. Fassler. 1998. Mouse myoblasts can fuse and form a normal sarcomere in the absence of beta1 integrin expression. *J Cell Sci*. 111 (Pt 16):2397-2409.

Hirschi, K.K., and P.A. D'Amore. 1996. Pericytes in the microvasculature. *Cardiovascular*

research. 32:687-698.

Hodges, B., Y. Hayashi, I. Nonaka, W. Wang, K. Arahata, and S. Kaufman. 1997. Altered expression of the alpha7beta1 integrin in human and murine muscular dystrophies. *J Cell Sci*. 110:2873-2881.

Hoffman, E.P., R.H. Brown, and L.M. Kunkel. 1987. Dystrophin: The protein product of the duchenne muscular dystrophy locus. *Cell*. 51:919-928.

Huard, J., B. Cao, and Z. Qu-Petersen. 2003. Muscle-derived stem cells: potential for muscle regeneration. *Birth defects research. Part C, Embryo today : reviews*. 69:230-237.

Hughes, P.E., F. Diaz-Gonzalez, L. Leong, C. Wu, J.A. McDonald, S.J. Shattil, and M.H. Ginsberg. 1996. Breaking the integrin hinge. A defined structural constraint regulates integrin signaling. *J Biol Chem*. 271:6571-6574.

Humphries, M.J. 2000. Integrin structure. *Biochem Soc Trans*. 28:311-339.

Humphries, M.J., E.J.H. Symonds, and A.P. Mould. 2003. Mapping functional residues onto integrin crystal structures. *Current Opinion in Structural Biology*. 13:236-243.

Hynes, R.O. 2002. Integrins: bidirectional, allosteric signaling machines. *Cell*. 110:673-687.

Hynes, R.O., and K.M. Yamada. 1982. Fibronectins: multifunctional modular glycoproteins. *J Cell Biol*. 95:369-377.

Hynes, R.O., and Q. Zhao. 2000. The Evolution of Cell Adhesion10.1083. *J. Cell Biol.* 150:89F-96.

Isaji, T., Y. Sato, Y. Zhao, E. Miyoshi, Y. Wada, N. Taniguchi, and J. Gu. 2006. N-Glycosylation of the beta -propeller domain of the integrin alpha 5 subunit is essential for alpha 5beta 1 heterodimerization, expression on the cell surface and its biological function. *J. Biol. Chem.*:M607771200.

Jackson, K.A., T. Mi, and M.A. Goodell. 1999. Hematopoietic potential of stem cells isolated from murine skeletal muscle. *Proceedings of the National Academy of Sciences of the United States of America*. 96:14482-14486.

Jasiulionis, M.G., R. Chammas, A.M. Ventura, L.R. Travassos, and R.R. Brentani. 1996. alpha6beta1-Integrin, a major cell surface carrier of beta1-6-branched oligosaccharides, mediates migration of EJ-ras-transformed fibroblasts on laminin-1 independently of its

glycosylation state. *Cancer research*. 56:1682-1689.

Kaariainen, M., J. Kaariainen, T.L. Jarvinen, L. Nissinen, J. Heino, M. Jarvinen, and H. Kalimo. 2000. Integrin and dystrophin associated adhesion protein complexes during regeneration of shearing-type muscle injury. *Neuromuscular disorders : NMD*. 10:121-132.

Kaariainen, M., L. Nissinen, S. Kaufman, A. Sonnenberg, M. Jarvinen, J. Heino, and H. Kalimo. 2002. Expression of {alpha}7{beta}1 Integrin Splicing Variants during Skeletal Muscle Regeneration. *Am J Pathol*. 161:1023-1031.

Kapsa, R., A.J. Kornberg, and E. Byrne. 2003. Novel therapies for Duchenne muscular dystrophy. *The Lancet Neurology*. 2:299-310.

Karceski, S. 2008. Gene therapy and muscular dystrophies. *Neurology*. 71:e6-8.

Kassar-Duchossoy, L., B. Gayraud-Morel, D. Gomes, D. Rocancourt, M. Buckingham, V. Shinin, and S. Tajbakhsh. 2004. Mrf4 determines skeletal muscle identity in Myf5:Myod double-mutant mice. *Nature*. 431:466-471.

Katz, B. 1961. The terminations of the afferent nerve fibre in the muscle spindle of the frog. *Philosophical Transactions of the Royal Society of London*. 243.

Kaufman, S.J., and R.F. Foster. 1988. Replicating myoblasts express a muscle-specific phenotype. *Proceedings of the National Academy of Sciences of the United States of America*. 85:9606-9610.

Khurana, T.S., S.C. Watkins, P. Chafey, J. Chelly, F.M. Tome, M. Fardeau, J.C. Kaplan, and L.M. Kunkel. 1991. Immunolocalization and developmental expression of dystrophin related protein in skeletal muscle. *Neuromuscular disorders : NMD*. 1:185-194.

Kim, M., C.V. Carman, W. Yang, A. Salas, and T.A. Springer. 2004. The primacy of affinity over clustering in regulation of adhesiveness of the integrin {alpha}L{beta}2. *J Cell Biol*. 167:1241-1253.

Kirchhofer, D., L.R. Languino, E. Ruoslahti, and M.D. Pierschbacher. 1990. Alpha 2 beta 1 integrins from different cell types show different binding specificities. *J Biol Chem*. 265:615-618.

Kirsch, T., G. Harrison, E.E. Golub, and H.D. Nah. 2000. The roles of annexins and types II and X collagen in matrix vesicle-mediated mineralization of growth plate cartilage. *J Biol Chem*. 275:35577-35583.

Koenig, M., E.P. Hoffman, C.J. Bertelson, A.P. Monaco, C. Feener, and L.M. Kunkel. 1987.

Complete cloning of the duchenne muscular dystrophy (DMD) cDNA and preliminary genomic organization of the DMD gene in normal and affected individuals. *Cell*. 50:509-517.

Kolodziej, M.A., G. Vilaire, S. Rifat, M. Poncz, and J.S. Bennett. 1991. Effect of deletion of glycoprotein IIb exon 28 on the expression of the platelet glycoprotein IIb/IIIa complex. *Blood*. 78:2344-2353.

Koopman, G., C.P. Reutelingsperger, G.A. Kuijten, R.M. Keehnen, S.T. Pals, and M.H. van Oers. 1994. Annexin V for flow cytometric detection of phosphatidylserine expression on B cells undergoing apoptosis. *Blood*. 84:1415-1420.

Kramer, R.H., M.P. Vu, Y.F. Cheng, D.M. Ramos, R. Timpl, and N. Waleh. 1991. Laminin-binding integrin alpha 7 beta 1: functional characterization and expression in normal and malignant melanocytes. *Cell regulation*. 2:805-817.

Kranz, A., J. Fu, K. Duerschke, S. Weidlich, R. Naumann, A.F. Stewart, and K. Anastassiadis. 2010. An improved Flp deleter mouse in C57Bl/6 based on Flpo recombinase. Genesis. 48:512-520.

Kretzschmar, K., and F.M. Watt. 2012. Lineage tracing. *Cell*. 148:33-45.

Kronqvist, P., N. Kawaguchi, R. Albrechtsen, X. Xu, H.D. Schroder, B. Moghadaszadeh, F.C. Nielsen, C. Frohlich, E. Engvall, and U.M. Wewer. 2002. ADAM12 alleviates the skeletal muscle pathology in mdx dystrophic mice. *Am J Pathol*. 161:1535-1540.

Kuhl, U., M. Ocalan, R. Timpl, and K. von der Mark. 1986. Role of laminin and fibronectin in selecting myogenic versus fibrogenic cells from skeletal muscle cells in vitro. *Dev Biol*. 117:628-635.

Kunath, T., M.K. Saba-El-Leil, M. Almousailleakh, J. Wray, S. Meloche, and A. Smith. 2007. FGF stimulation of the Erk1/2 signalling cascade triggers transition of pluripotent embryonic stem cells from self-renewal to lineage commitment. *J Cell Sci*. 120:2752.

Law, D.J., A. Caputo, and J.G. Tidball. 1995. Site and mechanics of failure in normal and dystrophin-deficient skeletal muscle. *Muscle Nerve*. 18:216-223.

Lee, J.-O., P. Rieu, M.A. Arnaout, and R. Liddington. 1995. Crystal structure of the A domain from the a subunit of integrin CR3 (CD11 b/CD18). *Cell*. 80:631-638.

Lehmann, M., V. Rigot, N.G. Seidah, J. Marvaldi, and J.C. Lissitzky. 1996. Lack of integrin alpha-chain endoproteolytic cleavage in furin-deficient human colon adenocarcinoma cells LoVo. *Biochem J*. 317 (Pt 3):803-809.

Leitinger, B., A. McDowall, P. Stanley, and N. Hogg. 2000. The regulation of integrin function by Ca2+. *Biochimica et Biophysica Acta (BBA) - Molecular Cell Research*. 1498:91-98.

Liemann, S., and R. Huber. 1997. Three-dimensional structure of annexins. *Cell Mol Life Sci*. 53:516-521.

Liu, S., D.A. Calderwood, and M.H. Ginsberg. 2000. Integrin cytoplasmic domain-binding proteins. *J Cell Sci*. 113 (Pt 20):3563-3571.

Lu, C., J. Takagi, and T.A. Springer. 2001. Association of the membrane proximal regions of the alpha and beta subunit cytoplasmic domains constrains an integrin in the inactive state. *J Biol Chem*. 276:14642-14648.

Mandarino, L.J., N. Sundarraj, J. Finlayson, and H.R. Hassell. 1993. Regulation of fibronectin and laminin synthesis by retinal capillary endothelial cells and pericytes in vitro. *Experimental eye research*. 57:609-621.

Madisen, L., T.A. Zwingman, S.M. Sunkin, S.W. Oh, H.A. Zariwala, H. Gu, L.L. Ng, R.D. Palmiter, M.J. Hawrylycz, A.R. Jones, E.S. Lein, and H. Zeng. 2010. A robust and high-throughput Cre reporting and characterization system for the whole mouse brain. Nature neuroscience. 13:133-140.

Marcantonio, E.E., J.L. Guan, J.E. Trevithick, and R.O. Hynes. 1990. Mapping of the functional determinants of the integrin beta 1 cytoplasmic domain by site-directed mutagenesis. *Cell regulation*. 1:597-604.

Maroto, M., R. Reshef, A.E. Munsterberg, S. Koester, M. Goulding, and A.B. Lassar. 1997. Ectopic Pax-3 Activates MyoD and Myf-5 Expression in Embryonic Mesoderm and Neural Tissue. *Cell*. 89:139-148.

Martin, P.T., S.J. Kaufman, R.H. Kramer, and J.R. Sanes. 1996. Synaptic integrins in developing, adult, and mutant muscle: selective association of alpha1, alpha7A, and alpha7B integrins with the neuromuscular junction. *Dev Biol*. 174:125-139.

Masumoto, A., and M.E. Hemler. 1993. Mutation of putative divalent cation sites in the alpha 4

subunit of the integrin VLA-4: distinct effects on adhesion to CS1/fibronectin, VCAM-1, and invasin. *J Cell Biol*. 123:245-253.

Mauro, A. 1961. Satellite cell of skeletal muscle fibers. *The Journal of biophysical and biochemical cytology*. 9:493-495.

Mayer, U. 2003. Integrins: redundant or important players in skeletal muscle? *J Biol Chem*. 278:14587-14590.

Mayer, U., G. Saher, R. Fassler, A. Bornemann, F. Echtermeyer, H. von der Mark, N. Miosge, E. Poschl, and K. von der Mark. 1997. Absence of integrin alpha 7 causes a novel form of muscular dystrophy. *Nat Genet*. 17:318-323.

McCullagh, K.J., and R.C. Perlingeiro. 2014. Coaxing stem cells for skeletal muscle repair. *Advanced drug delivery reviews*.

Megeney, L.A., B. Kablar, K. Garrett, J.E. Anderson, and M.A. Rudnicki. 1996. MyoD is required for myogenic stem cell function in adult skeletal muscle. *Genes Dev*. 10:1173-1183.

Michishita, M., V. Videm, and M.A. Arnaout. 1993. A novel divalent cation-binding site in the A domain of the beta 2 integrin CR3 (CD11b/CD18) is essential for ligand binding. *Cell*. 72:857-867.

Miosge, N., C. Klenczar, R. Herken, M. Willem, and U. Mayer. 1999. Organization of the myotendinous junction is dependent on the presence of alpha7beta1 integrin. *Laboratory investigation; a journal of technical methods and pathology*. 79:1591-1599.

Miyamoto, S., H. Teramoto, O.A. Coso, J.S. Gutkind, P.D. Burbelo, S.K. Akiyama, and K.M. Yamada. 1995. Integrin function: molecular hierarchies of cytoskeletal and signaling molecules. *J Cell Biol*. 131:791-805.

Miyoshi, E., K. Noda, J.H. Ko, A. Ekuni, T. Kitada, N. Uozumi, Y. Ikeda, N. Matsuura, Y. Sasaki, N. Hayashi, M. Hori, and N. Taniguchi. 1999. Overexpression of alpha1-6 fucosyltransferase in hepatoma cells suppresses intrahepatic metastasis after splenic injection in athymic mice. *Cancer research*. 59:2237-2243.

Moghadaszadeh, B., R. Albrechtsen, L.T. Guo, M. Zaik, N. Kawaguchi, R.H. Borup, P. Kronqvist, H.D. Schroder, K.E. Davies, T. Voit, F.C. Nielsen, E. Engvall, and U.M. Wewer. 2003. Compensation for dystrophin-deficiency: ADAM12 overexpression in skeletal muscle results in increased alpha 7 integrin, utrophin and associated glycoproteins. *Hum Mol*

Genet. 12:2467-2479.

Mollenhauer, J., and K. von der Mark. 1983. Isolation and characterization of a collagen-binding glycoprotein from chondrocyte membranes. *Embo j*. 2:45-50.

Morgan, J.E., D.J. Watt, J.C. Sloper, and T.A. Partridge. 1988. Partial correction of an inherited biochemical defect of skeletal muscle by grafts of normal muscle precursor cells. *J Neurol Sci*. 86:137-147.

Morrison, S.J., A.M. Wandycz, H.D. Hemmati, D.E. Wright, and I.L. Weissman. 1997. Identification of a lineage of multipotent hematopoietic progenitors. *Development*. 124:1929-1939.

Moss, R.L., G.M. Diffee, and M.L. Greaser. 1995. Contractile properties of skeletal muscle fibers in relation to myofibrillar protein isoforms. *Reviews of physiology, biochemistry and pharmacology*. 126:1-63.

Nakamura, A., and S. Takeda. 2011. Exon-skipping therapy for Duchenne muscular dystrophy. *Lancet*. 378:546-547.

Nakamura, A., and S.i. Takeda. 2009. Exon-skipping therapy for Duchenne muscular dystrophy. *Neuropathology*. 29:494-501.

Nakashima, H., T. Kibe, and K. Yokochi. 2009. 'Congenital muscular dystrophy caused by integrin α7 deficiency'. *Developmental Medicine & Child Neurology*. 51:245-245.

Nawrotzki, R., M. Willem, N. Miosge, H. Brinkmeier, and U. Mayer. 2003. Defective integrin switch and matrix composition at alpha 7-deficient myotendinous junctions precede the onset of muscular dystrophy in mice. *Hum Mol Genet*. 12:483-495.

Negroni, E., G.S. Butler-Browne, and V. Mouly. 2006. Myogenic stem cells: regeneration and cell therapy in human skeletal muscle. *Pathologie-biologie*. 54:100-108.

Nehls, V., and D. Drenckhahn. 1993. The versatility of microvascular pericytes: from mesenchyme to smooth muscle? *Histochemistry*. 99:1-12.

Nermut, M.V., N.M. Green, P. Eason, S.S. Yamada, and K.M. Yamada. 1988. Electron microscopy and structural model of human fibronectin receptor. *EMBO J*. 7:4093-4099.

Nolte, M., R.B. Pepinsky, S.Y. Venyaminov, V. Koteliansky, P.J. Gotwals, and M. Karpusas. 1999. Crystal structure of the alpha1beta1 integrin I-domain: insights into integrin I-domain

function. *FEBS Letters*. 452:379-385.

Öcalan, M., S.L. Goodman, U. Kühl, S.D. Hauschka, and K. von der Mark. 1988. Laminin alters cell shape and stimulates motility and proliferation of murine skeletal myoblasts. *Developmental Biology*. 125:158-167.

Ott, M.O., E. Bober, G. Lyons, H. Arnold, and M. Buckingham. 1991. Early expression of the myogenic regulatory gene, myf-5, in precursor cells of skeletal muscle in the mouse embryo. *Development*. 111:1097-1107.

Oxvig, C., and T.A. Springer. 1998. Experimental support for a beta-propeller domain in integrin alpha-subunits and a calcium binding site on its lower surface. *Proceedings of the National Academy of Sciences of the United States of America*. 95:4870-4875.

Paquet-Fifield, S., H. Schluter, A. Li, T. Aitken, P. Gangatirkar, D. Blashki, R. Koelmeyer, N. Pouliot, M. Palatsides, S. Ellis, N. Brouard, A. Zannettino, N. Saunders, N. Thompson, J. Li, and P. Kaur. 2009. A role for pericytes as microenvironmental regulators of human skin tissue regeneration. *J Clin Invest*. 119:2795-2806.

Paratore, and Sommer. 2006.

Pardo, J.V., J.D. Siliciano, and S.W. Craig. 1983. A vinculin-containing cortical lattice in skeletal muscle: transverse lattice elements ("costameres") mark sites of attachment between myofibrils and sarcolemma. *Proceedings of the National Academy of Sciences of the United States of America*. 80:1008-1012.

Partridge, T., Q.L. Lu, G. Morris, and E. Hoffman. 1998. Is myoblast transplantation effective? *Nat Med*. 4:1208-1209.

Partridge, T.A., J.E. Morgan, G.R. Coulton, E.P. Hoffman, and L.M. Kunkel. 1989. Conversion of mdx myofibres from dystrophin-negative to -positive by injection of normal myoblasts. *Nature*. 337:176-179.

Payne, C.M., L.Z. Stern, R.G. Curless, and L.K. Hannapel. 1975. Ultrastructural fiber typing in normal and diseased human muscle. *J Neurol Sci*. 25:99-108.

Pearce, M., D.J. Blake, J.M. Tinsley, B.C. Byth, L. Campbell, A.P. Monaco, and K.E. Davies. 1993. The utrophin and dystrophin genes share similarities in genomic structure. *Hum Mol Genet*. 2:1765-1772.

Peault, B., M. Rudnicki, Y. Torrente, G. Cossu, J.P. Tremblay, T. Partridge, E. Gussoni, L.M.

Kunkel, and J. Huard. 2007. Stem and progenitor cells in skeletal muscle development, maintenance, and therapy. *Mol Ther*. 15:867-877.

Petrof, B.J., J.B. Shrager, H.H. Stedman, A.M. Kelly, and H.L. Sweeney. 1993. Dystrophin protects the sarcolemma from stresses developed during muscle contraction. *Proceedings of the National Academy of Sciences of the United States of America*. 90:3710-3714.

Petrof, B.J., H.H. Stedman, J.B. Shrager, J. Eby, H.L. Sweeney, and A.M. Kelly. 1993. Adaptations in myosin heavy chain expression and contractile function in dystrophic mouse diaphragm. *The American journal of physiology*. 265:C834-841.

Pujades, C., R. Alon, R.L. Yauch, A. Masumoto, L.C. Burkly, C. Chen, T.A. Springer, R.R. Lobb, and M.E. Hemler. 1997. Defining extracellular integrin alpha-chain sites that affect cell adhesion and adhesion strengthening without altering soluble ligand binding. *Mol Biol Cell*. 8:2647-2657.

Qu, A., and D.J. Leahy. 1995. Crystal structure of the I-domain from the CD11a/CD18 (LFA-1, alpha L beta 2) integrin. *Proceedings of the National Academy of Sciences*. 92:10277-10281.

Rando, T.A. 2001. The dystrophin-glycoprotein complex, cellular signaling, and the regulation of cell survival in the muscular dystrophies. *Muscle Nerve*. 24:1575-1594.

Rando, T.A. 2005. The adult muscle stem cell comes of age. *Nat Med*. 11:829-831.

Rando, T.A. 2007. Non-viral gene therapy for Duchenne muscular dystrophy: progress and challenges. *Biochim Biophys Acta*. 1772:263-271.

Relaix, F., D. Rocancourt, A. Mansouri, and M. Buckingham. 2004. Divergent functions of murine Pax3 and Pax7 in limb muscle development. *Genes Dev*. 18:1088-1105.

Relaix, F., D. Rocancourt, A. Mansouri, and M. Buckingham. 2005. A Pax3/Pax7-dependent population of skeletal muscle progenitor cells. *Nature*. 435:948-953.

Relaix, F., and P.S. Zammit. 2012. Satellite cells are essential for skeletal muscle regeneration: the cell on the edge returns centre stage. *Development*. 139:2845-2856.

Rescher, U., and V. Gerke. 2004. Annexins--unique membrane binding proteins with diverse functions. *J Cell Sci*. 117:2631-2639.

Reynolds, L.E., L. Wyder, J.C. Lively, D. Taverna, S.D. Robinson, X. Huang, D. Sheppard, R.O. Hynes, and K.M. Hodivala-Dilke. 2002. Enhanced pathological angiogenesis in mice lacking beta3 integrin or beta3 and beta5 integrins. *Nat Med*. 8:27-34.

Rodriguez-Garcia, J.L., A. Paule, J. Dominguez, J.R. Garcia-Escribano, and M. Vazquez. 1999. Effects of the angiotensin II antagonist losartan on endothelin-1 and norepinephrine plasma levels during cold pressor test in patients with chronic heart failure. *International journal of cardiology*. 70:293-301.

Rogers, L.K.a.M., U. 2006. Insights into Integrin Function in Skeletal Muscle. *In* Integrins and Development. Vol. Chapter 9. Landes Biosciences, Landes Biosciences. 138-151.

Rojas, E., H.B. Pollard, H.T. Haigler, C. Parra, and A.L. Burns. 1990. Calcium-activated endonexin II forms calcium channels across acidic phospholipid bilayer membranes. *J Biol Chem*. 265:21207-21215.

Rooney, J.E., J.V. Welser, M.A. Dechert, N.L. Flintoff-Dye, S.J. Kaufman, and D.J. Burkin. 2006. Severe muscular dystrophy in mice that lack dystrophin and alpha7 integrin. *J Cell Sci*. 119:2185-2195.

Rouget, C. 1873. Mémoire sur le développment, la structure et les propertiés physiologiques des capillaries sanguins et lymphatiques. . *Arch Physiol Norm Pathol*. 5.

Rudnicki, M.A., P.N. Schnegelsberg, R.H. Stead, T. Braun, H.H. Arnold, and R. Jaenisch. 1993. MyoD or Myf-5 is required for the formation of skeletal muscle. *Cell*. 75:1351-1359.

Sabourin, L.A., A. Girgis-Gabardo, P. Seale, A. Asakura, and M.A. Rudnicki. 1999. Reduced differentiation potential of primary MyoD-/- myogenic cells derived from adult skeletal muscle. *J Cell Biol*. 144:631-643.

Sackstein, R., J.S. Merzaban, D.W. Cain, N.M. Dagia, J.A. Spencer, C.P. Lin, and R. Wohlgemuth. 2008. Ex vivo glycan engineering of CD44 programs human multipotent mesenchymal stromal cell trafficking to bone. *Nat Med*. 14:181-187.

Saito, T., J.E. Dennis, D.P. Lennon, R.G. Young, and A.I. Caplan. 1995. Myogenic Expression of Mesenchymal Stem Cells within Myotubes of mdx Mice in Vitro and in Vivo. *Tissue engineering*. 1:327-343.

Salem, H.K., and C. Thiemermann. 2010. Mesenchymal stromal cells: current understanding and clinical status. *Stem Cells*. 28:585-596.

Sampaolesi, M., Y. Torrente, A. Innocenzi, R. Tonlorenzi, G. D'Antona, M.A. Pellegrino, R. Barresi, N. Bresolin, M.G. De Angelis, K.P. Campbell, R. Bottinelli, and G. Cossu. 2003. Cell therapy of alpha-sarcoglycan null dystrophic mice through intra-arterial delivery of

mesoangioblasts. *Science*. 301:487-492.

Samson, T., C. Will, A. Knoblauch, L. Sharek, K. von der Mark, K. Burridge, and V. Wixler. 2007. Def-6, a guanine nucleotide exchange factor for Rac1, interacts with the skeletal muscle integrin chain alpha7A and influences myoblast differentiation. *J Biol Chem*. 282:15730-15742.

Sanes, J.R. 2003. The basement membrane/basal lamina of skeletal muscle. *J Biol Chem*. 278:12601-12604.

Sassoon, D.A., I. Garner, and M. Buckingham. 1988. Transcripts of alpha-cardiac and alpha-skeletal actins are early markers for myogenesis in the mouse embryo. *Development*. 104:155-164.

Sastry, S.K., M. Lakonishok, D.A. Thomas, J. Muschler, and A.F. Horwitz. 1996. Integrin alpha subunit ratios, cytoplasmic domains, and growth factor synergy regulate muscle proliferation and differentiation. *J Cell Biol*. 133:169-184.

Schlaepfer, D.D., and T. Hunter. 1998. Integrin signalling and tyrosine phosphorylation: just the FAKs? *Trends Cell Biol*. 8:151-157.

Schwander, M., M. Leu, M. Stumm, O.M. Dorchies, U.T. Ruegg, J. Schittny, and U. Muller. 2003. Beta1 integrins regulate myoblast fusion and sarcomere assembly. *Dev Cell*. 4:673-685.

Schwartz, M.A., M.D. Schaller, and M.H. Ginsberg. 1995. Integrins: emerging paradigms of signal transduction. *Annu Rev Cell Dev Biol*. 11:549-599.

Seale, P., A. Asakura, and M.A. Rudnicki. 2001. The potential of muscle stem cells. *Dev Cell*. 1:333-342.

Seale, P., L.A. Sabourin, A. Girgis-Gabardo, A. Mansouri, P. Gruss, and M.A. Rudnicki. 2000. Pax7 is required for the specification of myogenic satellite cells. *Cell*. 102:777-786.

Segers, V.F., I. Van Riet, L.J. Andries, K. Lemmens, M.J. Demolder, A.J. De Becker, M.M. Kockx, and G.W. De Keulenaer. 2006. Mesenchymal stem cell adhesion to cardiac microvascular endothelium: activators and mechanisms. *American journal of physiology. Heart and circulatory physiology*. 290:H1370-1377.

Seidah, N.G., and M. Chretien. 1997. Eukaryotic protein processing: endoproteolysis of precursor proteins. *Current opinion in biotechnology*. 8:602-607.

Seidah, N.G., R. Day, M. Marcinkiewicz, and M. Chretien. 1998. Precursor convertases: an evolutionary ancient, cell-specific, combinatorial mechanism yielding diverse bioactive

peptides and proteins. *Ann N Y Acad Sci*. 839:9-24.

Shi, M., J. Li, L. Liao, B. Chen, B. Li, L. Chen, H. Jia, and R.C. Zhao. 2007. Regulation of CXCR4 expression in human mesenchymal stem cells by cytokine treatment: role in homing efficiency in NOD/SCID mice. *Haematologica*. 92:897-904.

Sicinski, P., Y. Geng, A.S. Ryder-Cook, E.A. Barnard, M.G. Darlison, and P.J. Barnard. 1989. The molecular basis of muscular dystrophy in the mdx mouse: a point mutation. *Science*. 244:1578-1580.

Siminovitch, L., E.A. McCulloch, and J.E. Till. 1963. The Distribution of Colony-Forming Cells among Spleen Colonies. *J Cell Physiol*. 62:327-336.

Skrahina, T., A. Piljic, and C. Schultz. 2008. Heterogeneity and timing of translocation and membrane-mediated assembly of different annexins. *Exp Cell Res*. 314:1039-1047.

Skuk, D., M. Goulet, B. Roy, V. Piette, C.H. Cote, P. Chapdelaine, J.Y. Hogrel, M. Paradis, J.P. Bouchard, M. Sylvain, J.G. Lachance, and J.P. Tremblay. 2007. First test of a "high-density injection" protocol for myogenic cell transplantation throughout large volumes of muscles in a Duchenne muscular dystrophy patient: eighteen months follow-up. *Neuromuscular disorders : NMD*. 17:38-46.

Solowska, J., J.L. Guan, E.E. Marcantonio, J.E. Trevithick, C.A. Buck, and R.O. Hynes. 1989. Expression of normal and mutant avian integrin subunits in rodent cells. *J Cell Biol*. 109:853-861.

Song, W.K., W. Wang, R.F. Foster, D.A. Bielser, and S.J. Kaufman. 1992. H36-alpha 7 is a novel integrin alpha chain that is developmentally regulated during skeletal myogenesis. *J Cell Biol*. 117:643-657.

Song, W.K., W. Wang, H. Sato, D.A. Bielser, and S.J. Kaufman. 1993. Expression of alpha 7 integrin cytoplasmic domains during skeletal muscle development: alternate forms, conformational change, and homologies with serine/threonine kinases and tyrosine phosphatases. *Journal of Cell Science*. 106:1139-1152.

Spence, H.J., Y.J. Chen, and S.J. Winder. 2002. Muscular dystrophies, the cytoskeleton and cell adhesion. *Bioessays*. 24:542-552.

Springer, M.L., C.R. Ozawa, and H.M. Blau. 2002. Transient production of alpha-smooth muscle actin by skeletal myoblasts during differentiation in culture and following intramuscular implantation. *Cell motility and the cytoskeleton*. 51:177-186.

Springer, T.A. 1997. Folding of the N-terminal, ligand-binding region of integrin α-subunits into a β-propeller domain *Proceedings of the National Academy of Sciences*. 94:65-72.

Srinivas, S., T. Watanabe, C.S. Lin, C.M. William, Y. Tanabe, T.M. Jessell, and F. Costantini. 2001. Cre reporter strains produced by targeted insertion of EYFP and ECFP into the ROSA26 locus. *BMC developmental biology*. 1:4.

Staatz, W.D., S.M. Rajpara, E.A. Wayner, W.G. Carter, and S.A. Santoro. 1989. The membrane glycoprotein Ia-IIa (VLA-2) complex mediates the Mg++-dependent adhesion of platelets to collagen. *J Cell Biol*. 108:1917-1924.

Stedman, H.H., H.L. Sweeney, J.B. Shrager, H.C. Maguire, R.A. Panettieri, B. Petrof, M. Narusawa, J.M. Leferovich, J.T. Sladky, and A.M. Kelly. 1991. The mdx mouse diaphragm reproduces the degenerative changes of Duchenne muscular dystrophy. *Nature*. 352:536-539.

Streuli, C.H., N. Bailey, and M.J. Bissell. 1991. Control of mammary epithelial differentiation: basement membrane induces tissue-specific gene expression in the absence of cell-cell interaction and morphological polarity. *J Cell Biol*. 115:1383-1395.

Strynadka, N.C., and M.N. James. 1989. Crystal structures of the helix-loop-helix calcium-binding proteins. *Annual review of biochemistry*. 58:951-998.

Tajbakhsh, S., and M. Buckingham. 2000. The birth of muscle progenitor cells in the mouse: spatiotemporal considerations. *Current topics in developmental biology*. 48:225-268.

Tajbakhsh, S., E. Vivarelli, G. Cusella-De Angelis, D. Rocancourt, M. Buckingham, and G. Cossu. 1994. A population of myogenic cells derived from the mouse neural tube. *Neuron*. 13:813-821.

Tamkun, J.W., D.W. DeSimone, D. Fonda, R.S. Patel, C. Buck, A.F. Horwitz, and R.O. Hynes. 1986. Structure of integrin, a glycoprotein involved in the transmembrane linkage between fibronectin and actin. *Cell*. 46:271-282.

Taverna, D., M.H. Disatnik, H. Rayburn, R.T. Bronson, J. Yang, T.A. Rando, and R.O. Hynes. 1998. Dystrophic muscle in mice chimeric for expression of alpha5 integrin. *J Cell Biol*. 143:849-859.

Tidball, J.G., and T.L. Daniel. 1986. Myotendinous junctions of tonic muscle cells: structure and loading. *Cell Tissue Res*. 245:315-322.

Tidball, J.G., and M. Wehling-Henricks. 2004. Expression of a NOS transgene in dystrophin-

deficient muscle reduces muscle membrane damage without increasing the expression of membrane-associated cytoskeletal proteins. *Molecular Genetics and Metabolism*. 82:312-320.

Tidball, J.G., and M. Wehling-Henricks. 2004. Evolving therapeutic strategies for Duchenne muscular dystrophy: targeting downstream events. *Pediatric research*. 56:831-841.

Till, J.E., and C.E. McCulloch. 1961. A direct measurement of the radiation sensitivity of normal mouse bone marrow cells. *Radiation research*. 14:213-222.

Timpl, R., and J.C. Brown. 1996. Supramolecular assembly of basement membranes. *Bioessays*. 18:123-132.

Tinsley, J.M., D.J. Blake, A. Roche, U. Fairbrother, J. Riss, B.C. Byth, A.E. Knight, J. Kendrick-Jones, G.K. Suthers, D.R. Love, and et al. 1992. Primary structure of dystrophin-related protein. *Nature*. 360:591-593.

Tomatis, D., F. Echtermayer, S. Schober, F. Balzac, S.F. Retta, L. Silengo, and G. Tarone. 1999. The muscle-specific laminin receptor alpha7 beta1 integrin negatively regulates alpha5 beta1 fibronectin receptor function. *Exp Cell Res*. 246:421-432.

Trotter, J.A. 1993. Functional morphology of force transmission in skeletal muscle. A brief review. *Acta anatomica*. 146:205-222.

Trotter, J.A., and J.M. Baca. 1987. The muscle-tendon junctions of fast and slow fibres in the garter snake: ultrastructural and stereological analysis and comparison with other species. *Journal of muscle research and cell motility*. 8:517-526.

Vachon, P.H., H. Xu, L. Liu, F. Loechel, Y. Hayashi, K. Arahata, J.C. Reed, U.M. Wewer, and E. Engvall. 1997. Integrins (alpha7beta1) in muscle function and survival. Disrupted expression in merosin-deficient congenital muscular dystrophy. *The Journal of Clinical Investigation*. 100:1870-1881.

van der Flier, A., I. Kuikman, C. Baudoin, R. van der Neut, and A. Sonnenberg. 1995. A novel beta 1 integrin isoform produced by alternative splicing: unique expression in cardiac and skeletal muscle. *FEBS Lett*. 369:340-344.

van Deutekom, J.C., and G.J. van Ommen. 2003. Advances in Duchenne muscular dystrophy gene therapy. *Nature reviews. Genetics*. 4:774-783.

Velling, T., G. Collo, L. Sorokin, M. Durbeej, H. Zhang, and D. Gullberg. 1996. Distinct alpha 7A beta 1 and alpha 7B beta 1 integrin expression patterns during mouse development: alpha 7A is restricted to skeletal muscle but alpha 7B is expressed in striated muscle, vasculature, and nervous system. *Dev Dyn*. 207:355-371.

Voisin, V., and S. de la Porte. 2004. Therapeutic strategies for Duchenne and Becker dystrophies. *International review of cytology*. 240:1-30.

von der Mark, H., J. Durr, A. Sonnenberg, K. von der Mark, R. Deutzmann, and S.L. Goodman. 1991. Skeletal myoblasts utilize a novel beta 1-series integrin and not alpha 6 beta 1 for binding to the E8 and T8 fragments of laminin. *J Biol Chem*. 266:23593-23601.

von der Mark, H., I. Williams, O. Wendler, L. Sorokin, K. von der Mark, and E. Poschl. 2002. Alternative Splice Variants of alpha 7beta 1 Integrin Selectively Recognize Different Laminin Isoforms. *J. Biol. Chem.* 277:6012-6016.

Wakefield, P.M., J.M. Tinsley, M.J. Wood, R. Gilbert, G. Karpati, and K.E. Davies. 2000. Prevention of the dystrophic phenotype in dystrophin/utrophin-deficient muscle following adenovirus-mediated transfer of a utrophin minigene. *Gene therapy*. 7:201-204.

Watt, D.J., K. Lambert, J.E. Morgan, T.A. Partridge, and J.C. Sloper. 1982. Incorporation of donor muscle precursor cells into an area of muscle regeneration in the host mouse. *J Neurol Sci*. 57:319-331.

Webster, C., and H.M. Blau. 1990. Accelerated age-related decline in replicative life-span of Duchenne muscular dystrophy myoblasts: implications for cell and gene therapy. *Somatic cell and molecular genetics*. 16:557-565.

Weisel, J.W., C. Nagaswami, G. Vilaire, and J.S. Bennett. 1992. Examination of the platelet membrane glycoprotein IIb-IIIa complex and its interaction with fibrinogen and other ligands by electron microscopy. *J Biol Chem*. 267:16637-16643.

Weissman, I.L. 2000. Translating stem and progenitor cell biology to the clinic: barriers and opportunities. *Science*. 287:1442-1446.

Wennerberg, K., L. Lohikangas, D. Gullberg, M. Pfaff, S. Johansson, and R. Fassler. 1996. Beta 1 integrin-dependent and -independent polymerization of fibronectin. *J Cell Biol*. 132:227-238.

Wilcox, D.A., C.M. Paddock, S. Lyman, J.C. Gill, and P.J. Newman. 1995. Glanzmann

thrombasthenia resulting from a single amino acid substitution between the second and third calcium-binding domains of GPIIb. Role of the GPIIb amino terminus in integrin subunit association. *J Clin Invest*. 95:1553-1560.

Williamson, R.A., M.D. Henry, K.J. Daniels, R.F. Hrstka, J.C. Lee, Y. Sunada, O. Ibraghimov-Beskrovnaya, and K.P. Campbell. 1997. Dystroglycan is essential for early embryonic development: disruption of Reichert's membrane in Dag1-null mice. *Hum Mol Genet*. 6:831-841.

Wu, C., V.M. Keivens, T.E. O'Toole, J.A. McDonald, and M.H. Ginsberg. 1995. Integrin activation and cytoskeletal interaction are essential for the assembly of a fibronectin matrix. *Cell*. 83:715-724.

Xiong, J.P., T. Stehle, B. Diefenbach, R. Zhang, R. Dunker, D.L. Scott, A. Joachimiak, S.L. Goodman, and M.A. Arnaout. 2001. Crystal structure of the extracellular segment of integrin alpha Vbeta3. *Science*. 294:339-345.

Yablonka-Reuveni, Z., M.A. Rudnicki, A.J. Rivera, M. Primig, J.E. Anderson, and P. Natanson. 1999. The transition from proliferation to differentiation is delayed in satellite cells from mice lacking MyoD. *Dev Biol*. 210:440-455.

Yang, J.T., H. Rayburn, and R.O. Hynes. 1993. Embryonic mesodermal defects in alpha 5 integrin-deficient mice. *Development*. 119:1093-1105.

Yao, C.C., B.L. Ziober, A.E. Sutherland, D.L. Mendrick, and R.H. Kramer. 1996. Laminins promote the locomotion of skeletal myoblasts via the alpha 7 integrin receptor. *J Cell Sci*. 109 (Pt 13):3139-3150.

Yurchenco, P.D.a.J.O'Rear. 1993. Supramolecular organisation of basement membranes. *in Molecular and Cellular aspects of basement membrane*. D.M.Rohrbach and R. Timple, Editors:19-47.

Zammit, P.S., J.P. Golding, Y. Nagata, V. Hudon, T.A. Partridge, and J.R. Beauchamp. 2004. Muscle satellite cells adopt divergent fates: a mechanism for self-renewal? *J Cell Biol*. 166:347-357.

Zheng, M., H. Fang, and S. Hakomori. 1994. Functional role of N-glycosylation in alpha 5 beta 1 integrin receptor. De-N-glycosylation induces dissociation or altered association of alpha 5 and beta 1 subunits and concomitant loss of fibronectin binding activity. *J Biol Chem*.

269:12325-12331.

Zhidkova, N.I., A.M. Belkin, and R. Mayne. 1995. Novel Isoform of Î²1 Integrin Expressed in Skeletal and Cardiac Muscle. *Biochemical and Biophysical Research Communications*. 214:279-285.

Zhou, G.Q., H.Q. Xie, S.Z. Zhang, and Z.M. Yang. 2006. Current understanding of dystrophin-related muscular dystrophy and therapeutic challenges ahead. *Chinese medical journal*. 119:1381-1391.

Ziober, B.L., Y. Chen, and R.H. Kramer. 1997. The laminin-binding activity of the alpha 7 integrin receptor is defined by developmentally regulated splicing in the extracellular domain. *Molecular Biology of the Cell*. 8:1723-1734.